
NANOP

2017

NANOPHOTONICS
AND
MICRO/NANO OPTICS
INTERNATIONAL CONFERENCE

Sept 13-15, 2017

BARCELONA

BOOK OF ABSTRACTS

Prem 

Conferences, Events & Workshops

premc.org



An Open Access Journal by MDPI

Editor-in-Chief:

Prof. Dr. Nelson Tansu

Photonics Editorial Office
photonics@mdpi.com
MDPI AG
St. Alban-Anlage 66
4052 Basel, Switzerland
Tel: +41 61 683 77 34
Fax: +41 61 302 89 18
www.mdpi.com



Message from the Editor-in-Chief

Dear Colleagues,

You are invited to contribute a research article or a comprehensive review for consideration and publication in Photonics (ISSN 2304-6732). Photonics is an online open access journal covering both the fundamental and applications of optics and photonics. Photonics strives to provide an avenue to allow authors to disseminate their scientific findings—both theoretical / simulations and experimental works – in highly accessible peer-reviewed journal publications. The manuscript in Photonics will be handled with quick turnaround production processing time. We welcome authors to submit their manuscripts for publications in Photonics. Our goal in Photonics is to enable fast dissemination of high impact works to the scientific community.

Author Benefits

-  **Open Access** Unlimited and free access for readers
-  **No Copyright Constraints**
Retain copyright of your work and free use of your article
-  **Thorough Peer-Review**
-  **Rapid Processing and Immediate Publication upon Acceptance**
-  **No Space Constraints, No Extra Space or Color Charges**
No restriction on the length of the papers, number of figures or colors
-  **Discounts on Article Processing Charges (APC)**
If you belong to an institute that participates with the MDPI membership program
-  **High Visibility** Indexed in Emerging Sources Citation Index (ESCI - Web of Science), INSPEC (IET), Scopus



Special Issue

Microwave Photonics

Best Paper Award

Table of Contents

Two Grand Challenges for Nanophotonics: Tunable Coherent Optical Arrays and the Starshot Lightsail	1
<u>Prof. Harry Atwater</u>	
Plasmonics – a Scalable Path towards a Terabit/s-Technology?	2
<u>Prof. Juerg Leuthold</u>	
Tracking femtosecond dynamics at the nanoscale	3
<u>Prof. Niek van Hulst</u>	
Controlling Light-matter Interactions on the Nanometer Scale	4
<u>Prof. Lukas Novotny</u>	
Integration of magnetic plasmonic nanoantennas on a silicon chip	5
<u>Mr. Javier Losada, Dr. Alejandro Martínez</u>	
Optical properties of porphycenes in the regime of strong light-matter coupling.	6
<u>Mr. Wassie Takele, Dr. Lukasz Piatkowski, Prof. Jacek Waluk</u>	
Dynamic plasmonic colour display	7
<u>Mr. Xiaoyang Duan, Mr. Simon Kamin, Prof. Na Liu</u>	
Totally confined gigahertz mechanical mode with a complete phononic bandgap for a nano-optomechanic cavity	8
<u>Ms. Laura Mercadé Morales, Dr. Alejandro Martínez</u>	
Emission of a single colloidal quantum dot in a patch antenna	9
<u>Mr. Juan Uriel Esparza, Dr. Amit Raj Dhawan, Dr. Cherif Belacel, Dr. Catherine Schwob,, Dr. Micheal Nasilowski, Prof. Benoit Dubertret, Prof. Laurent Coolen, Prof. Pascale Senellart, Prof. Agnès Maître</u>	
Optical properties and charge trapping dynamics of single CsPbBr₃ nanocrystals	10
<u>Ms. Natalie A. Gibson, Mr. Brent A. Koscher, Prof. A. Paul Alivisatos, Prof. Stephen R. Leone</u>	
New luminescent nanostructural polymer materials	12
<u>Dr. Viktoria Lapina, Dr. Piotr Pershukevich, Dr. Pavich Tatsiana</u>	
Development of an optical genosensor based on gold nanoparticles for genomic detection of Mycobacterium bovis.	14
<u>Dr. Patricio Oyarzun, Mr. Braulio Contreras, Dr. Enrique Guzmán-Gutiérrez, Ms. Javiera Aguilar, Mr. Alejandro Maldonado, Prof. René Garcés</u>	
Control of Chiral Response in Clustered Nanoparticles through Cluster Geometry	16
<u>Mr. Dominykas Brickus, Dr. Sergej Orlov</u>	
A light detection system for a STM	17
<u>Mr. Yves Auad, Mr. Ricardo Peña Román, Mr. Edivar Carvalho, Ms. Isabela Rigo, Mr. Raone Guedes, Mr. Leonardo Santana, Mr. Ronaldo Vieira, Ms. Luiza Lober, Mr. Lucas Palhares, Ms. Maria Orfanelli, Prof. Luiz Fernando Zagonel</u>	

Surface holograms for sensing application	18
<u>Dr. Monika Zawadzka, Prof. Izabela Naydenova</u>	
Ge₂₄.9Sb₁₁.6S₆₃.5 thin films aged under various conditions	19
<u>Mr. Petr Kutálek, Mr. Petr Knotek, Ms. Eva Černošková, Mr. Ludvík Beneš, Mr. Petr Janíček</u>	
Metawire	20
<u>Dr. Alexey Tishchenko, Mr. Maxim Anokhin, Prof. Mikhail Strikhanov</u>	
Towards fabrication of high-precision microlens arrays for LED-based optoelectronic devices	21
<u>Ms. Daria Bezshlyakh, Mr. Benjamin Pogoda, Mr. Jannick Langfahl, Dr. Uwe Brand, Dr. Hutomo Suryo Wasisto, Prof. Andreas Waag</u>	
Investigation Of Crystal Growth And properties of 2 at%(Ln³⁺) Doped LiGd(WO₄)₂ with Ln; Eu, Er and Tm	23
<u>Dr. Brahim Rekik, Dr. Kheirreddine Lebbou, Prof. Mourad Derbal</u>	
Propagation of light beams in microstructured nematic liquid crystals	24
<u>Mrs. Volha Kabanava, Dr. Elena Melnikova, Dr. Alexei Tolstik</u>	
Integrated on-chip localized surface plasmon resonances in a subwavelength periodic array of gold nanowires	25
<u>Dr. Ricardo Tellez-Limon, Dr. Rafael Salas-Montiel, Dr. Victor Coello, Dr. Sylvain Blaize</u>	
Efficient detection of rare cells using CMOS-based low-cost quantum dot camera	27
<u>Mr. Kevin Huang, Mr. Benjamin Ding, Dr. Zhimin Ding</u>	
Active Hybrid Hydrogel-Metallic Nanostructures for Plasmonic Biosensor Applications	28
<u>Mr. Nestor Gisbert Quilis, Mr. Marcel van Dongen, Mr. Christian Petri, Prof. Ulrich Jonas, Prof. Wolfgang Knoll, Prof. Martin Möller, Dr. Ahmed Mourran, Dr. Jakub Dostalek</u>	
H⁺ ions beam irradiation-induced interconnections between Ni-NWs for transparent conducting electrodes	29
<u>Ms. Shehla Honey</u>	
Rational design of nanoscale building blocks: silver and gold D_{5h} nanostructures for sensing applications	30
<u>Ms. Nicole Ritter, Dr. Jennifer Chen, Dr. Vladimir Kitaev</u>	
Dynamics and kinetics study of individual QD at UME surface	31
<u>Mr. Abdallatif Alshalfouh</u>	
Organic microcavity laser based on high gain monolayer	32
<u>Dr. Alexander Palatnik, Dr. Hagit Aviv, Dr. Yaakov Tischler</u>	
Nonlocality in metallo-dielectric nanostructures	33
<u>Dr. Antoine Moreau, Mr. Armel Pitelet, Prof. Emmanuel Centeno, Mr. Nikolai Schmitt, Dr. Stéphane Lanteri, Dr. Claire Scheid</u>	
Super-resolution photoluminescence microspectroscopy of individual metal-halide perovskite nanowires: defect-induced local variation of crystal phase transition temperature	34
<u>Dr. Alexander Dobrovolsky, Dr. Aboma Merdasa, Dr. Eva Unger, Prof. Arkady Yartsev, Prof. Ivan Scheblykin</u>	
Optical spirals and Möbius strips on all-dielectric optical antennas	35
<u>Dr. Aitzol Garcia-Etxarri</u>	

Optical properties of Ag nanocap decorated SiO₂ opal plasmonic photonic crystals and their applications	36
<u>Prof. Hung-Chih Kan, Mr. Ti-Li Lin, Mr. Jiun-Hong Lin, Mr. Jian-Hung Chu</u>	
Local Charge Transfer and Enhanced Light Emission of Monolayer MoS₂ Hybridized with Copper Phthalocyanine Nanoparticles	37
<u>Mr. Ganesh Ghimire, Mr. Shrawan Roy, Mr. Subash Adhikari, Mr. Dinh Hoa Loung, Mr. Jinbao Jiang, Mr. Hyun Kim, Dr. Seong Gi Jo, Prof. Young Hee Lee, Prof. Jinsoo Joo, Prof. Jeongyong Kim</u>	
Hybrid plasmonic - all-dielectric nanodimers for second-harmonic generation	38
<u>Dr. Mihail Petrov, Mrs. Flavia Timpu, Dr. Nicholas R. Hendricks, Dr. Songbo Ni, Dr. Claude Renaut, Dr. Heiko Wolf, Prof. Lucio Isa, Prof. Yuri Kivshar, Prof. Rachel Grange</u>	
Extreme nonlinear optical phenomena enabled by plasmons in nanostructured graphene	40
<u>Dr. Joel Cox, Prof. Javier Garcia De Abajo</u>	
Dynamics of ultra small semiconductor lasers	41
<u>Prof. FREDERIC GRILLOT, Mr. Jean-maxime Sarraute, Dr. Kevin Schires, Prof. Sophie Larochelle</u>	
Bispectral second-harmonic-generation in snake-shaped AlGaAs nanowires	42
<u>Ms. Natália Morais, Dr. Marco Ravaro, Dr. Iannis Roland, Dr. Aristide Lemaitre, Prof. Stefan Wabnitz, Dr. Maurizio De Rosa, Dr. Ivan Favero, Prof. Giuseppe Leo</u>	
Electrostatic SHG from extreme nano-sized bi-metal structures	43
<u>Mr. Shlomo Levi, Dr. Avi Niv</u>	
Mid-Infrared Second Harmonic Spectroscopy of Tunable Phonon Polaritons in Atomic Scale Heterostructures	45
<u>Mr. Christopher Winta, Mr. Nikolai C Passler, Dr. Ilya Razdolski, Prof. Martin Wolf, Prof. Joshua D Caldwell, Dr. Alexander Paarmann</u>	
Spectroscopy of single gold nanoparticles reveals strong heterogeneity in the kinetics of ssDNA functionalization	46
<u>Mr. Matěj Horáček, Dr. Rachel E. Armstrong, Dr. Peter Zijlstra</u>	
Single protein detection by aptamer-labeled gold nanorods	47
<u>Dr. Rachel E. Armstrong, Dr. Peter Zijlstra</u>	
Plasmonic fluorescence enhancement for single-molecule electrochemistry	48
<u>Dr. Martin Caldarola, Ms. Weichun Zhang, Ms. Biswajit Pradhan, Prof. Michel Orrit</u>	
Improved Sensitivity of Optical Polarimetry with MEMS Machining and Microfluidics	50
<u>Mrs. Maab Al-hafidh, Dr. Andrew Glidle, Dr. Anthony Kelly, Dr. Julien Reboud, Prof. Jonathan Cooper</u>	
Surface Enhanced Raman Spectroscopy Assisted With Photonic Crystal	52
<u>Prof. Xiangwei Zhao</u>	
Plasmonic color-graded nanosystems with achromatic sub-wavelength architectures for light filtering and advanced SERS detection	53
<u>Dr. Francesco Bisio, Dr. Remo Proietti Zaccaria, Dr. Andrea Toma, Dr. Gobind Das, Prof. Enzo Di Fabrizio, Dr. Francesco De Angelis, Prof. Maurizio Canepa</u>	

Near field imaging of a nanofiber	54
<u>Dr. Vivien Loo</u> , Mr. Guillaume Blanquer, Mr. Maxime Joos, Dr. Quentin Glorieux, Dr. Yannick De Wilde, Dr. Valentina Krachmalnicoff	
Surface enhanced infrared absorption with highly doped InAsSb plasmonic nano-antenna arrays	56
Ms. Franziska Barho, Dr. Maria Jose Milla, Mr. Mario Bomers, <u>Dr. Fernando Gonzalez-Posada Flores</u> , Dr. Laurent Cerutti, Prof. Eric Tournié, Prof. Thierry Taliercio	
Enhanced molecular vibrational spectroscopy with phononic boron nitride antennas	58
<u>Dr. Marta Autore</u> , Dr. Peining Li, Ms. Irene Dolado, Mr. Francisco Javier Alfaro-Mozaz, Dr. Rubèn Esteban, Ms. Ainhoa Atxabal, Prof. Felix Casanova, Prof. Luis Hueso, Dr. Pablo Alonso González, Prof. Javier Aizpurua, Dr. Saül Velez, Dr. Alexey Nikitin, Prof. Rainer Hillenbrand	
Plasmonic sensing of single particle catalysis	60
<u>Dr. Su Liu</u> , Mrs. Svetlana Alekseeva, Mr. Ferry Nugroho, Dr. Lars Hellberg, Prof. Christoph Langhammer, Dr. Arturo Susarrery-arce	
Vibrational strong light-matter coupling using a wavelength tunable mid-Infrared open microcavity	61
Mr. Omree Kapon, <u>Dr. Yaakov Tischler</u>	
Gap plasmon resonance in electromagnetically-actuated nanomechanical silicon nitride strings	62
<u>Dr. Nicolas Cazier</u> , Mr. Pedram Sadhegi, Dr. Mostafa Shawrav, Mr. Andreas Steiger-Thirsfeld, Prof. Silvan Schmid	
Dielectric Resonator Antenna for Large Volume Microwave Magnetic Coupling to NV Centers in Diamond	63
<u>Dr. Polina Kapitanova</u> , Mr. Vladimir Soshenko, Mr. Vadim Vorobyov, Mr. Dmitry Dobrykh, Dr. Ilya Shadrivov, Prof. Pavel Belov, Prof. Alexey Akimov	
Quantum Emitters in Hexagonal Boron Nitride Have Spectrally Tunable Quantum Efficiency	65
<u>Dr. Mikael Svedendahl</u> , Dr. Andreas Schell, Prof. Romain Quidant	
CMOS-based low-cost quantum dot camera for fast and efficient molecular detection	66
<u>Dr. Zhimin Ding</u> , Dr. Aihua Fu	
Photonic Structuring of Colloidal Quantum-Dot Assemblies	67
<u>Dr. Ferry Prins</u>	
Dielectric leaky-wave nanoantennas for highly directional emission of light	68
<u>Prof. Jens Förstner</u> , Dr. Andre Hildebrandt, Prof. Thomas Zentgraf, Mr. Manuel Peter, Mr. Christian Schlickriede, Ms. Kimia Gharib, Prof. Stefan Linden	
Control of spontaneous emission rate in luminescent resonant diamond particles	70
<u>Dr. Roman Savelev</u> , Ms. Anastasiia Zalogina, Dr. Sergey Makarov, Dr. Dmitriy Zuev, Dr. Ilya Shadrivov	
Designer bulk plasmon polariton modes in hyperbolic metamaterials for sensing applications	71
<u>Dr. Tommi Isoniemi</u> , Dr. Nicolò Maccaferri, Ms. Sara Perotto, Prof. Michael Hinczewski, Prof. Giuseppe Strangi, Dr. Francesco De Angelis	
High-Efficiency Asymmetric Transmission of Circularly Polarized THz waves using a Dielectric Herringbone Metasurface	72
<u>Dr. Mitchell Kenney</u> , Mr. Shaoxian Li, Dr. Xueqian Zhang, Dr. Teun-teun Kim, Mr. Dongyang Wang, Dr. Dongmin Wu, Prof. Chunmei Ouyang, Prof. Jiaguang Han, Prof. Weili Zhang, Prof. Hong-bo Sun, Prof. Shuang Zhang	

Directional and singular surface plasmon generation in chiral and achiral nanostructures demonstrated by leakage radiation microscopy	74
<u>Ms. Aline Pham, Dr. Quanbo Jiang, Dr. Martin Berthel, Dr. Serge Huant, Prof. Joel Bellessa, Dr. Cyriaque Genet, Dr. Aurelien Drezet</u>	
Controlling Thermal Radiation Signatures using Materials Designed by Transformation Optics Theory	75
<u>Mr. ahmed Alwakil, Dr. Myriam Zerrad, Dr. Claude Amra</u>	
Hybrid optical surface waves supported by resonant anisotropic metasurfaces	76
<u>Dr. Dmitry Permyakov, Mr. Oleh Yermakov, Dr. Andrey Bogdanov, Dr. Anton Samusev, Dr. Ivan Mukhin, Mr. Ivan Sinev, Dr. Radu Malureanu, Dr. Osamu Takayama, Dr. Ivan Iorsh, Prof. Andrei Lavrinenko</u>	
Zero-index media: a loophole in effective medium theories	77
<u>Dr. Iñigo Liberal, Dr. Yue Li, Prof. Nader Engheta</u>	
Moving from Single Molecules to Controlled Cooperative Systems in Quantum Nano-Optics	78
<u>Prof. Vahid Sandoghdar</u>	
Chiral Nanophotonics and Quantum Optics	79
<u>Prof. Arno Rauschenbeutel</u>	
Polaritons for Chemistry and Materials Science	80
<u>Prof. Francisco Garcia-Vidal</u>	
Engineering light propagation with planar or conformable optical metasurfaces	81
<u>Dr. Patrice Genevet</u>	
Intrinsic emergence of optical spin-orbit interaction at the nanoscale	82
<u>Mr. J. Enrique Vázquez-Lozano, Dr. Alejandro Martínez</u>	
Synthesis and characterization of host material for phosphorescent organic light emitting diodes (PHOLEDs)	83
<u>Mr. Ji Su An, Prof. Choon Woo Lim</u>	
Dirac points manipulation using linear laser in Floquet crystals for Graphene superlattices	84
<u>Mrs. Shahd Alfadhli, Prof. Sergey Saveliev, Prof. Feo Kusmartsev</u>	
Optical Parameters of GaInAsSb Laser Diodes and Its Application for Carbon Monoxide Detection	86
<u>Mr. Dzmitry Kabanau, Dr. Yahor Lebiadok</u>	
Performance enhancement of bidirectional TWDM-PON by Rayleigh backscattering mitigation	87
<u>Mr. Ibrahim Elewah, Ms. Martina Kalds, Prof. Moustafa Aly</u>	
Universal description of 2D channel plasmons: from graphene and beyond	90
<u>Mr. Paulo André Gonçalves, Mr. Eduardo Dias, Prof. Sanshui Xiao, Prof. Mikhail Vasilevskiy, Prof. Sergey I. Bozhevolnyi, Prof. Nuno Peres, Prof. N. Asger Mortensen</u>	
Broadband bidirectional optical cloaking by a generalized Hilbert transform	91
<u>Mr. Zeki Hayran, Dr. Ramon Herrero, Dr. Muriel Botey, Prof. Kestutis Staliunas, Dr. Hamza Kurt</u>	
Dispersion relations for electromagnetic surface waves on the boundary vacuum- metamaterial	93
<u>Ms. Olga Porvatkina, Dr. Alexey Tishchenko, Prof. Mikhail Strikhanov</u>	

Color-selective diffractive optical components based on composite multilayer structures including phase-change materials	94
<u>Mr. Chi-Young Hwang, Dr. Yong-Hae Kim, Dr. Gi Heon Kim, Mr. Won-Jae Lee, Mr. Han Byeol Kang, Dr. Jong-Heon Yang, Mr. Jae-Eun Pi, Mr. Ji Hun Choi, Dr. Kyunghye Choi, Mrs. Hee-Ok Kim, Dr. Chi-Sun Hwang</u>	
Effect of plasmonic gold nanoparticles morphology and silica layer on efficient light induced carbon dioxide photo-conversion to formic acid in whole solar spectrum region	96
<u>Dr. Dinesh Kumar, Ms. Ji Yeon Lee, Prof. Chan Hee Park, Prof. Cheol Sang Kim</u>	
Measuring Quantum Yield of Perylene Bisimide Dyes by Lifetime Modifications Using a Metal Ball	97
<u>Mr. Ersan Özelci, Prof. Ute Resch-Genger, Prof. Oliver Benson</u>	
Fractal Metasurface Absorbers with Octave-Spanning Bandwidth	99
<u>Dr. Mitchell Kenney, Dr. James Grant, Dr. Yash Shah, Dr. Ivonne Escorcia-carranza, Mr. Mark Humphreys, Prof. David Cumming</u>	
Plasmon-enhanced fluorescence biosensor utilizing metallic nanostructures and responsive hydrogel binding matrix	101
<u>Ms. Simone Hageneder, Mr. Stefan Fossati, Mr. Christian Petri, Prof. Ulrich Jonas, Prof. Wolfgang Knoll, Dr. Jakub Dostalek</u>	
Super-resolution optical imaging of nanostructures using SMAL (Super-resolution Microsphere Amplifying Lens)	102
<u>Dr. Sorin Laurentiu Stanescu, Dr. Sébastien Vilain, Mr. Valerio Galieni, Dr. George Goh, Ms. Katarzyna Karpinska, Mr. Chao Wei, Mr. Alex Sheppard, Mr. Steve Wright, Dr. Wei Guo, Prof. Lin Li</u>	
KeV Argon Ions Beam Irradiation Induced Changes in Optical Properties of Ni-NWs	103
<u>Ms. Shehla Honey, Dr. Shahzad Naseem, Dr. Ahmad Ishaq, Dr. Malik Maaza</u>	
Interface defects and silicon impurities in AlGaAs/GaAs heterostructures and its relationship to registration efficiency of quantum well infrared photodetector	104
<u>Dr. Yahor Lebiadok, Ms. Alena Shalayeva</u>	
Thermal Dynamics of Xanthene Dye in Polymer Matrix Excited by Two-Photon Laser Radiation	105
<u>Dr. Iliia Samusev, Mr. Rodion Borkunov, Mr. Maksim Tsarkov, Ms. Elizaveta Konstantinova, Prof. Yury Antipov, Dr. Maksim Demin, Prof. Valery Bryukhanov</u>	
Anomalous Hall effect and magnetic properties of GaMnSb thin films grown by DC Magnetron co-Sputtering for spintronics applications	106
<u>Prof. Fredy Mesa, Dr. Jorge Calderon, Prof. Anderson Dussan, Prof. Rafael Gonzalez-hernandez</u>	
Colour Gamut Enhancement with Remote Light Conversion Mechanism	107
<u>Dr. Devrim Koseoglu, Mr. Emrah Bakan, Mr. Kivanc Karsli, Mr. Yusuf Sinan Sezer</u>	
Numerical Analysis of Microstructured Optical Fiber for Applications in SPR Sensing	108
<u>Mr. Arthur Aprígio De Melo, Ms. Márcia Fernanda Da Silva Santiago, Ms. Talita Brito Da Silva, Prof. Rossana Moreno Santa Cruz, Prof. Cleumar da Silva Moreira</u>	
Intersubband-surface-plasmon-polaritons in all-semiconductor planar plasmonic resonators	109
<u>Prof. Mirosław Zaluzny</u>	

Ratiometric Sensor for Levodopa Detection Based on Quenching Effect of Polylevodopa Nanoparticles on the Fluorescence Intensity of CdTe Quantum Dots	110
<u>Mr. Ahmad Moslehi Pour, Dr. Mohammad Reza Hormozi-nezhad</u>	
Study of efficient energy transfer depending on Zn-porphyrin compound ratio in pyrene based metal-organic frameworks by time-resolved spectroscopy	112
<u>Mr. Ganesh Ghimire, Mr. Changwon Seo, Mr. Jubok Lee, Mr. Kyoung Chul Park, Prof. Chang Yeon Lee, Prof. Jeongyong Kim</u>	
Selective control of reconfigurable plasmonic metamolecules	113
<u>Prof. Anton Kuzyk</u>	
Graphene-based random metalasers	114
<u>Dr. Andrea Marini, Prof. Javier Garcia De Abajo</u>	
Terahertz light emission and lasing in graphene-based heterostructure 2D material systems -theory and experiments	115
<u>Prof. Taiichi Otsuji</u>	
Optical rotation in chiral van der Waals stacks.	117
<u>Mr. Dmitrii Kazanov, Mr. Alexander Poshakinskiy, Dr. Tatiana Shubina, Dr. Sergey Tarasenko</u>	
Tamm plasmon/surface plasmon mode beating for spatially controlled plasmon generation	118
<u>Dr. Clementine Symonds, Dr. Jean-michel Benoit, Prof. Pascale Senellart, Dr. Aristide Lemaitre, Prof. Jean-Jacques Greffet, Dr. Christophe Sauvan, Prof. Joel Bellessa</u>	
Near Unity Transmission and Full Phase Control with Huygens' Dielectric Metasurfaces based on Cuboid Shape Silicon Nanoresonators	119
<u>Dr. Xinan Liang, Dr. Ramon Paniagua-dominguez, Dr. Yefeng Yu, Dr. Yuan Hsing Fu, Dr. Arseniy Kuznetsov</u>	
Revealing the spectral response of a plasmonic structure using tunnel electrons	121
<u>Dr. Eric Le Moal, Mrs. Shuiyan Cao, Dr. Aurelien Drezet, Dr. Serge Huant, Prof. Jean-Jacques Greffet, Dr. Jean-Paul Hugonin, Dr. Gérald Dujardin, Dr. Elizabeth Boer-Duchemin</u>	
Quantum Dynamics of an Interacting Electron Gas in a Nanosphere	123
<u>Ms. Alexandra Crai, Dr. Andreas Pusch, Dr. Doris E Reiter, Prof. Tilmann Kuhn, Prof. Ortwin Hess</u>	
Nanomechanical 2D-scanning photothermal microscopy for analysis and imaging of single sub-10 nm nanoparticles	124
<u>Ms. Miao-Hsuan Chien, Prof. Silvan Schmid</u>	
Controlling On-chip Optical Radiation with All-Dielectric Antennas: Reconfigurable Interconnects and Lab-on-a-chip Devices	126
<u>Mr. Sergio Lechago, Dr. Carlos Garcia-Meca, Prof. Javier Marti</u>	
Nanostructured silica based optical coatings for high power laser systems	129
<u>Dr. Tomas Tolenis, Ms. Lina Grinevičiūtė, Dr. Andrius Melninkaitis, Dr. Rytis Buzelis, Ms. Lina Mažulė</u>	
Enhancement of optical micro-cavity effect coupled with surface plasmon in an organic light emitting device with nanosized multi-cathode structure	130
<u>Prof. Akiyoshi Mikami</u>	

Fano resonances in Al-based multilayer structures	132
Prof. Shinji Hayashi, Mr. Yudai Fujiwara, Mr. KANG BYUNGJUN, Prof. Minoru Fujii, Dr. Dmitry Nesterenko, Prof. Zouheir Sekkat	
Nanoscale Precision Design of Metal Catalysts Using Plasmonic Nanoreactors	133
Ms. Evgenia Kontoleta, Dr. Sven Askes, Dr. Erik Garnett	
Optical properties of GaP/Si active microdisks containing InGaAs/GaP quantum dots	135
Mr. Ronan Tremblay, Mr. Tony Rohel, Dr. Yoan Léger, Dr. Alain le corre, Dr. Rozenn Bernard, Dr. Nicolas Bertru, Prof. Olivier Durand, Dr. Charles Cornet	
Measuring the directional Local Density of States (LDOS) of quantum and classical plasmons using near-field scanning optical microscopy	136
Dr. Aurelien Drezet, Dr. Martin Berthel, Ms. Aline Pham, Dr. Quanbo Jiang, Dr. Serge Huant, Prof. Joel Bellessa, Dr. Cyriaque Genet	
Modification of Förster Resonance Energy Transfer using Plasmonic Nanogaps	137
Mr. <u>Abdullah Hamza</u> , Mr. Francesco Narda Viscomi, Dr. Jean-Sebastien G. Bouillard, Dr. Ali M. Adawi	
Characterization of the wavelength-dependent coupling function from nitrogen-vacancy fluorescence into surface plasmon polaritons	139
Dr. Cesar E. Garcia-Ortiz, Dr. Victor Coello, Dr. Shailesh Kumar, Prof. Sergey I. Bozhevolnyi	
Enhancement and Inhibition of Spontaneous Photon Emission by dielectric photonic antennas	140
Dr. Mathieu Mivelle, Mr. Dorian Bouchet, Dr. Julien Proust, Dr. Bruno Gallas, Dr. Igor Ozerov, Prof. Maria Garcia-parajo, Dr. Yannick De Wilde, Dr. Nicolas Bonod, Dr. Valentina Krachmalnicoff, Dr. Sebastien Bidault	
Plasmon-exciton coupling evolution by dynamic molecular aggregation	142
Dr. Francesco Todisco, Dr. Milena De Giorgi, Mr. Marco Esposito, Dr. Luisa De Marco, Ms. Alessandra Zizzari, Dr. Monica Bianco, Dr. Lorenzo Dominici, Dr. Dario Ballarini, Dr. Valentina Arima, Prof. Giuseppe Gigli, Dr. Daniele Sanvitto	
Exploring electron induced photon radiation in plasmonic nanostructures by angle and polarization-resolved cathodoluminescence spectroscopy	143
Dr. Viktor Myroshnychenko, Prof. Javier García de Abajo, Prof. Jens Förstner, Prof. Naoki Yamamoto	
Magneto-optics of single-molecule magnets with optical nanoantennas	145
Dr. Francesco Pineider, Dr. Addis Mekonnen Adamu, Dr. Michele Serri, Dr. Valentina Bonanni, Dr. Giulio Campo, Dr. Matteo Mannini, Dr. Cesar De Julián Fernández, Dr. Claudio Sangregorio, Prof. Massimo Gurioli, Prof. Alexandre Dmitriev, Prof. Roberta Sessoli	
Active control of transmission and helicity of nanostructured optical beams via magnetoplasmonic vortex lens	147
Dr. <u>Nicolò Maccaferri</u> , Dr. Yuri Gorodetski, Dr. Pierfrancesco Zilio, Dr. Francesco De Angelis, Dr. Denis Garoli	
GaSb oxidation for plasmonic enhanced mid-IR molecular spectroscopy	149
Mr. Mario Bomers, Ms. Franziska Barho, Dr. Aude Mezy, Dr. Maria Jose Milla, Dr. Laurent Cerutti, Dr. Fernando Gonzalez-Posada Flores, Prof. Eric Tournié, Prof. Thierry Taliercio	
Holographic reconstruction via sub-wavelength aperture tips	151
Dr. Nancy Rahbany, Dr. Ignacio Izeddin, Dr. Valentina Krachmalnicoff, Prof. Rémi Carminati, Prof. Gilles Tessier, Dr. Yannick De Wilde	

Nanometre scale monitoring of the quantum confined stark effect and emission efficiency droop in multiple GaN/AlN quantum disks in nanowires	153
<u>Prof. Luiz Fernando Zagonel, Dr. Luiz Tizei, Mr. Gabriel Vitiello, Dr. Gwénolé Jacopin, Dr. Lorenzo Rigutti, Dr. Maria Tchernycheva, Dr. Francois Julien, Dr. Rudeesun Songmuang, Dr. Tomas Ostasevicius, Dr. Francisco De La Peña, Dr. Caterina Ducati, Prof. Paul Midgley, Dr. Mathieu Kociak</u>	
Second harmonic generation in AlGaAs nanodisk dimers	155
<u>Mr. Valerio Flavio Gili, Mr. Davide Rocco, Dr. Lavinia Ghirardini, Dr. Luca Carletti, Prof. Andrea Locatelli, Dr. Michele Celebrano, Prof. Marco Finazzi, Prof. Costantino De Angelis, Dr. Aristide Lemaitre, Dr. Ivan Favero, Prof. Giuseppe Leo</u>	
Active near-field probe based on ultrabroadband hot luminescence of Si/Au nanoparticle	156
<u>Dr. Anton Samusev, Dr. Sergey Makarov, Mr. Ivan Sinev, Dr. Valentin Milichko, Mr. Filipp Komissarenko, Dr. Dmitry Zuev, Dr. Elena Ushakova, Dr. Ivan Mukhin, Dr. Yefeng Yu, Dr. Arseniy Kuznetsov, Dr. Pavel Belov, Dr. Ivan Iorsh, Dr. Alexander Poddubny, Prof. Yuri Kivshar</u>	
Generation of continuous terahertz wave by differential-frequency-mixing in a GaAs/AlAs multiple quantum well	158
<u>Prof. Osamu Kojima, Mr. Yuki Tarui, Prof. Takashi Kita, Mrs. Avan Majeed, Dr. Edmund Clark, Dr. Pavlo Ivanov, Prof. Richard Hogg</u>	
Mid-infrared nonlinear polaritonics using surface phonon polaritons	160
<u>Dr. Christopher Gubbin, Dr. Simone De Liberato</u>	
Second Harmonic generation from an array of gold nanocylinders up to a single nanocylinder.	162
<u>Dr. christian jonin, Prof. Pierre-françois Brevet, Dr. Emeric Bergmann, Prof. Pierre-michel Adam, Dr. Anne-laure Baudrion, Dr. Sergei Kochtcheev</u>	
PT-axisymmetric VCSELS	164
<u>Mr. Waqas W. Ahmed, Dr. Muriel Botey, Dr. Ramon Herrero, Prof. Kestutis Staliunas</u>	
Biocompatible Random Lasers for Biosensing	165
<u>Ms. Soraya Caixeiro, Dr. Michele Gaio, Dr. Van Duong Ta, Dr. Benedetto Marelli, Prof. Fiorenzo Omenetto, Dr. Francisco Fernandes, Dr. Riccardo Sapienza</u>	
Designing Gold Nanoparticles for Photothermal Therapy & Multimodal Therapeutic Strategies	166
<u>Mr. emre doruk önal, Prof. Kaan Guven</u>	
Nanostructured Color Filter based Wearable Optobiomedical Sensor for Non-invasive Diagnosis	167
<u>Mr. Wenze Wu, Mr. Gregor Scholz, Mr. Jan Gülink, Ms. C.b. Rojas Hurtado, Dr. Joan Daniel Prades, Prof. Stefanie Kroker, Prof. Rainer Macdonald, Dr. Hutomo Suryo Wasisto, Prof. Andreas Waag</u>	
Optical scattering and microscopic imaging of cellular exo- and endocytosis	168
<u>Mr. Dylan Marques, Dr. Adelaide Miranda, Prof. Ana G. Silva, Dr. Peter Munro, Dr. Pieter De Beule</u>	
Super-resolution imaging of single-molecule DNA interactions with plasmonic nanoparticles	170
<u>Dr. Adam Taylor, Dr. Peter Zijlstra</u>	
Propagation Characteristics of Myelinated and Un-myelinated Nerve Fibres in guiding 200 nm to 2000 nm EM Wave	172
<u>Dr. Enayetur Rahman, Dr. Iasonas F. Triantis</u>	

Dielectric and semiconductor nanoantennas	174
<u>Dr. Arseniy Kuznetsov</u>	
Integrating Nanofluidics with Single Particle Plasmonics	175
<u>Prof. Christoph Langhammer</u>	
Exploring the Nanoscale Dynamics of Single Molecules with Optical Microcavities	176
<u>Prof. Frank Vollmer</u>	
Metasurfaces with Nonlinear Berry Phases in Space and Time	177
<u>Prof. Thomas Zentgraf</u>	
Properties of CaF₂ ceramics obtained by Hot Isostatic Pressing	178
<u>Dr. Krzysztof Perkowski</u> , <u>Dr. Magdalena Gizowska</u> , <u>Ms. Izabela Kobus</u> , <u>Dr. Milena Zalewska</u> , <u>Mr. Gustaw Konopka</u> , <u>Mrs. Irena Witosławska</u> , <u>Dr. Marcin Osuchowski</u>	
Optical bound state in the continuum in the one-dimensional photonic structures: transition into a resonant state	180
<u>Ms. Zarina Sadrieva</u> , <u>Mr. Ivan Sinev</u> , <u>Mr. Kirill Koshelev</u> , <u>Dr. Anton Samusev</u> , <u>Dr. Osamu Takayama</u> , <u>Dr. Radu Malureanu</u> , <u>Dr. Andrey Bogdanov</u> , <u>Prof. Andrei Lavrinenko</u>	
Plasmonic nanohole arrays with thermo-responsive hydrogel for flow-through biosensor	182
<u>Mrs. Daria Kotlarek</u> , <u>Dr. Jakub Dostalek</u>	
Powerful Laser Diode Matrixes for Active Vision Systems	183
<u>Mr. Denis Shabrov</u> , <u>Dr. Boris Kuntsevich</u>	
Numerical investigation of plasmonic metasurfaces for improved MIR absorption	185
<u>Dr. Roxana Tomescu</u> , <u>Dr. Cristian Kusko</u> , <u>Dr. Mihai Kusko</u>	
Application of luminescent converters for the correction of the spectra of white LEDs	186
<u>Dr. Piotr Pershukevich</u> , <u>Dr. Pavich Tatsiana</u> , <u>Dr. Viktoria Lapina</u>	
Fabrication and characterization of plasmonic gold Sierpinski nanocarpets	187
<u>Mr. Nikhil Santh Puthiya Purayil</u> , <u>Dr. Francesco De Nicola</u> , <u>Mr. Mario Miscuglio</u> , <u>Dr. Davide Spirito</u> , <u>Dr. Andrea Tomadin</u> , <u>Dr. Francesco Tantussi</u> , <u>Dr. Francesco De Angelis</u> , <u>Dr. Marco Polini</u> , <u>Dr. Roman Krahne</u> , <u>Dr. Vittorio Pellegrini</u>	
Evaporated anisotropic nano-structured coatings for polarization control in high-power lasers	189
<u>Ms. Lina Grinevičiūtė</u> , <u>Mr. Laurynas Petronis</u> , <u>Dr. Rytis Buzelis</u> , <u>Dr. Tomas Tolenis</u>	
Structural and optical properties of silver-doped gold clusters AgAun-1 (n=1-8): a comparison with pure gold clusters	190
<u>Dr. Mohand Akli TAFOUGHALT</u>	
Hydrogel-based plasmonic sensor system	191
<u>Mr. Christoph Kroh</u> , <u>Mr. Roland Wuchrer</u> , <u>Dr. Margarita Günther</u> , <u>Prof. Gerald Gerlach</u> , <u>Dr. Thomas Härtling</u>	
Synthesis of meta-atoms and bottom-up fabrication of three-dimensional plasmonic nanostructures	192
<u>Ms. Rossella Grillo</u> , <u>Prof. Thomas Buergi</u>	
GaN/AlN Interface Characteristics in Presence of Point Defects	194
<u>Dr. Yahor Lebiadok</u> , <u>Dr. Tatyana Bezyazychnaya</u> , <u>Dr. Ivan Alexandrov</u> , <u>Dr. Konstantin Zhuravlev</u>	

Microstructure control of yttria nanopowders obtained by solution combustion synthesis	196
<u>Dr. Magdalena Gizowska, Ms. Izabela Kobus, Dr. Krzysztof Perkowski, Dr. Milena Zalewska, Mr. Gustaw Konopka, Mrs. Irena Witosławska, Dr. Marcin Osuchowski</u>	
Micro-Photoluminescence Mapping for evaluation of the Surface Plasmon Enhanced Emissions	198
<u>Mr. Kazutaka Tateishi, Dr. Pangpang Wang, Dr. Sou Ryuazki, Prof. Mitsuru Funato, Prof. Yoichi Kawakami, Prof. Koichi Okamoto, Prof. Kaoru Tamada</u>	
UV controlled optical properties of polymer porous PET films filled with a liquid crystal	200
<u>Dr. Dina Shmeliova, Prof. Sergey Pasechnik, Dr. Alex Dubtsov, Mr. Sergey Trifonov</u>	
Contribution of type II quantum dot InAlAs/AlGaAs to enhance solar cell performance	201
<u>Dr. Rim Neffati</u>	
Hexagonal Metamaterial Filter On and Off Embedded Metallic Inclusion for Microwave Applications	202
<u>Dr. toto saktioto, Mr. Romi Fadli Syahputra, Mr. Mohammad Fandi Kurnia</u>	
Superiority of localized surface plasmon resonance technique in characterization of ultra-thin metallic films	203
<u>Mr. Sudheer ., Ms. P Tiwari, Ms. S Bhartiya, Dr. C Mukherjee, Dr. S. K. Rai, Dr. A. K. Sinha, Dr. V. N. Rai, Dr. A. K. Srivastava</u>	
3D Simulations of Spatially Dispersive Metals with a Finite Element Time Domain Method	205
<u>Mr. Nikolai Schmitt, Dr. Stéphane Lanteri, Dr. Claire Scheid</u>	
Solution combustion synthesis as a method of YAG nanopowders obtaining	206
<u>Dr. Milena Zalewska, Dr. Magdalena Gizowska, Ms. Izabela Kobus, Dr. Krzysztof Perkowski, Mr. Gustaw Konopka, Mrs. Irena Witosławska, Dr. Marcin Osuchowski</u>	
Synthesis and characterization of new host molecules available as red phosphorescent OLED host material	208
<u>Mr. Dae Ryun Kwon, Prof. Choon Woo Lim</u>	
Optical Perturbation of Atoms in weak localization	209
<u>Dr. Afifa Yedjour</u>	
Simple and Rapid Detection of L-Dopa Based on in Situ Formation of Polylevodopa Nanoparticles	210
<u>Mr. Ahmad Moslehi Pour, Dr. Mohammad Reza Hormozi-nezhad</u>	
Hot-carrier Dynamics in Photoexcited Gold Nanostructures: Analysis of Plasmon Excitation, Interband Transitions and Ballistic Transport	212
<u>Dr. Giulia Tagliabue, Mr. Adam Jermyn, Prof. Ravishankar Sundararaman, Ms. Alex Welch, Dr. Joseph Du Chene, Dr. Ragip Pala, Dr. Artur Davoyan, Dr. Prineha Narang, Prof. Harry Atwater</u>	
Solid state ITO Au-NPs TiO₂ plasmonic based solar cells	213
<u>Mr. Adam Ginsburg, Dr. Assaf Y. Anderson, Prof. Arie Zaban</u>	
Low-loss Adiabatic Dielectric-Plasmonic Hybrid Waveguide for HAMR Applications	214
<u>Mr. Chuan Zhong, Mr. Brian Jennings, Mr. Patrick Flanigan, Mr. Frank Bello, Mr. Nicolás Abadía, Ms. Gwenael Acheson, Mr. Richard Hobbs, Mr. David McCloskey, Mr. John Donegan</u>	
Microspectroscopy of plasmonic crystal cavity by cathodoluminescence STEM	216
<u>Dr. Hikaru Saito, Prof. Naoki Yamamoto</u>	

UV light driven synthesis of plasmonic nanoparticles on ceria support: optimisation and potential applications in photocatalysis	217
<u>Mrs. Eva Raudonyte-Svirbutaviciene, Dr. Arturas Katelnikovas</u>	
Analytical Investigation of In-plane Focusing Surface Plasmon Modes by a Dielectric Lens	219
<u>Ms. Fahimeh Armin, Prof. Mir Mojtaba Mirsalehi</u>	
Subnanometric control of the coherent coupling between a single molecule and a plasmonic nanocavity	220
<u>Dr. Yao Zhang, Dr. Qiu-shi Meng, Dr. Yang Zhang, Mr. Yang Luo, Mr. Yun-jie Yu, Mr. Li Zhang, Dr. Ruben Esteban, Prof. Zhen-chao Dong, Prof. Javier Aizpurua</u>	
All optical band engineering of Dirac materials	221
<u>Mr. Kevin DINI, Dr. Ivan Iorsh, Prof. Oleg Kibis, Prof. Ivan Shelykh</u>	
Guided mode resonance enhanced upconversion fluorescence of rare earth nanoparticles in aqueous solution using a low refractive index resonant waveguide grating	223
<u>Prof. C. C. Hsu, Mr. V. D. Vu, Mr. H. W. Chiu, Ms. R. Nababan, Prof. Q. M. Le, Prof. S. W. Kuo, Prof. L. K. Chau, Prof. C. C. Ting, Prof. H. C. Kan</u>	
Suppression of fluorescence quenching in plasmonic nanocavities	224
<u>Mr. Nuttawut Kongsuwan, Dr. Angela Demetriadou, Mr. Rohit Chikkaraddy, Dr. Felix Benz, Dr. Vladimir A Turek, Dr. Ulrich F Keyser, Prof. Jeremy J Baumberg, Prof. Ortwin Hess</u>	
Knife-Edge Method At Nanoscale: Why It Fails And How To Correct It?	225
<u>Dr. Sergej Orlov</u>	
Hybrid Plasmons in Graphene Nano-slits	227
<u>Mr. Paulo André Gonçalves, Prof. Sanshui Xiao, Prof. Nuno Peres, Prof. N. Asger Mortensen</u>	
Large angle directional beaming control by metal aperture-corrugation structures	228
<u>Dr. Guoguo Kang</u>	
Light controlled conductivity of graphene on photorefractive lithium niobate	229
<u>Mr. Jon Gorecki, Dr. Nikitas Papisimakis, Dr. Sakellaris Mailis, Dr. Vasilis Apostolopoulos</u>	
Enhancement of light transmission through random copper thin-films near the percolation threshold	231
<u>Dr. Luis Guillermo Mendoza Luna, Prof. José Luis Hernández Pozos, Ms. Eva Mayra Rojas Ruiz</u>	
Cathodoluminescence characteristics of light emission properties of axial ZnO/Zn_{1-x}MgxO multiple quantum wells on vertical ZnO microrods	232
<u>Ms. Agnieszka Pieniążek, Dr. Henryk Teisseyre, Mr. Dawid Jarosz, Dr. Bartłomiej S. Witkowski, Mrs. Anna Reszka, Mr. Krzysztof Kopalko, Prof. Adrian Kozanecki, Prof. Marek Godlewski, Prof. Bogdan J. Kowalski</u>	
Terahertz Generation via Excitation of Surface States Formed from Spatially Separated Electrons and Holes in Nanocomposites	233
<u>Dr. Oleg Khasanov, Dr. Olga Fedotova, Mr. Grigory Rusetsky, Dr. Vladimir Gayvoronsky, Prof. Sergey Pokutnyi, Dr. Eugenijus Gaizauskas, Dr. Virgilijus Vaicaitis</u>	
Microstructured photonic polymer membranes for modulation of the reflectivity in the mid infrared	234
<u>Mr. Salim Assaf, Ms. Maud Viallon, Dr. Alexander Korovin, Prof. Yan Pennec, Dr. Anthony Treyzebre, Dr. Vincent Thomy, Dr. Vincent Senez, Dr. Daniel Dupont, Mr. Michel Caillibotte, Prof. Bahram Djafari-rouhani</u>	

Gain Media In Plasmonic Nanostructures: From Superradiance To Lasing	236
<u>Dr. Renaud Vallée</u> , Dr. Pierre Fauché, Dr. Atsushi Yamada, Prof. Daniel Neuhauser, Prof. Brahim Lounis	
NanoPlasmonic Sensing spectroscopy as a novel route for monitoring CH₃NH₃PbI₃ perovskite formation in mesoporous TiO₂ films	237
<u>Dr. Fahd Rajab</u> , Prof. Farid Harraz	
Nanomechanical membrane resonator as a novel platform for the detection and analysis of FEBID plasmonic nanostructures	238
<u>Ms. Miao-Hsuan Chien</u> , Dr. Mostafa Shawrav, Dr. Heinz Wanzenboeck, Prof. Silvan Schmid	
Transmission of optical signals in coupled cavity resonators based on quasi-one-dimensional periodic nanobeam based structures	239
<u>Dr. Alexander Korovin</u> , Prof. Yan Pennec, Prof. Bahram Djafari-rouhani	
Accurate detection of resonance by monitoring wavepacket width	240
Dr. Rémi Pollès, Dr. Martine Mihailovic, Prof. Emmanuel Centeno, <u>Dr. Antoine Moreau</u>	
Non-plasmonic nanoparticle heaters with temperature control	242
<u>Mr. George Zograf</u> , Dr. Mihail Petrov, Dr. Dmitriy Zuev, Dr. Valentin Milichko, Dr. Sergey Makarov, Prof. Pavel Belov	
Dielectric nanoantennas for surface-enhanced fluorescence spectroscopy and efficient harmonic generation	243
<u>Dr. Gustavo Grinblat</u> , Dr. Yi Li, Mr. Toshihiko Shibamura, Mr. Javier Cambiasso, Dr. Michael Nielsen, Dr. Emiliano Cortes, Dr. Pablo Albella, Dr. Aliaksandra Rakovich, Dr. Rupert F Oulton, Prof. Stefan Maier	
Plasmon Voltammetry to Sense pH-dependent Surface Oxidation of Gold	244
<u>Mr. Bernhard Steinhauser</u> , Dr. Cynthia Vidal, Mrs. Ruxandra-Aida Barb, Prof. Johannes Heitz, Dr. Calin Hrelescu, Prof. Thomas Klar	
Broadening effects of absorption and emission bands in InP/ZnS quantum dots	245
Mr. Sergey Savchenko, Dr. Alexander Vokhmintsev, <u>Prof. Ilya Weinstein</u>	
Multi-color luminescent ZnO nanoparticles produced by pulsed laser ablation in water	247
<u>Prof. Marco Cannas</u> , Dr. Pietro Camarda, Dr. Lavinia Vaccaro, Dr. Fabrizio Messina, Dr. Gianpiero Buscarino, Prof. Simonpietro Agnello, Prof. Franco Gelardi	
Silicon Oxycarbide Waveguides for Photonics Applications	248
<u>Dr. Faisal Ahmed Memon</u> , Dr. Francesco Morichetti, Prof. Andrea Melloni	
Demultiplexing surface waves with silicon nanoantennas	249
<u>Mr. Ivan Sinev</u> , Dr. Andrey Bogdanov, Mr. Filipp Komissarenko, Ms. Kristina Frizyuk, Dr. Mihail Petrov, Dr. Ivan Mukhin, Dr. Sergey Makarov, Dr. Anton Samusev, Prof. Andrei Lavrinenko, Dr. Ivan Iorsh	
Multiple Spherical Reactor	251
<u>Prof. Humberto Ramirez Hernandez</u> , Prof. Francisco Espinosa, Prof. Salvador Fernandez Tavizon, Prof. Alfonso Mercado, Prof. Armando Zaragoza	

Two Grand Challenges for Nanophotonics: Tunable Coherent Optical Arrays and the Starshot Lightsail

Wednesday, 13th September - 09:05 - Plenary Speeches - Auditorium - Oral - Abstract ID: 515

Prof. Harry Atwater¹

1. California Institute of Technology

Research in nanophotonics is yielding advances that are opening paths for conceptually new “grand challenge” photonic technologies that have not previously been achievable. One such example is tunable coherent optical arrays, which are enabling phased-array optical beam steering and forming in a manner previously accessible mainly at microwave frequencies. A combination of the rapid progress in metasurface design, together with new concepts for dynamical tuning of optical phase and amplitude in nanoantennas is enabling coherent array at optical and infrared frequencies. A second grand challenge for humanity is design of spacecraft capable of interstellar travel. Recently, the Breakthrough Starshot initiative has captured scientific imagination and advanced a proposal for light-driven spacecraft that could reach nearby stars within a human lifetime. I will show that this audacious concept may be closer than we imagine, if advances in nanophotonics can enable key concepts for spacecraft propulsion, instrumentation and communications.

Plasmonics – a Scalable Path towards a Terabit/s-Technology?

Wednesday, 13th September - 09:40 - Plenary Speeches - Auditorium - Oral - Abstract ID: 512

Prof. Juerg Leuthold¹

1. ETH Zurich

Plasmonics has increasingly the potential to replace traditional photonics. And indeed, a new generation of passive and active plasmonic elements is emerging. Unlike photonic devices these plasmonic elements feature a tiny footprint in combination with an almost unlimited bandwidth. Yet, plasmonic devices also suffer from high losses. The question then is where and when plasmonics really can make a difference. In this talk, we will review and comment the latest generation of plasmonic devices encompassing plasmonic electro-optical modulators, detectors, RF-receivers, couplers and waveguides. Finally, we will introduce plasmonic devices that feature not only lowest power consumption but also a footprint at the single atom level.

Tracking femtosecond dynamics at the nanoscale

Wednesday, 13th September - 10:45 - Plenary Speeches - Auditorium - Oral - Abstract ID: 254

Prof. Niek van Hulst¹

1. ICFO – the Institute of Photonic Sciences, Barcelona

NanoPhotonics and NanoOptics (NANOP) addresses the interaction of light with nanostructures that are too small and complex to be described by traditional continuum methods, and the structuring and manipulation of optical fields to control these interactions at the nano-scale. Applications are found in 2D-materials, perovskites, photo-voltaics, polymers, molecular biophysics, cold atoms, quantum optics etc... Natural Photosynthetic systems in plants and bacteria constitute a particular Nano-Micro system ranging from individual chlorophylls to full complex networks, moreover acting on the ultrafast fs-ps scale. Photosynthetic light harvesting works highly efficient and even signatures of coherent energy transfer have been revealed. Yet the complexes in natural membranes are too small and fast to track the nanoscale light transfer. We aim to combine ultrasmall and ultrafast, to couple efficiently to single units, to track fs transient spectra and to control the interaction.

I will introduce a novel experimental technique that allows for the direct recording of ultrafast transient absorption spectra of single molecules in a broadband fashion, at room temperature, with a temporal resolution of 25 fs, to reveal a dynamic Stokes-shift alongside vibrational cooling within the first tens of femtoseconds after photoexcitation. Beyond single molecule detection by fluorescence, I'll enter into the alternative detection of stimulated emission.

Finally, imaging nanoscale light transport requires local excitation and detection far beyond the diffraction limit. I will address the use of scanning resonant antenna probes and nanoholes to confine the light field and couple effectively to single emitters on the nanoscale. The plasmonic antenna acts as a nano cavity with relative strong coupling (~100GHz), speeding up the radiative decay to picosecond time scale, enhancing the photostability and allowing > GHz single photon emission.

I will conclude with an outlook of the challenges ahead and the perspectives of addressing coupled networks in real nano-space and on femtosecond timescale.

Controlling Light-matter Interactions on the Nanometer Scale

Wednesday, 13th September - 11:25 - Plenary Speeches - Auditorium - Oral - Abstract ID: 8

Prof. Lukas Novotny¹

1. ETH Zurich

The past 20 years have brought exceptional control over light-matter interactions on the nanoscale. Today, localized optical fields are being probed with nanoscale materials, and, vice versa, nanoscale materials are being controlled and manipulated with localized fields.

I will discuss both early and recent developments in near-field optical spectroscopy and optical nanomanipulation and then focus on recent experiments on antenna-coupled quantum emitters and vacuum-levitated nanoparticles.

Integration of magnetic plasmonic nanoantennas on a silicon chip

Wednesday, 13th September - 13:30 - Poster Session - Gallery - Poster - Abstract ID: 127

*Mr. Javier Losada*¹, *Dr. Alejandro Martínez*²

1. Valencia Nanophotonics Technology Center (NTC), 2. Universitat Politècnica de València

Introduction

Metallic nanoantennas with subwavelength dimensions have become extremely powerful elements to manipulate light at the nanoscale. Their properties, associated to the existence of localized surface plasmon resonances (LSPRs) with either electric or magnetic character, can be used for different applications: directional light scattering, broadband absorption or enhanced nonlinear interactions. In particular, magnetic nanoantennas supporting an LSPR with magnetic character have been used for directional coupling of guided waves, enhanced nonlinear interaction or as fundamental building block of negative-index metamaterials. Taking account this idea, we have demonstrated that a plasmonic nanoantenna showing an magnetic LSPR can be efficiently excited if inserted within a subwavelength gap created into a waveguide and fed by the fundamental TM waveguide mode.

Characterization

Figure 1(a) describes schematically the system we are proposing. A subwavelength gap (g) separates two silicon waveguides with rectangular cross-section. Figure 1(b) shows schematically the distribution of the fields in the sandwich nanoantenna in order to get a magnetic LSPR. When the TM mode is used we can see that the field components (namely the E_z , Fig. 1(c), and H_x , Fig. 1(d)), perfectly match with the requirements in the nanoantenna to obtain a magnetic response. In order to optimize the magnetic field response (H_x) within the insulator several full-3D numerical simulations have been run using CST Microwave Studio. The waveguide is made of silicon with a cross section of $220 \times 450 \text{ nm}^2$. For the nanoantenna we consider indium tin oxide (ITO), with a permittivity of $1.02 + j0.96$ at the wavelength of $1.6 \mu\text{m}$, and gold. Figure 2 shows the results obtained in the optimization step which has led to a magnetic response at telecom wavelength.

Conclusion

We demonstrate the viability of a magnetic nanoantenna embedded in a photonic waveguide fed by the TM mode of a silicon waveguide. Moreover, we have study the effect of the sandwich-like antenna geometrical parameters, concluding that, first, optimal response occurs for an insulator thickness of 40 nm in a gap with a length of 100 nm , and secondly, for gap lengths larger than 150 nm the resonant magnetic response disappears. Next steps will include the fabrication and testing of the structure under study.

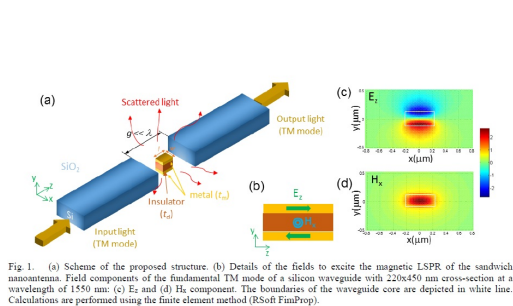


Fig. 1. (a) Scheme of the proposed structure. (b) Details of the fields to excite the magnetic LSPR of the sandwich nanoantenna. Field components of the fundamental TM mode of a silicon waveguide with $220 \times 450 \text{ nm}$ cross-section at a wavelength of 1550 nm : (c) E_z and (d) H_x component. The boundaries of the waveguide core are depicted in white line. Calculations are performed using the finite element method (RSoft FimProp).

Fig1.description of the system.jpg

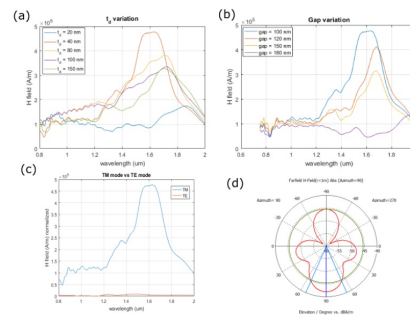


Fig. 2. (a) H_x field spectra in insulator layer for insulator thickness (t_i) varying from 20 to 150 nm . (b) H_x field spectra in the insulator for gap lengths varying from 100 nm (minimum gap length feasible in fabrication) to 180 nm . (c) H_x field spectrum in the insulator for TM excitation vs TE excitation for the optimized configuration of the antennas. (d) Radiation pattern at the resonant wavelength ($1.6 \mu\text{m}$) for optimized antenna configuration with TM excitation.

Fig2.optimization step.jpg

Optical properties of porphycenes in the regime of strong light-matter coupling.

Wednesday, 13th September - 13:30 - Poster Session - Gallery - Poster - Abstract ID: 408

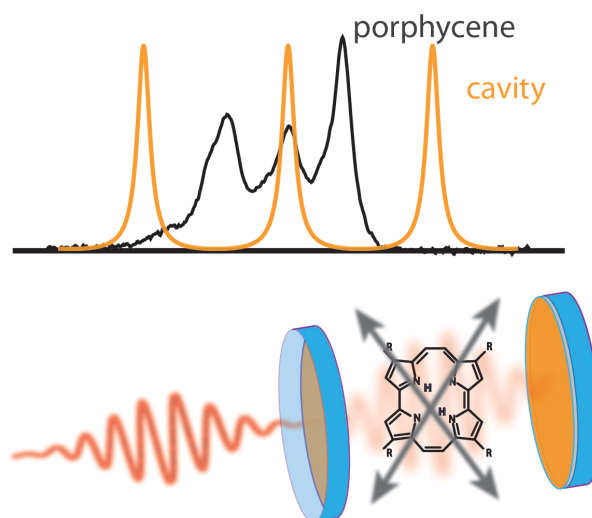
Mr. Wassie Takele¹, Dr. Lukasz Piatkowski¹, Prof. Jacek Waluk¹

1. Institute of Physical Chemistry, Polish Academy of Sciences

Interaction of molecules with light can be modified by placing the molecules in an optical microcavity. When the interaction between the properly oriented transition dipole moment of a molecule and the cavity mode occurs at a rate faster than any competing dissipation process, the so-called strong coupling of light and matter develops, which results in a formation of hybrid light-matter states (polaritons). These new states have interesting optical and electronic properties possessed neither by the original molecule or the optical mode.

Because of their large transition dipole moment organic dyes have been extensively used for the strong coupling experiments. However, an interesting family of molecules, yet to be studied under strong light-matter coupling regime, is porphycenes. They possess an intriguing property of undergoing ultrafast (fs-ps) tautomerization reaction. As a result of this process, the electronic transition dipole moments significantly change their orientation. This leads to a fascinating situation where the degree of the strong coupling regime in a molecule embedded in a microcavity may vary following the reorientation of the transition dipole moment.

In the experiment, parent and substituted porphycene molecules, either in a solution or in a polymer matrix, are placed in a tunable, Fabry-Pérot type optical microcavity comprising of two silver coated mirrors. The cavity is then tuned to be resonant with different electronic transitions of the molecule. We study the effect of the cavity on both the absorption and emission properties of porphycenes. The preliminary experiments are carried out to check whether porphycene molecules indeed enter the strong coupling regime with the optical cavity modes. We want to demonstrate that by tuning the optical cavity and therefore controlling the coupling strength between the molecules and cavity modes, one can control the tautomerization rate. Coupling-induced splitting of the energy levels likely causes the asymmetry in the double-well potential for the tautomerization reaction. We thus hypothesise that inducing asymmetry in the otherwise symmetric double-well potential will affect the tautomerization rate and, in extreme conditions, may even stop it.



Porphycene in an optical microcavity.jpg

Dynamic plasmonic colour display

Wednesday, 13th September - 13:30 - Poster Session - Gallery - Poster - Abstract ID: 167

Mr. Xiaoyang Duan¹, **Mr. Simon Kamin**², **Prof. Na Liu**³

1. Max Planck Institute for Intelligent Systems & University of Heidelberg, 2. Max Planck Institute for Intelligent Systems, 3. Max Planck Institute for Intelligent Systems & University of Heidelberg,

Plasmonic colour printing based on engineered metasurfaces has revolutionized colour display science due to its unprecedented subwavelength resolution and high-density optical data storage. However, advanced plasmonic displays with novel functionalities have remained in their infancy. Here we demonstrate a dynamic plasmonic colour display technique which enables all the aforementioned functionalities using catalytic magnesium metasurfaces. Controlled hydrogenation and dehydrogenation of the constituent magnesium nanoparticles, which serve as dynamic pixels, allow for plasmonic colour printing, tuning, erasing, and restoration of colour. In this work, we demonstrate a dynamic plasmonic display technique based on catalytic Mg metasurfaces. Different from other hydrogen-storage metals such as palladium (Pd) and yttrium, which are associated with poor optical response, Mg exhibits excellent plasmonic properties at high frequencies. For example, Mg nanostructures have been used for chiral sensing in the UV spectral range and for hydrogen sensing in the visible spectral range¹⁻⁴. Most importantly, the unique hydrogenation/dehydrogenation kinetics of Mg nanoparticles is ideally suited for creating dynamic plasmonic systems.

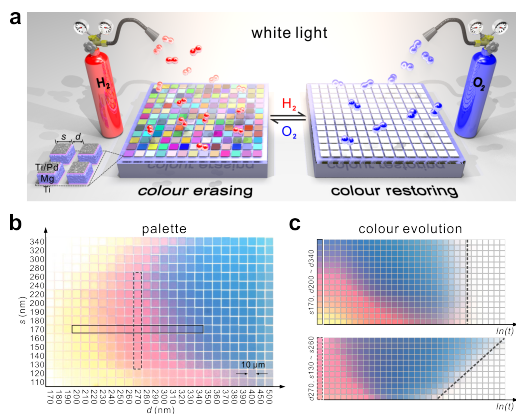


Figure1.png

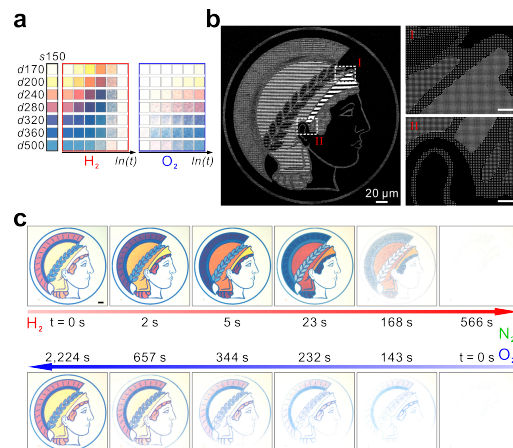


Figure2.png

Totally confined gigahertz mechanical mode with a complete phononic bandgap for a nano-optomechanic cavity

Wednesday, 13th September - 13:30 - Poster Session - Gallery - Poster - Abstract ID: 122

*Ms. Laura Mercadé Morales*¹, *Dr. Alejandro Martínez*¹

¹. *Universitat Politècnica de València*

INTRODUCTION

One-dimensional optomechanical crystals are commonly defined as quasi-periodic structures in which propagation and coupling of optical and mechanical waves can be engineered. Here, we present a nano-optomechanical cavity that incorporates two different unit cells based on high optical quality factor cavities, which have been modified to have a complete phononic bandgap. An optomechanical coupling rate of 600 kHz, an optical quality factor of $3.8 \cdot 10^4$ and a mechanical frequency of 5.3 GHz has been found.

METHODS

The design of the nano-optomechanic cavity has been performed through an analysis of the phononic and photonic diagram bands evaluated using finite element methods (FEM) as COMSOL and RSoft Bandsolve, respectively. On the one hand, solving these eigenvalue problems, it was possible to design the corrugated unit cell to have the mechanical cavity frequency of 5.3 GHz inside the total bandgap, as can be seen in Fig. 1. On the other hand, the proper middle cavity was built according to *Appl. Phys. Lett.* **101**, 081115 (2012), with a waveguide width of 500 nm and a quadratic variation of the lattice parameter along the structure in order to fit with the corrugated optomechanical crystal in the surroundings. This corrugated one-dimensional crystal was used to shield the acoustic mode of the cavity and it is based on *Nat. Commun.* **5**, 4452 (2014).

RESULTS

The fundamental optical and mechanical defect modes are presented in Fig. 2 besides the total structure. Both modes show an optomechanical coupling rate of 600 kHz where its main contribution is given by the photoelastic effect (PE), instead of the moving boundary effect (MB), as can be seen in Fig 1c. As both contributions are additive, the optimization process being performed works in order to be able to maximize both simultaneously.

DISCUSSION

The main advantage of this structure is that the optical properties can be tuned with the width beam and hole spacing and size of the center of the structure and, separately, the mechanical properties can be tuned with the corrugated unit cell in the surroundings. Furthermore, its design enables coupling via lateral bend waveguides.

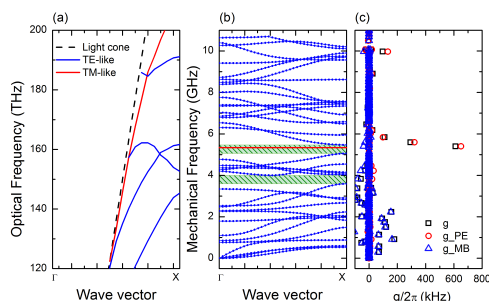


Figure 1: (a, b) Photonic and phononic band diagrams of the corrugated unit cell placed at the surroundings. (c) Vacuum optomechanical coupling, g , and its moving boundaries and photoelastic effect contributions corresponding to the idealized cavity.

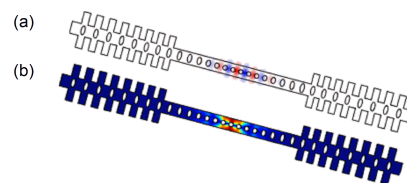


Figure 2: FEM simulations corresponding to (a) the normalized E_y field of the fundamental optical mode and (b) displacement field, $|Q|/\max\{|Q|\}$, of the mechanical mode at 5.3 GHz

Figure2 fem modes.png

Figure1 bands and coupling.png

Emission of a single colloidal quantum dot in a patch antenna

Wednesday, 13th September - 13:30 - Poster Session - Gallery - Poster - Abstract ID: 166

Mr. Juan Uriel Esparza¹, Dr. Amit Raj Dhawan², Dr. Cherif Belacel³, Dr. Catherine Schwob⁴, Dr. Micheal Nasilowski⁵, Prof. Benoit Dubertret⁵, Prof. Laurent Coolen¹, Prof. Pascale Senellart⁶, Prof. Agnès Maître¹

1. Université Pierre et Marie Curie, 2. Institute of Fundamental and Frontier Sciences and University of Pierre et Marie Curie, 3. Centre Développement Technologies Avancées, 4. Univ. Pierre et Marie Curie, 5. Ecole Supérieure de Physique et de Chimie Industrielles de la Ville de Paris, 6. Laboratoire de photonique et nanostructures

In the study of light-matter interaction significant efforts have attempt to improve the coupling between single quantum emitters and metallic sub-wavelength nanostructures. A patch antenna [1] has already demonstrated strong acceleration of spontaneous emission and control of radiation pattern when aggregates of nanocrystals (around 50) were coupled to a plasmonic patch antenna. Purcell factor (ratio of LDOS with and without antenna) of 80 has been obtained [2].

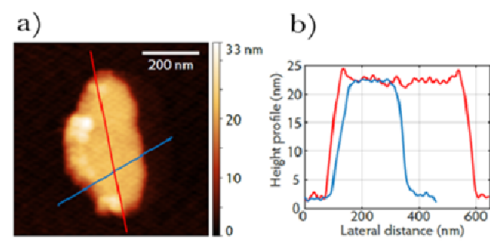
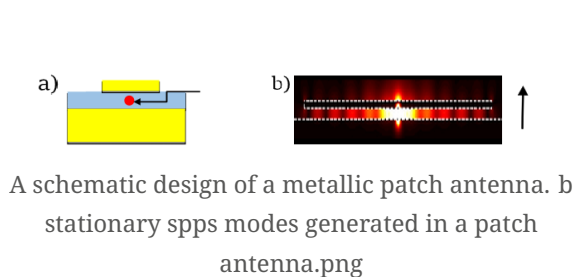
The design of a patch antenna consists of a metal-insulator-metal structure where a thick gold layer is used as an optical mirror and a thin gold nanodisk is placed some nanometers above the emitter using in-situ optical lithography protocol [3]. The thickness of the spacer between both metallic layers should ensure the excitation of surface plasmon polariton modes (SPP's) and leads the maximum confined field avoiding quenching due to non-radiative channels.

We will present the fabrication of a deterministic plasmonic patch antenna when a single CdSe/CdS colloidal quantum dot is used as source of light. Depending of the dimension of the patch antenna and the emitter orientation, different Purcell factors could be achieved leading to different optical properties. For moderate Purcell factors, patch antennas are single photon sources. For higher Purcell factors, the spontaneous emission acceleration makes the multiexciton radiative recombination competitive with Auger recombination. Very bright and efficient antennas could be achieved.

[1] R. Esteban, T.V. Teperik, J.J. Greffet, "Optical patch antennas for single photon emission using plasmonic resonance", *Phys.Rev. Lett.***104**, 026802 (2010).

[2] C. Belacel, B. Habert, F. Bigourdan, F. Marquier, J-P. Hugonin, S. Michaelis de Vasconcellos, X. Lafosse, L. Coolen, C. Schwob, C. Javaux, B. Dubertret, J-J. Greffet, P. Senellart, A. Maître, Controlling spontaneous emission with plasmonic optical patch antennas, *Nanoletters***13** 1516 (2013).

[3] Dousse, A. et al. Controlled light-matter coupling for a single quantum dot embedded in a pillar microcavity using far-field optical lithography. *Phys. Rev. Lett.* 101, 267404 (2008).



Optical properties and charge trapping dynamics of single CsPbBr₃ nanocrystals

Wednesday, 13th September - 13:30 - Poster Session - Gallery - Poster - Abstract ID: 390

***Ms. Natalie A. Gibson*¹, *Mr. Brent A. Koscher*¹, *Prof. A. Paul Alivisatos*¹, *Prof. Stephen R. Leone*¹**

1. University of California, Berkeley

Semiconductor nanocrystals are attractive materials for a range of optoelectronic devices, due in large to their tunable optical and electronic properties. However, the localization of excited charges at defect states impedes both charge mobility and radiative recombination and limits the efficiency of any nanocrystal-based device. Since this leads to intermittencies in the emitted photoluminescence (PL) of a single nanocrystal, it can be directly probed by analyzing PL trajectories of individual nanocrystals.

While such experiments have contributed to an understanding of light-matter interactions in type II-VI, III-V and IV-VI semiconductors,¹ these interactions in an emerging class of semiconductor nanocrystals, lead halide perovskites, are largely unknown.

Time-correlated single photon counting is used to record PL trajectories of single CsPbBr₃ nanocrystals. An embedding polymer used to prevent aggregation also decreases the photostability and quantum yield of the nanocrystals. To overcome these issues, a low repetition rate laser is used to avoid rapid photobleaching, and a bin-free changepoint analysis (CPA) method^{2,3} is used to analyze trajectories that lack a clear separation of intensity levels.

Figure 1 shows a PL trajectory of a single CsPbBr₃ nanocrystal, obtained by binning photon counts (black) and using CPA (red). Once a trajectory is separated into distinct 'on' and 'off' levels via CPA, the kinetics of each level can be investigated by calculating a probability distribution. This is found to follow an exponentially-truncated power law, $P(\tau) = \tau^{-m} \exp(-\tau/\tau_c)$, where $P(\tau)$ is the probability that a duration of length τ occurs, m is the power-law exponent, and τ_c is the time at which the power law diverges into an exponential.

The intensity dependence of the on-state τ_c is investigated in over 130 nanocrystals, and appears to decrease with increasing excitation intensity (Figure 2). A superlinear dependence at low exciton formation is observed, followed by a rapid saturation (Figure 3).

These results suggest that a single-exciton mechanism, or a combination of single and multi-exciton mechanisms, is responsible for the intermittent PL behavior in CsPbBr₃ nanocrystals.⁴ Future studies will focus on isolating the nanocrystals in a polymer-free environment to understand the role of the surrounding polymer.

[1] 10.1021/jp0467548

[2] 10.1021/acs.jpcc.6b09780

[3] 10.1039/C2CS35452G

[4] 10.1063/1.1993567

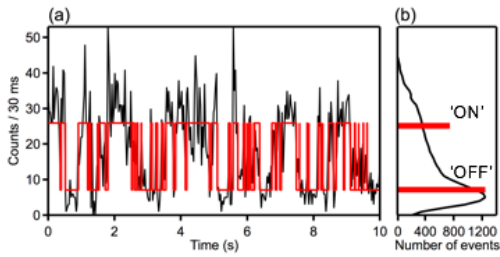


Figure 1. (a) 10 s of a PL trajectory binned at 30 ms in black, overlaid with corresponding CPA trajectory in red. (b) Intensity histograms for both methods.

Figure 1 pl trajectory of a single cspbbr3 nanocrystal.png

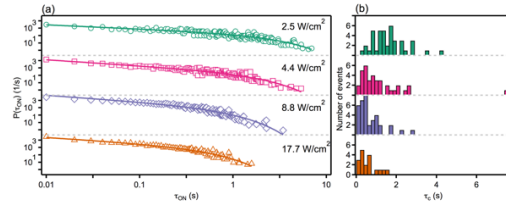


Figure 2. (a) Sample on-state probability distributions of a single nanocrystal excited at four different intensities. (b) Corresponding distribution of truncation times, τ_c , for all nanocrystals studied at the four excitation intensities.

Figure 2 intensity dependence of the on state kinetics.png

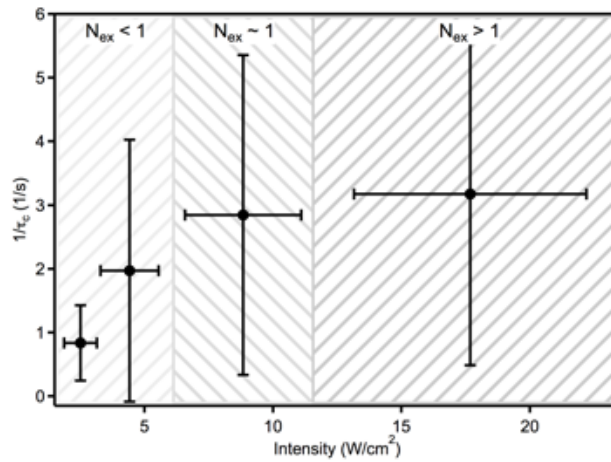


Figure 3. Average inverse truncation time, $1/\tau_c$, versus excitation intensity. Three excitation regimes are labeled: below, near, and above $\langle N_{ex} \rangle = 1$ (average formation of one exciton per pulse).

Figure 3 saturation behavior of the on state truncation time.png

New luminescent nanostructural polymer materials

Wednesday, 13th September - 13:30 - Poster Session - Gallery - Poster - Abstract ID: 245

***Dr. Viktoria Lapina*¹, *Dr. Piotr Pershukevich*¹, *Dr. Pavich Tatsiana*²**

1. Institute of Physics NAS of Belarus, 2. Institute of Physics NAN Belarus

Introduction

Polymer guest-host systems composed of a solid polymer matrix and functional molecules such as luminophores are of interest for a broad range of applications in the area of optical information technology and sensors. The use of such composite systems offers a variety of advantages. The polymer matrix contributes, for instance, good film forming capabilities, sufficient adhesion on solid substrates and good mechanical properties. Combination of the effective luminophores with suitable polymers can lead to creation of new advanced optical materials.

Materials: Our work is concerned with development new optical materials based on supramolecular complexes composed of nanodiamonds particles and rare earth elements introducing into polymeric matrix. As guest host systems were involved with amorphous polymer hosts such as polycarbonate, and polystyrene.

Methods: For synthesis luminescent complexes the method template synthesis was used, for fabrication of thin composite films – the spin-coating procedure. The main photophysical characteristics were investigated using the methods luminescent spectroscopy, SEM, time-resolution kinetic spectroscopy.

Results:

Complex of europium with bataphenanthrolyne (4,7-diphenyl-1,10-phenanthrolyne): $\text{Eu}(\text{BPhen})_3$ and nanodiamonds - ND- $[\text{Eu}(\text{BPhen})_{2-3}]$ were obtained and on their basis there have been fabricated the composites as polymer films with the thickness of ~ 300 nm. It was established that in dependence on type of polymer both spectra of luminescence excitation and luminescence of complexes can be change essentially. The fabricated luminescent polymer materials have revealed strong luminescence and high quantum output, up to 70%, enhanced photostability. Besides it, distinguished attribute of such films is excellent adhesion to surface due to presence of nanodiamonds particles.

Fig.1. Spectra of luminescence excitation (1, 2) under $\lambda_{\text{reg.}} = 613$ nm (a) and luminescence (1, 2) under $\lambda_{\text{ex.}} = 300$ nm (b) powders: 1 – complex $\text{Eu}(\text{BPhen})_2(\text{NO}_3)_3$, 2 – supramolecular complex $(\text{ND}-\text{Eu}(\text{BPhen})_2(\text{NO}_3)_2)$

Fig.2. Spectra of luminescence excitation (1, 2) under $\lambda_{\text{reg.}} = 613$ nm (left) and luminescence (3,4) under $\lambda_{\text{ex.}} = 300$ nm (right) PMMA samples: 1, 3 – complex $\text{Eu}(\text{BPhen})_2(\text{NO}_3)_3$, 2, 4 – supramolecular complex $(\text{ND}-\text{Eu}(\text{BPhen})_2(\text{NO}_3)_2)$

Conclusion: developed new advanced optical materials can be used as luminophors, active components of functional devices, detectors, in microelectronics at manufacture of OLED (polymer nanocomposite materials).

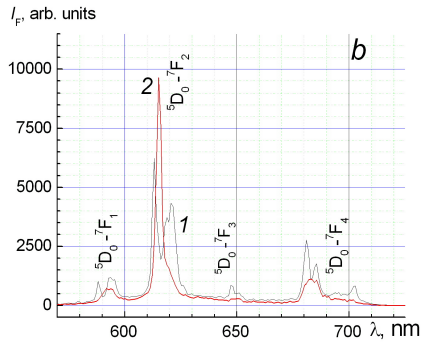


Fig.1b porosh na-eu-bpen .jpg

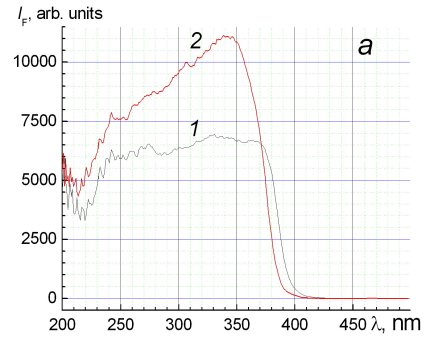


Fig1a porosh na-eu-bphen .jpg

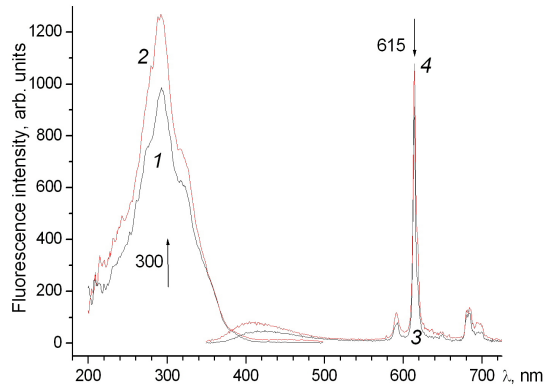


Fig2 pmma na-eu-bph2.jpg

Development of an optical genosensor based on gold nanoparticles for genomic detection of *Mycobacterium bovis*.

Wednesday, 13th September - 13:30 - Poster Session - Gallery - Poster - Abstract ID: 168

Dr. Patricio Oyarzun¹, Mr. Braulio Contreras¹, Dr. Enrique Guzmán-Gutiérrez¹, Ms. Javiera Aguilar¹, Mr. Alejandro Maldonado¹, Prof. René Garcés¹

1. Universidad San Sebastián

Introduction

Food safety is gaining prominence as a global issue, driving the demand for rapid, simple, on-site and low-cost biosensor technologies. Biosensors have emerged as a cheap and quick alternative to traditional chromatographic methods. Gold nanoparticles (AuNPs) exhibit optical properties (surface plasmon resonance) offering the prospect for label-free and real-time measurements. AuNPs can be biofunctionalized with oligonucleotides (probes) that are specific for recognition of food pathogens, giving rise to nano-biosensors (genosensors) with applications in food quality and safety assurance. Optical excitation of plasmons is responsible for their large absorption and scattering properties, which can be controlled by modifying the behavior of the nanoparticles in solution (aggregation/dispersion).

Methods

AuNPs were chemically synthesized by the citrate reduction method. The nanoparticles were functionalized by oligonucleotides hybridizing genomic DNA of *Mycobacterium bovis* (bovine tuberculosis), which correspond to a segment of the RD4 gene (5'-CGCCTTCCTAACCAGAATTG-3'). The alkanthiol-modified probe was reduced with DTT to form the thiol group needed for chemisorption of the oligonucleotides onto the AuNP surface, and was chromatographically purified (Sephadex G-50). The genosensor was built by functionalizing AuNPs with the thiolated probe. Detection of *M. bovis* genomic DNA was performed previous denaturation of the DNA (95°C for 5 min). The hybridation was carried out at 55°C, and color change was followed spectrophotometrically upon addition of HCl 0.1 N.

Results

AuNPs were analysed spectrophotometrically (Figure 1) and by dynamic light scattering, showing homogeneous dispersion of nanoparticles with an average diameter of 10 nm (Figure 2). Optical detection of *M. bovis* was demonstrated using samples contaminated with different amounts of genomic DNA. A shift was observed on the AuNPs absorption spectrum, which was associated to a color change from red to purple ($\lambda_{max} = 520$ nm to $\lambda_{max} = 620$ nm). A standard curve was obtained by correlating the color change (A_{520}/A_{620}) with the DNA concentration (Figure 3).

Discussion

AuNPs aggregate in the absence of genomic DNA. Under this condition, the color change (red to purple) is attributable to the absence of hybridization between the genosensor aptamers and DNA that stabilize the nanoparticles, while color red gets more intense in the presence of the DNA.

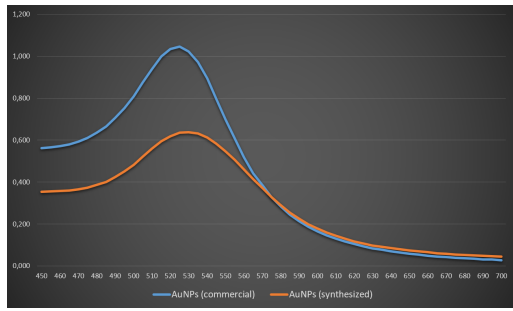


Fig 1 spectrogram.png

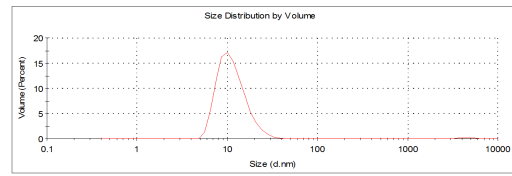


Fig 2 size distribution.png

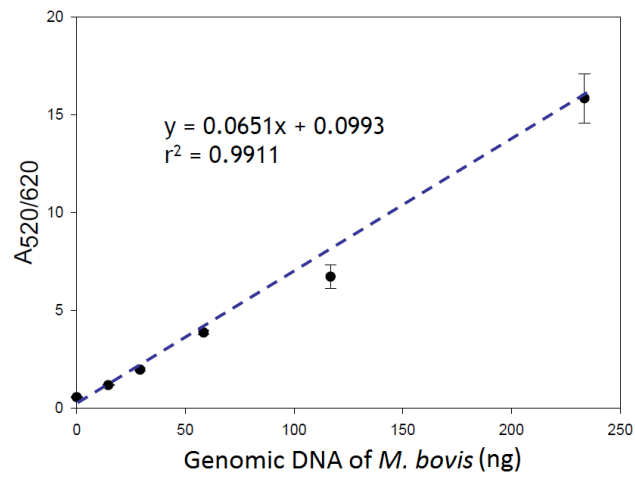


Fig 3 curve.png

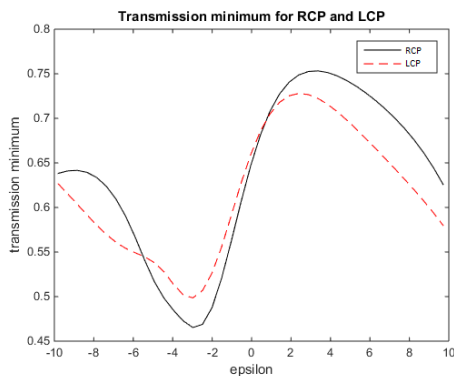
Control of Chiral Response in Clustered Nanoparticles through Cluster Geometry

Wednesday, 13th September - 13:30 - Poster Session - Gallery - Poster - Abstract ID: 436

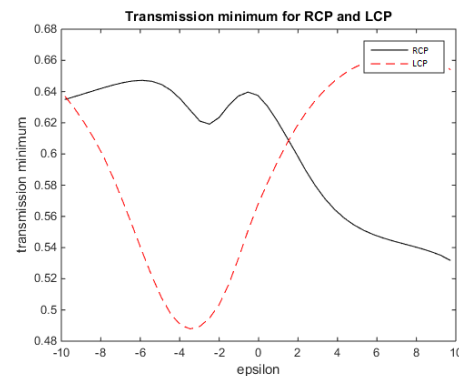
Mr. Dominykas Brickus¹, Dr. Sergej Orlov¹

1. Center for Physical Sciences and Technology, Industrial Laboratory for Photonic Technologies

Chiral materials have different response to right and left circular polarized light. This chiral response is generally very weak for most chiral molecules, but for nano-scale structures it could possibly be orders of magnitude higher. Modern fabrication techniques for nano-materials allow to create such meta-materials where chirality is controlled via shape and geometry. One known technique is structured thin films with helical nano-structures. However, even much simpler achiral structures such as arrangements of nano-spheres can produce a chiral behavior purely from geometrical properties of a three-dimensional arrangement together with incoming light beam. The optical response of such nano-cluster depends strongly on the particle material composition, arrangement geometry, location in the focal plane and the incoming beam properties and polarization state. This problem can be modeled by making use of the so called T-matrix method, which is faster than finite element methods and allows to consider more parameters. Using this method chiral response is analyzed in a two-dimensional cluster, made from single nano-spheres of different sizes and materials. The resulting chirality is induced here by the choice of cluster geometry and material composition. Numerical results are reported and the optimal geometry to maximize chiral response in planar structures is investigated.



Homogenous 90deg.png



Heterogenous 90deg.png

A light detection system for a STM

Wednesday, 13th September - 13:30 - Poster Session - Gallery - Poster - Abstract ID: 439

Mr. Yves Auad¹, Mr. Ricardo Peña Román¹, Mr. Edivar Carvalho¹, Ms. Isabela Rigo¹, Mr. Raone Guedes¹, Mr. Leonardo Santana¹, Mr. Ronaldo Vieira¹, Ms. Luiza Lober¹, Mr. Lucas Palhares¹, Ms. Maria Orfanelli¹, Prof. Luiz Fernando Zagonel¹

1. University of Campinas – UNICAMP

Several processes in a scanning tunneling microscope (STM) may induce light emission by the sample. Among others, such light can be emitted by plasmonic nanoparticles, direct band-gap semiconductors and color centers.[1,2] The spectroscopy of such emitted light can be very rich and provide insightful information about the electronic structures of semiconductors or about the plasmon resonances of metallic nanoparticles. Moreover, in the STM, luminescence mapping can be coupled with usual STM imaging and even with spectroscopy information such as scanning tunneling spectroscopy (STS).

Efficient detection of light emitted inside an STM can be challenging due the several restrictions imposed by the STM and even more so in the case of UHV and Low Temperature devices. In this project, we are striving to build a high efficiency light detection system that provides high collection efficiency while preserving good energy resolution of the emitted light for a LT UHV STM. This light detection system applies patented solutions and tries to solve specific problems in the context of the STM.[3,4] The solution uses a mirror collector with high numerical aperture which is positioned with sub-micrometric precision to ensure an accurate alignment. Numerical simulations predict a solid angle above 70% of a hemisphere. Light is then couple by optical fibers into an optical spectrometer. A software is under development to allow the acquisition of luminescence maps (hyper spectral imaging) automatically and simultaneously with regular images, similarly to cathodoluminescence in a Scanning Transmission Electron Microscope (CL-STEM).[5]

Once operational, we plan on applying our LT UHV STM with the custom built high efficiency light detection system to the study of nano-structured luminescent materials such as semiconducting nanoparticles and 2D materials as WSe₂. [6]

[1] Klaus Kuhnke *et al.* Chem. Rev. 2017, 117, 5174–5222.

[2] D. Frank Ogletree *et al.* Adv. Mater. 2015, 27, 5693–5719.

[3] M. Kociak, *et al.* WO Patent 2011/148072, 2011.

[4] M. Kociak, *et al.* WO Patent 2011/148073, 2011.

[5] L. F. Zagonel *et al.* Nanotechnology 23 (2012) 455205.

[6] Acknowledgements: FAPESP funding 2014/23399-9.

Surface holograms for sensing application

Wednesday, 13th September - 13:30 - Poster Session - Gallery - Poster - Abstract ID: 511

Dr. Monika Zawadzka¹, Prof. Izabela Naydenova¹

1. Centre for Industrial and Engineering Optics, School of Physics, Clinical and Optometric Sciences, College of Sciences and Health, Dublin Institute of Technology

Surface holograms, in which the interference pattern is inscribed on the surface rather than in the volume of the material, can be formed using various approaches. One method involves formation of surface relief structures upon exposure of a photoresist to a patterned light (using holographic recording or exposure through a mask). This approach requires wet processing in order to develop the surface profile. In mass production, the photoresist structures are copied to create a master which is used in embossing. Another method of surface hologram fabrication consists of holographic patterning of material using high power pulsed laser which ablates locally material from the surface.^[1] This technique is a very flexible patterning method that can be easily applied to a range of materials. Moreover, provided that the material being patterned is sensitive to chemical or physical stimuli, the surface hologram can act as a sensor. Exposure of the hologram to the stimulus induces changes to the refractive index modulation resulting in the change of the diffraction efficiency, which constitutes the working principle behind such surface hologram based sensor (Fig. 1). To maximise the efficiency of the sensor, the characteristics of both of the holographic grating and of the sensing material must be optimised. The approach to the fabrication of this novel type of sensors using high power laser holographic ablation method will be discussed. The advantages and challenges of the technique being used will be presented. The experimental data will be compared with theoretical predictions concerning holographic structures diffraction efficiency.

[1] Q. Zhao, A. K. Yetisen, C. J. Anthony, W. R. Fowler, S. H. Yun, H. Butt, Appl. Phys. Lett. 106, 041115 (2015).

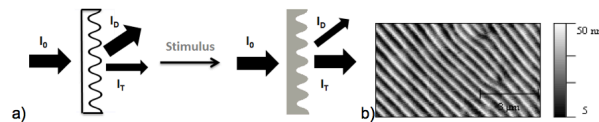


Fig. 1 a) Working principle of a surface hologram based sensor where I_0 , I_D and I_t are intensities of incident, transmitted and diffracted light; change in the refractive index of the material upon exposure to stimulus induces changes in the diffraction efficiency $\eta = I_D/I_0$ b) AFM image of the surface patterned via ablation using pulsed laser in a holographic set-up.

Principle of a surface hologram based.png

Ge_{24.9}Sb_{11.6}S_{63.5} thin films aged under various conditions

Wednesday, 13th September - 13:30 - Poster Session - Gallery - Poster - Abstract ID: 24

Mr. Petr Kutálek¹, Mr. Petr Knotek¹, Ms. Eva Černošková¹, Mr. Ludvík Beneš¹, Mr. Petr Janíček¹

1. University of Pardubice

Introduction

Although the chalcogenide glasses and amorphous thin films find application in a number of fields, the limitation of such materials could be the uncontrolled drift in their exploitation characteristics over time. This means that the properties can vary over a period of time as the state tries to reach a more energetically favorable state. This phenomenon is known as ageing and restricts the wider practical implementation of these materials.

Methods

Amorphous Ge_{24.9}Sb_{11.6}S_{63.5} thin films prepared by thermal evaporation were aged for more than 1 year under various conditions: in a dark in a desiccator (DES), in a dark and humid atmosphere (RH75) and under laboratory conditions under daylight (SUN). Changes in thin films during/due to ageing were studied by the EDX analysis, FTIR spectroscopy, AFM and ellipsometry. The photo-sensitivity of virgin thin film and variously stored thin films during the ageing was also compared.

Results and Discussion

The bleaching of thin films (the blue shift of the optical band gap) was observed with the magnitude depending on the storage conditions. The lowest magnitude of bleaching was observed for the thin films stored in a dark in a desiccator, while the highest magnitude of bleaching was observed for the thin films stored under laboratory conditions under daylight. The overall kinetics of ageing (bleaching) follow well the stretch-exponential function with the formal rate depending on the storage conditions and the stretch parameter slightly varying in the region of 0.54 – 0.6. This means that during the aging of films in various types of storages the effective dimensionality of the samples is not changing. The photo-sensitivity of the aged thin films was significantly affected by storage conditions and was found to decrease with the increasing time of ageing.

Metawire

Wednesday, 13th September - 13:30 - Poster Session - Gallery - Poster - Abstract ID: 209

Dr. Alexey Tishchenko¹, **Mr. Maxim Anokhin**¹, **Prof. Mikhail Strikhanov**¹

1. National Research Nuclear University MEPhI (Moscow Engineering Physics Institute)

Despite the fact that metamaterials consist of the microscopic (or even nanoscopic) elements which characteristics define the “meta”-properties, the problem of multiscale and accurate theoretical description is rather complicated. Here we construct the theory describing macroscopic properties of a wire consisting of a chain of micro-particles (molecules, nanoparticles, quantum dots, etc). Using the local field theory approach, we managed to describe the macroscopic properties given by the analogues of permittivity and permeability for the wire through the microscopic properties of its constituent objects: electric and magnetic polarizabilities, and interspacing. Moreover, the expressions obtained for the chain of particles are analogues of the well-known Clausius-Mossotti expression. This chain is considered as a meta-object: we discuss the conditions for microscopic parameters, when permittivity and permeability become negative, as it occurs in double-negative metamaterials.

The work was supported by the Competitiveness Programme of National Research Nuclear University “MEPhI” and partially by the Ministry of Science and Education of the Russian Federation, grant № 3.2621.2017/4.6.

References

1. M.N. Anokhin, A.A. Tishchenko, M.N. Strikhanov, Microscopic calculations of dielectric properties for hyperbolic metamaterials, *Appl. Phys. A* **123**, 88 (2017).
2. V.M. Shalaev, Optical negative-index metamaterials, *Nature Photonics* **1**, 41 (2007).
3. M.I. Ryazanov, A.A. Tishchenko, Clausius-Mossotti-Type relation for planar monolayers, *JETP* **103**, 539 (2006).
4. A.J. Hoffman, L. Alekseyev, S. S. Howard et al., Negative refraction in semiconductor metamaterials, *Nature Materials* **6**, 946–950 (2007).

Towards fabrication of high-precision microlens arrays for LED-based optoelectronic devices

Wednesday, 13th September - 13:30 - Poster Session - Gallery - Poster - Abstract ID: 473

***Ms. Daria Bezshlyakh*¹, *Mr. Benjamin Pogoda*¹, *Mr. Jannick Langfahl*², *Dr. Uwe Brand*², *Dr. Hutomo Suryo Wasisto*¹, *Prof. Andreas Waag*¹**

1. Institute of Semiconductor Technology (IHT), Technische Universität Braunschweig, 2. Department 5.1 Surface Metrology, Physikalisch-Technische Bundesanstalt (PTB)

Introduction

The trend to system miniaturization is moving the semiconductor technology toward creation of micro- and nanostructured light sources (i.e., micro- and nanoLEDs). To increase the efficiency of LED light extraction and outcoupling, high-precision microoptical elements are required. Thus, in this work, precisely positioned microlens arrays were designed and manufactured using a thermal reflow method to be combined with LED devices. Even though this lens fabrication technique had been well known, its processing reproducibility and output quality were not yet analyzed in detail. Further optimization and characterization therefore was combined with nanometrological methods in order to obtain replicable manufacturing processes of microlens arrays.

Methodology and Results

The fabrication process starts with defining the parameters of the spincoating and photolithography steps in accordance with the required geometrical and optical properties (e.g., focal length, diameter, and maximum center thickness) of the microlenses. The spincoating parameters should be controlled very precisely to obtain a photoresist layer with a constant thickness and required aspect ratio of resist thickness and lens radius, otherwise the lens morphology would be different from the desired semi-spherical shape (Figs. 1(a)-(c)). The semi-spherical microlenses were obtained by thermal reflow of the photoresist cylinders formed at the photolithography step. To estimate their performance, optical characterization was carried out by observing and analyzing the shape of the light beam, which was formed by each lens (Figs. 2(a) and (b)). From the measurement results, the microlens arrays have exhibited high uniformity over the whole substrates with parameters agreeing to the calculated values. Besides, integration of the microlens arrays into structured LED wafers is currently being executed using spin-on-glass, which is more mechanically and chemically stable, and its results will be presented.

Discussion

Semi-spherical microlens arrays with high quality and precision were designed and fabricated by combining photolithography and enhanced thermal reflow processes. 3D confocal laser scanning microscopy and optical metrology were carried out for ensuring the quality of their shapes, focal lengths, surface profiles and outcoupling performance, respectively. Further integration of these microoptical elements with structured light-emitting diode wafers will pave the way to realize ultra-compact optoelectronic sensing and manipulation devices.

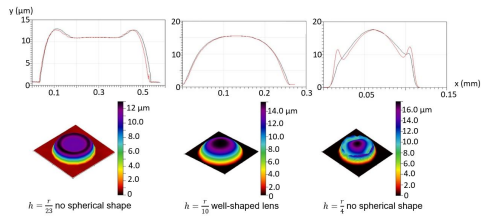


Fig. 1 3d confocal laser scanning microscopy surface profiles top and images bottom of the photoresist microlenses.jpg

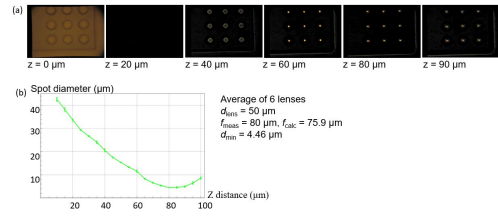


Fig. 2 optical characterization of an array of microlenses. dependence of the spot diameter on the distance along the optical z-axis..jpg

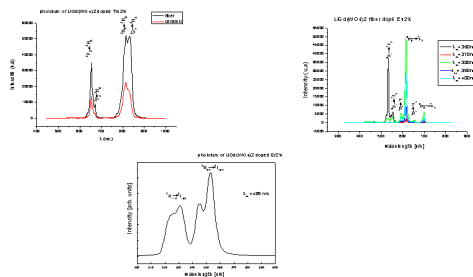
Investigation Of Crystal Growth And properties of 2 at%(Ln³⁺) Doped LiGd(WO₄)₂ with Ln; Eu, Er and Tm

Wednesday, 13th September - 13:30 - Poster Session - Gallery - Poster - Abstract ID: 256

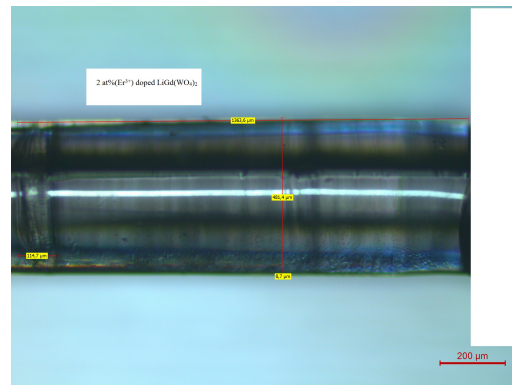
Dr. Brahim Rekik¹, Dr. Kheirredine Lebbou², Prof. Mourad Derbal³

1. University Saad Dahlab Blida1 , Laboratory LASICOM, 2. institut Lumière Matière, université Claude Bernanrd Lyon 1, 3. université Saad Dahleb Blida 1 Laboratory Lasicom

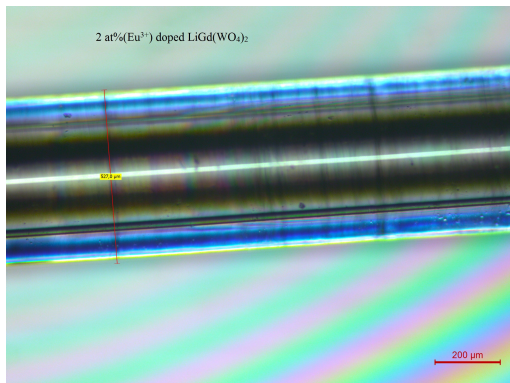
Spectroscopic and luminescent properties of Europium, Erbium, Thulium doped LiGd(WO₄)₂ fibers crystal, present high performances for investigation in laser application . We have successfully grown Eu, Er and Tm-doped LiGd(WO₄)₂ single-crystal fiber by the Micro Pulling Down (μ-PD) technique (they melt above 1115°C). The corresponding crystallization interface was flat, with meniscus length equal to the fiber radii. The pulling rate used was in the range of 15 mm h⁻¹. Spectroscopic investigations of these rare earth 2% doped fibers are given, the emission spectra recorded in the visible and Infrared domain with fluorescence corresponding to the ¹G₄ → ³H₅ and ³F₂ → ³H₆ for the Thulium, and Europium ⁵D₁ → ⁷F₂, ⁵D₀ → ⁷F₁₋₂₋₃₋₄, and Erbium ⁴S_{3/2} → ⁴I_{15/2} , ²H_{11/2} → ⁴I_{15/2} in visible and ⁴I_{11/2} → ⁴I_{15/2} , ⁴I_{13/2} → ⁴I_{15/2} in IR domain, The fluorescence decay times associated to these intenses transitions were investigated, the Raman vibration in LiGd(WO₄)₂:Ln³⁺(2 mol %) single crystal are given at 913 cm⁻¹ for the highest energy transition.



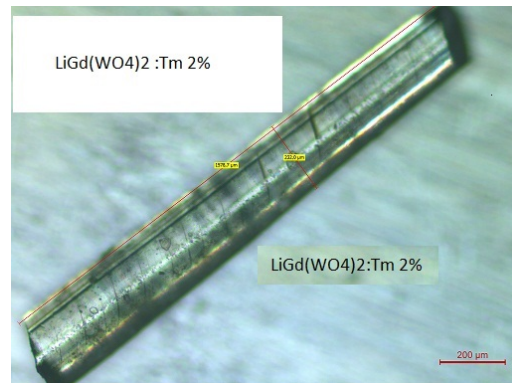
Emission spectra of ligd wo4 2 doped eu er and tm.png



Lgw fiber doped er 2 .jpg



Lgw fiber doped eu 2 .jpg



Lgw fiber doped tm 2 2 .jpg

Propagation of light beams in microstructured nematic liquid crystals

Wednesday, 13th September - 13:30 - Poster Session - Gallery - Poster - Abstract ID: 233

*Mrs. Volha Kabanava*¹, *Dr. Elena Melnikova*¹, *Dr. Alexei Tolstik*¹

1. Belarusian State University

Electrically controlled waveguides implemented in spatially structured liquid crystals (LC) are promising for use as switching elements of fiber-optic communication lines, in the devices for optical signal processing and transmission, are becoming more popular in today's market. Manifestation in the nematic LC media optical Fredericks transition effect and the nonlinear light-induced orientation effect make these materials promising functional environments for creating managed waveguide channels.

A method of creating an integrated optical devices based on LC waveguides for spatial-polarization control of the light beams is presented. Waveguide channels in planar nematic LC layer implemented by using a patterned electrode layer deposited on the one substrate of the LC cell. The periodic refractive index modulation in the LC layer appears due to the action of an external electric field and causes the formation of controlled LC waveguides in the cell. An external AC voltage applied to the LC element controls the depth of modulation of optical anisotropy. The waveguide properties of the LC cell disappear when external AC voltage is not applied.

The experimental picture of propagation of linearly polarized light beams along the waveguide channels with an optical power below the threshold of nonlinear light-induced orientation effect is shown in Fig.1. As seen from Fig.1 *a*, at low power light beam ($P = 0.5$ mW) waveguide mode propagation of light is realized under external voltage ($U=4$ V) significantly exceeding the threshold of the Fredericks transition ($U = 1.1$ V). Waveguide mode propagation of light beams in this case is realized by electrically controlled total internal reflection (TIR) effect in a microstructured nematic LC layer. Fig.1 *b* shows that in this case the effect of self-focusing and formation of spatial soliton can be observed even when the light beam power is $P = 3$ mW.

Thus, the combination of two mechanisms of the nematic LC director reorientation (electrical and optical) extends the functional characteristics of photonic devices based on the waveguide mode propagation of light and nonlinear light-induced orientation effects. Developed portable LC devices with low working voltages are promising for spatial-polarization control of light beams with different optical power.

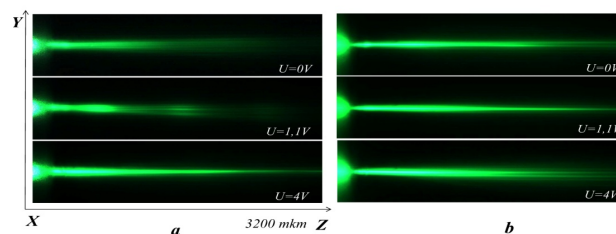


Fig1ab.jpg

Integrated on-chip localized surface plasmon resonances in a subwavelength periodic array of gold nanowires

Wednesday, 13th September - 13:30 - Poster Session - Gallery - Poster - Abstract ID: 328

Dr. Ricardo Tellez-Limon¹, **Dr. Rafael Salas-Montiel**², **Dr. Victor Coello**³, **Dr. Sylvain Blaize**²

1. CONACYT - CICESE Monterrey, 2. Université de technologie de Troyes, 3. CICESE Monterrey

Motivated by the miniaturization of optical devices for lab-on-a-chip applications, in this contribution we present an integrated hybrid plasmonic-photonic structure able to excite the localized surface plasmon resonance (LSPR) of a sub-diffractive periodic array of metallic nanowires (Fig. 1a). The system, fabricated with e-beam lithography and thermal evaporation processes, consists of a periodic array of 500 gold nanowires of thickness $h_x=30$ nm, width $w_z=75$ nm, length $L_y=300$ μm and period $\Lambda=185$ nm (Fig. 1b and c), integrated on top of an ion-exchanged glass waveguide (IExWg).

The device was experimentally characterized in the far- and near-field regimes with the use of transmission spectroscopy with a white-light source, and near-field scanning optical microscopy (NSOM) with a laser source. Due to the invariance of the nanowires along the y direction, their LSPR is only excited when the fundamental TM₀ mode of the IExWg propagates through the structure (Fig. 2a), and not when propagating the fundamental TE₀ mode of the IExWg (Fig. 2b). The transmission spectrum of the TM₀ mode measured at the output facet of the waveguide, exhibits broad depth with a minimum value around $\lambda=675$ nm, corresponding to the excitation of the LSPR of the nanowires (Fig. 2c).

Using the NSOM technique (Fig. 3) and analyzing the resulting images in the Fourier space, we identified two modes radiated into the air and glass substrate with effective indices $n_{\text{eff,sup}}=1.058\pm 0.073$ and $n_{\text{eff,rad}}=1.35\pm 0.073$, respectively, and the propagating TM₀ mode of the hybrid structure with an effective index $n_{\text{eff,TM}_0}=1.496\pm 0.073$. No other mode was observed in the structure, implying that there is no light propagation along the metallic nanowires.

This interesting result means that even when the structure is a sub-diffractive metallic grating, there is no strong coupling of the plasmonic resonances between adjacent nanowires. Hence, the hybrid system can be regarded as a collection of almost individual localized light sources excited with the photonic TM₀ mode of the IExWg. Due to the ultra-low coupling loss with commercial single-mode optical fibers in the visible range, the proposed system opens new perspectives in the design of optical chips to control light at the nanoscale for biosensing applications.

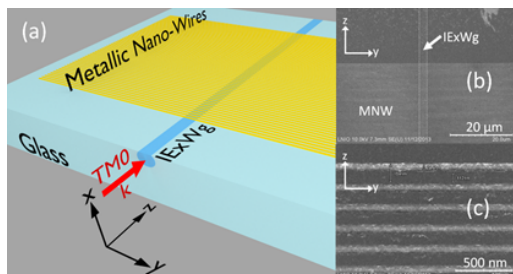


Fig1 structure.png

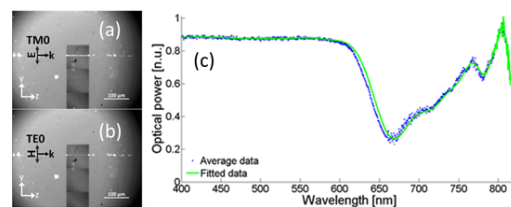


Fig2 far field.png

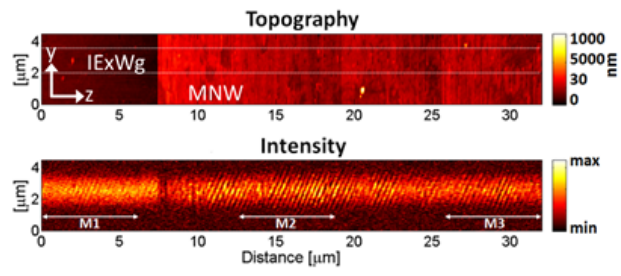


Fig3 near field.png

Efficient detection of rare cells using CMOS-based low-cost quantum dot camera

Wednesday, 13th September - 13:30 - Poster Session - Gallery - Poster - Abstract ID: 357

Mr. Kevin Huang¹, Mr. Benjamin Ding¹, Dr. Zhimin Ding¹

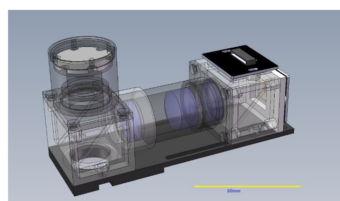
1. Anitoo Systems LLC

With the recent advancement in semiconductor process technology, new opportunities towards low-cost cell and molecular imaging have emerged. One application involves the detection of cancer cells that are tagged with antibody-conjugated nano-particles in the blood sample[1][2][3]. In this project, we present a multi-fluorescence camera that is small and portable. When combined with a disposable microfluidic chip carrier, it can be used to image and search for rare cells in a blood sample at point-of-care settings. This would potentially allow cancer monitoring and detection in patients without having to undertake painful and expensive lab tests. The camera utilizes multiple ultra-low-light CMOS sensor chips and a low power LED to visualize and manipulate quantum-dot labeled nanoparticles of interest in the bloodstream. Since fluorescence emitting quantum-dot materials have distinct emission spectrum while sharing the same excitation wavelength, quantum-dot labeled nanoparticles demonstrate excellent multiplexing capability and enables fast detection. In our system, once the desired fluorescent nano-particle images are captured, they are sent to a companion Android app via Bluetooth connection for further analysis. This app can be installed on any Android phone or tablet and features a user friendly interface to display imagery as well as generate diagnostic findings and recommendations. In this work, we take advantage of existing technological innovations in the IT world to provide potentially affordable, portable instrument and more user-friendly interface for cancer detection and cancer patient care.

[1] Nagrath, S. (2007, December 20). Isolation of rare circulating tumour cells in cancer patients by microchip technology. *Nature*. 450(7173): 1235–1239

[2] Thorban, S., Roder, J. D., Nekarda, H., Funk, A., Siewert, J. R., & Pantel, K. (1996). Immunocytochemical Detection of Disseminated Tumor Cells in the Bone Marrow of Patients With Esophageal Carcinoma. *JNCI Journal of the National Cancer Institute*, 88(17), 1222-1227. doi:10.1093/jnci/88.17.1222

[3] Wit, S. D., Dalum, G. V., Lenferink, A. T., Tibbe, A. G., Hiltermann, T. J., Groen, H. J., . . . Terstappen, L. W. (2015, July 17). The detection of EpCAM+ and EpCAM- circulating tumor cells. <https://www.nature.com/articles/srep12270>



(Top) Miniaturized Quantum dot camera build with Ultra-low-light CMOS image sensor.

(Bottom) Detection of magnetic-beads tagged using 2-channel Quantum dot camera (Red 635nm, Green 540nm.)



Red channel

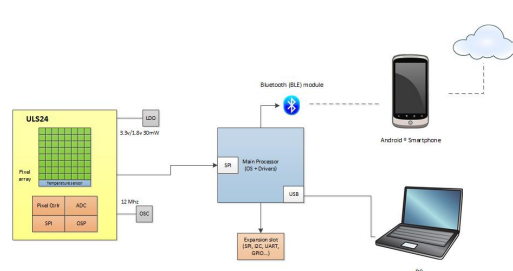


Green channel



Negative control

Qdcam.png



Blockdiagram.jpg

Active Hybrid Hydrogel-Metallic Nanostructures for Plasmonic Biosensor Applications

Wednesday, 13th September - 13:30 - Poster Session - Gallery - Poster - Abstract ID: 363

Mr. Nestor Gisbert Quilis¹, Mr. Marcel van Dongen², Mr. Christian Petri³, Prof. Ulrich Jonas³, Prof. Wolfgang Knoll¹, Prof. Martin Möller², Dr. Ahmed Mourran², Dr. Jakub Dostalek¹

1. Biosensor Technologies, AIT-Austrian Institute of Technology GmbH, 2. DWI - Leibniz Institute for Interactive Materials, Aachen, 3. Macromolecular Chemistry, Department Chemistry - Biology, University of Siegen

Plasmonic nanostructures offer attractive means for improving response in optical spectroscopy techniques that are employed for detection of ligand–analyte interactions. Metallic nanostructures have been exploited for strong signal amplification in areas including surface-enhanced Raman spectroscopy (SERS), surface enhanced infrared absorption spectroscopy (SEIRA), and surface plasmon-enhanced fluorescence spectroscopy (SPFS). The paper will present a novel method for preparing hybrid nanostructures composed of metallic nanoparticles and responsive hydrogel materials¹ by using template stripping² and UV laser interference lithography³. These structures are prepared over cm² area and exhibit tailored and actively tunable optical properties. The implementation of prepared responsive structures for sensitive monitoring of biomolecular binding events by SPFS will be demonstrated.

[1] Mateescu, A.; Wang, Y.; Dostalek, J.; Jonas, U. Thin hydrogel films for optical biosensor applications. *Membranes* 2012, 2 (1), 40-69.

[2] Sharma, N.; Keshmiri H.; Zhou X.; T.I. Wong, Petri, C.; Jonas, U.; , B. Liedberg, J. Dostalek, Tunable plasmonic nanohole arrays actuated by responsive hydrogel cushion, *Journal of Physical Chemistry C*, 2016, 120, 561-56

[3] Sharma, N.; Petri, C.; Jonas, U.; Dostalek, J. Reversibly tunable plasmonic bandgap by responsive hydrogel grating. *Optics Express* 2016, 24 (3), 2457.

H⁺ ions beam irradiation-induced interconnections between Ni-NWs for transparent conducting electrodes

Wednesday, 13th September - 13:30 - Poster Session - Gallery - Poster - Abstract ID: 505

Ms. Shehla Honey¹

1. University of the Punjab, Lahore

This study is based on fabrication of interconnections between Ni-NWs on small scale in various shapes such as II-, X-, V-, T-shapes etc by MeV H⁺ ions beam irradiation-induced nanoscale welding approach. Ni-NWs are exposed to 2.75 MeV H⁺ ions at beam fluence $\sim 1 \times 10^{16}$ ions/cm² and temperature is kept at room temperature. Transmission electron microscopy (TEM), scanning electron microscopy (SEM) and x-ray diffraction (XRD) results show that perfect interconnections are fabricated between Ni-NWs with stable crystal structure. Subsequently, a two-dimensional large scale random mesh of Ni-NWs is fabricated by 3 MeV H⁺ ions beam irradiation-induced nanoscale welding of Ni-NWs at contact positions. 3 MeV H⁺ ion beam induced large scale mesh fabrication of Ni-NWs is investigated by transmission electron microscopy (TEM) and scanning electron microscopy (SEM) and x-ray diffraction (XRD) techniques. Moreover, electrical and optical characterizations of these Ni-NWs are made using UV-VIS spectroscopy and four probe techniques. It is found that at a beam fluence of $\sim 10^{15}$ ions/cm², perfect II-, X-, and V-shape interconnects between Ni-NWs are achieved and finally lead to the fabrication of an optimum welded large scale Ni-NWs mesh with stable morphology and structure of NWs. These meshes are electrically conductive and optically transparent. Moreover, results show that Ni-NWs mesh is fabricated in three steps: (i) H⁺ Ions beam induced heat spikes leads to local heating of Ni-NWs, (ii) formation of interconnections between Ni-NWs on small scale, (iii) formation of interconnections between Ni-NWs on large scale. Large scale Ni-NWs meshes are suitable for application as transparent conducting electrodes in optoelectronic devices. H⁺ ions beam irradiation-induced nanoscale welding of Ni-NWs could improve electrical performance of Ni-NWs mesh by reducing contact resistance between NWs. This observation is also important for application of optoelectronic devices based on Ni-NWs in extreme environment such as in upper space where H⁺ ions are abundant in MeV to GeV energy range.

Rational design of nanoscale building blocks: silver and gold D_{5h} nanostructures for sensing applications

Wednesday, 13th September - 13:30 - Poster Session - Gallery - Poster - Abstract ID: 194

*Ms. Nicole Ritter*¹, *Dr. Jennifer Chen*², *Dr. Vladimir Kitaev*¹

1. Wilfrid Laurier University, 2. York University

Nanostructure design is a way of developing nanoscale building blocks with end functions in mind. The rational design pathway starts with the desired applications, assessing required properties for such applications, and then realizing those properties through nanoparticle synthesis. Noble metal nanoparticles exhibit a localized surface plasmon resonance (LSPR) that has proven advantageous in sensing applications such as surface plasmon resonance (SPR) spectroscopy and surface enhanced Raman spectroscopy (SERS). Desirable properties for these applications include sharp LSPR peaks and high stability for SPR, and structures with regular cavities by non-close packing (creation of hot spots in film preparation) and cavitation (creation of hot spots within nanostructures) for SERS. All of these properties can be achieved with silver and gold D_{5h} (decahedral) nanoparticles. Silver decahedral nanoparticles (AgDeNPs) are first prepared with low size dispersity (sharp LSPR peaks) and then used as seeds for gold plated/shell, bimorphic and star morphologies. Synthesis and LSPR tuning of these nanostructures will be presented, as well as preliminary testing in SPR and SERS. Briefly, the nanomole detection of halides using SPR, and 10⁷ enhancement with near monolayer films in SERS have been reliably achieved.

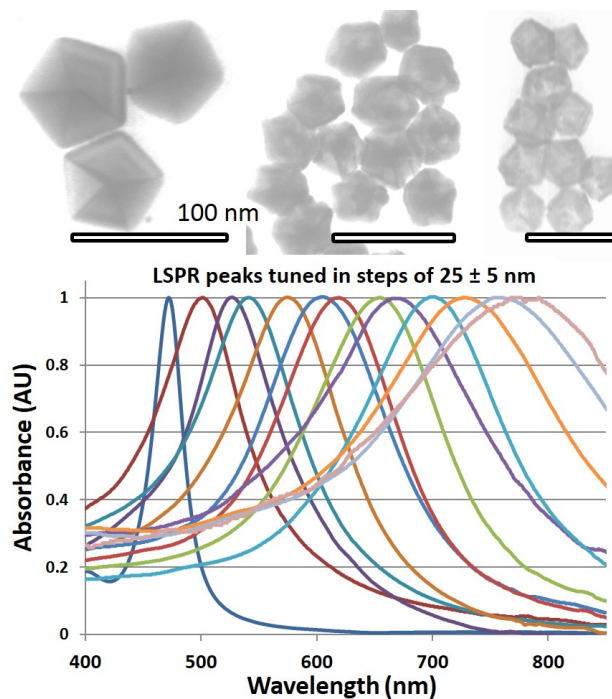


Figure1 lspr tuning.jpg

Dynamics and kinetics study of individual QD at UME surface

Wednesday, 13th September - 13:30 - Poster Session - Gallery - Poster - Abstract ID: 280

Mr. Abdallatif Alshalfouh¹

1. Carl von Ossietzky Universität Oldenburg

In the last decade, fluorescent semiconductor nanoparticles (quantum dots, QD) have gained increasing interest in various applications such as photovoltaic or bioanalytics. Although there have been several studies on QD redox- and electrochemistry like performed by Amelia et al. [1], the knowledge of dynamics and kinetics of individual QDs at electrode surfaces is still limited, because we cannot distinguish between electrochemically active and non active QDs in a heterogeneous mixture.

Adsorption and desorption of nanoparticles on microelectrodes already has been subject of investigation [2]. In order to obtain more detailed information, the electrochemical reactivity of single particles on the surface of an ultra microelectrode is observed via single molecule spectroscopy and time resolved fluorescence spectroscopy. These methods allow an effective observation of adsorption and desorption of QDs to the electrode surface, and furthermore kinetics of QD modification or degradation processes. In order to enable a correlation of optically registered events and electrochemical events, the diameter of the UME is matched to the size of the optical observation volume, typically around 1 μm . For data evaluation, cross correlation analysis is employed.

[1] M. Amelia, C. Lincheneau, S. , A.Credi, Electrochemical properties of CdSe and CdTe quantum dots, Chem.Soc. Rev., 2012, 41, 5728-5743.

[2] A. Boika, S. N. Thotgaard, A. J.Bard, Monitoring the electrophoretic migration and adsorption of single Insulating Nanoparticles at Ultramicroelectrodes, J. Phys. Chem. B., 2013, 117,4371-4380

Organic microcavity laser based on high gain monolayer

Wednesday, 13th September - 14:30 - Optical properties of nanostructures - Auditorium - Oral - Abstract ID: 360

Dr. Alexander Palatnik¹, Dr. Hagit Aviv¹, Dr. Yaakov Tischler¹

1. Bar-Ilan University

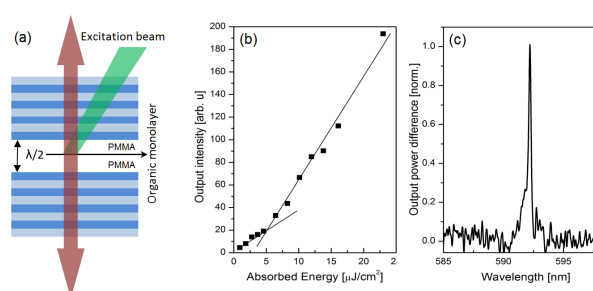
Microcavity lasers in which the emission occurs perpendicular to the device plane such as in a Vertical Cavity Surface Emitting Laser (VCSEL) are used in many applications including telecommunications and large-scale photonics integration, however no coherent emission from monolayer based microcavity devices have been observed so far. Commonly, in Organic VCSELs, the active media which provides optical gain is distributed between two mirrors of the microcavity. In this work fluorescent molecules are confined into a single molecular layer providing surprisingly high optical gain of more than 1000 cm^{-1} [1]. This is the first demonstration of lasing using an organic monolayer and the first demonstration of lasing with any monolayer in planar microcavity configuration.

The optical gain is provided by amphiphilic fluorescent dye, Lissamine Rhodamine B sulfonyl didodecyl amine (LRSD). LRSD was assembled into a monolayer via Langmuir-Blodgett deposition. Despite the relatively high concentration of molecules in the monolayer, $\sim 0.3/\text{nm}^2$, the dye shows high quantum yield. The device was assembled from two separately grown highly reflective mirrors with distance between them $\lambda/2$ using spacers of Poly(methyl methacrylate) (Fig. 1a). With such a design, we were able to achieve microcavity quality factor of $Q > 6000$.

Lasing was observed upon excitation by nanosecond pulses at a threshold absorbed energy density of $4.4\ \mu\text{J}/\text{cm}^2$, when 5% of the fluorescent molecules were excited. Lasing was accompanied by a change in slope of the output intensity curve, the appearance of polarized emission, and a narrow spectral line above the threshold (Fig. 1 b-c). Tuning the microcavity, we observed lasing in the spectral region between 585 nm and 610 nm.

Monolayer based Organic VCSELs have potential for gain layer optimization at the molecular level and can be useful in engineering energy transfer dynamics for fluorescence based chemical sensing applications. By localizing the gain to a single nanometer thick slice of the electromagnetic field, such devices can enable coherent coupling between excitons and thus ultimately lead to superradiant lasing and other fundamental studies on quantum coupling between light and molecules in monolayers.

[1] A. Palatnik et al., ACS Nano, 11(5), 4514-4520 (2017).



Monolayer laser.png

Nonlocality in metallo-dielectric nanostructures

Wednesday, 13th September - 14:47 - Optical properties of nanostructures - Auditorium - Oral - Abstract ID: 327

Dr. Antoine Moreau¹, ***Mr. Armel Pitelet***¹, ***Prof. Emmanuel Centeno***¹, ***Mr. Nikolai Schmitt***², ***Dr. Stéphane Lanteri***², ***Dr. Claire Scheid***²

1. Université Clermont Auvergne, 2. INRIA

Drude's model is at the very heart of plasmonics, providing the almost unique way to take into account the response of metals. In 2012, a landmark experiment showed that Drude's model is not able to accurately give the resonance of nanospheres closely coupled to a metallic film because it neglects the repulsion between electrons inside the metal. Since then, a lot of progress has been made from a theoretical and numerical point of view, by using a hydrodynamic model to better describe the response of metals.

Numerical tools solving the equations of the hydrodynamic model are now available for multilayers or even complex geometries. For multilayered structures, the solution being analytical, it is possible to generalize the scattering matrix formalism to take into account spatial dispersion very easily. A code implementing this technique has been recently made available. For complex geometries, numerical tools have been recently developed: while some authors have proposed comsol add-ons, recently, a Galerkin-discontinuous method has been developed and tested. Using the above mentioned numerical tools, it is possible to build on the idea that nonlocality cannot be neglected when plasmonic guided modes with high wavevectors are excited. Analytical calculations indeed show that the influence of spatial dispersion is controlled by a parameter proportional to the square of the wavevector. Physically this means that when the effective wavelength of the guided modes shrinks down to a scale close to the free mean path of electrons, then spatial dispersion has a real influence on the guided mode.

We have been working in the direction of proposing feasible experiments that would allow to measure accurately the nonlocal parameters. Using the most realistic and conservative material and model parameters, we came up with several designs that should be sensitive to nonlocality. This includes prism couplers, grating couplers in high-index dielectrics, nanoslit arrays and patch antennas.

Our work not only paves the way for future much needed experiments, it gives a much more accurate idea of what the limits of Drude's model actually are and in which situation issues are likely to arise.

Super-resolution photoluminescence microspectroscopy of individual metal-halide perovskite nanowires: defect-induced local variation of crystal phase transition temperature

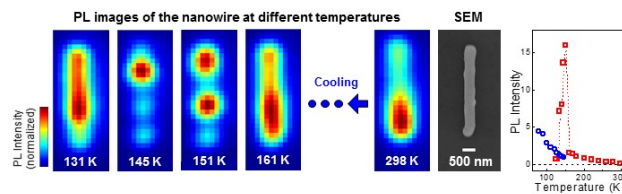
Wednesday, 13th September - 15:04 - Optical properties of nanostructures - Auditorium - Oral - Abstract ID: 453

Dr. Alexander Dobrovolsky¹, Dr. Aboma Merdasa¹, Dr. Eva Unger¹, Prof. Arkady Yartsev¹, Prof. Ivan Scheblykin¹
 1. Lund University

Solution-processed organometal halide perovskites are hybrid semiconductors that are of high interest for low-cost and efficient solar cells, light-emitting diodes and laser devices. Despite the rapid development of their applications, there is still limited understanding of the fundamental photophysics in these materials. These soft crystalline solids undergo phase transitions, which alter the electronic and optical properties of the material significantly. In the current contribution, we present the study of transition from the tetragonal to orthorhombic crystal phase in individual methylammonium lead triiodide $\text{CH}_3\text{NH}_3\text{PbI}_3$ nanowires by temperature-dependent photoluminescence microspectroscopy and super-resolution imaging which was very recently published [1]. A wide range of phase transition temperatures in $\text{CH}_3\text{NH}_3\text{PbI}_3$ has been reported in the literature; however, the cause of this variability remains unclear. Here we studied high-quality $\text{CH}_3\text{NH}_3\text{PbI}_3$ nanowires grown by a surface-initiated solution fabrication method. We directly observed that tetragonal and orthorhombic crystal phases coexist in the same intact nanowire crystal in the form of nano-domains in the phase transition temperature range below 160 degrees Kelvin. The characteristic sizes of crystal phase domains and their temperature variation were estimated by super-resolution analysis of the photoluminescence images. We show that the temperature of crystal phase transition in these nanowires is strongly influenced by the concentration and nature of local defects. We observed a drastic photoluminescence enhancement during cooling from 160 to 140 K and a high spatial inhomogeneity of the photoluminescence (see spotty intensity pattern on a figure), which can be explained by formation of domains with defects being pushed out to the high-bandgap orthorhombic phase. The photoluminescence then stems from the remaining less-defected low-bandgap tetragonal domains where the charge carriers generated in the orthorhombic domains are trapped. This effect may lead to new ideas for perovskite material manipulations to enhance their optoelectronic properties.

References

[1] A. Dobrovolsky, A. Merdasa, E.L. Unger, A. Yartsev, I.G. Scheblykin, "Defect-induced local variation of crystal phase transition temperature in metal-halide perovskites," *Nature Communications* **8**, 34 (2017).



Temperature dependences of the pl images and intensities of the pl bands associated with the tetragonal red squares and orthorhombic blue circles domains.jpg

Optical spirals and Möbius strips on all-dielectric optical antennas

Wednesday, 13th September - 15:21 - Optical properties of nanostructures - Auditorium - Oral - Abstract ID: 225

Dr. Aitzol Garcia-Etxarri¹

1. Donostia International Physics Center

The study of the optical response of high refractive index nano-particles has revealed that these resonant structures are capable of controlling different degrees of freedom of light fields with unprecedented versatility. The ability of these particles to control the intensity, phase and polarization of light has unveiled a plethora of new physical effects. To mention a few, these particles have allowed controlling the directionality of optical antennas in an unprecedented manner, they have shown promise in enhancing chiro-optical spectroscopic techniques and they have led to a generalized Brewster's condition to achieve full polarization of light.

In this talk, we unveil a two new phenomena that to the best of our knowledge were not reported up to date; the natural generation of an optical vortex in the back scattering of Silicon nanospheres and the emergence of a Möbius strip structure in the main axis of the polarization ellipse around lines where the scattered light is circularly polarized.

Firstly, based on singular optics arguments, we deduce the emergence of the vortex for a high index nano-particle illuminated by circularly polarized light at the first Kerker condition. Using the recently developed helicity and angular momentum conservation framework, we prove that the modulus of the topological charge of the vortex has to be equal to 2. We verify our predictions through analytic and numerical calculations (Figure 1a).

Secondly, we analyze the emergence of polarization singularities (C lines and L surfaces) in the scattering of optical resonators excited by linearly polarized light. We demonstrate both analytically and numerically that high refractive index spherical resonators present such topologically protected features and calculating the polarization structure of light around the generated C lines, we unveil a Möbius strip structure in the main axis of the polarization ellipse when calculated on a closed path around the C line (Figure 1b).

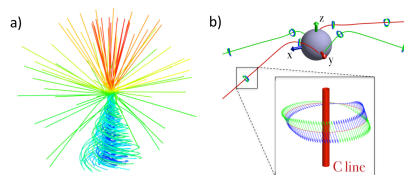


Figure abstract garciaetxarri.png

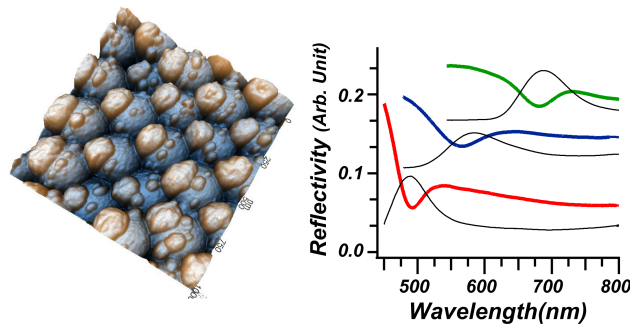
Optical properties of Ag nanocap decorated SiO₂ opal plasmonic photonic crystals and their applications

Wednesday, 13th September - 15:38 - Optical properties of nanostructures - Auditorium - Oral - Abstract ID: 391

***Prof. Hung-Chih Kan*¹, *Mr. Ti-Li Lin*², *Mr. Jiun-Hong Lin*¹, *Mr. Jian-Hung Chu*¹**

1. Department of Physics, National Chung Cheng University, 2. National Chung Cheng University

We fabricated plasmonic-photonic crystal that consists of SiO₂ nanosphere opal decorated with silver nanocaps with self-assembly methods. Optical measurements of the sample show anomalous suppression of the reflectivity in the spectral range of the photonic band gap of the opal structure, which results in an inverted reflection peak in the spectrum compared to that of a bare opal structure. Our numerical simulations indicate that the coupling between the excitation of Ag-cap surface plasmon and the scattering of the incident light inside the opal lead to the suppression of the opal reflection at the photonic bandgap wavelengths. We apply such coupling to identify light diffraction from the opals surfaces as the physical mechanism responsible for the the high-order reflection peaks in the specular reflection spectra, whose origin has been long searched since their discovery.



2017 abstract figures hck.png

Local Charge Transfer and Enhanced Light Emission of Monolayer MoS₂ Hybridized with Copper Phthalocyanine Nanoparticles

Wednesday, 13th September - 15:55 - Optical properties of nanostructures - Auditorium - Oral - Abstract ID: 96

*Mr. Ganesh Ghimire*¹, *Mr. Shrawan Roy*¹, *Mr. Subash Adhikari*¹, *Mr. Dinh Hoa Loung*¹, *Mr. Jinbao Jiang*¹, *Mr. Hyun Kim*¹, *Dr. Seong Gi Jo*², *Prof. Young Hee Lee*¹, *Prof. Jinsoo Joo*², *Prof. Jeongyong Kim*¹

1

1. Sungkyunkwan University, 2. Korea University

The study of external doping and hybridization of 2-dimensional monolayer transition metal dichalcogenides (1L-TMDs) with various organic and inorganic nanostructures for modifying their optoelectronic properties is the hot topic of research nowadays. However, hybridization of organic semiconducting nanostructure with 1L-TMDs are rarely reported. Organic semiconducting nanostructure and 1L-TMDs could be suitable for tailoring the optoelectronic properties of 1L-TMDs. In this study, we synthesized organic semiconducting copper phthalocyanine (CuPC) nanoparticles (NPs) of size ~30 nm, using re-precipitation method, and decorated on 1L-MoS₂ grown by chemical vapor deposition (CVD) method. We observed about 6-fold enhanced in photoluminescence (PL) of 1L-MoS₂ from the CuPC NPs decorated regions as shown in Fig. 1. This enhancement of PL of 1L-MoS₂ in CuPC decorated region is mainly due to localized p-doping effect caused by CuPC NPs. Such organic nanostructure/1L-MoS₂ hybrid system could be suitable for future optoelectronic device applications. Detail will be presented.

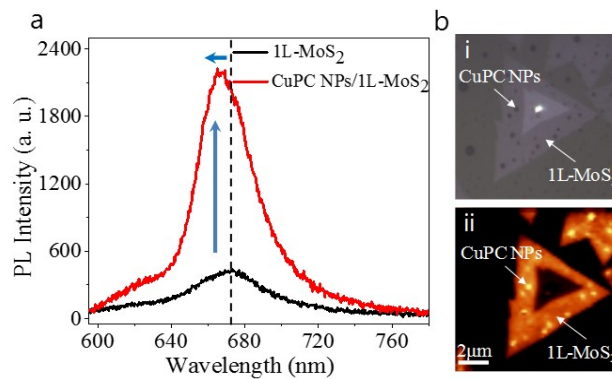


Figure 1: (a) PL spectra of pristine 1L-MoS₂ and CuPC NPs decorated 1L-MoS₂. (b) Optical micrograph (i) and PL mapping images (ii) of CuPC NPs decorated 1L-MoS₂ hybrid sample.

Figure1.jpg

Hybrid plasmonic - all-dielectric nanodimers for second-harmonic generation

Wednesday, 13th September - 14:30 - Nonlinear nano-optics - Room 207 - Oral - Abstract ID: 379

***Dr. Mihail Petrov*¹, *Mrs. Flavia Timpu*², *Dr. Nicholas R. Hendricks*², *Dr. Songbo Ni*³, *Dr. Claude Renault*², *Dr. Heiko Wolf*⁴, *Prof. Lucio Isa*³, *Prof. Yuri Kivshar*⁵, *Prof. Rachel Grange*²**

1. ITMO University, **2.** Optical Nanomaterial Group, Institute for Quantum Electronics, Department of Physics, ETH Zürich, **3.** Laboratory for Interfaces, Soft Matter, and Assembly, Department of Materials, ETH Zürich, **4.** IBM Research–Zurich, **5.** Nonlinear Physics Center, Australian National University

Hybrid nanoscale structures which combine properties of dielectric and plasmonic components, currently attract a lot of attention. Such structures would be particularly useful to combine nonlinear optical properties of dielectrics with linear plasmon resonances in order to enhance low-intensity signals at the nanoscale (see Fig. 1). Nowadays, it is feasible to fabricate nanodimers with a single material using the standard microelectronics techniques, but constructing hybrid nanodimers consisting of two dissimilar materials is still a challenge. Here, we demonstrate a template assisted colloidal assembly technique to fabricate nonlinear hybrid nanodimers composed of 80 nm gold (Au) and 100 nm BaTiO₃ nanoparticles. The dark-field optical images of isolated gold nanoparticles and after assembly with BaTiO₃ show a change of the scattering spectrum due to the effective nanoparticle interaction. The hybrid nanostructures benefit from the surface plasmon resonance of the Au nanoparticles at the second-harmonic wavelength to enhance a nonlinear signal originated from the BaTiO₃ nanoparticles. We measure a nonlinear signal from the hybrid nanodimers and demonstrate up to 10 times enhancement in comparison to isolated BaTiO₃ particles. The maximal enhancement is observed when the second-harmonic wavelength coincides with the resonance of localized surface plasmons of gold nanoparticle (see Fig. 2). The performed numerical calculations of both linear and nonlinear spectra of the hybrid nanodimer reveal that the Au particle in the dimer operates as a nanoantenna enhancing the emission at the second-harmonic wavelength. Moreover, we discuss the efficiency of nonlinear signal generation when the hybridization plasmonic and all-dielectric modes takes place.

The work has been supported by the Russian Ministry of Science and Education (project #RFMEFI58416X0018). The authors also acknowledge the Swiss National Science Foundation (SNSF) (grants IZLRZ2_163916 and PP00P2_150609) and the Australian Research Council.

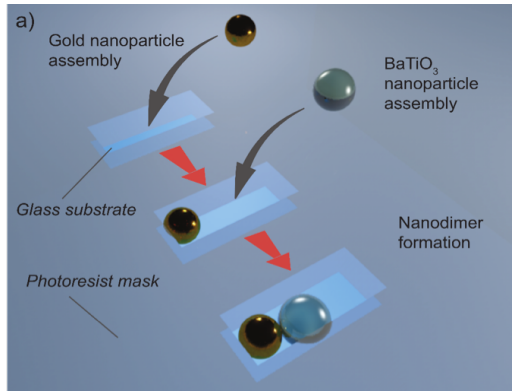


Fig1.png

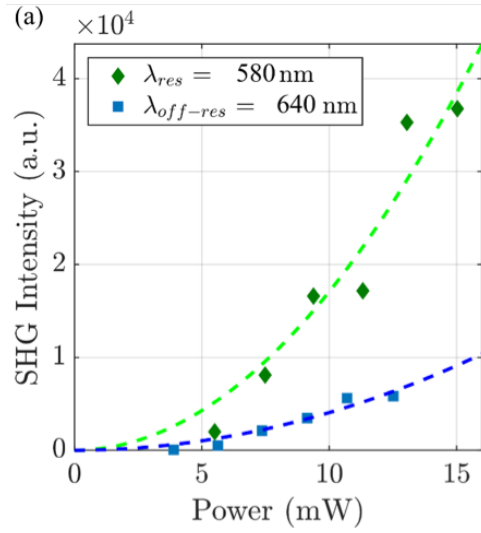


Fig2.png

Extreme nonlinear optical phenomena enabled by plasmons in nanostructured graphene

Wednesday, 13th September - 14:47 - Nonlinear nano-optics - Room 207 - Oral - Abstract ID: 195

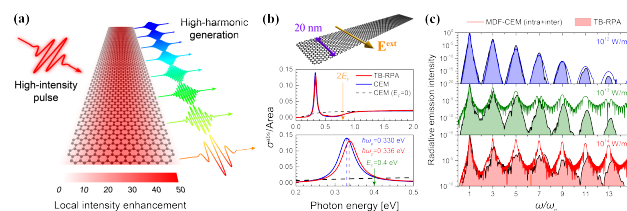
Dr. Joel Cox¹, Prof. Javier Garcia De Abajo²

1. ICFO-Institut de Ciències Fotoniques, The Barcelona Institute of Science and Technology, 08860 Castelldefels (Barcelona), Spain, 2. ICFO-The Institute of Photonic Sciences

The remarkably high intrinsic nonlinearity of graphene can be pushed even further when the frequency of impinging light matches that of its long-lived and electrically-tunable plasmon resonances. Through their enhanced absorption cross-sections, plasmons in highly-doped graphene provide the means to concentrate electromagnetic energy on extreme subwavelength scales, generating enormous local electric fields. We explore the regime of extreme nonlinear optics that is enabled by plasmonic near-field enhancement in nanostructured graphene. In particular we focus on (1) the generation of high-order harmonics and (2) transient absorption arising from elevated electronic temperatures in the carbon layer upon ultrafast optical pumping. Our studies of these plasmon-assisted nonlinear phenomena are based on rigorous time-domain simulations, where graphene structures are described using an atomistic tight-binding description of their electronic states combined with the random-phase approximation.

Our results indicate that high-harmonic generation can be achieved with remarkably low input optical powers by tuning the incident light wavelength to the localized plasmon resonances of ribbons and finite islands, while these resonances can be modulated via electrical gating. In contrast to atomic gases, we observe no cutoff in harmonic order, while a comparison of graphene plasmon-assisted high-harmonic generation to recent measurements in solid-state systems suggest that the yields from bulk semiconductors can be produced by graphene plasmons using 3-4 order of magnitude lower pulse fluence. At the fundamental excitation frequency, a delayed nonlinearity also takes place as a consequence of the strong dependence of the graphene response on the temperature of its conduction electrons. We demonstrate that strong transient modulation of the optical absorption associated with plasmonic excitations in graphene nanostructures can occur when electrons are optically pumped to an elevated temperature. Our results indicate that doped graphene nanostructures hold great promise for efficient higher-harmonic generation and all-optical switching applications in nonlinear nanophotonic devices.

Figure 1 shows (a) a schematic illustration of a doped nanoribbon illuminated by an intense optical pulse emitting high harmonics; (b) the absorption cross-section of a 20-nm wide nanoribbon exhibiting a prominent plasmonic mode; (c) the spectral decomposition of the light emission intensity under illumination by pulses centered at the plasmon resonance frequency.



Hhg from a graphene nanoribbon.png

Dynamics of ultra small semiconductor lasers

Wednesday, 13th September - 15:04 - Nonlinear nano-optics - Room 207 - Oral - Abstract ID: 61

Prof. FREDERIC GRILLOT¹, Mr. Jean-maxime Sarraute², Dr. Kevin Schires³, Prof. Sophie Larochelle²

1. Telecom ParisTech - Universite Paris-Saclay, 2. UNIVERSITE LAVAL, 3. Telecom ParisTech - Université Paris Saclay

Semiconductor lasers represent an exceptional success story of breakthroughs in fundamental physics. In particular, laser structures with small cavity volumes are becoming attractive candidates for high-speed direct modulation, with bandwidths much beyond those of conventional semiconductor lasers due to small volume and short radiative carrier lifetime. The attractiveness of ultra small devices relies in the dimensions of the optical cavity, close to or below diffraction limit. First, this offers promise for tighter integration of optoelectronic devices on a microchip and for reduced energy consumption per transmitted bit of information, which are of vital importance for optical interconnection applications. To the best of our knowledge, little is known on the dynamics of such small devices, in particular close to their threshold where there is strong competition between spontaneous and stimulated emissions as well as potential for super-radiance effects. This work aims first at investigating the impact of the spontaneous emission rate and the Purcell factor on the static and dynamical responses of semiconductor lasers for which the cavity dimensions become close to the lasing wavelength. In the limiting case of dimensions below the diffraction limit, our analysis unveils that relaxation oscillation frequency, damping factor and 3-dB bandwidth are not necessary increased when compared to standard edge emitters (macro-lasers) or micro-lasers (VCSEL) under comparable pumping conditions. The last part will focus on the nonlinear dynamics under optical injection, which can be used to enhance the modulation dynamics. In this case, the light from an external master laser is injected into the slave laser, which can lock onto the master wavelength. The direct-modulation response of the injection-locked laser then exhibits a resonance at the frequency detuning between the master and slave lasers, which allows reaching 3-dB bandwidths much larger than the free-running bandwidth of the slave laser. Results reveal that devices with smaller size from close to below the diffraction limit allow an increase of the stable-locking area. Overall, the presented results will unveil the importance of the device miniaturization on the laser dynamics, in the context of developing novel laser sources for the aforementioned applications.

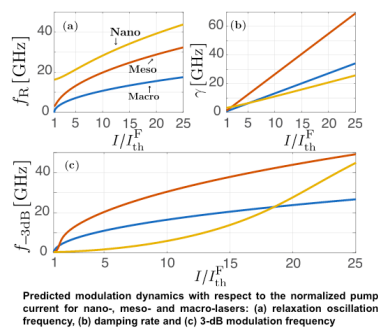


Illustration.png

Bispectral second-harmonic-generation in snake-shaped AlGaAs nanowires

Wednesday, 13th September - 15:21 - Nonlinear nano-optics - Room 207 - Oral - Abstract ID: 477

Ms. Natália Morais¹, Dr. Marco Ravano¹, Dr. Iannis Roland², Dr. Aristide Lemaitre³, Prof. Stefan Wabnitz⁴, Dr. Maurizio De Rosa⁵, Dr. Ivan Favero¹, Prof. Giuseppe Leo¹

1. Université Paris Diderot, 2. université, 3. Laboratoire de photonique et nanostructures, 4. Università di Brescia, 5. Istituto Nazionale di Ottica

High-contrast nonlinear nanophotonics is being increasingly recognized for its potential under different configurations, spanning from high-Q resonators to multi-pole nanoantennas, and nanowires. To confine photons at the nanoscale by total internal reflection, such devices rely on a high-refractive-index core surrounded by low-index cladding in one or more dimensions, and therefore they typically consist of semiconductor nanostructures that either lie on an oxide substrate or are suspended in air. Here we focus on periodically bent AlGaAs suspended nanowires with sub-wavelength cross section (about 0.1 μm height and 1 μm width) and macroscopic length (about 1 mm), whose $\chi^{(2)}$ nonlinearity benefits from a combination of birefringent phase matching and directional quasi-phase matching and results in second harmonic generation (SHG) in the telecom fiber wavelength range, with an efficiency $\eta_{\text{SHG}} \approx 10^{-3} \text{W}^{-1}$. Based on an $\text{Al}_{0.18}\text{Ga}_{0.82}\text{As}$ epitaxial layer on a [100] GaAs wafer, electron-beam lithography and inductively coupled plasma etching, we fabricated monolithic snake-shaped nanowires consisting of cascaded half-circles with opposite curvatures [1]. Since a 90° rotation around the (100) zinc-blend axis is equivalent to a crystallographic inversion [2], a virtual $\chi^{(2)}$ grating was implemented with a period equal to four 90° bends. By end-fire injecting a continuous-wave pump beam into the nanowires, we systematically reveal two distinct quasi-phase-matching spectral features whose separation in wavelength is set by the radius of curvature. While SHG in these nanowires can be seen as the unravelled version of the previously demonstrated SHG in a suspended microdisk [3], this is the first observation of a dual quasi-phase-matching resonance in a grating-less homogeneous waveguide.

REFERENCES

- [1] R. T. Horn and G. Weihs, "Directional Quasi-Phase Matching in Curved Waveguides", arXiv: 1008.2190 (2010).
- [2] Y. Dumeige and P. Feron, "Whispering-gallery-mode analysis of phase-matched doubly resonant second-harmonic generation", Phys. Rev. A 74, 063804 (2006).
- [3] S. Mariani et al., "Second-harmonic generation in AlGaAs microdisks in the telecom range", Optics Letters 39, 3062 (2014).

Electrostatic SHG from extreme nano-sized bi-metal structures

Wednesday, 13th September - 15:38 - Nonlinear nano-optics - Room 207 - Oral - Abstract ID: 510

Mr. Shlomo Levi¹, Dr. Avi Niv¹

1. Ben-Gurion University of the Negev

Introduction: Recent years saw the agglomeration of nonlinear optics (NLO) and nano-optics yielding new possibilities for nonlinear light matter interactions. Nonetheless the basic understanding of NLO has not changed since it was first introduced. We investigate the SHG from a metal nano-dimer where, unlike former accounts, dimer is made from two different metals. We show that the resulting SHG cannot be accounted for by existing theories if the dimer is made small enough. Encourage by this result we propose a new mechanism, beyond what is so far known, to explain our unique observations.

Methods: Samples are made by drying water immersed gold nanoparticles (GNPs) on a silver covered by SiO₂ separation layer. The dimer is obtained from the charges of these GNPs and their images within the silver. Samples are illuminated with a Ti:Sapphire laser, and the reflection is analyzed for SHG as shown in Fig. 1. The symmetry-breaking, which is essential for SHG, is obtained from the optical properties of the different metals, while its amount is controlled by the SiO₂ layer thickness - 5 nm for maximum interaction and up to 70 nm for disconnected sphere/surface.

Results: Figure 2 shows a scanned SHG images for 680 nm excitation of 5 nm GNPs for different SiO₂ layers. Dark regions indicate clustering of GNPs, while bright areas are sparse GNPs monolayers where data is collected from. Variations in SHG versus SiO₂ layer thickness are readily shown.

Discussion: Figure 3 shows the SHG of the GNPs nano-dimer in red. Note a maximum for 10 nm SiO₂ layer - an example of observation beyond existing theories. The prediction of a coupled harmonic-oscillator model with nonlinear Coulomb interaction is shown in blue. Good agreement indicates that such mechanism might be responsible for this unexpected result.

Summary: It is shown that nonlinear optics may hide yet unknown sources. Good agreement with a model gives rise to new possibilities for SHG as well as for NLO in general.

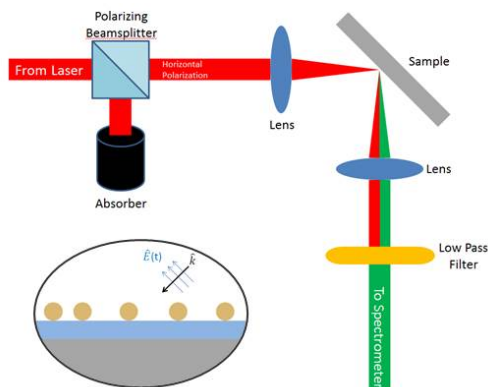


Fig1.jpg

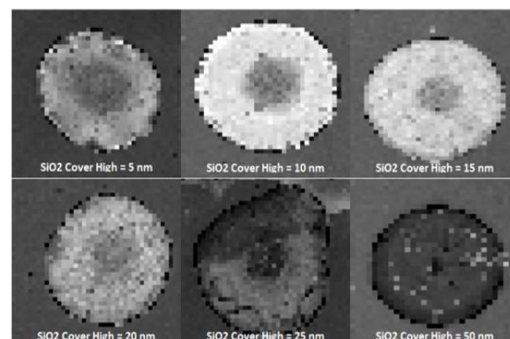


Fig2.jpg

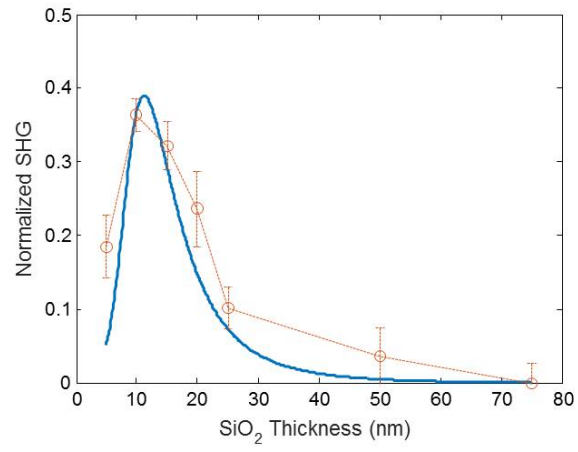


Fig3.jpg

Mid-Infrared Second Harmonic Spectroscopy of Tunable Phonon Polaritons in Atomic Scale Heterostructures

Wednesday, 13th September - 15:55 - Nonlinear nano-optics - Room 207 - Oral - Abstract ID: 334

Mr. Christopher Winta¹, Mr. Nikolai C Passler¹, Dr. Ilya Razdolski¹, Prof. Martin Wolf¹, Prof. Joshua D Caldwell², Dr. Alexander Paarmann¹

1. Fritz Haber Institute of the Max Planck Society, 2. Vanderbilt University

Surface polaritons are the key building block of nanophotonics, since these excitations provide sub-diffractive light localization accompanied by significant optical field enhancements. Many previous studies have focused on surface plasmon polaritons (SPPs) at the surface of noble metals.¹ Recently, an alternative approach was introduced using surface phonon polaritons (SPhPs)² which can be excited in the mid-infrared at the surface of polar dielectrics, where optical phonon resonances lead to the negative dielectric permittivity required for the surface polariton formation.

Here, we undertake a first step towards active tuning of the mid-infrared polaritonic properties in atomic-scale heterostructures of polar dielectric materials, so-called crystal hybrids.³ We employ mid-infrared second harmonic spectroscopy⁴ of AlN/GaN atomic scale superlattices to demonstrate active control over phonon polariton hybridization, that is tuning of hybrid phonon frequencies and linewidths with the relative and absolute AlN and GaN layer thicknesses. Additionally, we use Otto-type prism coupling⁵ to probe the evanescent modes of the crystal hybrid. These measurements provide a direct proof that the effective dielectric function of the hybrid material, as extracted from infrared ellipsometry, is fully predictive for the nanophotonic response of this new material. Our results lay out a novel route for tunable mid-infrared nanophotonics.

1. Maier, S. A. *Plasmonics: Fundamentals and applications. Plasmonics: Fundamentals and Applications* 1–223 (Springer US: 2007).
2. Caldwell, J. D. *et al.* Low-loss, infrared and terahertz nanophotonics using surface phonon polaritons. *Nanophotonics* **4**, 1–26 (2015).
3. Caldwell, J. D. *et al.* Atomic-scale photonic hybrids for mid-infrared and terahertz nanophotonics. *Nature Nanotechnology* **11**, 9–15 (2016).
4. Paarmann, A. *et al.* Second harmonic generation spectroscopy in the Reststrahl band of SiC using an infrared free-electron laser. *Applied Physics Letters* **107**, 081101 (2015).
5. Passler, N. C. *et al.* Second-Harmonic Generation from Critically Coupled Surface Phonon Polaritons. *ACS Photonics* **4**, 1048–1053 (2017).

Spectroscopy of single gold nanoparticles reveals strong heterogeneity in the kinetics of ssDNA functionalization

Wednesday, 13th September - 14:30 - Enhanced spectroscopy and sensing - Room 412 - Oral - Abstract ID: 365

Mr. Matěj Horáček¹, Dr. Rachel E. Armstrong¹, Dr. Peter Zijlstra¹

1. Molecular Biosensing for Medical Diagnostics, Faculty of Applied Physics, Eindhoven University of Technology, P.O. Box 513, 5600 MB, Eindhoven, The Netherlands

Plasmonic nanostructures have recently emerged as versatile and programmable nanomaterials for various applications. DNA-conjugated gold nanoparticles have great potential in fields of drug delivery or gene regulation and also constitute sensitive nanosensors for probing biological processes. The functionalization of gold nanoparticles with DNA has been studied extensively in solution, however these ensemble measurements do not reveal particle-to-particle differences. Here we study the functionalization of gold nanorods with single stranded DNA (ssDNA) at the single-particle level and find an unexpected kinetic heterogeneity.

We use single-particle scattering spectroscopy to show that the kinetics of ssDNA functionalization strongly depends on the pH and the ionic strength of the employed buffer, which we attribute to modulations of the effective charge on the ssDNA and on the particle. Surprisingly, we find binding rates that differ from particle-to-particle by an order of magnitude, even though the buffer conditions are identical. We analyse this behaviour in the context of DLVO theory, which indicates that this heterogeneity is caused by a distribution of energy barriers caused by particle-to-particle variations in surface charge.

In the future we plan to use these ssDNA-conjugated nanoparticles to study the conformational changes of single biomolecules using an asymmetric plasmon ruler consisting of a single gold nanorod and a tethered gold nanosphere. Conformational changes of the ssDNA result in modulations of the interparticle distance causing plasmon shifts. The bright and photostable plasmon allows us to probe these conformational changes on microsecond timescales and reveal the folding pathway in real-time.

Single protein detection by aptamer-labeled gold nanorods

Wednesday, 13th September - 14:47 - Enhanced spectroscopy and sensing - Room 412 - Oral - Abstract ID: 437

Dr. Rachel E. Armstrong¹, Dr. Peter Zijlstra¹

1. Molecular Biosensing for Medical Diagnostics, Faculty of Applied Physics, Eindhoven University of Technology, P.O. Box 513, 5600 MB, Eindhoven, The Netherlands

Introduction: Biosensors based on plasmonic gold nanorods have recently reached single-molecule sensitivity owing to the sensitivity of the nanorod plasmon to local dielectric changes. Previous studies have utilized gold nanorods to track protein-binding to the nanorod surface, but a system with tunable protein affinities, ie – aptamer-based systems, are attractive in that they are tunable to function at a range of biologically-relevant timescales and concentrations. Additionally, inhibition of nonspecific nanorod surface interactions is essential, as biological fluids contain a concentrated mixture of many proteins. In SPR studies, PEG molecule coatings have been demonstrated to effectively reduce surface charge and subsequently inhibit electrostatic attractions between large biomolecules and gold surfaces. Here, protein-targeting DNA aptamers were mixed with short, PEG molecules and appended to a gold nanorod surface. The plasmon wavelength was monitored to track single protein-aptamer binding events and the effect of PEG in suppressing non-specific interactions was investigated. **Method:** Following immobilization of gold nanorods on a coverslip, varying ratios of thiolated DNA aptamers and thiol-PEG were added to the coverslip. Next, protein solutions were introduced to the sample in a flow chamber setup. We employed dark-field, single-particle scattering spectroscopy to track the nanorod plasmon shifts due to single protein-aptamer binding events in real-time.

Results: In samples with mixed PEG:aptamer coverage, step-wise plasmon scattering intensity changes were observed upon protein addition, indicative of single protein binding events. In control samples without aptamer or PEG, non-specific interactions induced similar step-wise intensity changes. However, on nanorods coated with PEG alone, no plasmon scattering intensity change was observed, even at high protein concentrations.

Discussion: Single protein-aptamer binding events were successfully measured on samples containing a mixed PEG:aptamer surface, as indicated by step-wise changes in the plasmon scattering intensity. Additionally, surface coating with PEG successfully suppressed non-specific interactions with the nanorod surface. Future studies with this system include tuning the binding affinity of the aptamer to match biologically relevant concentrations and protein detection in biological fluids.

Plasmonic fluorescence enhancement for single-molecule electrochemistry

Wednesday, 13th September - 15:04 - Enhanced spectroscopy and sensing - Room 412 - Oral - Abstract ID: 149

*Dr. Martin Caldarola*¹, *Ms. Weichun Zhang*¹, *Ms. Biswajit Pradhan*¹, *Prof. Michel Orrit*¹

1. Leiden University

Introduction

Electrochemical (EC) reactions are of crucial importance in diverse fields of nanoscience. Here we achieved electrochemical measurements with fluorescent readout of the redox-sensitive dye, Methylene Blue (MB) at single-molecule (SM) level. Figure 1 shows the two-electron reduction reaction for MB, which is fluorescent in its oxidized state and non-fluorescent in the reduced state. Thus, by detecting the emitted fluorescent photons we can optically read the oxidation state of MB molecules.

Methods

In order to control the oxidation state of the molecules accurately and measure the optical response simultaneously we combined a fluorescence confocal microscope with a potentiostat. We work with immobilized MB molecules on a glass surface and we used two configurations, shown in figure 2: an ensemble of MB molecules (see Figure 2a), where no enhancement is needed, and single-molecule scheme, where we used gold nanorods to enhance fluorescence (see figure 2b). The surface chemistry was similar in both cases, with the addition of the gold nanorods and a lower MB superficial concentration to ensure that there is only one enhanced molecule at the tip of the nanorod.

Results and discussion

Firstly, we measured the fluorescence intensity from an ensemble of MB molecules at different applied electrochemical potentials to show our capability of reading the redox state optically, as evidenced in the curve of figure 3a. From these data we obtained a mid-point potential of 51 mV, shown with the dashed vertical line.

Secondly we studied the redox-induced blinking of single MB molecules. We measured *the same molecule* at different EC potentials (see figure 3b) and found that the blinking off-times increase when decreasing the EC potential (and vice versa for the on-times). We then plotted and fitted the ratio of on and off mean times at different potentials to extract the mid-point potential for every measured SM using the Nernst equation (figure 4a), obtaining the histogram of mid-point potentials shown in figure 4b.

In conclusion, we accessed the electrochemical properties of Methylene Blue at single-molecule level using an optical method based on fluorescence enhancement by individual gold nanorods.

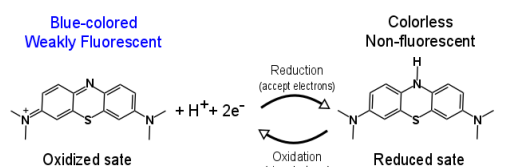


Figure 1: Two-electron reduction/oxidation reaction of Methylene Blue (MB). The oxidized species is fluorescent while the reduced is not.

Fig 1 mb redox reaction.png

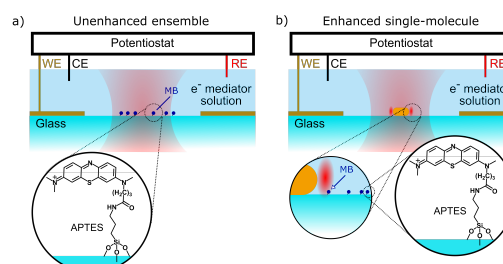


Figure 2: Electrochemistry with fluorescent readout. The schematics show the combined electrochemical-confocal setup and sample. a) unenhanced ensemble and b) enhanced single-molecule measurements (WE: working electrode, CE: counter electrode, RE: reference electrode). Note that there is no electrical connection between the MB molecules and the electrodes, thus an electron mediator solution is needed.

Fig 2 methods.png

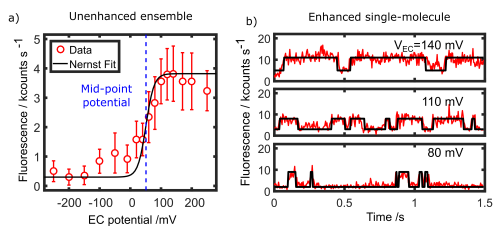


Figure 3: Electrochemical response of MB with fluorescence readout. a) unenhanced ensemble fluorescence signal for different applied electrochemical potentials. The black solid line is a Nernst fit. The dashed vertical line shows the mid-point potential at 51 mV. b) Enhanced single-molecule fluorescence time trace for the same molecule at different EC potentials. The blinking times are clearly responding to the EC potential. The black solid lines corresponds are the output of a step detection algorithm.

Fig 3 results 1.png

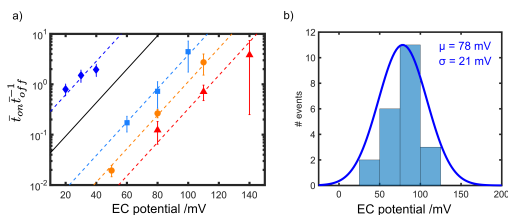


Figure 4: Single-molecule electrochemical properties of Methylene Blue. a) Ratio of on and off mean times from the blinking time traces as a function of applied EC potential. Each symbol represents a different molecule. The dashed lines are fits to the Nernst equation to extract the mid-point potential. The black line corresponds to the ensemble value. b) histogram of mid-point potentials obtained. The mean value is 78 mV and the dispersion 21 mV.

Fig 4 results 2.png

Improved Sensitivity of Optical Polarimetry with MEMS Machining and Microfluidics

Wednesday, 13th September - 15:21 - Enhanced spectroscopy and sensing - Room 412 - Oral - Abstract ID: 212

*Mrs. Maab Al-hafidh*¹, *Dr. Andrew Glidle*¹, *Dr. Anthony Kelly*², *Dr. Julien Reboud*¹, *Prof. Jonathan Cooper*¹

1. University of Glasgow/Biomedical Engineering, 2. University of Glasgow/Electronic and Nanoscale Engineering

Introduction

Polarimetry can provide important insights into the concentration and the molecular structure of chemical compounds in solution. The technique has been used in a variety of biochemical applications such as drug screening^[1]. Here we demonstrate a new method that significantly reduces the instrumentation required, without compromising performance, opening up the use of polarimetry in low volume, hand-held and multiplexed systems^[2].

We overcome the short optical path lengths inherent to microfluidic systems, which decrease optical rotation sensitivity, by using metal micromirrors to create multiple reflections across a capillary channel. Arranging the mirrors to obtain two reflections before passing through the sample volume (Figure 1) nullifies the 180 degrees flipping of the polarisation at each mirror before interrogating the sample through the subsequent pass, thus adding up rotation through multiple passes.

Methods

Our set-up (Figures 1 and 2) was modelled using simulations of the optical components in a Matlab environment, confirming functionality. It is controlled via computer programs (LabVIEW-Matlab), enabling to measure the polarisation of the He-Ne laser after three passes through solutions of D-glucose, using two reflections off silver mirrors at each step (Figures 1 and 2). The process was then repeated along the length of a capillary channel.

Results and Discussions

We analysed the increase in performance of the system but studying the rotation produced by different concentrations of glucose. The detection limit was enhanced 20 times when using only three passes with the mirrors (10 mM D-Glucose with (blue line) and 200 mM without reflections (red line) – Figure 3), while achieving an excellent linear correlation (Linear correlation $R^2 > 0.99$). The system achieved an angle resolution of 0.001 degrees, demonstrating the potential impact of our approach to increase sensitivity and thus open up microfluidic applications. We are now manufacturing micromirrors by taking advantage of the 45 degrees wet etching of silicon (Figure 4), to realise microfluidics-based polarimetry.

References

[1] Sofikitis, D., et al., “*Evanescent-wave and ambient chiral sensing by signal-reversing cavity ringdown polarimetry.*” *Nature*, **514**(7520): p. 76-79 (2014). [2] Tan, C., et al., *Frontiers of optofluidics in synthetic biology*. *Lab on a Chip*, **12**(19): p. 3654-3665 (2012).

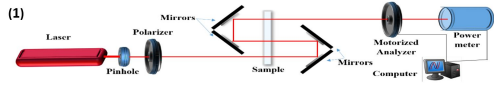


Figure1-system blog diagram.png

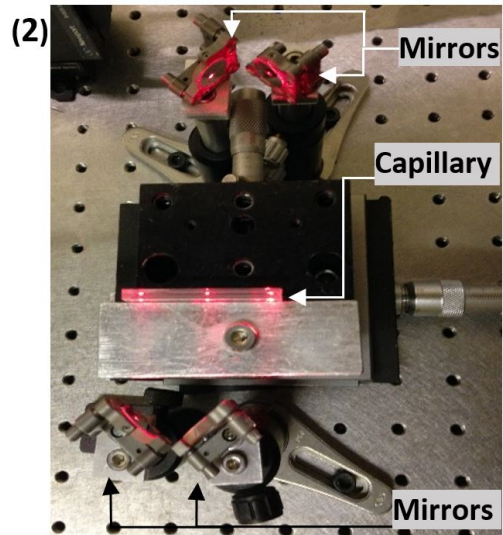


Figure2-experimental setup.png

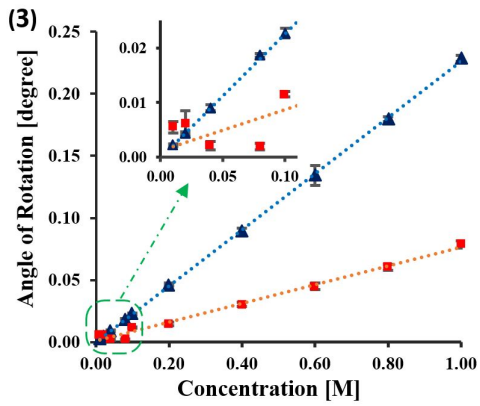


Figure3-optical rotation for different glucose concentrations for direct and multi-reflections setups.inset-for low concentrations.png

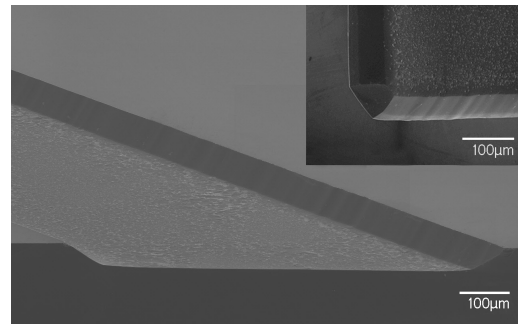


Figure4-koh etching of si 100 image to get 45degrees micro-mirrors.png

Surface Enhanced Raman Spectroscopy Assisted With Photonic Crystal

Wednesday, 13th September - 15:38 - Enhanced spectroscopy and sensing - Room 412 - Oral - Abstract ID: 23

Prof. Xiangwei Zhao¹

1. Southeast University

Raman-scattered photons from a molecule can directly reveal the signature of vibrational energy states of the molecule and their intensities can be greatly enhanced by plasmon of metal nanostructures or surfaces, which leads to high sensitivity. Therefore, surface enhanced Raman spectroscopy (SERS) attracts more and more attentions in bioanalysis recently. The probability of spontaneous Raman scattering is directly proportionally to the photon density of state (DOS) at related frequency. Therefore, structures that can increase DOS are desired in SERS applications. Photonic crystal (PC), which has periodic nanostructures relevant to the length of light, has photonic band gaps that forbidden the propagation of light in some frequency range. Therefore, PC has increased DOS at the band edge with respect to homogenous medium and provides a good candidate medium for the boost of light and plasmonic materials interactions. In this paper, I would like to discuss factors that affect SERS signals in the transducing process of biosensors and introduce our methods to boost SERS signals by combining self-assembled colloidal photonic crystal and plasmonic materials with respect to high sensitivity, multiplicity and simplicity. Our results showed that the micro/nano structure of photonic crystal could be used as a good platform for SERS sensors in biomedical applications like point of care testing (POCT), bacteria detection, cell analysis or multiplex bioassays.

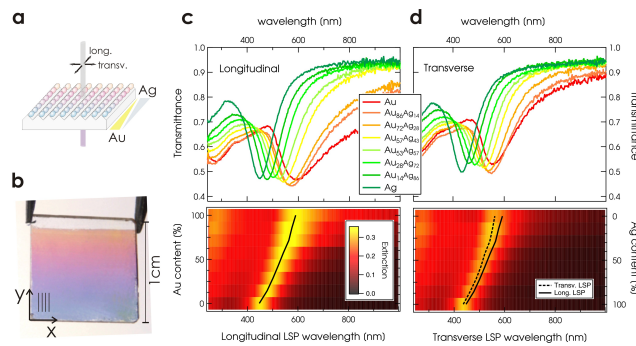
Plasmonic color-graded nanosystems with achromatic sub-wavelength architectures for light filtering and advanced SERS detection

Wednesday, 13th September - 15:55 - Enhanced spectroscopy and sensing - Room 412 - Oral - Abstract ID: 201

Dr. Francesco Bisio¹, **Dr. Remo Proietti Zaccaria**², **Dr. Andrea Toma**², **Dr. Gobind Das**³, **Prof. Enzo Di Fabrizio**³, **Dr. Francesco De Angelis**², **Prof. Maurizio Canepa**⁴

1. CNR-SPIN, 2. Istituto Italiano di Tecnologia, Department of Nanostructures, 3. King Abdullah University of Science and Technology, 4. Dipartimento di Fisica, Università di Genova

Plasmonic colour-graded systems are devices featuring a spatially variable plasmonic response over their surface. They are widely used as nanoscale colour filters; their typical size is small enough to allow integration with miniaturized electronic circuits paving the way to realize novel nanophotonic devices. Currently, most plasmonic colour-graded systems are intrinsically discrete, as their chromatic response exploits the tailored plasmon resonance of micro-architectures characterized by different size and/or geometry for each target colour. Here we report the realization of multifunctional plasmon-graded devices where continuously-graded chromatic response is achieved by smoothly tuning the composition of the resonator material while simultaneously maintaining an achromatic nanoscale geometry. The result is a new class of versatile materials: we show their application as plasmonic filters with a potential pixel size smaller than half of the exciting wavelength, but also as multiplexed surface-enhanced Raman spectroscopy (SERS) substrates. Many more implementations, like photovoltaic efficiency boosters or colour routers await, and will benefit from the low fabrication cost and intrinsic plasmonic flexibility of the presented systems.



Plasmongraded.jpg

Near field imaging of a nanofiber

Wednesday, 13th September - 16:40 - Strong light-matter interactions at the nanoscale - Auditorium - Oral -
Abstract ID: 381

Dr. Vivien Loo¹, Mr. Guillaume Blanquer¹, Mr. Maxime Joos², Dr. Quentin Glorieux², Dr. Yannick De Wilde³, Dr. Valentina Krachmalnicoff¹

1. ESPCI Paris, PSL Research University, CNRS, Institut Langevin, 1 rue Jussieu, F-75005, Paris, France, **2.** Laboratoire Kastler Brossel, Université Pierre et Marie Curie, Ecole Normale Supérieure and CNRS, UPMC Case 74, 4 place Jussieu, 75252 Paris Cedex 05, France, **3.** Institut Langevin, ESPCI Paris - CNRS

Introduction

Nanofibers have interesting properties, among which: fair coupling efficiency to emitters on their surface[1], light chirality[2], built-in integration to fibered systems. For these reasons they make an exciting playground for emitter-emitter interactions[3][4] and quantum optics in general. Using near field techniques, we probe the vicinity of a suspended nanofiber in the visible domain, and manipulate emitters on nanofibers.

Methods

An Atomic Force Microscope (AFM) tip is endowed with a radiative emitter (100 nm fluorescent bead). Its intensity and lifetime give information about the local density of states (LDOS) of the electromagnetic field near the nanofiber. The tip is scanning perpendicularly (x-direction) above the nanofiber and its height (z-direction) can be controlled, since the slightest contact with the fiber is detected by the AFM.

The nanofiber is suspended on an inverted microscope, thus, excitation of the emitter can be done in free space perpendicularly to the fiber or directly through it. Detection can also be done in either way. The bead can be dropped and retrieved on the nanofiber.

Results

As preliminary result, we can observe how the field is warped by a nanofiber (diameter is 600 nm) (fig. a)). 3D electromagnetic FDTD simulations show similar patterns (fig. b)). By comparing these two figures, the snap-in distance, height below which the AFM tip snaps into contact with the nanofiber due to attractive forces, is estimated around 400 nm.

Discussion

As we've already measured, the emitter in contact with the nanofiber exhibits a shorter lifetime (as well as a higher emission rate), due to a higher LDOS on the surface. If we can explore the 200 nm above the fiber we will map the LDOS of the evanescent field. To do so, stretching the fiber to its limits should reduce the snap-in distance.

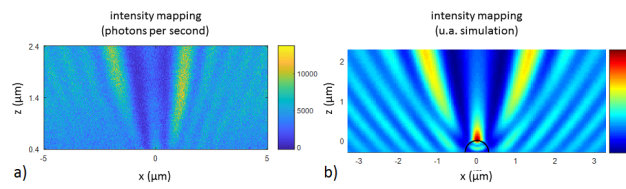
Once this milestone reached, we will proceed with single photons emitters (colloidal quantum dots), taking advantage of our ability to deterministically place several of them on the nanofiber.

[1]Schell *et al.*, *ACS Photonics*, 2017, **4**, 761–767

[2]Joos *et al.*, QIM 2017, QT2B.3

[3]Bouchet *et al.*, *Phys. Rev. Lett.* **116**, 037401

[4]Bouchet *et al.*, *Phys. Rev. A* **95**, 033828



Near field imaging of a nanofiber.png

Surface enhanced infrared absorption with highly doped InAsSb plasmonic nano-antenna arrays

Wednesday, 13th September - 16:57 - Strong light-matter interactions at the nanoscale - Auditorium - Oral - Abstract ID: 309

**Ms. Franziska Barho¹, Dr. Maria Jose Milla¹, Mr. Mario Bomers¹,
Dr. Fernando Gonzalez-Posada Flores¹, Dr. Laurent Cerutti¹, Prof. Eric Tournié¹, Prof. Thierry Taliercio²**

1. University of Montpellier / CNRS, 2. Université de Montpellier / CNRS

Introduction

Resonant surface enhanced infrared absorption (SEIRA) spectroscopy relies on advanced nanofabrication to tailor plasmonic antenna resonances at targeted wavelengths.[1] Strongest signal enhancement is obtained with plasmonic resonances tuned to molecular absorption features. This helps lower the IR spectroscopy detection limit and enables the minute detection of analyte quantities.

The tunability of the plasmonic antenna resonances is achieved by their geometry, size or interaction. Doped semiconductors go beyond, as the doping level is an additional parameter to tune the plasma frequency, contrariwise to noble metals where it is a material constant. In the IR, doped semiconductors are advantageous due to their lower carrier density, which engenders low Ohmic losses and resonances close to their plasma frequency.[2]

In this work, we investigate SEIRA performance of highly doped InAs_{0.91}Sb_{0.09} plasmonic nanoantenna arrays with different models and molecular layers.

Methods

Plasmonic resonators were fabricated by large-area surface patterning (interferential or UV lithography) and selective chemical etching from epitaxial highly doped InAs_{0.91}Sb_{0.09} films grown on GaSb substrates. Analyte layers were deposited by spin- or drop casting. SEIRA signals were evaluated using a normalization to the plasmonic background, to extract the vibrational signals from FTIR spectroscopy in reflectance mode. Additionally, finite-difference time-domain (FDTD) simulations were used to calculate far-field spectra and near-field profiles.

Results and discussion

Firstly, a higher doping level was correlated to a higher SEIRA signal using PDMS layers in line nanoantenna arrays. The highest doping induces in FDTD simulations an electric field less pinned inside the nanoantennas. Secondly, broadband resonant SEIRA of vanillin molecules is demonstrated using rectangular nanoantenna arrays with low aspect ratio. The Fano line vibrational shape features spectrally covered by the large LSPR evidences the coupling. Due to their anisotropy, the nanoantennas display polarization switchable mid-IR plasmonic resonances in two spectral bands. SEIRA signals were measured on characteristic benzene ring fingerprint vibrations, interesting for pharmaceutical applications or environmental monitoring. Finally, recent results using SiO₂ layers deposited by e-beam are under study for industrial coating controls. In sum, we will present SEIRA for different materials using semiconductor nanoantenna arrays.

References

- [1] F.Neubrech *et al.* Chem.Rev.2017,117,5110-5145.
- [2] A.Boltassevva *et al.* Science,2011,331,290-291.

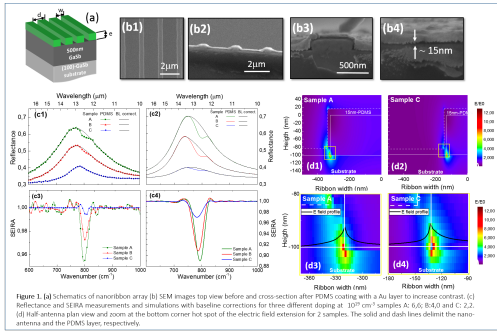


Figure 1 - seira of pdms with nanoribbon array.png

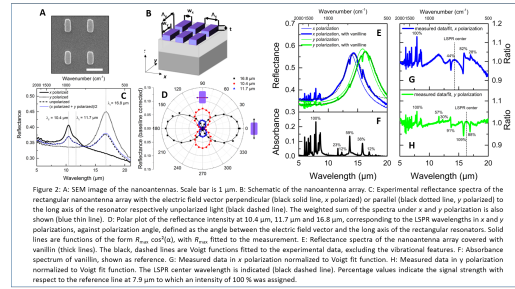


Figure 2 - seira of vanillin with nanoantenna array.png

Enhanced molecular vibrational spectroscopy with phononic boron nitride antennas

Wednesday, 13th September - 17:14 - Strong light-matter interactions at the nanoscale - Auditorium - Oral - Abstract ID: 407

***Dr. Marta Autore*¹, *Dr. Peining Li*², *Ms. Irene Dolado*², *Mr. Francisco Javier Alfaro-Mozaz*¹, *Dr. Rubèn Esteban*³, *Ms. Ainhoa Atxabal*¹, *Prof. Felix Casanova*¹, *Prof. Luis Hueso*¹, *Dr. Pablo Alonso González*⁴, *Prof. Javier Aizpurua*³, *Dr. Saül Velez*¹, *Dr. Alexey Nikitin*¹, *Prof. Rainer Hillenbrand*¹**

1. CIC nanoGUNE, **2.** CIC - nanoGUNE, **3.** Center for Material Physics (CSIC - UPV/EHU and DIPC), **4.** Universidad de Oviedo

Introduction

Surface enhanced infrared spectroscopy (SEIRA) is a powerful strategy to increase the weak vibrational signature of molecules in FTIR spectroscopy, by means of the confined and enhanced field on the surface of plasmonic objects [1]. Another possibility to enhance and confine infrared light into subwavelength scale is to exploit phonon polaritons in polar crystals [2] or layered materials, such as van der Waals crystals. In particular, the vdW material hexagonal boron nitride (hBN) hosts low-loss hyperbolic phonon polaritons with extremely high momenta, in the reststrahlen band frequency range (1360-1610 cm^{-1}) [3] With hBN nanocones and nanorods, extremely narrow resonances (Q up to 283) have been already demonstrated experimentally [4].

In this work we employ for the first time well-defined phononic antennas, hBN ribbons, to detect small amounts of organic molecules.

Methods

We fabricated hBN ribbons by e-beam lithography and etching. FTIR spectroscopy was employed to record infrared spectra of bare ribbons and ribbons with a thermally evaporated thin layer of organic molecules.

Results and discussion

Transmission FTIR spectra demonstrate SEIRA of thin organic molecular layers using hBN ribbons, reaching femtomolar sensitivity. We observe a remarkable shift of the phonon-polariton resonance and a strong anti-absorption feature in correspondence of the molecular vibration (see Fig 1). Our results show that phonon polaritons in engineered nanostructures represent a novel platform for SEIRA of thin molecular layers.

[1] Aroca, Ricardo. *Surface-enhanced vibrational spectroscopy*. John Wiley & Sons, 2006.

[2] Hillenbrand, R., Taubner, T., & Keilmann, F. (2002). Phonon-enhanced light-matter interaction at the nanometre scale. *Nature*, 418(6894), 159-162.

[3] Caldwell, J. D., & Novoselov, K. S. (2015). Van der Waals heterostructures: Mid-infrared nanophotonics. *Nature materials*, 14(4), 364-366.

[4] Caldwell, J. D. et al. (2014). Sub-diffractive volume-confined polaritons in the natural hyperbolic material hexagonal boron nitride. *Nature Communications*, 5, 5221.

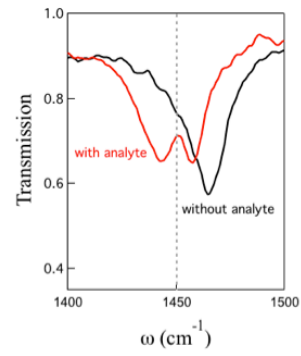


FIG 1. Transmission FTIR spectra for a bare hBN ribbon array (black), and for ribbons with a thin layer of organic molecules on top. Grey line marks the vibrational mode of the molecule.

Nanop2017 autore fig1.png

Plasmonic sensing of single particle catalysis

Wednesday, 13th September - 17:31 - Strong light-matter interactions at the nanoscale - Auditorium - Oral -
Abstract ID: 272

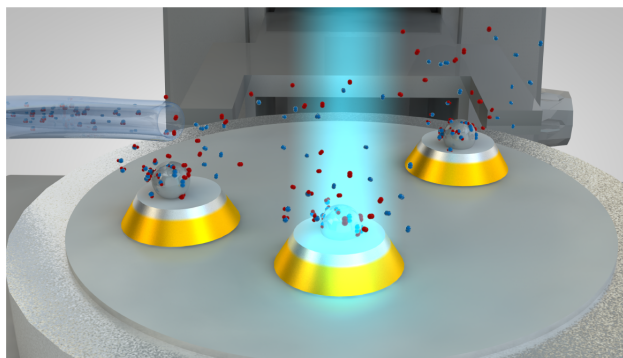
***Dr. Su Liu*¹, *Mrs. Svetlana Alekseeva*¹, *Mr. Ferry Nugroho*¹, *Dr. Lars Hellberg*¹, *Prof. Christoph Langhammer*¹, *Dr. Arturo Susarrery-arce*²**

1. Chalmers University of Technology, Department of Physics, 2. Ch

Nanoscale heterogeneous catalysts are heavily involved in modern chemical production, as well as in pollution mitigation, and generally advantageous due to their high number of active sites per unit of material. Characterizing individual catalyst nanoparticles *in operando* is a dream of catalysis science because any detrimental ensemble averaging effects could be completely eliminated. For this reason, a number of approaches to study single nanoparticle catalysis are emerging (1). However, a method to directly correlate physical and chemical properties of single catalyst nanoparticles with their catalytic activity is still missing mostly because existing approaches monitor either only the catalyst or the reactants. In this work, we present our efforts towards correlating single particle plasmonic nanospectroscopy (2) and mass spectrometry (MS) to simultaneously monitor the catalyst state and activity/selectivity *in operando* at atmospheric pressure reaction conditions. As shown in the figure below, we illustrate our concept on the example of hydrogen and carbon monoxide oxidation over Pt and a characterization of the kinetic phase transition (3) on nanoparticles of different size and over different support materials.

References

1. Sambur JB & Chen P (2014) *Annual Review of Physical Chemistry* 65(1):395-422.
2. Syrenova S, et al. (2015) *Nature Materials* 14:1236-1244.
3. Larsson EM, Langhammer C, Zoric I, & Kasemo B (2009) *Science* 326(5956):1091-1094.



Concept illustration.png

Vibrational strong light-matter coupling using a wavelength tunable mid-Infrared open microcavity

Wednesday, 13th September - 17:48 - Strong light-matter interactions at the nanoscale - Auditorium - Oral - Abstract ID: 354

Mr. Omree Kapon¹, Dr. Yaakov Tischler¹

1. Bar-Ilan University

An open microcavity (OMC) is an optical system that is composed of two mirrors, where one is fixed and the second is on a movable stage. OMCs enable tuning the optical resonances of the system and insertion of different materials between the mirrors, and are therefore of large scientific interest due to their many potential applications. Strong light-matter coupling of the vibrational transitions of organic molecules with the optical modes of a microcavity generates new polaritonic states in the mid-infrared (mid-IR) spectral region. Here, we achieve strong light-matter coupling in the mid-IR using a low optical-loss OMC, that is, wavelength tunable via a piezoelectric actuator. A thin film of Polymethyl methacrylate (PMMA) was deposited on to one of the mirrors to couple the narrow and intense absorption peak of the carbonyl stretch mode at 1731 cm^{-1} to the OMC. Polaritonic states are observed in FTIR transmission measurements when an OMC resonance is matched to the carbonyl stretch. By dynamically varying the cavity photon mode around the resonance condition, we determine the normal mode polariton dispersion relation and obtain a maximum Rabi-splitting $\hbar W_R = 7.0\text{ meV}$. Different cavity linewidths and Rabi-splittings can be achieved by changing the mirror separation, thus providing control of the coupling strength relative to dephasing. The ability to insert multiple materials inside an OMC and generate strong light-matter coupling over a large range of wavelengths can open new paths toward chemical reaction modification and energy transfer studies in the mid-IR.

Gap plasmon resonance in electromagnetically-actuated nanomechanical silicon nitride strings

Wednesday, 13th September - 18:05 - Strong light-matter interactions at the nanoscale - Auditorium - Oral - Abstract ID: 406

Dr. Nicolas Cazier¹, **Mr. Pedram Sadhegi**¹, **Dr. Mostafa Shawrav**¹, **Mr. Andreas Steiger-Thirsfeld**²,
Prof. Silvan Schmid¹

1. Institute of Sensor and Actuator Systems, TU Wien, Vienna, Austria, 2. University Service Center for Transmission Electron Microscopy, TU Wien, Vienna, Austria

We present a new kind of electromagnetically-actuated nanoplasmonomechanical string resonator. This nanomechanical resonator is made of two gold covered silicon nitride (SiN) strings separated by a 100 nm wide gap. These strings were cut into a SiN membrane with focused ion beam milling, as shown in the SEM image of the resonator on Figure 1. Besides supporting the induced plasmon resonance, the gold strips additionally act as actuation elements, being electrically connected. Placed in a static magnetic field (using neodymium magnets), the nanomechanical resonators are actuated by passing an oscillating current through one of the strings (see the schematic of the experimental setup on Figure 2). The induced Lorentz force makes the string vibrate, which varies the gap size between the two SiN strings. The string vibration is detected from the modulation of a tunable probe laser polarized perpendicularly to the direction of the strings, with a maximal scattering at the mechanical resonance frequency of the electromagnetically-actuated string. This can be seen on Figure 3, where we plotted the measured optical intensity and phase of the transmitted signal as a function of the frequency of the oscillating current, for an applied voltage of 1 mV and a laser wavelength of 780 nm. This kind of structure enables the investigation of the plasmonic resonances of plasmonic structures in close proximity, by electromagnetically-controlling the distance between those structures. This is particularly interesting in order to analyze the internal optical forces between plasmonic structures or to study quantum phenomena such as tunneling effects between these structures for gaps smaller than 1 nm.

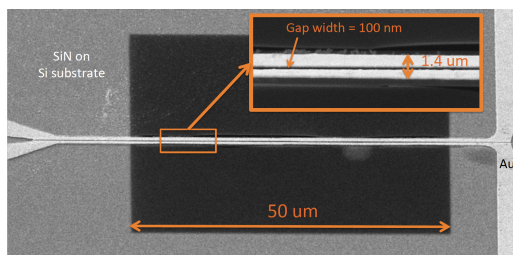


Fig1 sin strings cut with fib sem image.png

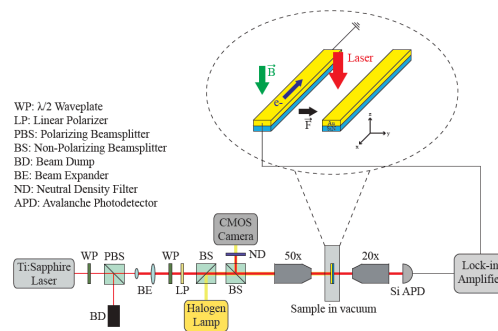


Fig2 experimental setup.png

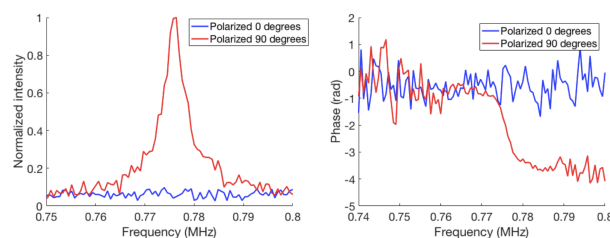


Fig3 measured plasmonic response.png

Dielectric Resonator Antenna for Large Volume Microwave Magnetic Coupling to NV Centers in Diamond

Wednesday, 13th September - 16:40 - Quantum dots and colour centres - Room 207 - Oral - Abstract ID: 442

Dr. Polina Kapitanova¹, **Mr. Vladimir Soshenko**², **Mr. Vadim Vorobyov**², **Mr. Dmitry Dobrykh**¹, **Dr. Ilya Shadrivov**³, **Prof. Pavel Belov**¹, **Prof. Alexey Akimov**⁴

1. Department of Nanophotonics and Metamaterials, ITMO University, St. Petersburg 197101, Russia, **2.** P.N. Lebedev Physical Institute, 119991 Moscow, Russia, **3.** Nonlinear Physics Centre, Australian National University, Canberra ACT 0200, Australia, **4.** Texas A & M University, College Station, TX 77843, USA

The NV center is a pointdefect in diamond. The interest to this defect is rising up during the lastdecade due to many possibilities of practice applications like ultra-precisemagnetometers, biocompatible thermometry, electron and nuclear magnetoresonance imaging etc. In most of the applications large ensembles of NV centersin single diamond plate are used [1] to increase the sensitivity of detectors.For sensor applications the electron spins at NV centers, localized at atomicscales, has to be manipulated. At room temperature it possible to applymagnetic field using a microwave antenna. The main requirement to the antennais the creation of uniform and strong microwave magnetic field over relativelylarge volume. A planar split-ring resonator (SRR) design foruniform and efficient coupling of microwave magnetic field into NV centers indiamond has been recently studied [2] However the SRR is not suitablefor manipulating NV centers spins in volume, because its magnetic field decaysdramatically in perpendicular direction from the SRR providing only 2D-uniformfield.

Here we present the microwavedielectric resonator antenna (DRA) for spin manipulation of large volumeensemble of NV centers in a bulk diamond. The proposed design is based on ahigh permittivity hollow dielectric resonator excited by a symmetric microstriploop resonating at the TE₀₁₈ mode of the dielectric resonator.

We have designed, fabricated and experimentally studied the DRAfor homogeneous control of spatially large spin ensembles. The Fig.1 representsthe design of the DRA, measured reflection coefficient in the comparison to thesimulated one, the Rabi oscillation frequency dependence and the calculatedaverage value of the magnetic field inside the dielectric resonator.

Demonstrated uniformity of the microwave magnetic field insidethe entire bore of the DRA is over 99% in volume of 8 cubic millimeters, whilethe magnitude of the field is enough to reach 15 MHz Rabi frequency at 5.2 Wfeeding power. This way our work paves the wave for building ultra-precisesensors, based on dense spin ensembles in solid state, such as NV centers indiamond.

[1] Clevenson, H.; Trusheim, M. E.; Schroder, T.; Teale, C.;Braje, D.; Englund, D. Nat. Phys. 2015, 11 (May), 393397.

[2] Bayat, K.; Choy, J.; Farrokh Baroughi, M.; Meesala, S.;Loncar,M. Nano Lett. 2014, 14 (3), 12081213.

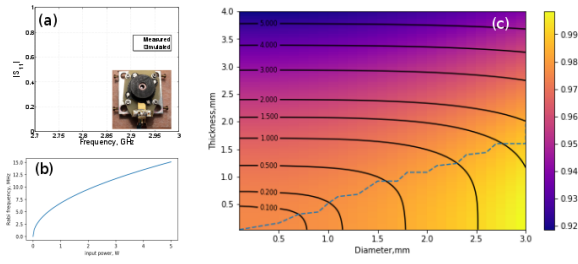


Fig1.png

Quantum Emitters in Hexagonal Boron Nitride Have Spectrally Tunable Quantum Efficiency

Wednesday, 13th September - 16:57 - Quantum dots and colour centres - Room 207 - Oral - Abstract ID: 429

*Dr. Mikael Svedendahl*¹, *Dr. Andreas Schell*¹, *Prof. Romain Quidant*¹

1. ICFO-Institut de Ciències Fòniques, The Barcelona Institute of Science and Technology, 08860 Castelldefels (Barcelona), Spain

Revealing the properties of novel solid-state quantum emitters is crucial for a number of applications, ranging from quantum optics to biology. Quantum emitters in 2D-materials have recently been discovered and defects in hexagonal boron nitride (hBN) has proven to efficiently supply single photons at room temperature with narrow emission lines and great photostability.¹

These quantum emitters have been studied at different emission wavelengths and operating temperatures. Various mechanisms to create defects or modify the emission wavelength have been investigated. Nevertheless, up to date, details of the emitters' level structure remain elusive.

In this contribution,² we present a study of the energy level structure using photoluminescence excitation spectroscopy on single quantum emitters (Fig. 1a). We varied the excitation wavelength using an optical parametric oscillator, and monitored the emission spectrum and intensity through a fiber-coupled spectrometer and APDs in a HBT-configuration. The samples were hBN nanoflakes, which we drop casted on clean silicon wafers. Figure 1b-c show SEM of different hBN nanoflakes at 35° and 80° incidence, respectively.

As an example, Fig. 1d show the photoluminescence for excitation wavelengths 530-620 nm. Two distinct peaks are visible, at 656 and 676 nm. The saturation curves (Fig. 1e) for the two main emission lines, using three different wavelengths, indicate that the saturation intensity and the saturation count rate vary with excitation wavelength. From fits to the data we calculate the relative quantum efficiencies (Figure 1f, 656 nm – orange, 676 nm - black). Our results show that bright single photon emission with high quantum efficiency is highly dependent on matching the excitation wavelength to the individual emitter. This is a strong indication that the level scheme is complex and cannot be described by simple two or three level systems.

The excitation dependence of the emission thus allow us to gain further insight to the internal level scheme and demonstrate how to distinguish different emitters both spatially as well as in terms of their photon correlations.

[1] Tran et al. Nature Nanotech. 2015, 11, 37-41

[2] Schell et al. arXiv:1706.0830

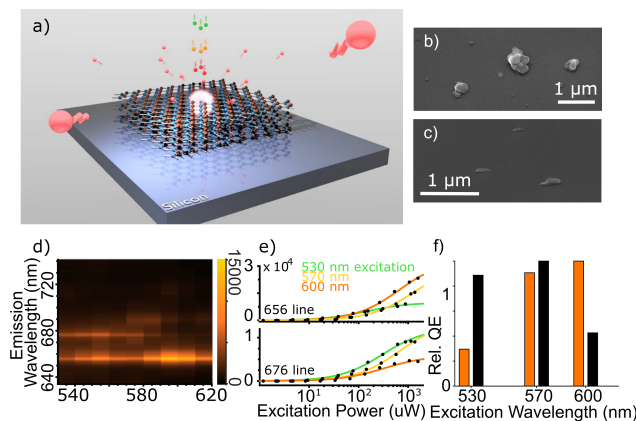


Figure 1.png

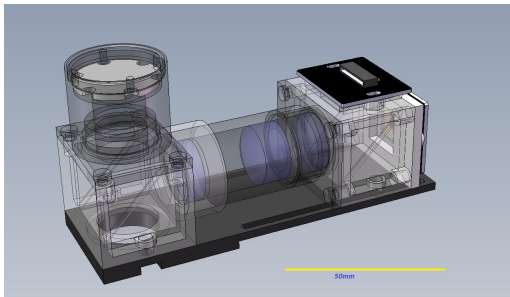
CMOS-based low-cost quantum dot camera for fast and efficient molecular detection

Wednesday, 13th September - 17:14 - Quantum dots and colour centres - Room 207 - Oral - Abstract ID: 397

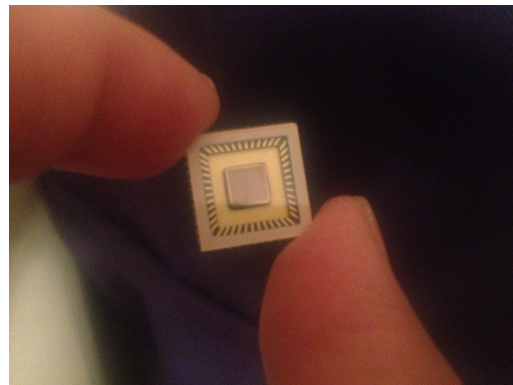
Dr. Zhimin Ding¹, Dr. Aihua Fu²

1. Anitoa Systems LLC, 2. Nvigen Inc

There is currently an emerging trend in biosensor design that utilize bio-conjugated nanoparticles, with magnetic and optical properties, to provide efficient performance for immunoassay, molecular and cell separation and detection. These nanoparticles have found many potential use in molecular or cell-based diagnostics for infectious diseases and cancer. In these applications, it is essential to be able to monitor and detect these nanoparticles efficiently and preferably in real time, using fluorescence and chemiluminescence signaling principles. In this work, we report the design and construction of a multi-fluorescence channel camera for detecting kinetically the activities of quantum dot-labeled nanoparticles in a microfluidic chip carrier. Based on the latest ultra-low-light CMOS image sensor chip and LED, we demonstrate a miniaturized camera that can detect quantum dot-labeled nanoparticles with good sensitivity, selectivity and superior speed. In our design, high efficiency multiplexing and high speed detection is achieved by taking advantage of the fact that fluorescence emitting quantum-dot materials have distinct emission spectrum while sharing the same excitation wavelength. This combination of technologies pave the way for potentially low-cost and portable diagnostic platforms for circulating tumor cells and infectious DNA biomarkers in a point-of-care setting.



Cfi 224qd.jpg



Cmosimager.jpg

Photonic Structuring of Colloidal Quantum-Dot Assemblies

Wednesday, 13th September - 17:31 - Quantum dots and colour centres - Room 207 - Oral - Abstract ID: 40

*Dr. Ferry Prins*¹

1. ETH Zurich

Colloidal quantum-dots (cQDs), or semiconductor nanocrystals, are highly versatile building blocks that combine size-tunable optical properties with low-cost wet-chemical methods. High quantum yields (>90%) and spectrally narrow emission throughout the visible and near-infrared range have placed cQDs among the highest color-quality emitters available.^{1,2} As such, they are ideal candidates for the bottom-up construction of photonic devices, where the combined tunability of the nanoscale building-block and the wavelength-scale photonic structure introduces new levels of control over light-matter interactions.

Here, we present a methodology to produce such patterned colloidal assemblies using template stripping.³ Mechanical cleaving (i.e. “stripping”) of a cQD film from a patterned hard silicon template allows for high-fidelity transfer of almost arbitrary shapes, yielding high resolution (<100 nm) and wafer-scale photonic structuring of cQD films. Using this technique, we are able to construct fully functioning photonic components composed purely out of cQDs. Examples include low-loss waveguides, high quality-factor ring resonators, and distributed feedback lasers with heavily reduced thresholds. Moreover, we will demonstrate how synthetic control over the cQD building block can enhance the performance of these photonic devices, for example through wavelength tuning and core-shell based Stokes-shift engineering.

[1] Y. Shirasaki, G. Supran, M. G. Bawendi, V. Bulovic, *Nature Photonics* 7, (2013) 13–23

[2] A. Nurmikko, *Nature Nanotechnology* 10 (2015) 1001-1004

[3] F. Prins, D.K. Kim, J. Cui, E. De Leo, L.L. Spiegel, K.M. McPeak, D.J. Norris, *Nano Letters* 17 (2017) 1319–1325

Dielectric leaky-wave nanoantennas for highly directional emission of light

Wednesday, 13th September - 17:48 - Quantum dots and colour centres - Room 207 - Oral - Abstract ID: 400

*Prof. Jens Förstner*¹, *Dr. Andre Hildebrandt*¹, *Prof. Thomas Zentgraf*¹, *Mr. Manuel Peter*², *Mr. Christian Schlickriede*², *Ms. Kimia Gharib*², *Prof. Stefan Linden*²

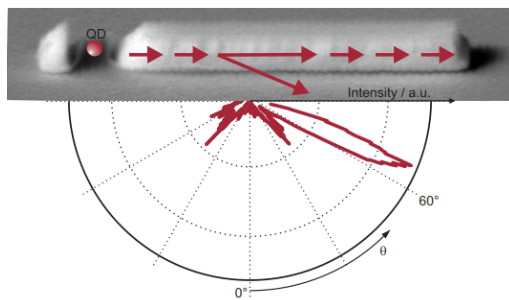
1. Paderborn University, 2. Universität Bonn

An important source of innovation in nanophotonics is the idea to scale down known radio wavetechnologies to the optical regime. One thoroughly investigated example of this approach are metallic nanoantennas which employ plasmonic resonances to couple localized emitters to selected far-field modes. While metals can be treated as perfect conductors in the microwave regime, their response becomes Drude-like at optical frequencies. Thus, plasmonic nanoantennas are inherently lossy. Moreover, their resonant nature requires precise control of the antenna geometry. A promising way to circumvent these problems is the use of broadband nanoantennas made from low-loss dielectric materials.

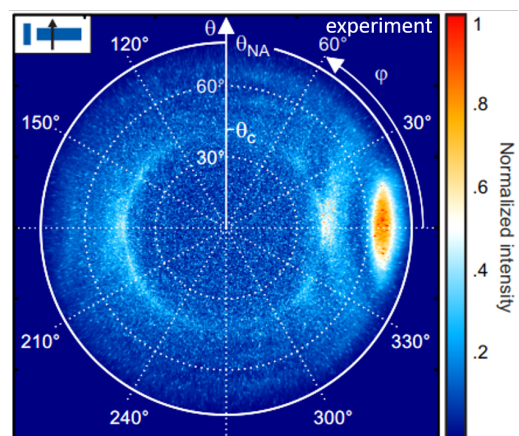
On the basis on theoretical considerations and numerical simulations we discovered a design rule for broadband dielectric optical leakywaveguide antennas being very robust to fabrication tolerances and showing high directional emission for a wide choice of material combinations.

Here, we report on the theoretical modelling and experimental realization of dielectric leaky-wavenanoantennas made of Hafnium dioxide nanostructures deposited on a glass substrate with high directional light emission. Colloidal semiconductor quantum dots deposited in the nanoantenna feed gap serve as a local light source. The emission patterns of hybrid nanoantennas with different sizes are measured by Fourier imaging and agree very well with our simulations. We find for all antenna sizes a highly directional emission, underlining the broadband operation of our design.

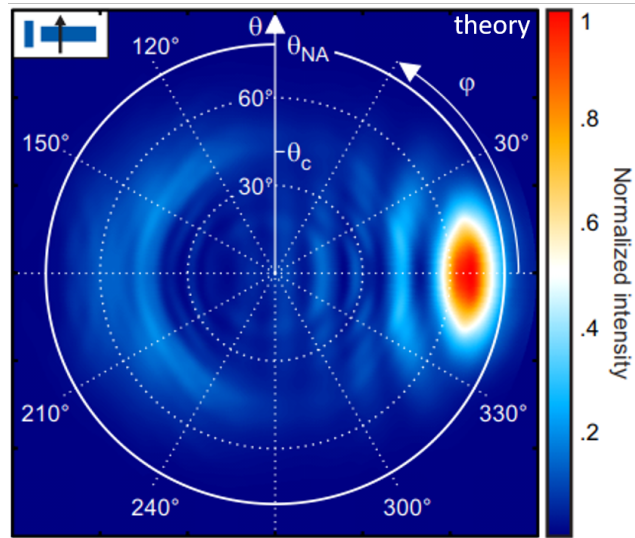
[1] M. Peter, A. Hildebrandt, C. Schlickriede, K. Gharib, T. Zentgraf, J. Förstner, and S. Linden, „Directional Emission from Dielectric Leaky-Wave Nanoantennas“, *Nano Letters* 7, 4178 (2017).



Toc bild.png



Exp2.png



Theory2.png

Control of spontaneous emission rate in luminescent resonant diamond particles

Wednesday, 13th September - 18:05 - Quantum dots and colour centres - Room 207 - Oral - Abstract ID: 389

Dr. Roman Savelev¹, **Ms. Anastasiia Zalogina**¹, **Dr. Sergey Makarov**², **Dr. Dmitriy Zuev**¹, **Dr. Ilya Shadrivov**³

1. Department of Nanophotonics and Metamaterials, ITMO University, 2. ITMO University, 3. Nonlinear Physics Center, Australian National University

Resonant high-refractive-index nanoparticles and nanostructures represent a promising platform for effective light manipulation at nanoscale and pave the way for creation of novel photonic devices. Interaction of a quantum emitter with one or several dielectric particles allows to significantly alter its radiation pattern and spontaneous emission rate [1]. Diamond particles containing colour centers such as nitrogen-vacancy, silicon-related and nickel-related centers [2] are of special interest in this context. They can be viewed as a single photonic nanodevice with emitting source embedded inside a diamond particle. Indeed, relatively high refractive index ($n \sim 2.4$) of the diamond and almost zero absorption in visible region make it possible to exploit the morphology- and size-dependent resonance properties of the diamond particles to control the emission properties of luminescent centers [3].

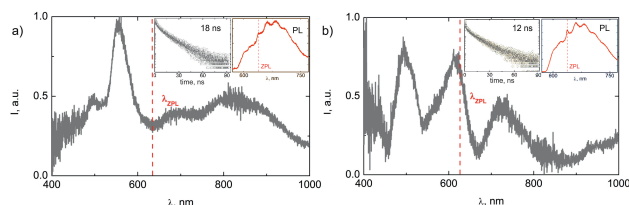
Here, we study the properties of luminescent diamond particles of different sizes (up to 1 μm) containing multiple NV-centers. NV-centers were incorporated into the sample during the growing of diamond film by plasma-enhanced chemically vapor deposition method. After milling the fabricated film the obtained diamond particles were characterized by dark-field spectroscopy method. In luminescence experiments, NV-centers were non-resonantly excited with 532 nm laser and the lifetime measurements of the excited state were carried out by the time-correlated single photon counting method.

We compare the luminescence properties of the diamond particles that exhibit resonances in the spectral region of NV-center luminescence. Fig.1 demonstrates the dark-field scattering spectra, photoluminescence intensity spectra and the time dependencies of the luminescence signal for these two cases. We observe that the spectral position of the resonance of diamond particle has a direct influence on the lifetime at zero-phonon line providing lifetime reduction in the resonant case by 1.5 times as compared to non-resonant one.

[1] A.I. Kuznetsov et.al, "Optically resonant dielectric nanostructures", *Science*, v.354, p.aag2472, 2016.

[2] I. Aharonovich, "Diamond photonics", *Nat. Photon.*, v.5, 397, p.2011.

[3] D.A. Shilkin et.al., "Optical magnetism and fundamental modes of nanodiamonds", *ACS Photon.*, v.4, p.1153, 2017.



Optical properties of luminescent diamond particles.jpg

Designer bulk plasmon polariton modes in hyperbolic metamaterials for sensing applications

Wednesday, 13th September - 16:40 - Metamaterials - Room 412 - Oral - Abstract ID: 335

*Dr. Tommi Isoniemi*¹, *Dr. Nicolò Maccaferri*¹, *Ms. Sara Perotto*¹, *Prof. Michael Hinczewski*², *Prof. Giuseppe Strangi*², *Dr. Francesco De Angelis*¹

1. Istituto Italiano di Tecnologia, Genova, 2. Case Western Reserve University, Cleveland, Ohio

Optical metamaterials are composed of sub-wavelength structures and exhibit unusual electromagnetic properties [1]. These materials can enable applications with negative refraction, sub-wavelength imaging and nanoscale light confinement. One class of them, hyperbolic metamaterials (HMM), are highly anisotropic media composed of alternating dielectric and metal layers. As such, the motion of free electrons is confined in one or two spatial dimensions, and the dispersion relation of HMMs is hyperbolic [1]. In addition to the usual surface plasmon polaritons (SPPs) on metal surfaces, HMMs can support bulk Bloch plasmon polaritons (BPPs) localized inside the multilayer structure, which can be used for nanoscale spectroscopic sensing due to the highly confined fields associated with these modes [2].

For this application we demonstrate theoretically and experimentally the excitation of BPPs through a grating coupling technique based on the excitation of SPPs. The structures consist of metallic diffraction gratings and an artificial HMM made of alternating layers of gold and alumina (Fig. 1), which can be called a hypergrating. We fabricated the multilayers with e-beam evaporation and atomic layer deposition, and produced the gratings with electron beam lithography.

The angle-dependent plasmon polariton modes can be seen in reflection spectra: in Fig. 2 the SPP is visible at 600-800 nm wavelengths and several BPP modes are seen in the near-infrared (1000-1800 nm). These measurements are well reproduced by simulations with different numerical methods. Our theory predicts configurations with almost zero reflection for BPP modes, as well as very narrow spectral features in the visible-near-infrared range. As the modes are sensitive to the dielectric medium in the immediate vicinity of the plasmon polariton, these systems are useful for ultrasensitive sensor applications, both for single-molecule detection and sub-wavelength optical imaging [1].

[1] Poddubny et al., Nature Photonics 7, 948–957 (2013).

[2] Sreekanth et al., Nature Materials 15, 621–627 (2016).

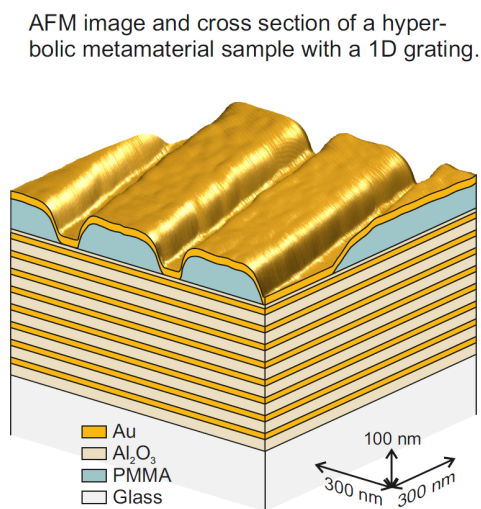


Fig. 1. structure of a hmm sample.png

Optical reflectance of the sample in Fig. 1 at p -polarization, incident plane perpendicular to the grating line axis.

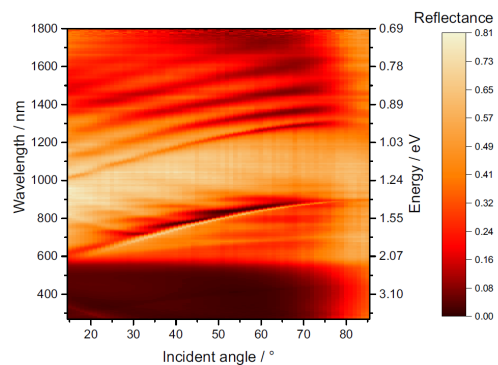


Fig. 2. reflectance of the hmm sample.png

High-Efficiency Asymmetric Transmission of Circularly Polarized THz waves using a Dielectric Herringbone Metasurface

Wednesday, 13th September - 16:57 - Metamaterials - Room 412 - Oral - Abstract ID: 443

Dr. Mitchell Kenney¹, **Mr. Shaoxian Li**², **Dr. Xueqian Zhang**², **Dr. Teun-teun Kim**³, **Mr. Dongyang Wang**², **Dr. Dongmin Wu**⁴, **Prof. Chunmei Ouyang**², **Prof. Jianguang Han**², **Prof. Weili Zhang**², **Prof. Hong-bo Sun**⁵, **Prof. Shuang Zhang**³

1. University of Glasgow, 2. Tianjin University, 3. University of Birmingham, 4. Chinese Academy of Sciences, 5. Jilin University

An interesting topic is that of metamaterials imparting chiral responses which invoke a disparity between opposite handednesses of circularly polarised (CP) light. Most chiral metamaterials are either 3D-helical structures [1] or stacked metallic structures with twisted orientations [2]. These structures allow selective transmission of one CP whilst prohibiting or reflecting the other, termed Circular Dichroism. However, for 2D chiral metamaterials, this is not so. Instead, the cross-polarisation conversion of one CP to another is different. The original work in [3] used an anisotropic lossy planar-chiral “fish-scale” structure to exhibit this effect, termed Asymmetric Transmission (AT). However, these responses are small with efficiencies less than 25%. Works to improve efficiency used 3D arrangements. Work in [4] achieved much higher efficiency than for the 2D planar-chiral structures, but due to the metallic construction absorption losses were unavoidable; such losses were given as 37%.

Here, we propose a means of achieving AT using a loss-free mechanism at 1THz frequency by constructing Monolithic Herringbone metamaterials from a dielectric medium [5]. This device works by a spin-selective interference of CP light, due to Pancharatnam-Berry (PB) phases, in conjunction with a propagative dynamic phase (Fig. 2) causing constructive interference for TRL and destructive for TLR Jones matrix components. An analytical derivation (Fig. 1a) was found to agree well with numerical simulations (Fig. 1b) for the design. These results indicate a conversion efficiency of LCP to RCP (TRL) exceeding 80%. Fabrication of Intrinsic Silicon was used for the devices (Fig. 2) and THz Time Domain Spectroscopy (THz-TDS) was used to characterise the samples, showing a 60% spin-conversion efficiency (Fig. 3). Such a device is robust and is not easily degraded by errors in fabrication.

[1] J. Gansel, M. Thiel, M. Rill *et al.*, *Science* **325**, 1513 (2009).

[2] A. Rogacheva, V. Fedotov *et al.*, *Phys. Rev. Lett.* **97**, 177401 (2006)

[3] V. Fedotov, P. Mladyonov, S. Prosvirnin *et al.*, *Phys. Rev. Lett.* **97**, 167401 (2006)

[4] C. Pfeiffer, C. Zhang, V. Ray *et al.*, *Phys.Rev. Lett.* **113**, 023902 (2014)

[5] M. Kenney, S. Li, X. Zhang *et al.*, *Adv.Mater.* **28**, 9567 (2016)

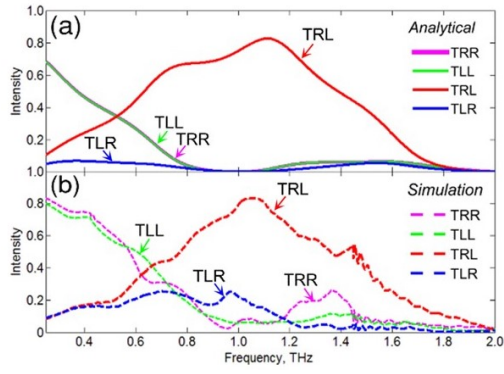


Figure 1 - analytical and simulation.jpg

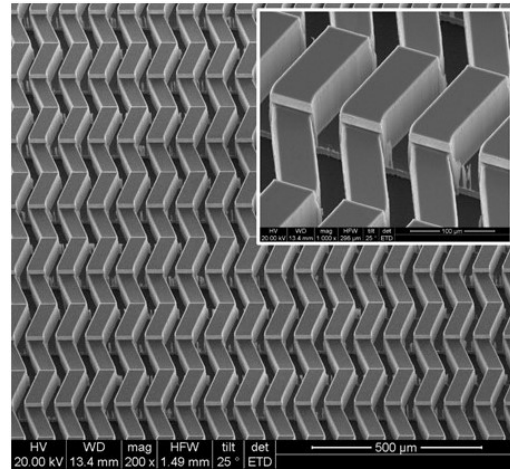


Figure 2 - structure sem.jpg

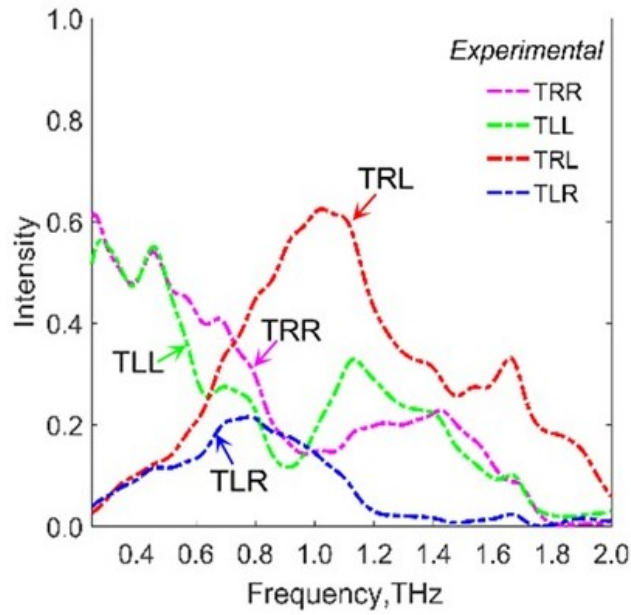


Figure 3 - experimental.jpg

Directional and singular surface plasmon generation in chiral and achiral nanostructures demonstrated by leakage radiation microscopy

Wednesday, 13th September - 17:14 - Metamaterials - Room 412 - Oral - Abstract ID: 152

***Ms. Aline Pham*¹, *Dr. Quanbo Jiang*¹, *Dr. Martin Berthel*², *Dr. Serge Huant*¹, *Prof. Joel Bellessa*³, *Dr. Cyriaque Genet*⁴, *Dr. Aurelien Drezet*⁵**

1. Institut Neel, 2. Laboratoire Ondes et Matière d'Aquitaine, 3. institut Lumière Matière, 4. ISIS, university of Strasbourg, 5. Institut Néel, CNRS, Université Grenoble Alpes

Chiral plasmonic nanostructures have received considerable attention due to their peculiar responses such as asymmetric transmission and optical vortex generation, arising from the spin-orbit interactions of light via plasmonic nanostructures. Owing to the additional degree of freedom added by the incident spin, chiral plasmonic couplers, such as T-shaped aperture arrays, have been reported to induce surface plasmons (SP) emission with spin-controlled directionality, opening new possibilities in manipulation of light at the nanoscale. Due to the inherently confinement of the SP, near-field optical detection has been widely employed in the past to image SP propagation. In the present work, we propose a complementary and versatile far-field approach based on leakage radiation microscopy (LRM) allowing quantitative and polarization analysis in both direct and Fourier spaces. We report on the quantitative characterization and comparison of the directional coupling associated with a chiral and an achiral plasmonic coupler made of T- and Λ -shaped apertures array, respectively. Both spin-driven propagation as well as vortex generation of SP is demonstrated. This study allows clarifying the role of the phase and symmetry breaking in the directional SP launching mechanism which is analytically described in terms multidipolar model. We expect our method to bring an important contribution in future characterization and design optimization of new directional couplers for integrated optics.

Controlling Thermal Radiation Signatures using Materials Designed by Transformation Optics Theory

Wednesday, 13th September - 17:31 - Metamaterials - Room 412 - Oral - Abstract ID: 421

Mr. ahmed Alwakil¹, Dr. Myriam Zerrad¹, Dr. Claude Amra¹

1. Aix-Marseille Université, CNRS, Centrale Marseille, Institut Fresnel, UMR 7249, 13013 Marseille, France

Above 0K all objects thermally radiate and each object has its own thermally radiated signature, depending on its geometric shape and its constitutive parameters. In our theoretical work, we investigate design methodologies based on transformation optics theory [1] to control the emitted thermal radiation signature. In this talk, we extend transformation optics theory to the field of near field thermal radiation [2]. We first summarize fluctuational electrodynamics theory [3] which is a mathematical framework to describe the electromagnetic thermal radiation as a linear response of Maxwell's equations due to thermal electric and magnetic currents. These sources are governed by stochastic processes and their statistical properties are determined by the fluctuation dissipation theorem which relates the losses of a linear system to the fluctuations of its internal thermal energy. These losses are related to the constitutive parameters of the thermal emitter. Then, we show that it is possible for objects residing in virtual and physical space to have the same thermal radiation pattern if their complex permittivities and permeabilities are related by the standard transformation optics such that the fluctuation electrodynamics problem is invariant under transformation, such invariance allows the illusion procedure in thermal radiation. 2D thermal camouflage [4] scheme is illustrated and numerical computations confirm the developed theory within our hypothesis framework. Finally, we extend the theoretical scheme for thermal radiation from reciprocal and non-reciprocal bi-anisotropic media [5].

Acknowledgements: This work was supported by the French National Research Agency (ANR- INPACT project).

References:

1. Pendry, J. B., Schurig, D. and D. R. Smith, "Controlling electromagnetic fields," *science*, Vol. 312, No. 5781, 1780-1782, 2006.
2. Howell, J. R., Menguc, M. P. and R. Siegel, *Thermal radiation heat transfer*, CRC press, 2010.
3. Rytov, S.M. "Theory of electric fluctuations and thermal radiation," *Air Force Cambridge Research Center, Bedford MA*, 1959.
4. A. Alwakil, M. Zerrad, M. Bellieud, and C. Amra, "Inverse heat mimicking of given objects," *Sci. Rep.* 7, (2017).
5. I. V. Lindell, A. H. Sihvola, S. A. Tretykov, and A. J. Viitanen, *Electromagnetic waves in Chiral and Bi-Isotropic Media*, *Artech House*, 1994.

Hybrid optical surface waves supported by resonant anisotropic metasurfaces

Wednesday, 13th September - 17:48 - Metamaterials - Room 412 - Oral - Abstract ID: 427

Dr. Dmitry Permyakov¹, Mr. Oleh Yermakov¹, Dr. Andrey Bogdanov¹, Dr. Anton Samusev¹, Dr. Ivan Mukhin², Mr. Ivan Sinev¹, Dr. Radu Malureanu³, Dr. Osamu Takayama⁴, Dr. Ivan Iorsh¹, Prof. Andrei Lavrinenko⁵

1. ITMO University, 2. ITMO University; St. Petersburg Academic University, 3. Department of Photonics Engineering, Technical University of Denmark; National Centre for Micro- and Nano-Fabrication, Technical University of Denmark, 4. Department of Photonics Engineering, Technical University of Denmark, 5. Technical University of Denmark; ITMO University

Significant advance in the field of nanophotonics has been achieved with the help of metamaterials - artificially created composite structures, whose electromagnetic properties drastically differ from the properties of the natural materials. However, three-dimensional metamaterials are poorly compatible with planar technology, which is a significant obstacle for their applications in the optical range. One of the possible ways to overcome this problem is to use metasurfaces, a two-dimensional analogue of metamaterials. Along with unprecedented control over reflected and transmitted waves and provide precise engineering of phase, amplitude, polarization, propagation direction, and wavefront of electromagnetic field.

In the framework of effective medium approximation, anisotropic metasurface can be described by a two-dimensional conductivity tensor. The dispersion relation can be directly derived from the Maxwell's equations by using effective conductivity tensor. We provide an experimental approach which allows to determine effective conductivity tensor of the particular metasurface, and predicts coexistence of unusual surface waves with TE-, TM- and hybrid polarizations.

In the present work we analyzed spectrum of the surfaces waves propagating along plasmonic metasurfaces consisting of anisotropic gold subwavelength particles placed on a silica substrate. We have shown that the spectrum of plasmonic metasurfaces consists of two hybrid polarized quasi-TE and quasi-TM surface modes which could have very high directivity and demonstrate non-diverging propagation. The strong anisotropy of the gold particles could result in appearance of a hyperbolic regime of the metasurfaces at the frequencies closed to the plasmonic and Mie resonances of the gold particles, respectively.

We provided an experimental study of surface waves localized on plasmonic metasurface and fully confirm our theoretical findings. In addition to the quasi-TE and quasi-TM modes predicted theoretically we observed a near dispersionless surface mode. We have shown that this mode is formed due to the interaction of quadrupole resonances of the gold nanoparticles.

Zero-index media: a loophole in effective medium theories

Wednesday, 13th September - 18:05 - Metamaterials - Room 412 - Oral - Abstract ID: 296

Dr. Iñigo Liberal¹, **Dr. Yue Li**², **Prof. Nader Engheta**³

1. Universidad Pública de Navarra, 2. Tsinghua University, 3. University of Pennsylvania

Effective medium theories (EMTs) are a powerful tool that enable the description of complex electromagnetic systems in terms of simple effective parameters (e.g., effective permittivity, permeability, chirality...). In fact, homogenization techniques associated with EMTs lie at the core of metamaterial science. Indeed, they describe the emergence of exotic properties (e.g., artificial magnetism, negative refraction...) as a consequence of the structure of their constitutive particles. However, EMTs suffer from strict limitations on their range of applicability. Typically, they are only valid for a sufficiently large number of particles, which must be small in size, and arranged with high density.

Thus, a two-dimensional (2D) structure such as that depicted in Fig.1a, would usually have no hope to be described via EMTs. However, the situation is exceptional if the refractive index of the host approaches zero. As we demonstrated in a recent work [Liberal *et al.* Science 355(6329), 1058-1063 (2017)], the limitations of EMTs can be circumvented in 2D epsilon-near-zero (ENZ) media. In this manner, an arbitrarily shaped body made of zero-index medium containing an arbitrary number of particles, and of any size, can still be described with effective material parameters. Furthermore, each particle contributes to the effective constitutive parameters in an additive, noninteracting, manner; an effect we named as ‘photonic doping’.

This methodology offers new possibilities in engineering light-matter interactions. For example, it allows for synthesizing exotic materials such as epsilon-and-mu-near-zero media and perfect-magnetic-conductors (see Figs. 1). It also facilitates the control of a large body with a single, arbitrarily located, particle, and this effect persists even when realistic material parameters are taken into consideration (see Fig. 2). Pathological effects, different from those in conventional EMTs, also appear when the filling factor of the particles approaches one. In our presentation, we will discuss the theory and underlying principles of this concept. We will also cover some proposals for practical implementations in the mid-IR based on silicon carbide (SiC), and we will review a number of potential applications, including flexible and reconfigurable metasurfaces, nonlinear optics, as well as thermal and nonclassical light sources.

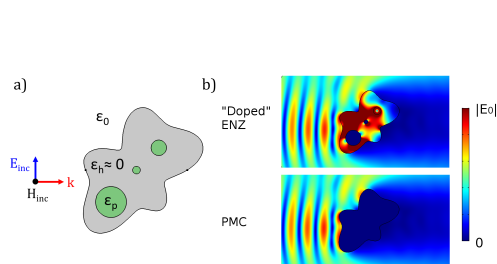


Fig1 sketch photonic doping pmc synthesis.png

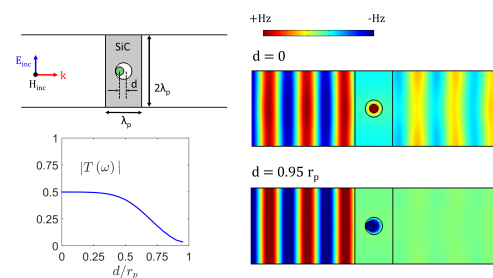


Fig2 sic implementation reconfigurable metasurface.png

Moving from Single Molecules to Controlled Cooperative Systems in Quantum Nano-Optics

Thursday, 14th September - 09:00 - Plenary Speeches - Oral - Abstract ID: 513

Prof. Vahid Sandoghdar¹

1. Max Planck Institute for the Science of Light

An emerging challenge in quantum nano-optics is to extend the toolbox generated from experiments with single emitters and single photons towards interfacing of a well-defined number of photons and quantum emitters. The resulting complex optical network would enable studies of many-body quantum optical phenomena and novel states of light and matter. Here, we discuss a chip-based scalable platform, which relies on the evanescent coupling of organic molecules to subwavelength dielectric waveguides (nanoguides) embedded in an organic matrix. The highly confined mode of a nanoguide allows a substantial mode overlap with the emission pattern of an emitter, resulting in large coupling efficiencies. As a result, we can observe coherent extinction signals from many different molecules in the transmission signal of a nanoguide [1]. Furthermore, the efficient linear coupling of photons and molecules paves the way for achieving nonlinear effects such as switching or amplification at very low light power [1, 2]. We also elaborate on future efforts towards the realization of on-chip polaritonic states [3] and integration of further optical elements such as microresonators [4,5], which would enhance and tailor the coupling of molecules to each other.

[1] P. Türschmann, et al, Nano Lett.17, 4941 (2017).

[2] A. Maser, et al, Nature Photonics 10, 450 (2016).

[3] H. R. Haakh, et al, Phys. Rev. A 94, 053840 (2016).

[4] N. Rotenberg, et al, Opt. Express 25, 5397 (2017).

[5] D. Wang, et al, Phys. Rev. X 7, 021014 (2017).

Chiral Nanophotonics and Quantum Optics

Thursday, 14th September - 09:40 - Plenary Speeches - Oral - Abstract ID: 514

Prof. Arno Rauschenbeutel¹

1. Vienna Center for Quantum Science and Technology, Atominstitut, TU Wien, Stadionallee 2, 1020 Wien, Austria

Controlling the interaction of light and matter is the basis for diverse applications ranging from light technology to quantum information processing. Nowadays, many of these applications are based on nanophotonic structures.

It turns out that the confinement of light in such nanostructures imposes an inherent link between its local polarization and its propagation direction, also referred to as spin–momentum locking of light [1]. Remarkably, this leads to chiral, i.e., propagation direction-dependent effects in the emission and absorption of light, and elementary processes of light–matter interaction are fundamentally altered [2]. For example, when coupling plasmonic particles or atoms to evanescent fields, the intrinsic mirror symmetry of the particles' emission can be broken. In our group, this allowed us to realize chiral nanophotonic interfaces in which the emission direction of light into the structure is controlled by the polarization of the excitation light [3] or by the internal quantum state of the emitter [4], respectively. Moreover, we employed this chiral interaction to demonstrate an integrated optical isolator [5] which operates at the single-photon level and which exhibits low loss. The latter was the first example of a new class of nonreciprocal nanophotonic devices which exploit the chiral interaction between quantum emitters and transversally confined photons.

References

- [1] K. Y. Bliokh, F. J. Rodríguez-Fortuño, F. Nori, and A. V. Zayats, Spin-orbit interactions of light, *Nat. Photon.* 9, 796 (2015).
- [2] P. Lodahl, S. Mahmoodian, S. Stobbe, A. Rauschenbeutel, P. Schneeweiss, J. Volz, H. Pichler, and P. Zoller, Chiral Quantum Optics, *Nature* 541, 473, (2017).
- [3] J. Petersen, J. Volz, and A. Rauschenbeutel, Chiral nanophotonic waveguide interface based on spin-orbit coupling of light, *Science* 346, 67 (2014).
- [4] R. Mitsch, C. Sayrin, B. Albrecht, P. Schneeweiss, and A. Rauschenbeutel, Quantum state-controlled directional spontaneous emission of photons into a nanophotonic waveguide, *Nature Commun.* 5, 5713 (2014).
- [5] C. Sayrin, C. Junge, R. Mitsch, B. Albrecht, D. O'Shea, P. Schneeweiss, J. Volz, and A. Rauschenbeutel, Nanophotonic Optical Isolator Controlled by the Internal State of Cold Atoms, *Phys. Rev. X* 5, 041036 (2015).

Polaritons for Chemistry and Materials Science

Thursday, 14th September - 10:45 - Plenary Speeches - Auditorium - Oral - Abstract ID: 3

Prof. Francisco Garcia-Vidal¹

1. Universidad Autonoma de Madrid

Exciton transport plays a crucial role in natural phenomena such as photosynthesis and in artificial devices such as organic solar cells, but is inefficient in many organic materials. We will discuss how the formation of collective polaritonic modes can dramatically enhance exciton conductance when the molecules are strongly coupled to an electromagnetic mode [1], which can be exploited to “harvest” and direct excitations to specific positions by tuning the spatial distribution of the EM mode [2]. We then show that in systems with a discrete EM mode spectrum, strong-coupling-enhanced exciton transport can proceed through “dark” modes that acquire a delocalized character in the strong-coupling regime [3].

In the second part, we discuss the influence of strong coupling on internal molecular structure and chemical reactions. While most models of strong coupling are based on simple two-level models, pioneering experiments have shown modifications of chemical reaction rates under strong coupling [4]. In order to address this mismatch, we have developed a first-principles model that takes into account both electronic and nuclear degrees of freedom [5]. We will first discuss the applicability of the Born-Oppenheimer approximation, which is challenged by the introduction of the new intermediate timescale of energy exchange between the molecule and the field. Based on these findings, we then show how photochemical reactions such as photoisomerization can be almost completely suppressed under strong coupling [6]. Finally, we show that this suppression works more efficiently when many molecules are coupled to a single light mode due to a “collective protection” effect in the delocalized polaritonic state.

[1] J. Feist and F. J. Garcia-Vidal, *Phys. Rev. Lett.* **114**, 196402 (2015).

[2] C. Gonzalez-Ballester, J. Feist, E. Moreno, and F. J. Garcia-Vidal, *Phys. Rev. B* **92**, 121402(R) (2015).

[3] C. Gonzalez-Ballester, J. Feist, E. Gonzalo-Badia, E. Moreno, and F. J. Garcia-Vidal, *Phys. Rev. Lett.* **117**, 156402 (2016).

[4] J. A. Hutchison et al., *Angew. Chemie* **124**, 1624 (2012).

[5] J. Galego, F. J. Garcia-Vidal, and J. Feist, *Phys. Rev. X* **5**, 041022 (2015).

[6] J. Galego, F. J. Garcia-Vidal, and J. Feist, *Nature Communications* **7**, 13841 (2016).

Engineering light propagation with planar or conformable optical metasurfaces

Thursday, 14th September - 11:25 - Plenary Speeches - Auditorium - Oral - Abstract ID: 278

*Dr. Patrice Genevet*¹

1. CRHEA - UCA- CNRS

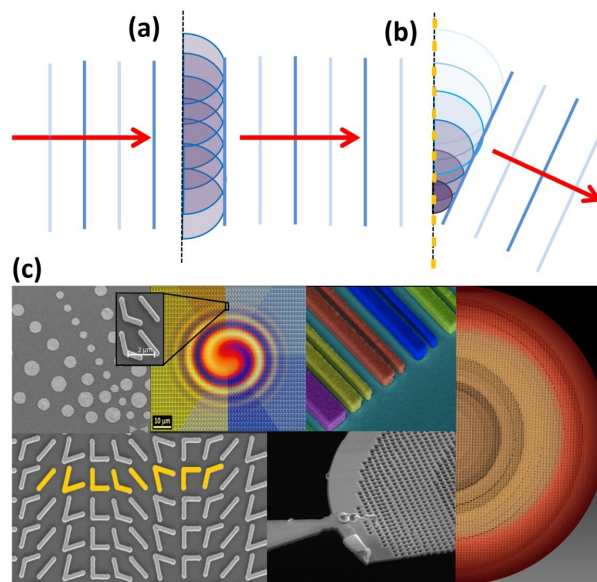
Abrupt modifications of the fields across an interface can be engineered by depositing an array of sub-wavelength resonators specifically tailored to address local amplitude, phase and polarization changes [1]. Physically, ultrathin nanostructure arrays, called “metasurfaces”, control light by engineering artificial boundary conditions of Maxwell’s equations. Metasurfaces have been implemented to obtain various sorts of optical functionalities, ranging from the basic control of the transmission and reflection of light, to the control of the radiation patterns for comprehensive wavefront engineering [2]. Here, we review the recent works in this field and explain which physical mechanisms are utilized for the design of efficient planar optical components. We will present our results on free-standing semiconductor metasurfaces and conclude with the concept of conformal boundary optics: an analytical method based on first-principle derivation to engineer transmission and reflection at free-form interfaces [3].

[1] Yu, Genevet, et al., Science 334,333 (2011)

[2] Genevet, et al. Optica 4 (1), 139-152 (2017)

[3] Han, Wong, Molardi & Genevet, PRA 94, 023820 (2016).

Acknowledgments:PG acknowledges support from ERC Grant agreement no. 639109.



Gif1.jpg

Intrinsic emergence of optical spin-orbit interaction at the nanoscale

Thursday, 14th September - 13:30 - Poster Session - Gallery - Poster - Abstract ID: 170

*Mr. J. Enrique Vázquez-Lozano*¹, *Dr. Alejandro Martínez*¹

1. Universitat Politècnica de València

The extension of spin-orbit interaction (SOI) to the framework of optics is attributed to the seminal work authored by Liberman and Zel'dovich [1]. Their approach is based on the conservation of the state of polarization (SoP) when the light propagates in an optically inhomogeneous medium. Due to the vector character of the electromagnetic fields, light possess two types of rotations giving rise to the corresponding contributions termed as the spin angular momentum (SAM) and orbital angular momentum (OAM), respectively. Whereas the OAM is related with the spatial distribution and propagation of the optical field, SAM is generally determined by the SoP. Therefore, SOI is envisioned as the mutual influence between the SoP (spin) and the phase (orbit), i.e., provided the electromagnetic field can be expressed in a factorized form, that mutual influence is vanished, avoiding the occurrence of SOI.

In the past few years, motivated by the rapid advance of nanotechnology, SOI of light has been subject of intense research activity [2]. Main efforts were devoted to investigate novel photonic applications [3], leaving elusive the fundamental theory underlying its origin. In this regard it has only been argued that SOI of light is inherent to Maxwell's equations, arising from the transversality condition and described within the Berry phase formalism.

In this work we propose a new perspective to unveil the intrinsic emergence of optical SOI at the nanoscale. Taking into account the factorizability condition of the electromagnetic fields we show, by using an analytical full-vector description based on the spherical vector wave approach, that this condition is fulfilled only in the far-field limit [Fig.1a]. Indeed, since SOI come into play at the subwavelength scale, the usual treatment based on the scalar-like plane waves seems to be pretty naive. On the other side, in the near-field region, an additional relative phase hinders the factorization and reveals an intricate behavior capturing the main features of the spin-orbit coupling regime [Fig.1b].

[1]V.S. Liberman and B.Y. Zel'dovich, Phys. Rev. A 46, 5199 (1992).

[2]K.Y. Bliokh, et al., Nat. Photonics 9, 796 (2015).

[3]F. Cardano and L. Marrucci, Nat. Photonics 9, 776 (2015).

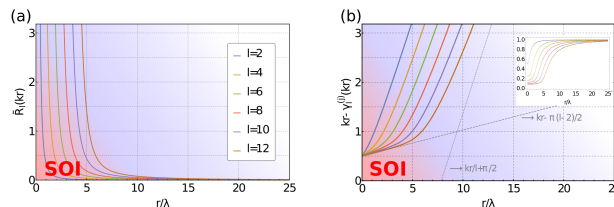


Figure 1: Amplitude (a) and phase (b) of the spin-orbit coupling term, $\Delta^{(s)}(kr) \equiv \frac{\hat{A}_l}{kr} \exp[\pm i(kr - \gamma^{(l)})]$, for different l-modes. The gradient color illustrates the transition from the coupling to decoupling regimes. The gray dashed lines show the asymptotic behavior of the phase. This is displayed in the inset by means of the slope of the relative phase with respect to kr .

Spin-orbit coupling term.png

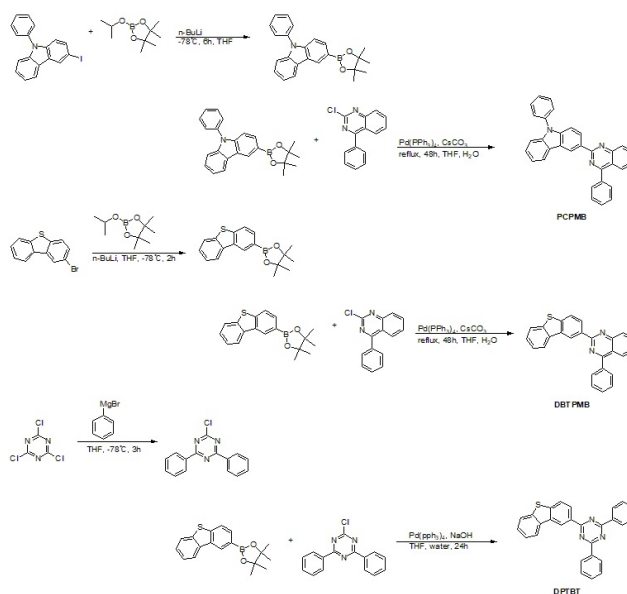
Synthesis and characterization of host material for phosphorescent organic light emitting diodes (PHOLEDs)

Thursday, 14th September - 13:30 - Poster Session - Gallery - Poster - Abstract ID: 468

Mr. Ji Su An¹, Prof. Choon Woo Lim¹

1. Department of Chemistry, College of Life Science and Nano-technology, Hannam University, Daejeon 305-811, Republic of Korea

Phosphorescent organic light-emitting diodes (PHOLEDs) have been attractive, because theoretical quantum efficiency of phosphorescent emitting material is four times higher than that of fluorescent emitter. We applied phenylquinazoline and triazine moieties which could provide good electron transport ability and the 9-phenylcarbazole and dibenzothiophene moieties which could provide good hole transport ability to obtain a bipolar host materials for PHOLEDs. Three host materials, PCPMB, DBTPMB and DPTBT were designed and synthesized, incorporating 9-phenylcarbazole(PC) and dibenzothiophene(DBT), respectively. Compounds PCPMB, DBTPMB and DPTBT were synthesized by Suzuki coupling reactions. DFT calculations were performed using Spartan' 08 software at the B3LYP level. The chemical structures were characterized by ¹H-NMR, ¹³C-NMR, GC-Mass. Thermal stability was analyzed by thermo gravimetric analysis (TGA) and differential scanning calorimetry (DSC). Optical properties of the host materials were analyzed by UV-vis absorption spectroscopy and PL spectroscopy.



Scheme1.jpg

Dirac points manipulation using linear laser in Floquet crystals for Graphene superlattices

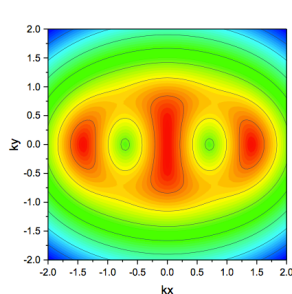
Thursday, 14th September - 13:30 - Poster Session - Gallery - Poster - Abstract ID: 132

*Mrs. Shahd Alfadhli*¹, *Prof. Sergey Saveliev*¹, *Prof. Feo Kusmartsev*¹

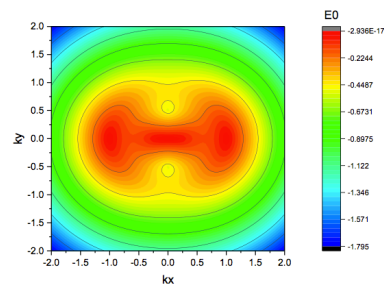
1. Loughborough University

Graphene has gained a huge interest since it has been illustrated as the first stable 2D crystal [1] [2]. Moreover, graphene is the basic structuring unit for all graphitic material [3]. Since this gapless material has been demonstrated, the main problem that has been investigated is the gap band opening and controlling in the energy spectrum of graphene. A variety of methods have been established to open a gap in graphene's band, some are based on destroying the honeycomb structure of graphene, where others maintain it. One of the most effective former methods is the application of an external field, which creates atomic sites with different electric potentials. However, this modification is only valid of multi-layered graphene as if a vertical field is applied to a single layer graphene there will be no gap in the band structure as the two sublattices remain equivalent. Hence, there is a demand for effective gap opening methods in single layer graphene that will maintain the high carrier mobility and allow manipulation of Dirac points. This study provides a theoretical analysis to investigate the band structure of single layer graphene in laser field (and graphene superlattices by analogy [4]), and some of its electronic properties. We show that the spectra and the current flow of Dirac electrons in graphene can be controlled by applying linearly polarised laser field to a graphene sheet under the application of static fields (Electric or Magnetic). We demonstrate how Dirac points can be manipulated by altering the laser field parameters based on Floquet theory and the resonance approximation. Electrons' ac current can be manipulated with a describable intensity.

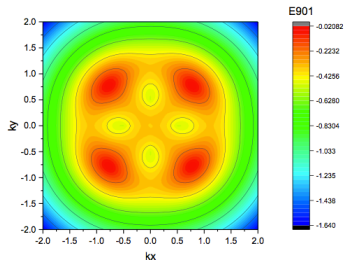
[1] Novoselov et al. (2004) Electric field effect in atomically thin carbon films, Science 306, 666.[2] Meyer et al. (2007) The structure of suspended graphene sheets, Nature 446, 60. [3] O'Hare et al. (2012) A stable flat form of two-dimensional crystals: could graphene, silicene, germanene be minigap semiconductors, Nano Lett. 12,1045[4] Savel'ev, S. E. and Alexandre, A.S (2011) Massless Dirac fermions in laser field as a counterpart of graphene superlattices, Physical Review B 84, 035428.



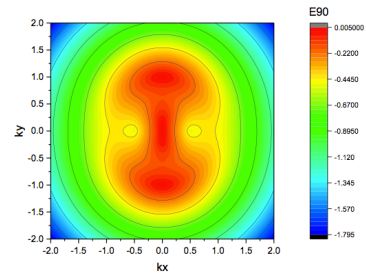
The energy spectrum of 1 layer graphene in the application of linearly laser field parallel to a static electric field .png



The energy spectrum of 1 layer graphene in the application of linearly laser field parallel to a static magnetic field .png



The energy spectrum of 1 layer graphene in the application of linearly laser field vertical to a static electric field .png



The energy spectrum of 1 layer graphene in the application of linearly laser field vertical to a static magnetic field .png

Optical Parameters of GaInAsSb Laser Diodes and Its Application for Carbon Monoxide Detection

Thursday, 14th September - 13:30 - Poster Session - Gallery - Poster - Abstract ID: 214

Mr. Dzmitry Kabanau¹, Dr. Yahor Lebiadok¹

1. SSPA "Optics, Optoelectronics & Laser Technology"

The optical and energy characteristics of laser diodes with quantum active layer GaInAsSb lasing in the range of 2.30-2.35 μm are analyzed in this report. The active region of the laser under investigation consists of two strained $\text{Ga}_{0.65}\text{In}_{0.35}\text{As}_{0.11}\text{Sb}_{0.89}$ quantum wells, each is of 10 nm thick. The thickness of waveguide layers made of AlGaAsSb is equal to 375 nm. Waveguide layers are bounded by wide-gap layers of p- and n-AlGaAsSb. The energy diagram of the laser structures under consideration is shown in Fig. 1.

The bandgap energy temperature dependence was obtained for $\text{Ga}_{0.65}\text{In}_{0.35}\text{As}_{0.11}\text{Sb}_{0.89}$ on the base of luminescence spectra (see Fig.1).

The lasing spectra of the laser diode with double quantum well and its temperature dependence were investigated in detail with the purpose of carbon monoxide detection (see Fig. 2).

The bandgap calculation method, lasing and amplified luminescence spectra are discussed in the report.

This work was partially supported by BRFFR, grant F17M-087

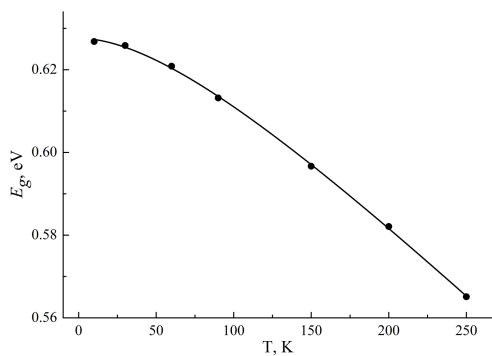


Fig1.jpg

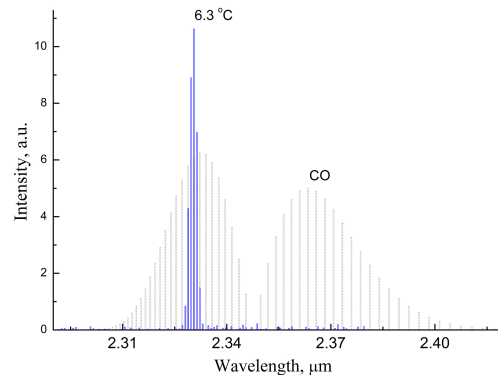


Fig2.jpg

Performance enhancement of bidirectional TWDM-PON by Rayleigh backscattering mitigation

Thursday, 14th September - 13:30 - Poster Session - Gallery - Poster - Abstract ID: 221

***Mr. Ibrahim Elewah*¹, *Ms. Martina Kalds*², *Prof. Moustafa Aly*³**

1. American College of the Middle East ACM, 2. Higher Technological Institute, 3. Arab Academy for Science, Technology and Maritime Transport

A bidirectional time wavelength division multiplexing-passive optical network (TWDM-PON) with a centralized light source (CLS) is designed and evaluated. TWDM-PON is the promising solution for PON future expansion and migration. The most important issue that limits optical fiber transmission length is the interferometric noise caused by Rayleigh backscattering (RB). In this study, we demonstrate a TWDM-PON architecture with subcarrier at the remote node (RN) to mitigate the RB effect. A successful transmission with 8 optical channels is achieved using wavelength division multiplexing (WDM). Each optical channel is splitted into 8 time slots to achieve TWDM. The proposed scheme is operated over 20 km bidirectional single mode fiber (SMF). The proposed system has the advantage of expanding the downstream (DS) capacity to be 160 Gb/s (8 channels×20 Gb/s) and 20 Gb/s (8 channels×2.5 Gb/s) for the upstream (US) transmission capacity. This is accomplished by a remarkable bit error rate (BER) and low complexity.

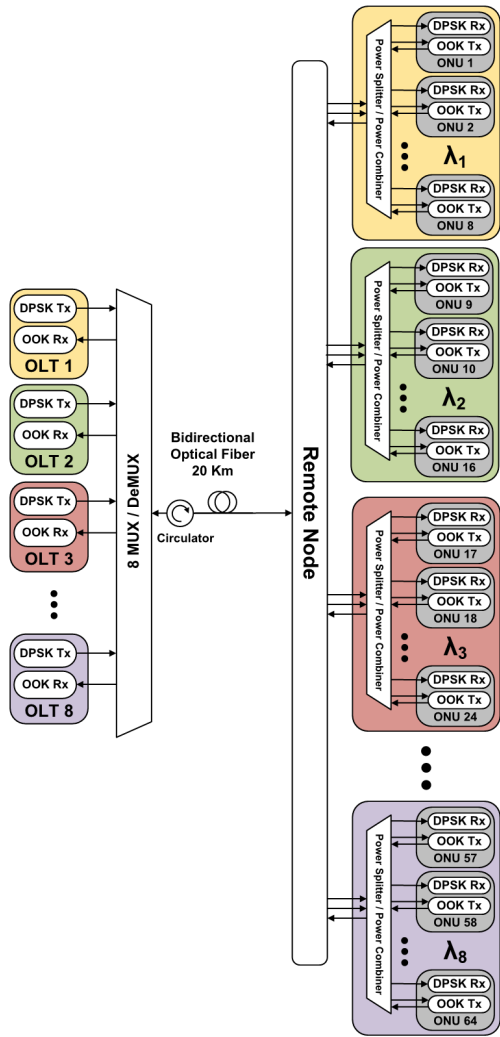


Figure 1.png

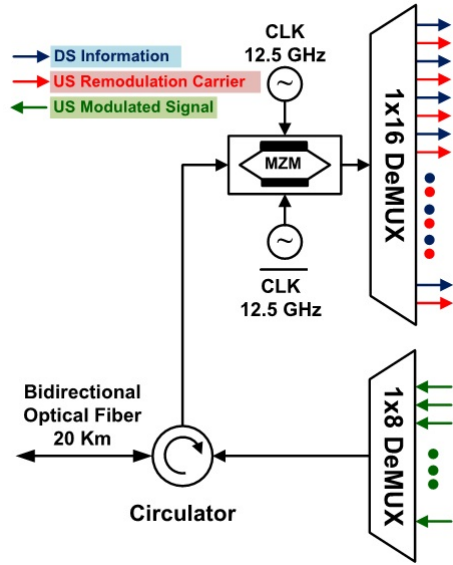


Figure 2.jpg

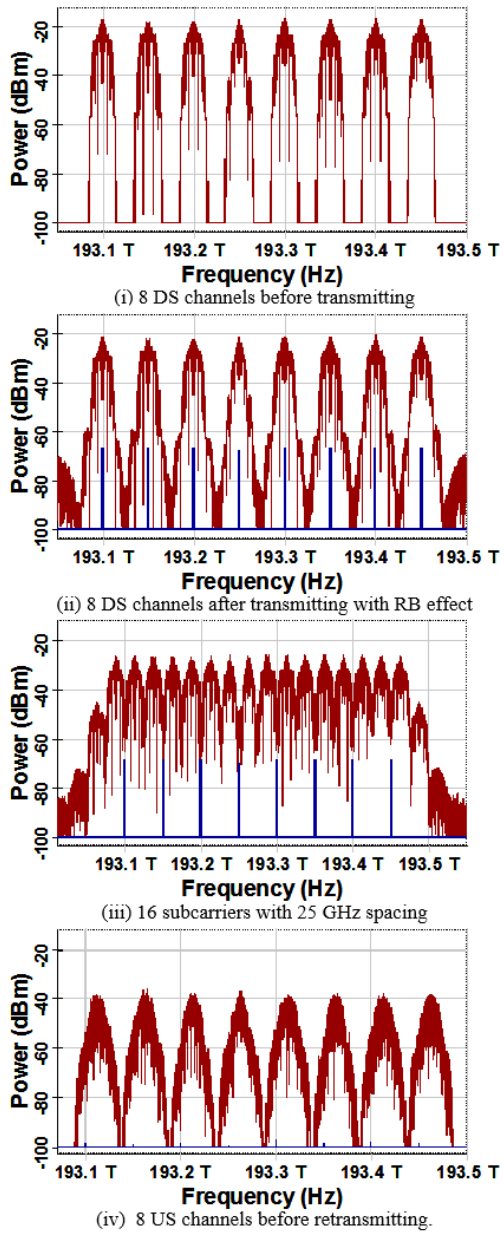


Figure 7. Channels spectrum for each stage

Figure 7.png

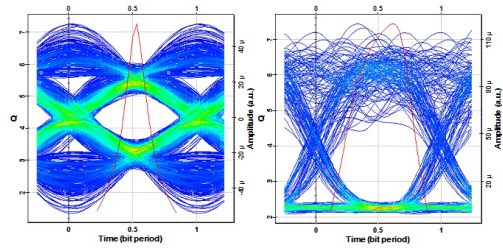


Figure 8. (i) DS eye diagram (ii) US eye diagram

Figure 8.jpg

Universal description of 2D channel plasmons: from graphene and beyond

Thursday, 14th September - 13:30 - Poster Session - Gallery - Poster - Abstract ID: 489

*Mr. Paulo André Gonçalves*¹, *Mr. Eduardo Dias*², *Prof. Sanshui Xiao*¹, *Prof. Mikhail Vasilevskiy*²,
*Prof. Sergey I. Bozhevolnyi*³, *Prof. Nuno Peres*², *Prof. N. Asger Mortensen*³

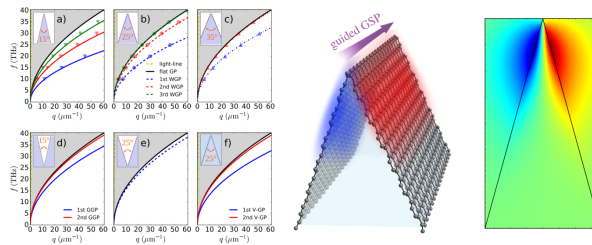
1. Technical University of Denmark, 2. University of Minho, 3. University of Southern Denmark

Introduction: Controlling and routing electromagnetic radiation below the diffraction limit is a key feature for future photonic-based circuitry. Here, we propose an alternative solution to conventional metal-based plasmonics by exploiting the subwavelength localization and tunability of 2D materials' plasmons guided along a V-shaped triangular channel.

Methods: We present both a rigorous quasi-analytical theory and a simpler effective-index method (EIM) to describe the plasmonic eigenmodes and corresponding field distributions of 2D-covered triangular channels.

Results: We have found that the dispersion of 2D channel plasmons follows the same functional dependence as their flat-plasmons counterparts, but now scaled by a purely geometric factor in which all the information about the system's geometry is incorporated. In addition, we show that the solution of the EIM reduces to solving a Schrödinger-like equation, whose eigenvalue determines the plasmon dispersion.

Discussion: The plasmonic spectrum calculated using both methods agrees well with full-wave numerical simulations. The modal distributions for each of the channel's modes are also obtained. We believe our results pave the way for the emergence of customized photonic devices for subwavelength waveguiding and localization of light based on novel 2D materials.



2d channel plasmons dispersion and field distribution.png

Broadband bidirectional optical cloaking by a generalized Hilbert transform

Thursday, 14th September - 13:30 - Poster Session - Gallery - Poster - Abstract ID: 218

Mr. Zeki Hayran ¹, Dr. Ramon Herrero ², Dr. Muriel Botey ³, Prof. Kestutis Staliunas ⁴, Dr. Hamza Kurt

¹

1. TOBB University of Economics and Technology, 2. Universitat Politècnica de Catalunya, 3. Univeritat Politècnica de Catalunya, 4. Institució Catalana de Recerca i Estudis Avançats, Catalonia

Cloaking objects, such that their optical response mimics wave propagation in free space, has been a long sought goal since the advent of transformation optics [1]. However, the complexity of the required materials or other inherent problems as the device area severely limit practical realizations. Therefore, many proposed cloaking schemes generally scarpify the perfect scattering cancellation [2]. A recent powerful proposal based on the spatial Kramers-Kronig relations, provides a valuable insight to the intimate relation between the material properties and their optical behaviour [3]; still suffering from serious difficulties in terms of practical realizations as it requires infinitely extended permittivity profiles including complex (lossy) materials.

We here propose a different approach following our recently developed general theorem to control the scattering behaviour of an arbitrary object on a specific demand [4], to attain bidirectional optical cloaking for any object with arbitrary shape and size. The design method is based on a generalized Hilbert transform (relating the real and imaginary permittivity) to locally tailor the scattering potential of an arbitrary object as explained in Fig. 1. Furthermore, to extend this idea to cover a specific operational bandwidth rather than a single frequency, as shown in Figs. 1(a), a “half-moon” shaped k -area can be employed to modify the index profile of the initial object, in Fig. 1(b), see Fig. 1(c). We note that the resulting index profile is locally isotropic and we reveal that it is always possible to produce local refractive indices larger than one avoiding the use of gain nor lossy materials. Numerical calculations, using the two-dimensional FDTD method, evidence the bidirectional cloaking with a broad operational bandwidth and wide angular aperture for both directions, working under both polarizations, see Fig.2.

The reported cloaking concept can be easily realized to operate in a wide electromagnetic spectrum from microwaves down to visible wavelengths and to other kind of waves (acoustics), and the operational principle can also be extended to three-dimensional geometries.

- [1] *Science* 312, 1780–1782, 2006.
- [2] *Phys. Rev.w Appl.*4, 037001, 2015.
- [3] *Nat. Photonics* 9, 1–4, 2015.
- [4] *arXiv preprint*, arXiv:1703.09490 [physics.optics], 2017.

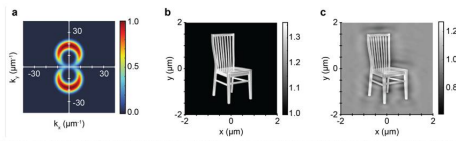


Figure 1. (a) Area of invisibility wavevector domain to be removed from the scattering potential. (b) Spatial index distribution of the original and, (c) corresponding modified object (exhibiting cloaking effect).

Fig1-cloaking.emf.jpg

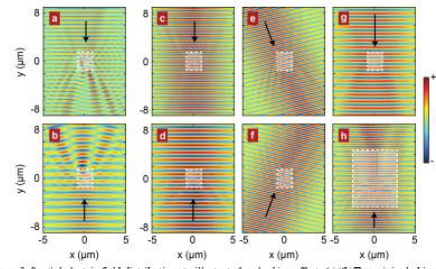


Figure 2. Spatial electric field distributions to illustrate the cloaking effect. (a)-(b) The original object causes strong wave scattering and, for both +/-y propagation directions. (c, d) The modified object, eliminates nearly all backward and forward scattered waves, displaying a bidirectional cloaking effect. (e, f) The bidirectional cloaking behaviour is still present with an oblique source incident angle of 18° with respect to normal incidence. (g) The same object exhibits optical cloaking also for a TE-polarized source. (h) The optical cloaking effect still survives even if the object is enlarged (in this case, the object is three times larger than in the previous cases). The operational frequencies correspond to $0.65 \mu\text{m}$, $1.20 \mu\text{m}$, $0.65 \mu\text{m}$, $1.20 \mu\text{m}$, $0.70 \mu\text{m}$, $1.10 \mu\text{m}$ and $0.80 \mu\text{m}$ for (a), (b), (c), (d), (e), (f), (g) and (h), respectively. The operational frequencies have been chosen so that the figures simultaneously demonstrate the broadband behaviour. Furthermore, the black arrows reveal the direction of the wave propagation and the white dashed lines outline the position of the 'chair' object.

Fig2-cloaking.jpg

Dispersion relations for electromagnetic surface waves on the boundary vacuum- metamaterial

Thursday, 14th September - 13:30 - Poster Session - Gallery - Poster - Abstract ID: 187

Ms. Olga Porvatkina ¹, Dr. Alexey Tishchenko ¹, Prof. Mikhail Strikhanov ¹

1. National Research Nuclear University MEPhI (Moscow Engineering Physics Institute)

Metamaterials are usually constructed as arrays of split-ring resonators. As the distance between resonators is comparable with their size, there is strong interaction between resonators, which results in rather strong absorption. As a result, absorbing volumes are not so convenient for experiments with metamaterials, and boundary phenomena become very attractive. In the present work we proceed from the local-field approach [1] and show that the natural variation in properties of near-surface layer [2,3] enables the existence of electromagnetic surface waves on the boundary vacuum-metamaterial. The dispersion relation for surface TE-waves is obtained (Pic.1) for condition (Pic.2), where $\varepsilon(\omega)$, $\mu(\omega)$ are permittivity and permeability of metamaterial; $\eta(\omega)$ is a phenomenological parameter defining properties of the near-surface layer. For nonmagnetic media our results coincide with those from [3]. When the influence of the near-surface layer is negligible, we can neglect surface currents and charges, and our results coincide with [4]. Thus, we argue that the surface waves can exist on the surface of metamaterials owing to the natural variation in properties of its near-surface layer. We envision that our results open new opportunities to realize devices based on the special properties of surface waves propagation.

The work was supported by the Competitiveness Programme of National Research Nuclear University "MEPhI" and partially by the Ministry of Science and Education of the Russian Federation, grant No 3.2621.2017/4.6.

REFERENCES

1. O.V. Porvatkina, A.A. Tishchenko, M.N. Strikhanov, "Permeability tensor for a metamaterial adjacent to a metal," *Appl. Phys. A*, vol. 123, p. 2, 2017.
2. O.V. Porvatkina, A.A. Tishchenko, M.N. Strikhanov, "Permittivity and permeability of semi-infinite metamaterial," *IOP Conf. Ser.*, vol. 740, p. 012011, 2016.
3. M.I. Ryazanov, "The effect of the natural variation in the polarization of a near-surface layer on electromagnetic surface waves," *Zh. Eksp. Teor. Fiz.*, vol. 110, pp. 959-965, 1996.
4. N.V. Ilin, A.I. Smirnov, I.G. Kondratiev, "Features of surface modes in metamaterial layers," *Metamaterials*, vol.3, pp.82-89, 2009.

$$q^2 = \frac{-\frac{\omega^2}{c^2} \left((\mu^2(\omega) - 1)(\varepsilon(\omega)\mu(\omega) - \mu^2(\omega)) - \frac{\omega^2}{c^2} \eta^2(\omega)(\mu^2(\omega) + 1) \right)}{(\mu^2(\omega) - 1)^2} \pm \frac{2\frac{\omega^3}{c^3} \eta(\omega)\mu(\omega) \sqrt{\frac{\omega^2}{c^2} \eta^2(\omega) + (\varepsilon(\omega)\mu(\omega) - 1)(1 - \mu^2(\omega))}}{(\mu^2(\omega) - 1)^2}$$

Pic1.png

$$(\varepsilon(\omega)\mu(\omega) - 1)(1 - \mu^2(\omega)) \geq 0,$$

Pic2.png

Color-selective diffractive optical components based on composite multilayer structures including phase-change materials

Thursday, 14th September - 13:30 - Poster Session - Gallery - Poster - Abstract ID: 301

Mr. Chi-Young Hwang¹, Dr. Yong-Hae Kim¹, Dr. Gi Heon Kim¹, Mr. Won-Jae Lee¹, Mr. Han Byeol Kang¹, Dr. Jong-Heon Yang¹, Mr. Jae-Eun Pi¹, Mr. Ji Hun Choi¹, Dr. Kyunghee Choi¹, Mrs. Hee-Ok Kim¹, Dr. Chi-Sun Hwang¹

1. Electronics and Telecommunications Research Institute

We present a composite multilayer resonance structure for color-selective diffractive optical components in the visible region. The structure consists of stacked layers of indium tin oxide (ITO), a phase-change material $\text{Ge}_2\text{Sb}_2\text{Te}_5$ (GST), and silicon dioxide (SiO_2) on an aluminum substrate. By printing binary spatial patterns on the imbedded GST layer using an ultraviolet laser patterning technique, color-selective diffractive properties with a moderate bandwidth can be obtained [1]. Figure 1(a) shows the design of the proposed structure, in which the dispersive profile of the first-order diffraction efficiency can be tuned by controlling the thickness of the SiO_2 layer.

To verify the proposed structure, numerical simulations are conducted to reveal the relationship between the thickness of the SiO_2 layer and the spectral diffraction efficiency for normally incident plane waves, as shown in Fig. 1(b). Based on this relationship, we fabricated a full-color computer-generated hologram (CGH) using a spatial multiplexing technique [2] capable of reconstructing holographic images with red, green, and blue light with wavelengths of 660, 532, and 473 nm, respectively. Accordingly, three SiO_2 thicknesses of $d = 252$, 390, and 150 nm were selected considering the relative diffraction efficiency at the selected wavelengths. The corresponding profiles are shown in Fig. 1(c). Figure 2 shows the fabricated full-color CGH and a zoomed-in image of the CGH. The printed CGH pattern has a pixel pitch of $2\ \mu\text{m}$, and a resolution of $16,384 \times 16,384$. During the CGH generation step, the right and left source images shown in Fig. 3(a) are positioned at distances of $d = 0.12$ and 0.15 m from the hologram plane, respectively. Figure 3(b) shows experimentally measured reconstruction images at two different focal planes, from which sharply focused “ETRI RGB” and a checkered pattern can be observed at the intended distances. The results demonstrate the effectiveness of the proposed method.

This work was supported by ‘The Cross-Ministry Giga KOREA Project’ grant from the Ministry of Science, ICT, and Future Planning, Korea [GK17D0100].

[1] S.-Y. Lee *et al.*, Scientific Reports 7, 41152 (2017)

[2] Y. Tsuchiyama *et al.*, Opt. Express 25, 2016-2030 (2017)

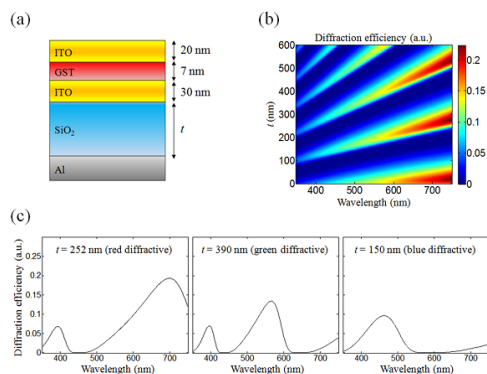


Fig. 1.png

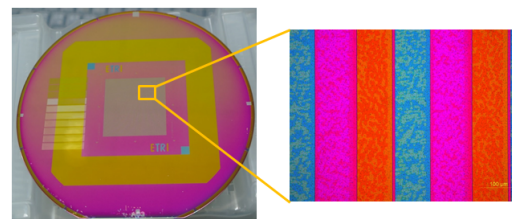
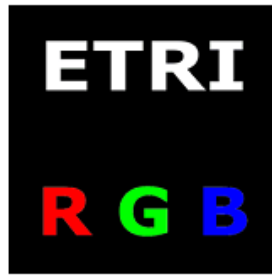
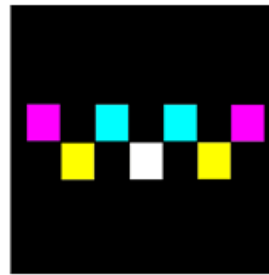


Fig. 2.png

(a)



$d = 0.12 \text{ m}$



$d = 0.15 \text{ m}$

(b)



$d = 0.12 \text{ m}$



$d = 0.15 \text{ m}$

Fig. 3.png

Effect of plasmonic gold nanoparticles morphology and silica layer on efficient light induced carbon dioxide photo-conversion to formic acid in whole solar spectrum region

Thursday, 14th September - 13:30 - Poster Session - Gallery - Poster - Abstract ID: 320

***Dr. Dinesh Kumar*¹, *Ms. Ji Yeon Lee*¹, *Prof. Chan Hee Park*¹, *Prof. Cheol Sang Kim*¹**

1. Chonbuk National University, Jeonju, South Korea

Plasmonic nanoparticles have unique optical properties such as scattering, absorption, enhanced electromagnetic field, fluorescence quenching, and hot-electron generation because of the localized surface plasmon resonance [1]. These properties were extensively explored for their use in numerous photochemical and biological applications.

Here, we have highlighted the preparation of silica coated plasmonic hybrid gold nanoparticles with different morphologies and their application for light induced photoreduction of carbon dioxide to formic acid. We have used Xe lamp (visible light), NIR laser and solar simulator as the light source in order to examine the feasibility of using whole solar spectrum region for carbon dioxide photoconversion. Silica coated gold nanorods (AuNR), nanostars (AuNS) and spherical nanoparticles (AuNP) were prepared by utilizing simple solution-based synthetic strategies. The hot electron generation, which is excited plasmon with higher energy than fermi-level after light absorption in the nanostructures and LSPR excitation, is useful to increase the catalytic activity of plasmonic nanomaterials efficiently [2]. Silica coated AuNS, AuNP and AuNR have shown chemical yield of 1.14%, 0.92% and 0.44% in visible light, 0.3%, 0.2% and 0.64% in NIR light and 0.22%, 0.15% and 0.11% in sun light for formic acid formation when irradiated for 5 h, respectively. Silica coated AuNS shown better efficiency in visible light irradiation and there was more than 100 fold increases in the conversion efficiency after AuNS coated with silica. Surface plasmon resonance band and efficient water oxidation ability of silica layer played vital role in the conversion efficiency of CO₂ to HCOOH.

References

- D. Pissuwan, S. M. Valenzuela and M. B. Cortie, *Trends Biotechnol.* 24, 62 (2006).
- D. Kumar, A. Lee, T. Lee, M. Lim and D. K. Lim, *Nano Lett.* 16, 1760 (2016).

Measuring Quantum Yield of Perylene Bisimide Dyes by Lifetime Modifications Using a Metal Ball

Thursday, 14th September - 13:30 - Poster Session - Gallery - Poster - Abstract ID: 324

Mr. Ersan Özelci¹, **Prof. Ute Resch-Genger**², **Prof. Oliver Benson**³

1. Humboldt-Universität zu Berlin, 2. Bundesanstalt für Materialforschung und -prüfung (BAM), 3. Humboldt Universität zu Berlin

A key parameter for fluorescence applications presents the photoluminescence quantum yield (QY), the number of emitted per number of absorbed photons, which can be determined by optical methods either relative to a standard with known QY or absolutely with integrating sphere spectroscopy [1]. An interesting alternative, expandable to single emitters, utilizes the modification of the spontaneous emission of a fluorophore in the neighborhood of a metallic surface according to the pioneering experiment by Drexhage [2]. This quantum electrodynamic approach enables the direct measurement of QY by changing the local density of states (LDOS) [3]. Our goal is to quantitatively compare both approaches to establish reliable QY measurements over a vast concentration range from macroscopic ensembles down to single emitters.

In our experimental approach, we use a spherical ball coated with silver as in [3] instead of a mirror. These balls in tripod configuration are placed on a PMMA-coated glass substrate (Fig. 1). Then, fluorescence lifetime imaging (FLIM) studies are performed, here with a dye exemplary chosen from the class of perylene bisimides (PBIs), used in organic electronics, photovoltaics, and as sensor materials [4], employing a scanning piezo stage and a confocal microscope. This yields FLIM map (inset of Fig.2). The concentric rings, centered with respect to the contact point of the sphere and the PMMA surface, reflect the increasing distance between the PBI molecules and the silver surface, which can be regarded as locally flat. The variation of the fluorescence lifetime as a function of the molecule-to-sphere distance can then be extracted from the FLIM map. Also, we fitted these data to theoretical curves considering a semi-infinite glass substrate, vacuum, the silver sphere's SiO₂ coating, and the semi-infinite silver layer [5] (Fig.2) and derived the QY of our PBI dye. In the future, we will combine this experimental concept with a microfluidics setup for solution studies.

[1] C. Würth et al., Nat Protocols 2013.

[2] K.Drexhage et al, J.Lumin, 1-2, 693 (1970).

[3] Lunnemann et al, ACS Nano 2013, 5984-5992.

[4] Würthner et al. Chem.Commun. 2004,1564-1579.

[5] Paulus et al., Phys. Rev. E 2000, 62, 5797–5807.

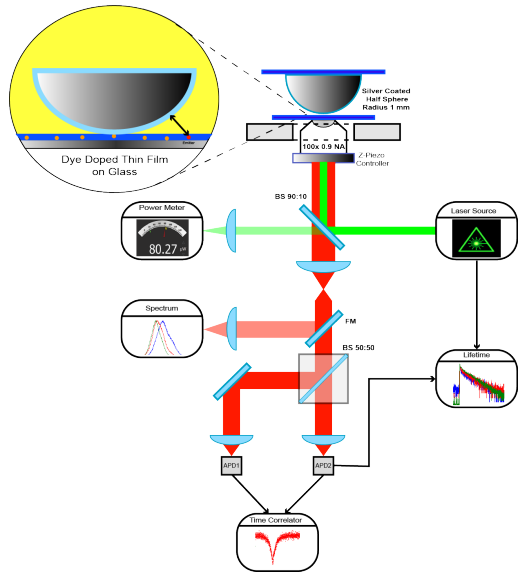


Figure1.png

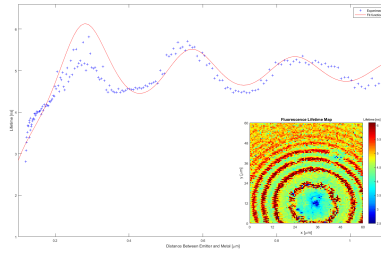


Figure2.png

Fractal Metasurface Absorbers with Octave-Spanning Bandwidth

Thursday, 14th September - 13:30 - Poster Session - Gallery - Poster - Abstract ID: 417

***Dr. Mitchell Kenney*¹, *Dr. James Grant*², *Dr. Yash Shah*², *Dr. Ivonne Escorcía-carranza*², *Mr. Mark Humphreys*², *Prof. David Cumming*²**

1. University of Glasgow, 2. University of Glasgow/Electronic and Nanoscale Engineering

Metasurfaces, the 2D equivalent of metamaterials, have been of great interest in the past few years. They offer a means of commercially integrable applications, and have produced novel devices involving chiroptics [1], highly-efficient holograms and mirrors [2,3], and beam manipulation [4,5]. Metasurface absorbers have been an interesting topic of research in the past few years, due to many potentially useful applications, including stealth and sensing. A particular focus has been on THz absorbers, due to the lack of naturally occurring materials having strong THz response. However, although most of these achieve high-absorption magnitude, many have limited bandwidth due to the highly resonant response of the meta-atoms. Devices which have both high-efficiency and broad bandwidth are typically multi-layered, hence involving complex design and fabrication. Here, we present a planar, ultrathin, broadband THz absorber, based on supercells ($P=40\mu\text{m}$) of fractal crosses (Fig.1). We employ the geometry-dependent frequency response of varying fractal crosses (size approximately $20\mu\text{m}$) to cover a broad FWHM bandwidth of 2.7THz (centred at 4.1THz), with a peak absorbance of 96% ($A=1-R$) (Fig.3). By utilising a unique absorption mechanism based on Salisbury screen and anti-reflection responses (Fig.2), we obtain high-magnitude dispersionless absorption over wide bandwidth. This design is distinct from typical metasurface absorbers, which utilise effective current loops to tailor the effective permeability. Experimental and simulated results are well-matched (Fig.3), where Frequency Domain calculations in CST Microwave Studio were used for numerical modelling. Both experiment and simulation were carried out at 30° incidence, showing good robustness to angle of incidence. Such a device is expected to be of great benefit to sensing technologies, and paves the way towards the development of a synthetic metasurface blackbody absorber in the THz band.

[1] M. Kenney, S. Li, X. Zhang *et al.*, *Adv. Mater.* **28**, 9567 (2016).

[2] G. Zheng, H. Mühlenbernd, M. Kenney *et al.*, *Nat. Nanotechnol.* **10**, 308 (2015).

[3] S. Xiao, H. Mühlenbernd, G. Li *et al.*, *Adv. Opt. Mater.* **4**, 654 (2016).

[4] L. Liu, X. Zhang, M. Kenney *et al.*, *Adv. Mater.* **26**, 5031 (2014).

[5] G. Zheng, G. Liu, M. Kenney *et al.*, *Opt. Express* **24**, 6749 (2016).

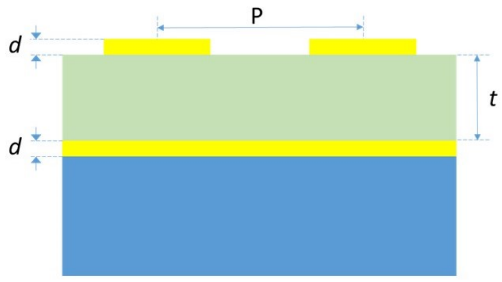


Fig 2 - absorber mim structure.jpg

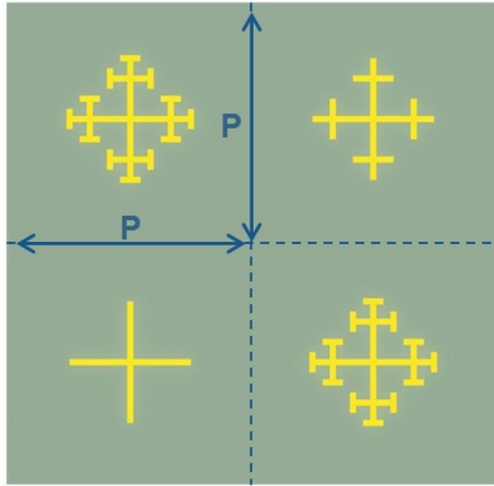


Fig 1 - fractal schematic.jpg

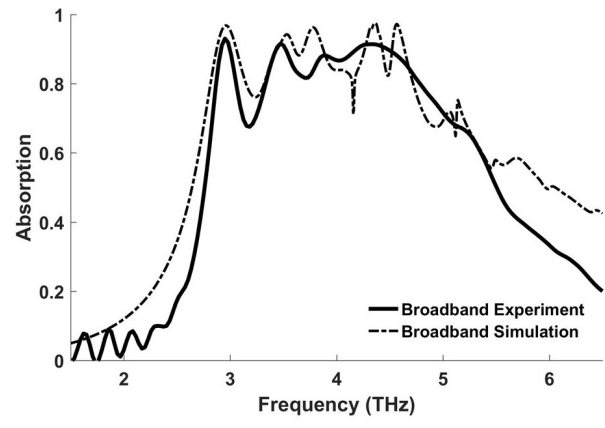


Fig 3 - experimental and simulated absorbance plots.jpg

Plasmon-enhanced fluorescence biosensor utilizing metallic nanostructures and responsive hydrogel binding matrix

Thursday, 14th September - 13:30 - Poster Session - Gallery - Poster - Abstract ID: 438

***Ms. Simone Hageneder*¹, *Mr. Stefan Fossati*¹, *Mr. Christian Petri*², *Prof. Ulrich Jonas*², *Prof. Wolfgang Knoll*¹, *Dr. Jakub Dostalek*¹**

1. Biosensor Technologies, AIT-Austrian Institute of Technology GmbH, 2. Macromolecular Chemistry, Department Chemistry - Biology, University of Siegen

Fast, cheap and reliable detection of biomolecules is of increasing need in various fields, including early diagnosis of cancer and infectious diseases [1,2]. Applications often concern the analysis of biomarkers present in bodily fluids at very low concentrations.

In order to sensitively detect trace amounts of biomarkers by the use of fluorescence assays, the plasmonic amplification of the fluorescence intensity associated with a specific capture of the target analyte has been pursued [3]. The highly increased field strength accompanied with the resonant excitation of surface plasmons at the adsorption and emission wavelengths of fluorophore labels allows enhancing the detected fluorescence intensity by a factor of 10^3 if the binding occurs at the plasmonic hotspot [4].

We report a strategy to selectively functionalize metallic nanostructures composed of gold and oxide features utilizing a responsive hydrogel binding matrix. A layer-by-layer (LBL) approach is used to attach a three dimensional pNIPAAm-based photo-cross-linkable hydrogel at the plasmonic hotspot. This hydrogel can be post-modified with ligand molecules to selectively capture the target analyte. After the analyte capture, the collapse of the hydrogel pulls the captured analyte towards the plasmonic hotspot where the sensitivity of detection can be most efficiently plasmonically enhanced.

This project has received funding from the European Union's Horizon 2020 research and innovation programme under grant agreement No 633937, project ULTRAPLACAD.

References:

- [1] Peeling, R. W., and D. Mabey. "Point-of-care tests for diagnosing infections in the developing world." *Clinical microbiology and infection* 16.8 (2010): 1062-1069.
- [2] Tothill, Ibtisam E. "Biosensors for cancer markers diagnosis." *Seminars in cell & developmental biology*. Vol. 20. No. 1. Academic Press, 2009.
- [3] Bauch, Martin, et al. "Plasmon-enhanced fluorescence biosensors: a review." *Plasmonics* 9.4 (2014): 781-799.
- [4] Kinkhabwala A, Yu ZF, Fan SH, Avlasevich Y, Mullen K, Moerner WE (2009) Large single-molecule fluorescence enhancements produced by a bowtie nanoantenna. *Nat Photonics* 3(11):654– 657

Super-resolution optical imaging of nanostructures using SMAL (Super-resolution Microsphere Amplifying Lens)

Thursday, 14th September - 13:30 - Poster Session - Gallery - Poster - Abstract ID: 497

***Dr. Sorin Laurentiu Stanescu*¹, *Dr. Sébastien Vilain*¹, *Mr. Valerio Galieni*¹, *Dr. George Goh*², *Ms. Katarzyna Karpinska*³, *Mr. Chao Wei*³, *Mr. Alex Sheppard*¹, *Mr. Steve Wright*¹, *Dr. Wei Guo*³, *Prof. Lin Li*³**

1. LIG Nanowise Limited, 2. LIG Biowise Limited, 3. The University of Manchester

Optical imaging is one of the most difficult tasks in characterizing nanostructures due to the diffraction limit. Using our novel SMAL (Super-resolution Microsphere Amplifying Lens) lens, we could image nanostructures with dimensions between 70 nm - 100 nm in wide field reflection mode. SMAL is a long lifespan super-resolution objective lens whose front lens assembly contains an attached optically aligned high refractive index microsphere which is replaceable. The microsphere is optically aligned along the XYZ axes and attached using a single refractive index medium between itself and the front hemispherical lens of the objective. We are offering a complementary technique to SEMs (Scanning Electron Microscopes) by offering simultaneous 3D multi-layer imaging and color information. SMAL can be easily applied for fluorescent samples as a complementary technique for STED (Stimulated emission depletion) and STORM (Stochastic Optical Reconstruction Microscopy) but without the need of fluorescent staining. The work presents full color wide area images of silicon nanostructures which come from different layers of microprocessors, SoCs (System-on-Chips) as well as bio samples. The imaging scanning is a contactless non-invasive and non-destructive process and has led to the development of a new microscope, NANOPSIS, with a custom software and optical optimization able to correct the distortions induced by the microsphere.

KeV Argon Ions Beam Irradiation Induced Changes in Optical Properties of Ni-NWs

Thursday, 14th September - 13:30 - Poster Session - Gallery - Poster - Abstract ID: 507

Ms. Shehla Honey¹, Dr. Shahzad Naseem¹, Dr. Ahmad Ishaq², Dr. Malik Maaza³

1. Centre of Excellence in Solid State Physics, University of Punjab, QAC, Lahore, Pakistan, 2. National Centre for Physics, Quaid-e-Azam University, Islamabad, Pakistan, 3. UNESCO-UNISA Africa Chair in Nanosciences/Nanotechnology, College of Graduate Studies, University of South Africa, Muckleneuk ridge, P O Box 392, Pretoria, South Africa

This contribution reports on KeV argon (Ar^+) ions beam irradiation-induced changes in optical properties of nickel nanowires (Ni-NWs) networks. Optical properties of Ni-NWs networks are studied systematically before and after irradiating at different fluencies of Ar^+ ions ranging from 7×10^{14} to 3×10^{16} ions/cm² at room temperature. The variation in optical properties of Ni-NWs networks is discussed after analysis of Ni-NWs networks using transmission electron microscopy (TEM) and X-ray diffraction (XRD) techniques. Moreover, optical characterization of these networks has been done using UV-VIS spectroscopy. Ni-NWs networks are found to be optically transparent and optical transparency is enhanced with increase in beam fluence of Ar^+ ions. The observed increase in optical transparency is thought to be due to Ar^+ ions beam induced sputtering of atoms from Ni-NWs lattices due to collision cascade of atomic displacements, which causes reduction of diameters of Ni-NWs and increase spaces between Ni-NWs in the network. Ion beam technology is therefore a promising approach that is capable of fabricating highly transparent Ni-NWs networks for transparent electrodes. Moreover, a method for thinning, slicing and cutting of Ni-NWs using ion beam technology is also discussed.

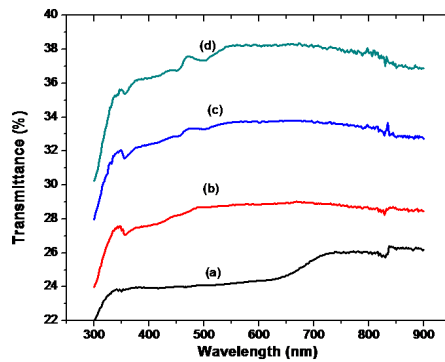


Fig. (a-d) represents the Plots of transmittance versus wavelength for Ni-NWs networks [(a) un-irradiated, and irradiated by Ar^+ ions at fluencies (b) 7×10^{14} ions/cm² (c) 3×10^{15} ions/cm² (d) 3×10^{16} ions/cm²].

Fig.png

Interface defects and silicon impurities in AlGaAs/GaAs heterostructures and its relationship to registration efficiency of quantum well infrared photodetector

Thursday, 14th September - 13:30 - Poster Session - Gallery - Poster - Abstract ID: 341

Dr. Yahor Lebiadok¹, Ms. Alena Shalayeva¹

1. SSPA "Optics, Optoelectronics & Laser Technology"

The influence of complex defects (gallium, arsenic and aluminum vacancies with corresponding interstitial atoms) in Al_{0.3}Ga_{0.7}As/GaAs heterointerface on quantum well infrared photodetector (QWIP) characteristics as well as "passivation" of the defects by silicon impurities are discussed in the report. The wavelength corresponding to the maximal absorption of QWIP is in the vicinity of 8.5-8.6 μm. The density functional theory calculations with the hybrid functionals B3LYP with Hay-Wadt effective core potentials for all the heavy atoms in a combination with Hay-Wadt valence basis were used. The energy characteristics (formation energy) and geometry of the defects (spatial distribution of the atoms and its charge near the interface defect) are presented in the report.

Thermal Dynamics of Xanthene Dye in Polymer Matrix Excited by Two-Photon Laser Radiation

Thursday, 14th September - 13:30 - Poster Session - Gallery - Poster - Abstract ID: 352

Dr. Ilia Samusev¹, Mr. Rodion Borkunov¹, Mr. Maksim Tsarkov¹, Ms. Elizaveta Konstantinova¹, Prof. Yury Antipov², Dr. Maksim Demin¹, Prof. Valery Bryukhanov¹

1. Immanuel Kant Baltic Federal University, 2. Kaliningrad State Technical University

Two-photon laser excitation of the molecules embedded in polymer media can be known to be a method of polymer thermal dynamics investigation.

The polyvinyl alcohol thin film (80 μm thick) doped with xanthene dye (0.5 mM) was excited by two-photon laser radiation: the first pulse of YAG:Nd³⁺ laser (532 nm, 20 J, 10 ns) caused the molecules to be excited on S₁ vibration-electron level and then, after time delay of 50 ms, the second pulse of CO₂ laser (10.6 μm , 20 W) made the molecules absorb an additional energy portion. The delayed fluorescence lifetime before and after IR-excitation were 17 and 50 ms respectively. The fluorescence intensity increase after the second laser pulsed allowed us to estimate the change in polymer media temperature (4 K).

In the second experimental stage, the samples were excited by two photon laser radiation: semiconductor laser (532 nm, J = 50 mJ) and pulsed CO₂ laser (10.6 μm , 20 W) with controlled time delay (from 50 to 200 ms). The dye delayed fluorescence lifetime appeared to be 4.7 s.

In order to simulate thermal and photophysical processes caused by two photon excitation, we solved heat transfer and energy deactivation differential equations numerically. The simulation allowed us to obtain the value of heat conductivity coefficient of PVA matrix: $a = 0.51 \cdot 10^{-6} \text{ m}^2/\text{s}$, which appeared to coincide with literature data.

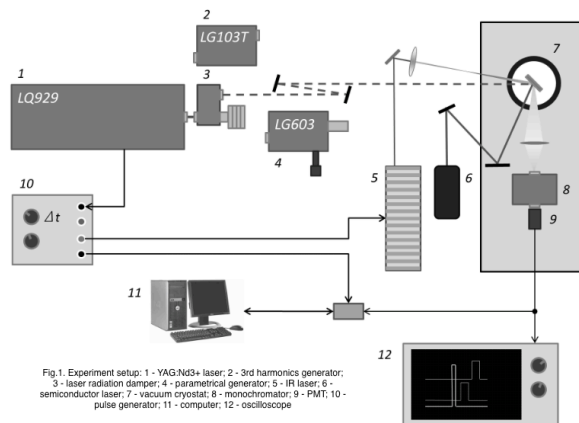


Fig 1.png

Anomalous Hall effect and magnetic properties of GaMnSb thin films grown by DC Magnetron co-Sputtering for spintronics applications

Thursday, 14th September - 13:30 - Poster Session - Gallery - Poster - Abstract ID: 128

Prof. Fredy Mesa¹, Dr. Jorge Calderon², Prof. Anderson Dussan², Prof. Rafael Gonzalez-hernandez³

1. Universidad del Rosario, 2. Universidad Nacional de Colombia, 3. Universidad del Norte

This work presents a study of the magnetic properties and Hall effect measurements on diluted magnetic semiconductors (GaMn)Sb obtained by DC magnetron co-sputtering method. Synthesis parameters, like substrate temperature (T_s), and deposition time (t_d) were varied while the magnetron power deposition applied to both targets, and the work pressure (WP) were kept constant. The values for t_d were 10 and 15 min; for T_s , these values were 423 and 523 K. The Mn_2Sb_2 and Mn_2Sb phases were identified through the X-ray diffraction measurements. The influence of synthesis parameters on the magnetic properties and Hall effect are discussed. Magnetization (M) studies as function of the applied magnetic field (H) at different temperatures (50, 150, and 300 K) were also performed. The paramagnetic and diamagnetic behavior, accompanied by the ferrimagnetic and ferromagnetic phases in two samples was evidenced through hysteresis curves. The Hall effect was used to establish carrier density (n_p) values between $3.19 \times 10^{15} \text{ cm}^{-3}$ and $2.86 \times 10^{20} \text{ cm}^{-3}$, consequently, the anomalous Hall effect was observed

Colour Gamut Enhancement with Remote Light Conversion Mechanism

Thursday, 14th September - 13:30 - Poster Session - Gallery - Poster - Abstract ID: 470

Dr. Devrim Koseoglu¹, Mr. Emrah Bakan¹, Mr. Kivanc Karsli¹, Mr. Yusuf Sinan Sezer¹

1. Vestel Electronics

The backlight unit spectrum of liquid crystal displays (LCD) directly affects the colour gamut. With the invention of GaN based blue light emitting diodes (LED), phosphors and quantum dots have gained considerable scientific interest due to their broad range of applications especially in lighting and display technologies. These phosphors and quantum dots are used to convert the blue light of the LEDs into white in general lighting. On the other hand, in display systems, they are used to generate red and green bands. There are different application methods such as on-chip and remote configurations of these particles. In this study, we concentrate on remote phosphor and quantum dot backlight configurations where the light conversion is done away from the chips. We use the GaN based blue LED flip-chips, since they are more efficient in terms of the light output and thermal management. Light conversion layers were placed in backlight units as a thin film for the emission of green and red bands. The composition of these layers were arranged to match the emission spectrum of the blue LEDs and the light conversion layer to the colour filters of the LCD, so that the green, blue, and red bands efficiently widens the colour space. The results were compared with the on-chip phosphor arrangements.

Colour Gamut Standard	On-chip yellow phosphor converted display		Display with remote light conversion layer	
	CIE 1931	CIE 1976	CIE 1931	CIE 1976
NTSC	69%	88%	87%	111%
DCI	71%	80%	91%	101%

Table 1 - The comparison of colour gamut measurements

Table 1.jpg

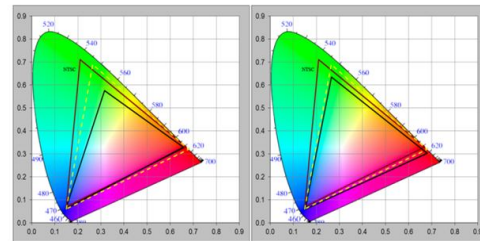


Figure 3 – The comparison of colour space diagrams

Figure 3.jpg

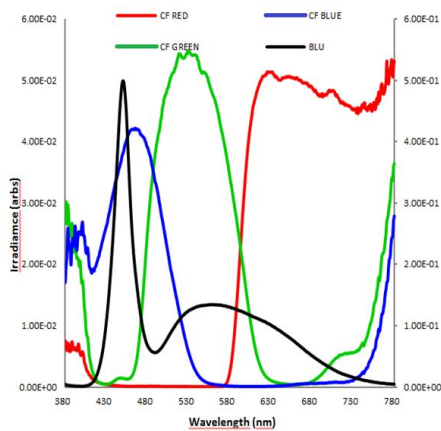


Figure 2 - BLU light conversion film and the colour filter spectrum

Figure 2.jpg

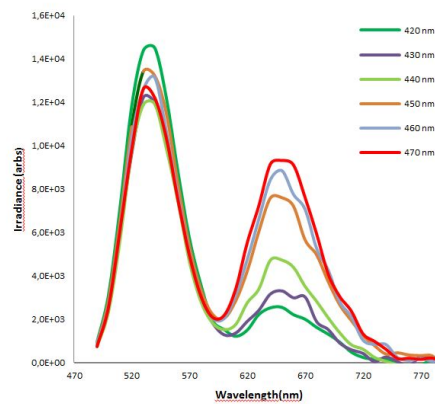


Figure 1 - Spectrum of light conversion film for different excitation wavelengths

Figure 1.jpg

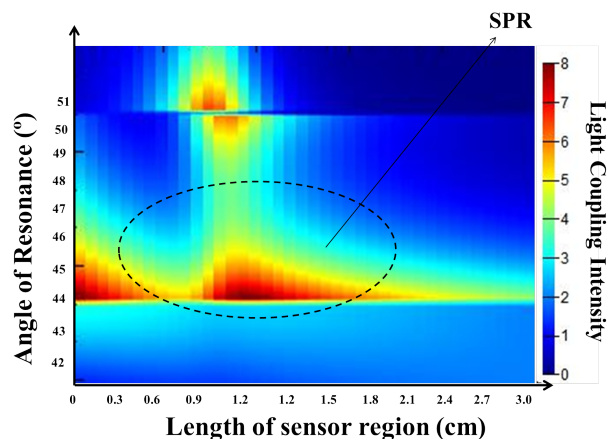
Numerical Analysis of Microstructured Optical Fiber for Applications in SPR Sensing

Thursday, 14th September - 13:30 - Poster Session - Gallery - Poster - Abstract ID: 451

*Mr. Arthur Aprígio De Melo*¹, *Ms. Márcia Fernanda Da Silva Santiago*¹, *Ms. Talita Brito Da Silva*¹,
*Prof. Rossana Moreno Santa Cruz*¹, *Prof. Cleumar da Silva Moreira*¹

1. IFPB

In recent years, fiber-optic sensor technology has been boosted to industrial and biomedical applications, with the emergence of sensors based on Surface Plasmon Resonance (SPR) phenomenon. During the 1990s, a new technology was introduced in the manufacture of optical fibers, where elements called photonic crystals became the raw material used for the construction and characterization of these fibers. This new technology has boosted interest in the study of photonic crystal fibers (PCFs), which consist of microstructured waveguides. The development of optical sensors in microstructured fibers becomes a very attractive alternative for several applications in sensing, and can be used in the monitoring of physical, chemical and biological parameters, relevant to the maintenance of the quality of products in the industry and in biomedical applications with the detection of pathologies through fluids, due to the development and optimization of devices for compact, accurate and low cost laboratory tests in comparison with the existing ones. This work presents the numerical analysis of a biosensor proposal constructed with fibers of photonic crystals of silica, using gold in the sensory region. Numerical characterization considers the Angular Interrogation Mode (AIM) with wavelength set at 800 nm. The numerical analysis was performed with the aid of software based on the finite element method (FEM). Using perfectly coupled layers and boundary conditions for light scattering. The metal layer and the analyte were placed in the outer layer of the D-shaped fiber in order to facilitate detection and practical implementation. This study served to validate the use of these fibers for the construction of SPR sensors. The future prospect is the manufacture of an optical biochip inspired by these fibers, with larger dimensions in order to facilitate manipulation and testing. The best polishing of the fabricated structure will also be defined in order to obtain the surface for deposition of the metal. Figure 1 shows the coupling of light in a solid-core PCF, where the occurrence of SPR in the fiber can be seen.



Nanop.png

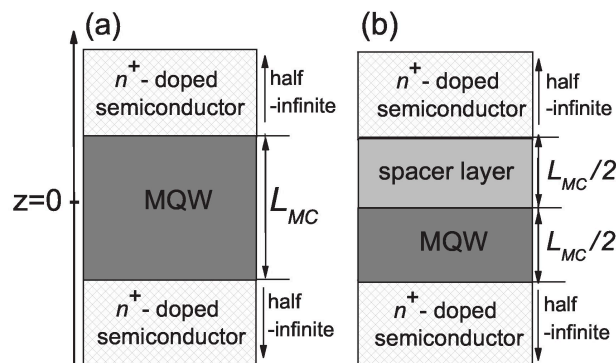
Intersubband-surface-plasmon-polaritons in all-semiconductor planar plasmonic resonators

Thursday, 14th September - 13:30 - Poster Session - Gallery - Poster - Abstract ID: 144

*Prof. Mirosław Żaluzny*¹

1. Institute of Physics, M. Curie-Skłodowska University, Lublin

The strong coupling between a collective intersubband excitation in a multiple quantum well (MQW) structure and the ground photonic mode of the semiconductor microcavity (MC) leads to formation of coherent mixed modes termed intersubband-cavity-polaritons. The intersubband-cavity-polaritons have attracted great attention of the research community. It is mainly due to the fact that intersubband optoelectronic devices operating in a strong coupling regime have potential for applications. The majority of work on the intersubband-cavity-polaritons has explored all dielectric, hybrid metal-dielectric or double metal MCs. In this paper we theoretically discuss the electromagnetic modes supported by the system consisting of an MQW embedded into planar resonator with semi-infinite highly doped semiconducting claddings (mirrors). We focus on the case when intersubband frequency is comparable with the frequency of the surface plasmon of the mirrors. Then the strong resonant coupling of the intersubband excitation with the symmetric and antisymmetric surface plasmon modes leads to the formation of the intersubband-surface-plasmon polariton (ISPP) branches. The characteristics of the ISPP branches are calculated numerically using a semiclassical approach supplemented by the effective-medium approximation. The symmetric structures, where QWs uniformly fill the space between the claddings (mirrors) and asymmetric structures, where QWs occupy only half of space between the mirrors are considered. Strong dependence of the ISPP characteristics on the cavity mirror separation is demonstrated. In particular, for certain parameters of the structures we observe formation of the zero group velocity points in the ISPP branches. It was observed that the properties of the ISPP branches in the symmetric (asymmetric) structures are well interpreted by a coupled two (three) oscillator model, provided that dispersive character of mirror material is taken into account. For sake of completeness, we also briefly discuss the formation (due to the nonresonant coupling of the intersubband excitation with higher resonator modes) of the additional features - the so-called in-gap polariton branches. They are located slightly below the intersubband frequency. The demonstrated possibility of the engineering the dispersion of the ISPP branches in all-semiconductor plasmonic resonators seems to be attractive from the viewpoint of intersubband polariton optoelectronics.



Structures.jpg

Ratiometric Sensor for Levodopa Detection Based on Quenching Effect of Polylevodopa Nanoparticles on the Fluorescence Intensity of CdTe Quantum Dots

Thursday, 14th September - 13:30 - Poster Session - Gallery - Poster - Abstract ID: 62

Mr. Ahmad Moslehi Pour¹, **Dr. Mohammad Reza Hormozi-nezhad**²

1. Sharif University of Technology and Bushehr petrochemical Company, 2. Institute for Nanoscience and Nanotechnology, Sharif University of Technology

Introduction

L-DOPA (L-3,4-dihydroxyphenylalanine) is a natural precursor of dopamine and useful drug for the treatment of Parkinson's disease. It can be cross the blood-brain barrier, whereas dopamine itself cannot.

Methods

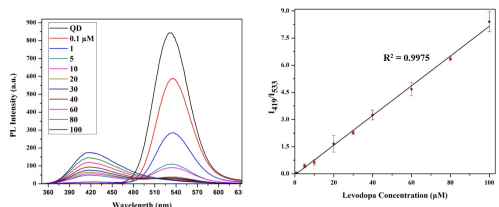
Certain μL amounts of a standard levodopa solution were added to a solution of the QDs (final concentration was $6.3 \mu\text{M}$) and the pH for each concentration was adjusted to 7.4 using phosphate buffer. To start the oxidation reaction, NaOH was added to the solution so that the final concentration was $20.0 \mu\text{M}$. The fluorescence intensities were recorded under the excitation wavelength of 400 nm. The calibration curves were plotted at two range of concentrations, one from zero to $12.8 \mu\text{M}$ (ratiometric) and another from 20 to $200 \mu\text{M}$ (The emission wavelength of 419 nm). To evaluate the selectivity of the method, the concentration of levodopa was set to $5.0 \mu\text{M}$ while the concentrations of all interfering chemicals were fixed at $500.0 \mu\text{M}$.

Results and discussion

Levodopa under alkaline conditions is unstable and is rapidly polymerized through covalent attachment and aggregation. Oxidation of levodopa in an alkaline environment is probably to be the principal mechanism by which intermolecular cross-linking occurs. Levodopa oxidizes into dopaquinone, followed by cyclization into dopachrome, which then undergoes oxidative polymerization into eumelanin. It was found that polymeric products can be quenched the fluorescence of the QDs. Up to now, studies on the interaction mechanism between QDs and polylevodopa nanoparticles in aqueous solutions are very rare.

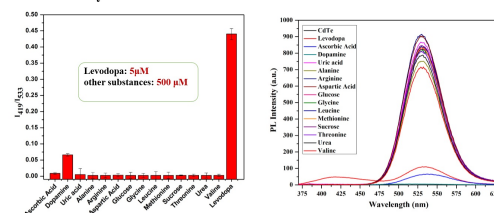
In the current study, we have studied the relationship between fluorescence intensity of CdTe nanocrystals and polylevodopa nanoparticles concentration that is nicely described by the Stern–Volmer equation. It was found, the emission of QDs is strongly dependent on time and the concentration of polylevodopa nanoparticles. Under optimized conditions, a very low detection limit (18.1 nM) and a great selectivity were achieved. Finally, it has been demonstrated that the assay is suitable for selective detection of l-DOPA in biological fluids, such as plasma, and no interference from dopamine, uric acid or ascorbic acid was observed.

Calibration Curve



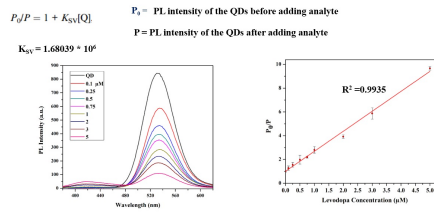
Calibration curve.jpg

Selectivity



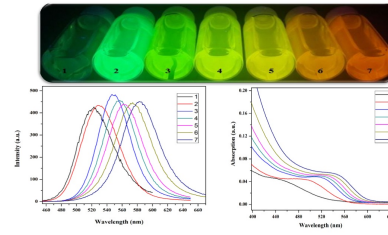
Selectivity.jpg

Stern-Volmer quenching constant (K_{SV})



Stern-volmer quenching constant.jpg

The Synthesis of CdTe QDs



Synthesis of qds.jpg

Study of efficient energy transfer depending on Zn-porphyrin compound ratio in pyrene based metal-organic frameworks by time-resolved spectroscopy

Thursday, 14th September - 13:30 - Poster Session - Gallery - Poster - Abstract ID: 112

***Mr. Ganesh Ghimire*¹, *Mr. Changwon Seo*¹, *Mr. Jubok Lee*¹, *Mr. Kyoung Chul Park*², *Prof. Chang Yeon Lee*², *Prof. Jeongyong Kim*¹**

1. Sungkyunkwan University, 2. Incheon National University

Metal-organic frameworks (MOFs) represent a class of solid-state hybrid compounds consisting of multitopic organic struts and metal-based nodes which are interconnected by coordination bonds.[1] Due to high porosity, chemical diversity and large surface areas,[2] MOF was studied for a broad range of potential applications including gas storage, catalysis, sensing, and light harvesting. NU-1000 is a Zr₆ based MOF structure which are well crystallized by pyrene ligands.[3] We studied energy transfer of new type of Zr based MOFs that replaced pyrene ligand to Zn-porphyrine ligand in NU-1000 by mixed ligand incorporation approach. The energy transfer between pyrene to Zn-porphyrin has been studied by confocal time-resolved photoluminescence spectroscopy. We found that Incorporation ratio of Zn-porphyrine in NU-1000 structure affects to energy transfer from pyrene to Zn-porphyrine. Pyrene emission peak was quenched while Zn-porphyrine enhanced, thereby increasing incorporation ratio of Zn-porphyrine. Also time-resolved photoluminescence results shows decay life time of pyrene is decreased while Zn-porphyrine is increased.

REFERENCES

- [1] Planas, N., J. E. Mondloch, S. Tussupbayev, J. Borycz, L. Gagliardi, J. T. Hupp, O. K. Farha and C. J. Cramer. "Defining the Proton Topology of the Zr₆-Based Metal-Organic Framework NU-1000," *J. Phys. Chem. Lett.* Vol. 5, NO. 21, 3716-3723, 2014.
- [2] Deria, P., J. E. Mondloch, E. Tylianakis, P. Ghosh, W. Bury, R. Q. Snurr, J. T. Hupp and O. K. Farha. "Perfluoroalkane Functionalization of NU-1000 via Solvent-Assisted Ligand Incorporation: Synthesis and CO₂ Adsorption Studies," *J. Am. Chem. Soc.* Vol. 135, No. 45, 16801-16804, 2013.
- [3] Deria, P., W. Bury, J. T. Hupp and O. K. Farha. "Versatile functionalization of the NU-1000 platform by solvent-assisted ligand incorporation," *Chem. Commun.*, Vol. 50, No.16, 1965-1968, 2014.

Selective control of reconfigurable plasmonic metamolecules

Thursday, 14th September - 14:30 - Metamaterials - Auditorium - Oral - Abstract ID: 154

Prof. Anton Kuzyk¹

1. Aalto University, School of Science

Selective configuration control of plasmonic nanostructures has remained challenging using both top-down and bottom-up approaches in the field of active plasmonics. Here we demonstrate the realization of DNA origami-based reconfigurable plasmonic metamolecules which can respond to a wide range of pH changes in a programmable manner (1). Such programmability allows for selective reconfiguration of different plasmonic metamolecule species coexisting in solution through simple pH tuning. Importantly, this approach enables discrimination of chiral plasmonic quasi-enantiomers as well as arbitrary tuning of chiroptical effects with unprecedented degrees of freedom (see Fig 1). Our work outlines a new blueprint for implementation of advanced active plasmonic systems, in which individual structural species can be programmed to perform multiple tasks and functions.

Figure 1. Enantioselective control of the chiral plasmonic metamolecules. (a) Selective reconfiguration process of the designated quasi-enantiomers. Left: At low pHs, the LH (red) and RH (blue) metamolecules coexist in equimolar amounts. LH and RH metamolecules are quasi-enantiomers, i.e., they are enantiomers as plasmonic object but functionalized with DNA locks with different TAT content. The mixture is quasi-racemic. Middle: Upon a pH increase, one type of the quasi-enantiomers (blue) undergoes a locked to relaxed transition. Right: Further pH increases result in both quasi-enantiomers being in the relaxed state. (b) Relative CD dependence on pH for a mixture of two quasi-enantiomers. (c) Relative CD dependence on pH for a quasi-racemic mixture composed of four different metamolecules in equimolar amount.

REFERENCES

1. Kuzyk, A. *et al.* "Selective control of reconfigurable chiral plasmonic metamolecules" *Science Advances* Vol. 3, e1602803, 2017.

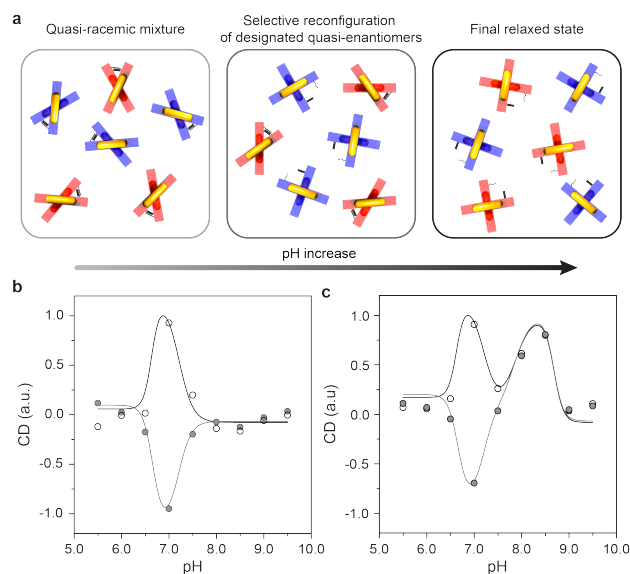


Figure1.png

Graphene-based random metalasers

Thursday, 14th September - 14:47 - Metamaterials - Auditorium - Oral - Abstract ID: 196

***Dr. Andrea Marini*¹, *Prof. Javier Garcia De Abajo*²**

1. ICFO - The Institute of Photonic Sciences, 2. ICFO-The Institute of Photonic Sciences

Traditional lasers are composed by three basic elements: an amplifying medium, an external pumping setup, and an optical cavity that confines and shapes the emitted light in well-determined modes and directions.

However, several modern approaches are extending this traditional laser paradigm into new avenues. Cavity-free stimulated emission of radiation has been widely studied in random lasers (RLs) [1], where the optical cavity modes of traditional lasers are replaced with multiple scattering in disordered media, while the interplay between gain and scattering determines the lasing properties.

In spite of their striking potential applications, RLs lack external tunability, reproducibility, and control over the spatial pattern of the output beam. Overcoming these limitations is central for the development and application of cost-effective cavity-free lasers. Inspired by the aforementioned challenges, here we investigate the optical properties of randomly-oriented undoped graphene flakes embedded in externally pumped amplifying media. We demonstrate a novel mechanism leading to stable and tunable single-mode cavity-free lasing characterized by a well-determined and highly coherent spatial pattern [2].

We find that the transverse size of the localized output beam, ranging from a few to several hundreds microns, can be accurately manipulated through the external pumping and through the volume density of graphene flakes. This cavity-free lasing mechanism profoundly relies on the extraordinary optical properties of graphene, and particularly on its highly-saturated absorption [3] at rather modest light intensities, a remarkable property which enables self-organization of light into a well determined spatial mode profile.

[1] D. S. Wiersma, "The physics and applications of random lasers," *Nat. Phys.* 4, 359 (2008).

[2] A. Marini and F. J. Garcia de Abajo, "Graphene-based active random metamaterials for cavity-free lasing," *Phys. Rev. Lett.* 116, 217401 (2016).

[3] A. Marini, J. D. Cox, and F. J. Garcia de Abajo, "Theory of graphene saturable absorption," *Phys. Rev. B* 95, 125408 (2017).

Terahertz light emission and lasing in graphene-based heterostructure 2D material systems -theory and experiments

Thursday, 14th September - 15:04 - Metamaterials - Auditorium - Oral - Abstract ID: 59

Prof. Taiichi Otsuji¹

1. RIEC, Tohoku University

Introduction

Graphene has attracted attention due to its massless and gapless energy spectrum. Carrier-injection pumping of graphene enables negative-dynamic conductivity in the terahertz (THz) range, which may lead to new types of THz lasers [1].

Method

The dual-gate graphene channel transistor (DG-GFET) structure serves carrier population inversion in the lateral p-i-n junctions under complementary dual-gate biased and forward drain biased conditions, promoting spontaneous incoherent THz light emission. A laser cavity structure implemented in the active gain area can transcend the incoherent light emission to the single-mode lasing.

Results

We designed/fabricated the distributed feedback (DFB) DG-GFET (Fig. 1) [2]. The GFET channel consists of a few layer (non-Bernal) epitaxial graphene [3], providing an intrinsic field-effect mobility exceeding 100,000 cm²/Vs [4]. The teeth-brash-shaped DG forms the DFB cavity having the fundamental mode at 4.96 THz. The modal gain and the Q factor at 4.96 THz were simulated to be ~5 cm⁻¹ and ~240, respectively (Fig. 2) [2]. THz emission from the sample was measured using a Fourier-transform spectrometer with a 4.2K-cooled Si bolometer. Broadband rather intense (~10~100 μW) amplified spontaneous emission from 1 to 7.6 THz (Fig. 3) and weak (~0.1~1 μW) single-mode lasing at 5.2 THz (Fig. 4) [2] were observed at 100K in different samples.

Discussion

When the substrate-thickness dependent THz photon field distribution could not meet the maximal available gain-overlapping condition, the DFB cavity cannot work properly, resulting in broadband LED-like incoherent emission. To increase the operating temperature and lasing radiation intensity, further enhancement of the THz gain and the cavity Q factor are mandatory. Plasmonic metasurface structures promoting the superradiance and/or instabilities [5] are promising for giant THz gain enhancement.

Acknowledgements: JSPS KAKENHI (16H06361), Japan.

1. V. Ryzhii et al., *J. Appl. Phys.* **101**, 083114 (2007); V. Ryzhii et al., *J. Appl. Phys.* **110**, 094503 (2011).
2. G. Tamamushi, et al., 74th Dev. Res. Conf. Dig., **1**, 225-226 (2016).
3. H. Fukidome et al., *Appl. Phys. Lett.* **101**, 041605 (2012).
4. A. Satou et al., *IEEE Trans. Electron Dev.*, **63**, 3300-3306 (2016).
5. V.V. Popov et al., *Phys. Rev. B* **86**, 195437 (2012); Y. Koseki et al., *Phys. Rev. B* **93**, 245408 (2016).

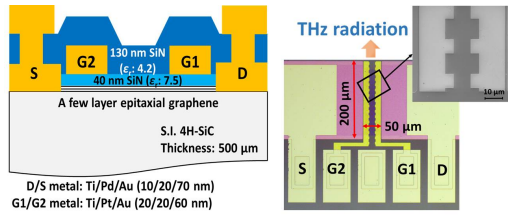


Fig.1.jpg

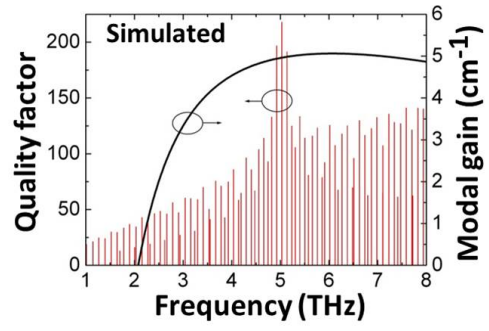


Fig.2.jpg

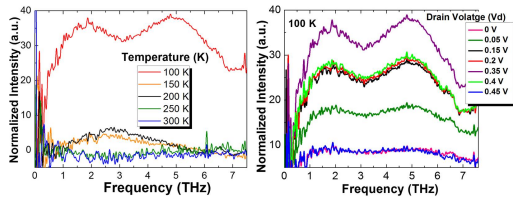


Fig.3.jpg

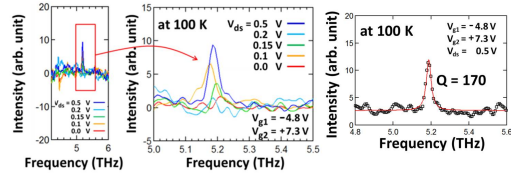


Fig.4.jpg

Optical rotation in chiral van der Waals stacks.

Thursday, 14th September - 15:21 - Metamaterials - Auditorium - Oral - Abstract ID: 158

Mr. Dmitrii Kazanov¹, **Mr. Alexander Poshakinskiy**¹, **Dr. Tatiana Shubina**¹, **Dr. Sergey Tarasenko**¹

1. A.F. Ioffe Physico-Technical Institute

Two-dimensional (2D) van der Waals heterostructures offer a unique opportunity to design nanodevices with desired optical properties [1]. Chiral nanostructures may manifest optical activity: when light is transmitted through such system its polarization plane is rotated. Recent experiments showed that the polarization rotation angle in the twisted bilayer graphene is several orders of magnitude larger than in natural materials [2].

Here we present the theory, which describes light transmittance through chiral stacks of 2D van der Waals monolayers, such as transition metal dichalcogenides (TMDC). The structure consists of a sequence of monolayers with strong exciton resonance [3], where each layer is rotated with respect to the precedent by a certain angle (Fig. 1). Due to low (chiral) symmetry such structure demonstrates optical activity and circular birefringence, although a single TMDC monolayer does not. Our calculations show that polarization rotation angle in realistic structures can reach 10 degrees per micrometer. Frequency dependence of polarization rotation angle reveals resonances at the energies of the eigen exciton modes of the stack. Interestingly, the resonances corresponding to both the superradiant symmetric mode and “dark” exciton modes are of the similar magnitude. Note that the “dark” modes that interact weakly with light are usually hidden in the optical transmittance and reflectance spectra. Therefore, spectra of optical rotation can be used to visualize the complete set of exciton modes in van der Waals stacks.

This work was supported by the Government of the Russian Federation (Project No. 14.W03.31.0011).

[1] A.K. Geim and I.V. Grigorieva, *Nature* **499**,419 (2013).

[2] C.-J. Kim et al., *Nat. Nanotechnol.* **11**, 520 (2016).

[3] C.Robert et al., *Phys Rev. B* **93**, 205423 (2016).

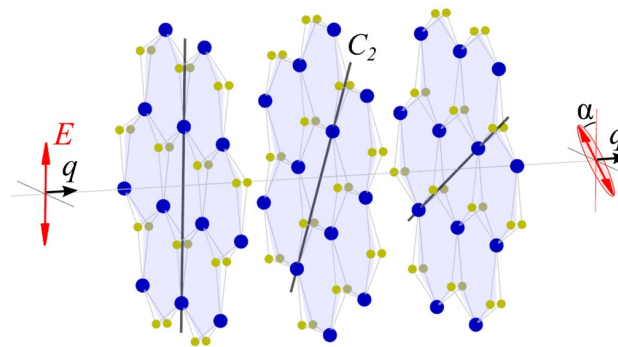


Fig 1. Chiral van der Waals stack of TMDC monolayers.

Chiral van der waals stack.jpg

Tamm plasmon/surface plasmon mode beating for spatially controlled plasmon generation

Thursday, 14th September - 15:38 - Metamaterials - Auditorium - Oral - Abstract ID: 323

*Dr. Clementine Symonds*¹, *Dr. Jean-michel Benoit*¹, *Prof. Pascale Senellart*², *Dr. Aristide Lemaitre*²,
*Prof. Jean-Jacques Greffet*³, *Dr. Christophe Sauvan*³, *Prof. Joel Bellessa*¹

1. *institut Lumière Matière*, 2. *C2N-CNRS*, 3. *Laboratoire Charles Fabry, Institut d'Optique*

Tamm plasmons (TPs) are electromagnetic modes formed at the interface between a photonic structure and a metallic layer [1]. They present optical properties at the boundary between microcavity modes and surface plasmons (SP). Compared to conventional SPs, Tamm plasmons present the advantage to be radiative and also to have reduced losses due to the larger penetration of the electric field in the dielectric part of the structure. The coupling between TP and semiconductor nanostructures (quantum dots, quantum wells) have led to the experimental demonstration of bright single photon sources [2], TP-exciton polaritons [3], and polarized laser emission [4]. Another very promising feature of TP modes is that they coexist outside the lightcone with the conventional SP present at the metal/air interface [5].

Here, we will report on the experimental observation of the electromagnetic coupling between TP and SP modes in a novel metal/semiconductor integrated structure comprising a buried quantum dot-based light source and a metallic surface grating for light extraction (Figure 1). The TP mode is excited by the photoluminescence emission of quantum dots grown in the top part of the dielectric mirror. This allows for indirect excitation of the SP at the silver/air interface, provided that a non-negligible spatial overlap between the two modes takes place in the thin metallic layer. The hybrid nature of such a TP/SP mode propagating in the planar silver thin film is demonstrated by the observation of a spatial beating along the propagation (Figure 2). This beating turns out to be in very good agreement with the results of numerical calculations, based on the wave-vector mismatch existing between the two modes. Our results pave the way to a new generation of hybrid metal/semiconductor integrated optical devices for both energy-sensitive surface detection and excitation of surface plasmons via Tamm plasmons.

- [1] M. Kaliteevski et al., *Phys.Rev. B* **76**, 165415 (2007)
 [2] O. Gazzano et al., *Appl.Phys.Lett.* **100**, 232111 (2012)
 [3] C. Symonds et al, *Appl.Phys. Lett.* **95**,151114 (2009)
 [4] G. Lheureux et al., *ACS Photonics* **2**, 842 (2015)
 [5] B.I. Afinogenov et al., *Appl. Phys. Lett.* **103**, 061112 (2013)

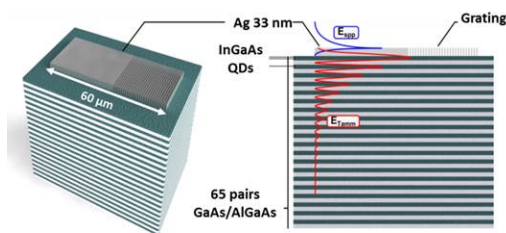


Figure1.jpg

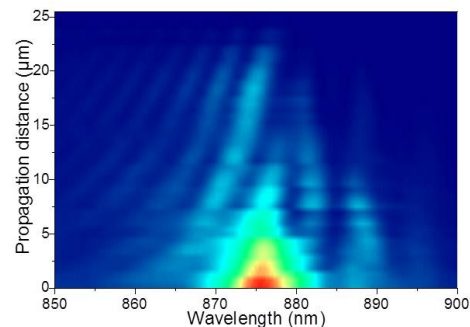


Figure2.jpg

Near Unity Transmission and Full Phase Control with Huygens' Dielectric Metasurfaces based on Cuboid Shape Silicon Nanoresonators

Thursday, 14th September - 15:55 - Metamaterials - Auditorium - Oral - Abstract ID: 52

*Dr. Xinan Liang*¹, *Dr. Ramon Paniagua-dominguez*¹, *Dr. Yefeng Yu*¹, *Dr. Yuan Hsing Fu*¹, *Dr. Arseniy Kuznetsov*¹

*1. Data Storage Institute, A*STAR (Agency for Science, Technology and Research)*

1. Introduction

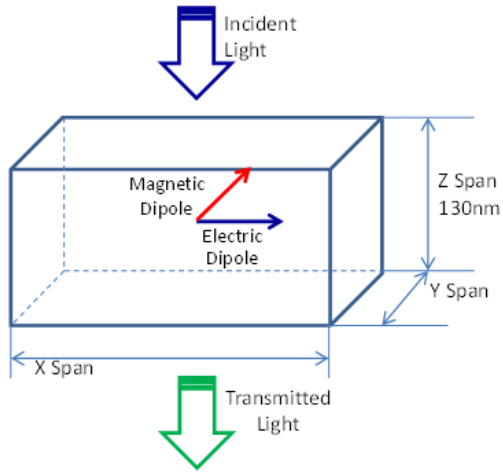
In resonant dielectric nanostructures, the simultaneous excitation and interference of magnetic and electric dipole resonances enables the suppression of backward scattering. The nanostructures then act as ideal Huygens' sources for which the phase of re-emitted light can be controlled by the actual phase of induced dipoles. The transmission and phase shift can be tailored by the nanostructure geometry. So far, disks and square prisms are most widely investigated. Although transmission $T > 80\%$ with full 2π phase control has been achieved, it is difficult to reach $T \approx 100\%$ over the whole range of phases for fixed thickness and periodicity. Here we show that, using cuboidal nanostructures, another degree of freedom is available to tune their optical performance, allowing improved resonance overlapping and $T \geq 95\%$ in 2π range of phase-shifts.

2. Method

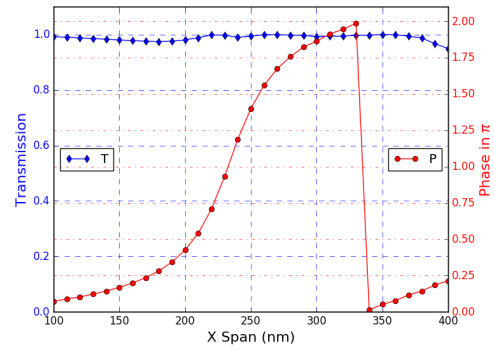
We investigate both theoretically and experimentally the transmission and phase shift obtained, under normal incidence illumination, with arrays of Silicon cuboids as a function of their lateral size along the polarization direction while keeping its size along the orthogonal direction and the array period fixed (Figure 1). The transmission and phase shift performance of the fabricated structures is characterized using a beam bending configuration and an 8-level computer generated hologram (CGH).

3. Results and Discussion

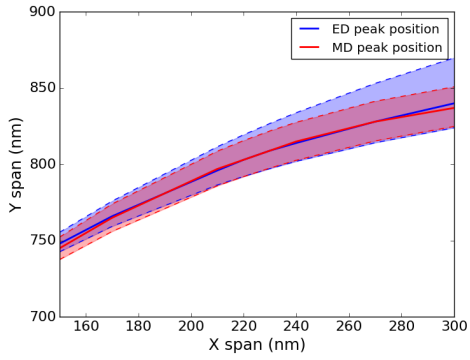
Figure 2 shows the simulated transmission and phase shift obtained for different sizes of cuboidal particle along the polarization direction at operating wavelength $\lambda = 800\text{nm}$. The particle height is around $\lambda/6$. As seen, $T > 95\%$ can be obtained for the whole range of 2π phase shift, which is due to perfect overlap and simultaneous spectral shift of the electric and magnetic resonances, as revealed by a multipole decomposition analysis (Figure 3). Using this configuration we designed gradient metasurfaces composed of 8 (and 12) elements for which 63% (71%) of the total transmitted light is deflected into the desired order. We also demonstrated broadband CGH, which was experimentally reconstructed using a supercontinuum laser with wavelength spanning from near IR to visible frequencies (Figure 4). The highest experimental diffraction efficiency of 72.8% of the total transmitted light was achieved at a wavelength of 770nm.



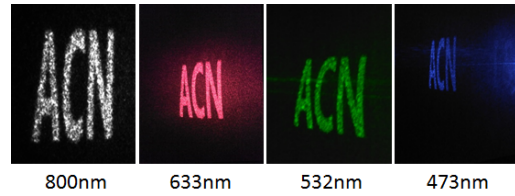
Nanop2017 figure1 sketch for resonant dielectric structure.png



Nanop2017 figure2 t p at wavelength of 800nm.png



Nanop2017 figure3 multipole decomposition results.png



Nanop2017 figure4 hologram reconstruction.png

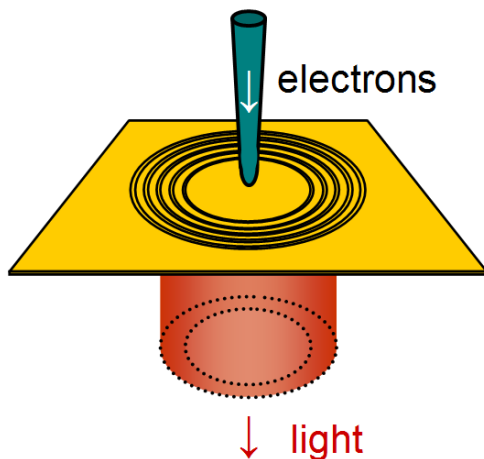
Revealing the spectral response of a plasmonic structure using tunnel electrons

Thursday, 14th September - 14:30 - Optical properties of nanostructures - Room 207 - Oral - Abstract ID: 88

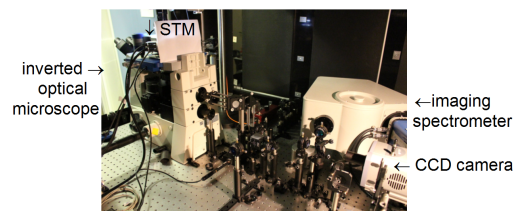
Dr. Eric Le Moal¹, **Mrs. Shuiyan Cao**¹, **Dr. Aurelien Drezet**², **Dr. Serge Huant**², **Prof. Jean-Jacques Greffet**³, **Dr. Jean-Paul Hugonin**³, **Dr. Gérald Dujardin**¹, **Dr. Elizabeth Boer-Duchemin**¹

1. Institut des Sciences Moléculaires d'Orsay (ISMO), CNRS, Université Paris-Sud, 2. Institut Néel, CNRS, Université Grenoble Alpes, 3. Laboratoire Charles Fabry, Institut d'Optique

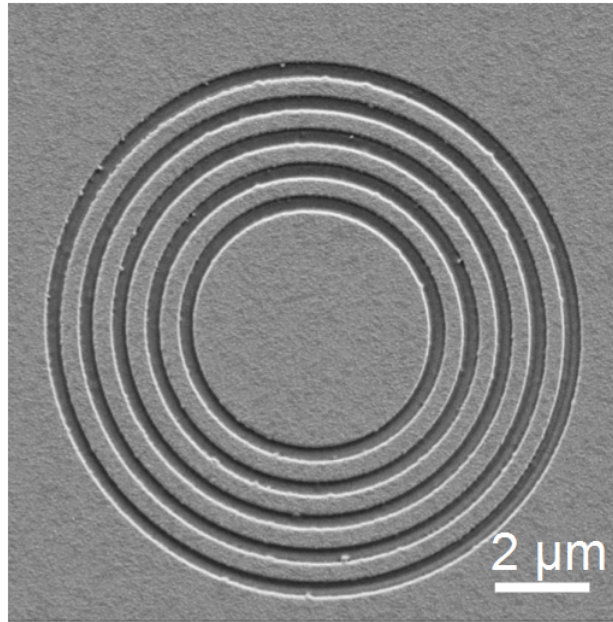
Plasmonic micro- and nanostructures may be used to locally convert electron current into light beams or surface plasmons and are thus expected to play a key role in integrating nanophotonics into electronic devices. Such structures are also used in all kinds of optical microcomponents and plasmonic circuits. Some of these structures, such as optical nanoantennas, plasmonic crystals or plasmonic lenses, have already been the subject of numerous studies in which they are excited by a laser beam or by near-field coupling to a fluorescent molecule. However, their excitation by electrical current, in particular by inelastic tunneling, has been rarely studied. A characteristic of inelastic tunneling is that it is extremely local and broadband in frequency, which requires adapting the design of the excited plasmonic structures that are often designed to operate at a given frequency. Thus, it is essential to be able to accurately measure the spectral response of these plasmonic structures under local electrical excitation. To this end, we have developed an experimental setup that combines a scanning tunneling microscope (STM), an optical microscope and an optical imaging spectrometer. The tunneling current is used to electrically excite surface plasmons on a gold microstructure under the STM tip. The scattering and leakage radiation of the excited surface plasmons are collected by the optical microscope and an image of this light emission in the Fourier space is projected on the entrance slit of the spectrometer which disperses light onto a cooled CCD camera. The spectral response of the plasmonic structure and the energy-wavevector dispersion of its modes are thus measured. We show that this technique may be used to optimize the design of plasmonic lenses for integrated electric microsources of radially polarized light beams.



Electrical light beam microsource.png



Experimental setup.png



Plasmonic lens.png

Quantum Dynamics of an Interacting Electron Gas in a Nanosphere

Thursday, 14th September - 14:47 - Optical properties of nanostructures - Room 207 - Oral - Abstract ID: 113

*Ms. Alexandra Crai*¹, *Dr. Andreas Pusch*¹, *Dr. Doris E Reiter*², *Prof. Tilmann Kuhn*², *Prof. Ortwin Hess*¹

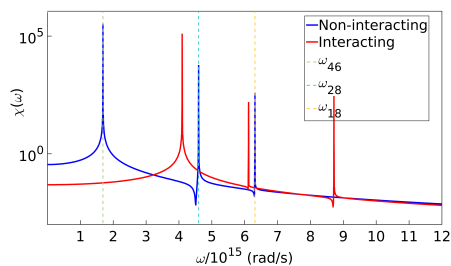
1. Imperial College London, 2. University of Münster

Plasmonic nanostructures provide a suitable environment for light-matter interaction on the nanoscale. The plasmonic excitation in the nanostructure generates hot electrons, with applications in chemistry, photovoltaics and photodetection devices. With the size of the nanoparticle becoming smaller and smaller, quantum effects will become increasingly important and the accuracy of classical models to describe the microscopic electronic structure is questionable. In this work, we study the optically generated many-particle dynamics using the density matrix formalism providing a quantum picture of the optical response of a metal nanosphere.

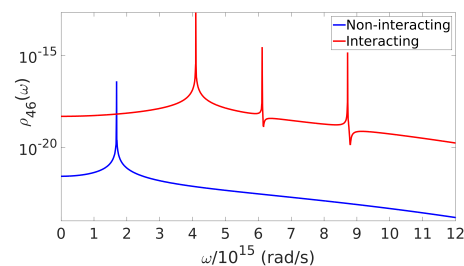
To describe the physical mechanism behind the short-lived non-equilibrium distribution, we use a microscopic density matrix theory. Our model describes a small nanosphere with discrete electronic states and analytic wave functions. The Hamiltonian takes into account both the Coulomb interaction between electrons and the interaction with an external electric field in dipole approximation. We analyse the linear optical response by exciting the partially filled few-electron system from the ground state with a weak short pulse. Specifically, we consider the case of 9 states, i.e., we take into account the lowest three s and p-shell states, filled with 5 electrons. We calculate the total induced macroscopic polarisation from the light-induced coherences between states in the density matrix. The resulting spectra display discrete resonances which, for the non-interacting case, are dipole-allowed transitions between an empty and a filled electron state.

When the electron-electron interaction is included, the spectrum is blue-shifted and the discrete resonances cannot be associated with transitions between eigenstates of the interacting multi-level system, unlike in the non-interacting case. Studying the light-induced coherences between states in the frequency domain reveals that the Coulomb interaction mixes the response of the individual states, indicating the formation of a collective oscillation.

In conclusion, we calculated the optically-induced electron dynamics in a fully-interacting few-electron system by determining its effective dielectric susceptibility. We showed that the Coulomb interaction is an essential factor in shifting the spectrum and obtaining a collective response of the interacting electron-system. Our work paves the way towards the microscopic description for the formation of plasmons.



Total induced dielectric susceptibility for 5 electrons in 9 possible excitation states.png



The fourier transform of the light-induced coherence between states 4 and 6..png

Nanomechanical 2D-scanning photothermal microscopy for analysis and imaging of single sub-10 nm nanoparticles

Thursday, 14th September - 15:04 - Optical properties of nanostructures - Room 207 - Oral - Abstract ID: 331

*Ms. Miao-Hsuan Chien*¹, *Prof. Silvan Schmid*¹

¹. *Micro and Nanosensors group, Institute of Sensor and Actuator Systems, TU Wien*

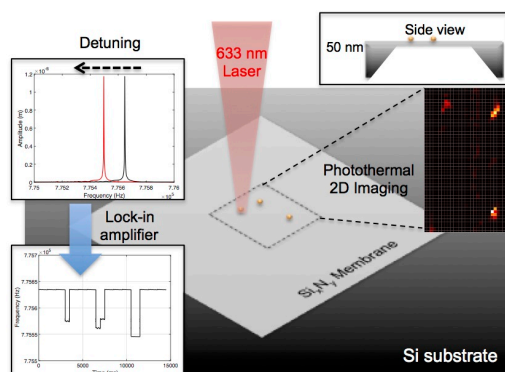
Label-free optical detection and imaging of single nanoparticles and molecules are of fundamental interests in many research fields due to its simpler detection scheme, reduced limitations on samples and higher stability. For sub-100 nm nanoparticles, absorption cross section exceeds scattering by several orders of magnitude, and the difference increases as the diameter of particles reduce, which makes photothermal spectroscopy a powerful technique for the imaging of single Au nanoparticles even under sub-10 nm regime. Instead of using inhomogeneous refractive index [1,2] to create contrast, photothermal analysis via the thermal frequency detuning of nanomechanical 1D string resonators of single metal [3] and polymer [4] nanoparticles has been demonstrated alternatively. We hereby introduce highly sensitive nanomechanical membrane resonator as a novel methodology and optical platform for single nanoparticle detection and 2D imaging, as shown in figure 1. The experiments were done with a rectangular silicon-rich silicon nitride membrane with 500 μm in width, 50 nm in thickness and pre-stress of 250 MPa and 30 MPa, and the results are shown in figure 2 and 3, respectively, along with their corresponding SEM images. When scanning a heating laser over the membrane, the local photothermal heating of the nanoparticles causes a heat influx into substrate and thus a measurable detuning of the membrane resonance frequency, which was monitored with a phase-locked loop. With pumping power of only 300 μW and spot size of 1 μm , we achieve the detection and imaging of 10 nm Au nanoparticles, as shown in figure 3, with a dissipated power of 300 fW and integration time of 100 ms, which demonstrates even higher sensitivity than state-of-the-art photothermal microscopy [1,2], making this novel spectroscopic technique a potential candidate toward single molecule detection and imaging.

[1] D. Boyer et al., *Science* 297, 1160–3, 2002.

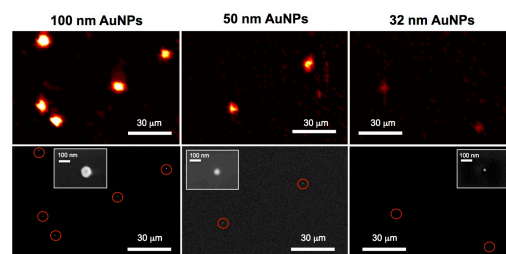
[2] A. Gaiduk et al., *Chem. Sci.* 1, 343–350, 2010.

[3] S. Schmid et al., *Nano Lett.* 14, 2318–2321, 2014.

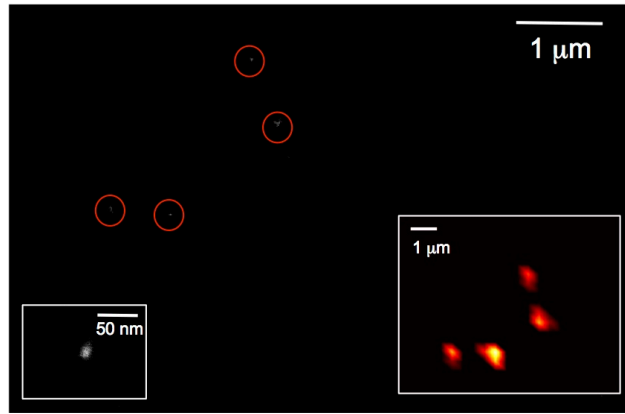
[4] T. Larsen et al., *ACS Nano* 7, 6188–6193, 2013.



Nanop fig1.jpg



Nanop fig2.jpg



Nanop fig3.jpg

Controlling On-chip Optical Radiation with All-Dielectric Antennas: Reconfigurable Interconnects and Lab-on-a-chip Devices

Thursday, 14th September - 15:21 - Optical properties of nanostructures - Room 207 - Oral - Abstract ID: 199

***Mr. Sergio Lechago*¹, *Dr. Carlos Garcia-Meca*¹, *Prof. Javier Marti*¹**

1. Universitat Politècnica de València

Introduction

Photonic integrated circuits (PICs) promise to open new avenues in high-performance computing, biosensing or optical beamforming, amongst others. Current PICs rely on the use of guided interconnects, hampering the creation of flexible and reconfigurable networks-on-a-chip and preventing the far-field light-matter interaction required for many sensing applications. In this work, we propose¹ a novel on-chip silicon antenna that, in contrast to their plasmonic counterparts², exhibits simultaneously an ultra-high directivity (>100), low loss, low reflections and a broadband response (Fig. 1). We propose the use of these nanoantennas as the main building blocks of a new wireless photonic platform that solves the aforementioned problems and considerably widens the range of achievable integrated photonic functionalities.

Methods

The studied antennas consist of inverted-taper silicon strips with additional structures behaving as directors, and were modelled via Huygens' Principle in combination with full-wave simulations (Fig. 1). The antennas were fabricated over silicon-on-insulator wafers using standard e-beam fabrication processes, assuring CMOS compatibility.

Results

As a first basic application, we demonstrated the first on-chip wireless data-streaming link, with a speed as high as 160 Gbit·s⁻¹ over a distance of 100 μm. Moreover, to illustrate the potential of these antennas for reconfigurable networks, we developed an electrically-controlled antenna-array beam-steering device, which allowed us to dynamically steer radiated beams by tuning the feeding waveguides phase (α) through silicon's thermo-optic effect (Fig. 2). Finally, we built an ultra-compact (with a footprint several orders of magnitude smaller than previous versions) lab-on-a-chip antenna-based microflow cytometer able to classify microparticles of different size via their time-dependent scattered-field signature with state-of-the-art resolution (Fig. 3).

Discussion

These results demonstrate the potential offered by the proposed wireless platform, providing much more flexible optical interconnects and the ability of developing reconfigurable architectures, as well as boosting new applications in other fields such as the generation of complex beams for material processing or optical tweezing. From a lab-on-a-chip perspective, the proposed microflow cytometer paves the way to point-of-care biomedical equipment and interesting additional applications such as on-chip dynamic light scattering, Raman spectroscopy or gas chromatography.

- *Light Sci App* 2017; **6**: e17053.

• *Nat Photonics* 2011;5:83-90.

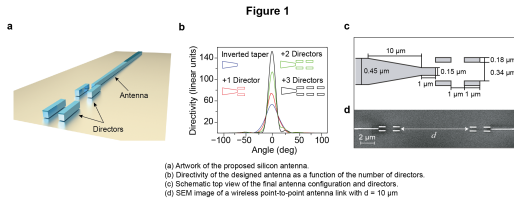
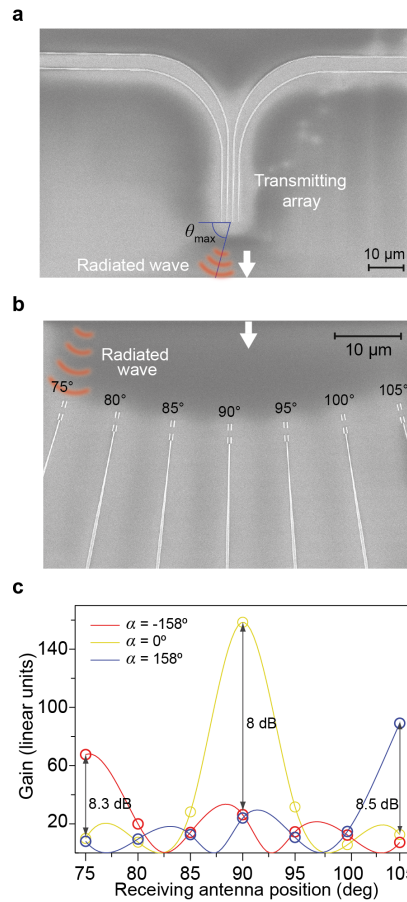


Figure1.png

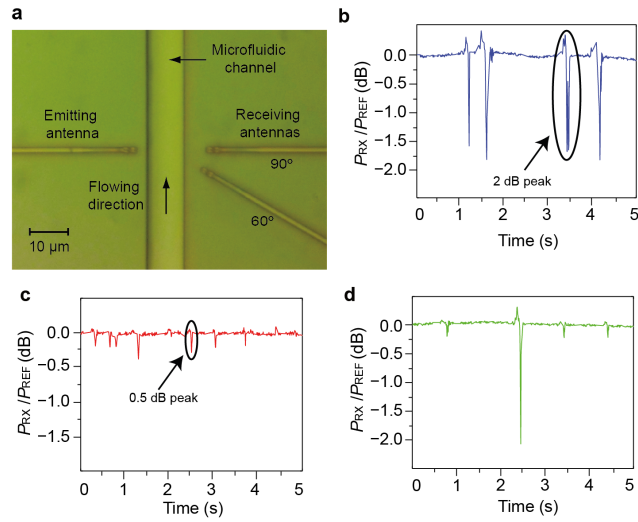
Figure 2



Experimental electrically reconfigurable beam steering

- (a) SEM image of the waveguides used to feed the emitting array
- (b) SEM image of the receiving subsystem consisting of 7 antennas placed in a hub configuration. The antennas at $75^\circ, 90^\circ$ and 105° are taken as the device output ports.
- (c) Total array gain associated with each receiving antenna ($d = 100 \mu\text{m}$, $\lambda = 1550 \text{ nm}$) for the three values of the transmitting array phase (α). Circles indicate measured values at each antenna position. The crosstalk at the output ports shows values always better than 8 dB.

Figure2.png

Figure 3

(a) Optical microscope image of the fabricated microflow cytometer.
(b-d) Power time-dependent efficiency measured at 60°. 0.5 dB and 2 dB peaks correspond to the detection of 1- μ m and 2- μ m microparticles respectively. P_{REF} is the received power with no particles flowing through the channel.

Figure3.png

Nanostructured silica based optical coatings for high power laser systems

Thursday, 14th September - 15:38 - Optical properties of nanostructures - Room 207 - Oral - Abstract ID: 146

***Dr. Tomas Tolenis*¹, *Ms. Lina Grinevičiūtė*¹, *Dr. Andrius Melninkaitis*², *Dr. Rytis Buzelis*¹, *Ms. Lina Mažulė*²**

1. Center for Physical Sciences and Technology, 2. Vilnius University

Most of optical coatings are formed using at least two materials with different refractive indexes. Silicon oxide is one of the materials with large band gap value. Therefore, high laser fluency is necessary to induce dielectric breakdown in it. Unfortunately, other typical high refractive index materials have low laser resistivity and limit the overall multilayer coating laser induced damage threshold.

A novel approach is presented to form the multilayer optical coatings based on nanostructured silica thin films. Glancing angle deposition method was employed to form silica sculptured thin films with different porosity. Tailoring the refractive index of individual layers, multilayer antireflection and high reflection coatings have been manufactured. Optical and structural characterization of nanostructured and standard coating, produced by sputtering technology, designs was performed and compared. Spectral performance of silica based antireflection coatings was found to exceed the two-material based coatings (see Fig. 1). Measured resistivity to laser radiation indicate the damage threshold of more than 15 J/cm² for silica coatings at the wavelength of 355 nm in nanosecond regime. High reflection all-silica mirrors also showed increased laser resistivity compared to standard dielectric mirrors. A possibility to obtain laser induced damage threshold of 65 J/cm² at the wavelength of 355 nm in nanosecond regime is demonstrated and presented in Fig. 2. The graph shows the possibility to damage optical component at different laser fluency. Optical losses of such multilayer nanostructured coatings were investigated by light scattering measurements and possible sources were analyzed. Also, combined techniques of standard and glancing angle deposition methods were used to form more spectrally favorable mirrors. Optical and structural analysis of such coatings indicate possible applications of nanostructured silica films for upgrading standard designs.

All-silica based multilayer coatings, produced by glancing angle deposition, were characterized by measuring optical performance and resistivity to laser radiation. Analysis indicate the advanced properties of nanostructured silica thin films. Tailored porosity of individual layers allows to form anti- and high-reflection coatings capable to withstand extremely high laser fluency.

Enhancement of optical micro-cavity effect coupled with surface plasmon in an organic light emitting device with nanosized multi-cathode structure

Thursday, 14th September - 15:55 - Optical properties of nanostructures - Room 207 - Oral - Abstract ID: 139

Prof. Akiyoshi Mikami¹

1. Kanazawa Institute of Technology

Organic light-emitting devices (OLEDs) are widely recognized as a high quality flat panel displays. The internal quantum efficiency of OLED has approaches to 100% by using phosphorescent materials. However, the external quantum efficiency (EQE) remains 20-25% because of a poor light extraction efficiency due to surface plasmon (SP) losses in a metal cathode. We found that the emission efficiency becomes higher by using multi-cathode (MLC) structure. In addition, the color purity in blue, green and red emission has improved by the external micro-cavity effect coupled with SP resonance.

Fig.1 [A] shows the device structure used in this work. The normal structure (a) consists of ITO/PEDOT:PSS/NPB/CBP:color dopant/Bu-PBD/MgAg cathode. MLC structure (b) has a feature of thin film stacked cathode consisting of a semi-transparent MgAg, ITO optical buffer and high reflection Ag. Fig.1 [B] shows optical power density as a function of normalized horizontal wave-vector (k_h/h_0) calculated by near-field optics. In the normal cathode, a strong SP band appears in an evanescent region in $k_h/h_0 > 1.8$. In contrast, it almost disappears and waveguide TM and substrate modes become dominant in the MLC structure. Fig.1 [C] shows a power density distribution obtained by FDTD analysis when a vertical dipole is excited. In the normal cathode, almost all the excitation power disappears in a short lifetime as SP loss in the cathode. However, we can see an intense forward emission as well as waveguide mode in the MLC structure. The optical efficiency has improved by a factor of 1.8. These phenomena can be explained by considering two kinds of SP resonance, long range SP and short range SP, which interact with each other on both sides of very thin MgAg layer.

Fig.2 shows electroluminescent spectra and three primary color coordinates in CIE diagram in the devices with and without MLC structure. Sharp emission band with narrower half-width is an advantage in the MLC structure because of the external micro-cavity effect enhanced by the increase of waveguide mode. Color coordinates of blue, green and red are shown in a table and color gamut has improved greatly.

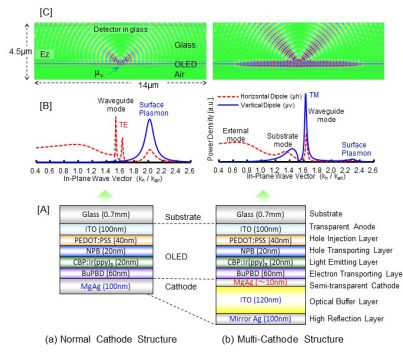


Fig. 1 Optical power spectra (power density vs. in-plane wave-vector), imaging of power intensity distribution and device structure with different cathode structure and refractive-index of glass substrate.

Fig1.png

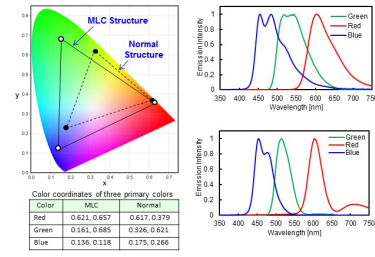


Fig2.png

Fano resonances in Al-based multilayer structures

Thursday, 14th September - 14:30 - Photonic & plasmonic nanomaterials - Room 412 - Oral - Abstract ID: 315

Prof. Shinji Hayashi¹, **Mr. Yudai Fujiwara**¹, **Mr. KANG BYUNGJUN**¹, **Prof. Minoru Fujii**¹, **Dr. Dmitry Nesterenko**², **Prof. Zouheir Sekkat**³

1. Kobe University, 2. Samara University, 3. MAScIR

Over the past decade, a great effort has been made to realize the Fano resonance in optical spectra of plasmonic nanostructures and metamaterials. High-Q Fano resonances have potential applications such as optical sensors and switches. However, the fabrication of desired nanostructures is time consuming and high cost, preventing real applications. Very recently, we have demonstrated both theoretically [1] and experimentally [2] the feasibility of realizing sharp Fano resonances in metal-dielectric multilayer structures, which can be fabricated without nanofabrication. The Fano resonance is a consequence of coupling between a surface plasmon polariton (SPP) mode acting as a bright mode and a planar waveguide (PWG) mode acting as a dark mode. Sharp Fano resonances were clearly observed in the attenuated total reflection (ATR) spectra of Kretschmann configurations consisting of Ag and organic dielectric layers [2].

To widen the applicability of our Fano structure, in particular to the UV light region, we prepared Al-based multilayer structures with inorganic dielectrics and studied experimentally and theoretically their Fano characteristics. Figure 1 shows schematically the sample attached to a prism (Kretschmann configuration). Figure 2 shows a typical angle-scan ATR spectrum obtained for the present sample. Without the Al₂O₃ waveguide layer, we observe only a broad dip corresponding to the excitation of SPP mode. However, in the presence of Al₂O₃ waveguide layer, we observe a sharp Fano resonance (TM₀F). The experimental spectrum (dots) is in good agreement with a theoretical curve (solid line) obtained by an electromagnetic calculation. One of the advantages of utilizing Al is its broad SPP resonance, to which the waveguide mode can easily be tuned. The present Fano structures exhibit Q factors an order of magnitude larger than those reported recently for plasmonic nanostructures, demonstrating high potentiality for a variety of applications.

[1] S. Hayashi et al., APEX, **8**, 022201 (2015), J. Phys. D : Appl. Phys., **48**, 325303 (2015).

[2] S.Hayashi et al, APL, **108**, 051101 (2016).

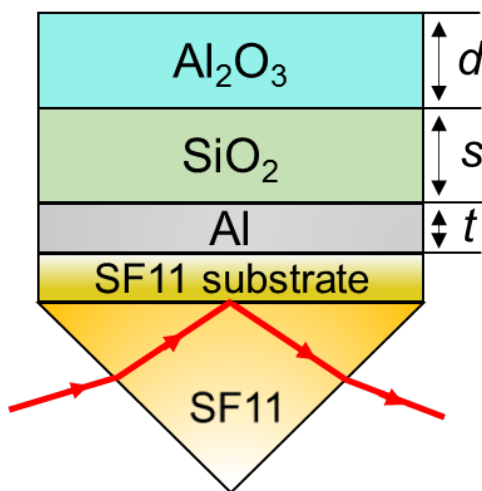


Fig. 1 sample structure..png

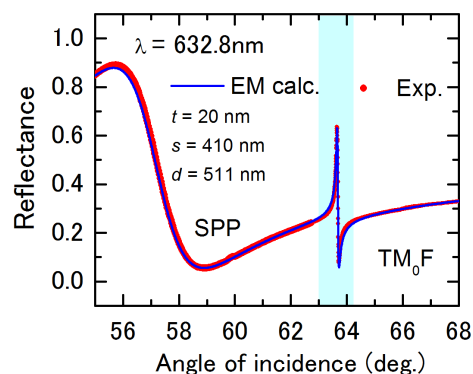


Fig.2 observed fano resonance..png

Nanoscale Precision Design of Metal Catalysts Using Plasmonic Nanoreactors

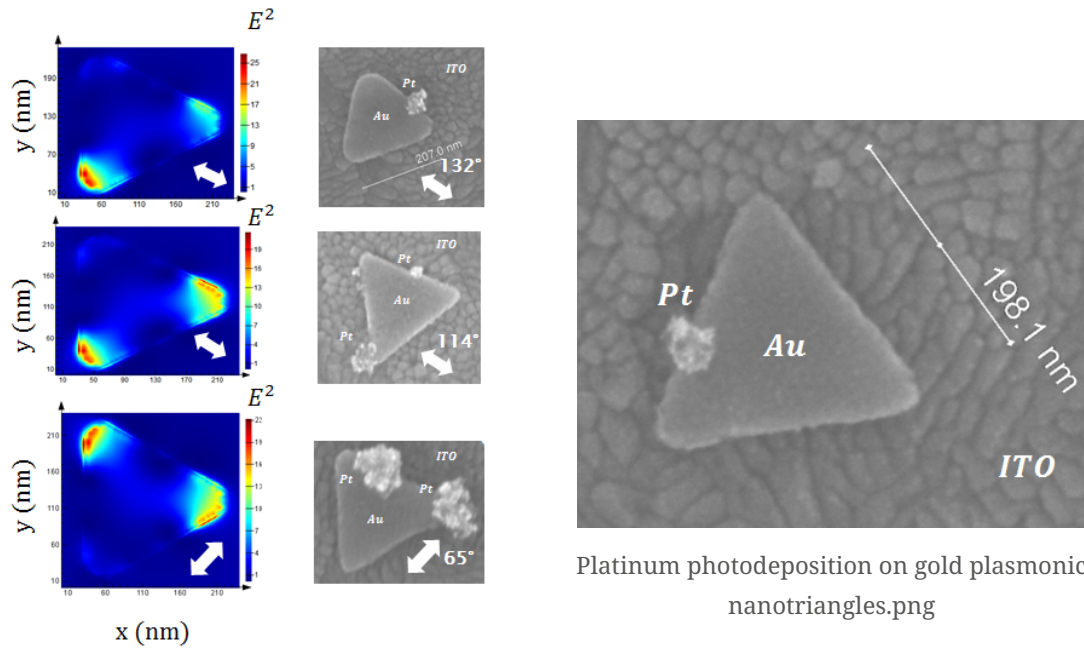
Thursday, 14th September - 14:47 - Photonic & plasmonic nanomaterials - Room 412 - Oral - Abstract ID: 384

Ms. Evgenia Kontoleta¹, Dr. Sven Askes¹, Dr. Erik Garnett¹

1. AMOLF Institute

The utilization of highly energetic charges (“hot-electrons/holes”) generated by the non-radiative decay of plasmons in metal nanostructures is an exciting emerging topic. Hot electrons have already been suggested as an explanation for increased kinetics and improved selectivity of illuminated metal nanoparticle catalysts. However, tracking the local generation and transfer of these hot electrons, their energy distribution and their relation to the underlying nanoparticle structure has been challenging. Here we use ultra-thin monocrystalline gold nanotriangles as a model system to study hot electron generation and activity in photoreduction reactions. A uniform illumination source is used for the excitation of the nanotriangles on a glass/ITO substrate, at their surface plasmon resonance, in presence of an aqueous solution of chloroplatinic acid. Scanning Electron Microscope images revealed local reduction of chloroplatinic acid to platinum nanoparticles only on the gold nanotriangles and only under optical illumination. An applied potential is used to tune the reaction kinetics, which allows for mapping out the hot electron distribution. By controlling the illumination polarization and wavelength, the spatial distribution of Pt nanoparticle deposition could be controlled. Optical simulations were conducted for different polarizations so as to study the electric field distribution around the plasmonic nanostructures. The results were compared with the experimental platinum formation sites on the gold nanotriangles and a nice match between them and the simulated location of the optical field “hot spots” was observed. Furthermore, a thin electron acceptor layer is found to increase the deposition kinetics, presumably by increasing the lifetime of hot-electrons.

Our approach provides fundamental insights into hot-electron reactions and opens up a new synthetic pathway for hierarchical nanostructures with both simple synthesis and high spatial control. Such highly controlled nanostructures could find applications in single-molecule spectroscopy, photoelectrochemical water splitting and CO₂ reduction.



Platinum photodeposition on gold plasmonic nanotriangles.png

Photodeposition of platinum nanoparticles on gold and polarization dependence.png

Optical properties of GaP/Si active microdisks containing InGaAs/GaP quantum dots

Thursday, 14th September - 15:04 - Photonic & plasmonic nanomaterials - Room 412 - Oral - Abstract ID: 189

**Mr. Ronan Tremblay¹, Mr. Tony Rohel¹, Dr. Yoan Léger¹, Dr. Alain le corre¹, Dr. Rozenn Bernard¹,
Dr. Nicolas Bertru¹, Prof. Olivier Durand¹, Dr. Charles Cornet¹**

¹. UMR FOTON, CNRS, INSA-Rennes

Taking advantage of low production costs and large integration scale, silicon photonics is a promising way to improve on-chip data routing and reduce electronic consumption. The small lattice mismatch between Si and GaP promotes the latter as a good candidate for III-V pseudomorphic integration, but questions remain on the interest of this platform for photonics. In this context, GaP/Si microdisks constitute a model system to explore the assets of the platform for optics [1]. GaP being an indirect material, nanostructure engineering is required to realize active devices. We presently focus on (In,Ga)As/GaP quantum dots (QDs), which theoretically feature a cross-over between direct/indirect bandgap emission and type-I/type-II depending on their In content, size and strain field [2], [3]. In this contribution, we investigate optical properties of these QDs by using temperature (Fig. 1) and excitation dependent PL experiments for various growth parameters to probe these electronic states and promote the direct emission. At low temperature, the appearance of a low energy contribution in the emission spectrum is reported. The origins of the PL peaks and their interplay will be discussed in the framework of type-I/type-II and direct/indirect transitions. Moreover, we demonstrate room temperature photoluminescence of these QDs in a GaP/Si microdisk where the QD layer is located at only 200nm from the III-V/Si interface (Fig. 2) highlighting overall good structural quality of the GaP/Si device. This research project is supported by the Labex Cominlabs project ANR-10-LABX-07-01 and the OPTOSI ANR project N°12-BS03-002-02.

- [1] P. Guillemé *et al.*, *Opt. Express*, vol. 24, n° 13, p. 14608, 2016.
 [2] C. Robert *et al.*, *Phys. Rev. B*, vol. 94, n° 7, 2016.
 [3] G. Stracke *et al.*, *Appl. Phys. Lett.*, vol. 104, n° 12, p. 123107, 2014.

Fig. 1. : Temperature dependent photoluminescence of (In,Ga)As/GaP QDs

Fig. 2. : (left) Scanning electron microscope image of a GaP microdisk on a Si pedestal. (Right) Room temperature photoluminescence of the microdisk

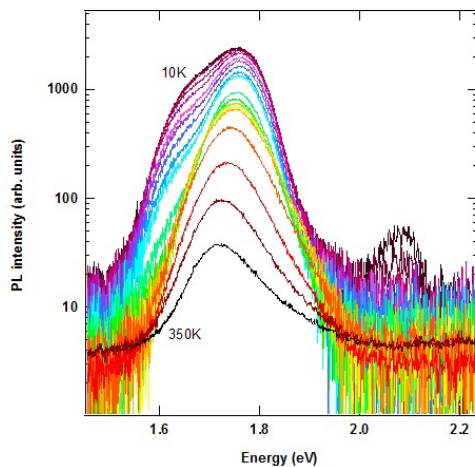


Fig. 1.jpg

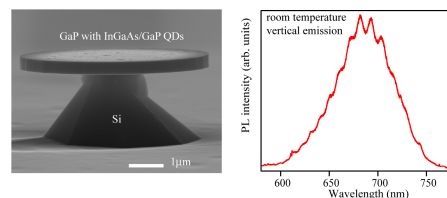


Fig.2.jpg

Measuring the directional Local Density of States (LDOS) of quantum and classical plasmons using near-field scanning optical microscopy

Thursday, 14th September - 15:21 - Photonic & plasmonic nanomaterials - Room 412 - Oral - Abstract ID: 125

Dr. Aurelien Drezet¹, **Dr. Martin Berthel**², **Ms. Aline Pham**², **Dr. Quanbo Jiang**², **Dr. Serge Huant**²,
Prof. Joel Bellessa³, **Dr. Cyriaque Genet**⁴

1. Institut Néel, CNRS, Université Grenoble Alpes, 2. Institut Neel, 3. institut Lumière Matière, 4. ISIS, university of Strasbourg

In this paper we will introduce the concept of local density of states (LDOS) associated with propagative surface plasmons (SPs) [1]. We will demonstrate how a near field scanning optical microscope (NSOM) coupled to a leakage radiation microscope (LRM) [2] can be used for mapping such LDOS in a plasmonic planar device [1]. We will show how to apply this method with a nitrogen vacancy (NV) based NSOM working in the quantum regime [3]. Then we will apply this method to the development and optimization of a planar SP device working as a plasmonic collimator [1]. We will compare this approach to other LDOS measurements of plasmonic observable with NSOM realized recently by our group [4,5].

Figure: Maps of partial LDOS associated with propagative SPs and recorded using an aperture NSOM probe [1]. (a) and (b) correspond to two different SP wave vectors. The inset show the agreement with the SP theory for LRM [2].

[1] M. Berthel, Q. Jiang, A. Pham, J. Bellessa, C. Genet, S. Huant, A. Drezet, Directional Local density of states of classical and quantum propagating surface plasmons, *Phys. Rev. Applied* 7, 014021 (2017).

[2] A. Drezet and C. Genet, Imaging surface plasmons: from leaky waves to far-field radiation, *Phys. Rev. Lett.* **110**, 213901 (2013).

[3] A. Cuche, O. Mollet, A. Drezet, and S. Huant, Deterministic Quantum Plasmonics, *Nano Lett* 10, 4566 (2010).

[4] A. Pham, M. Berthel, Q. Jiang, J. Bellessa, S. Huant, C. Genet, and A. Drezet, Chiral optical local density of states in a spiral plasmonic cavity, *Phys. Rev. A* 94, 053850 (2016).

[5] A. Cuche, M. Berthel, U. Kumar, G. Colas des Francs, S. Huant, E. Dujardin, C. Girard, A. Drezet, Near-Field Hyperspectral Quantum Probing of Multimodal Plasmonic Resonators, *Phys. Rev. B* 95, 121402R (rapid communications) (2017).

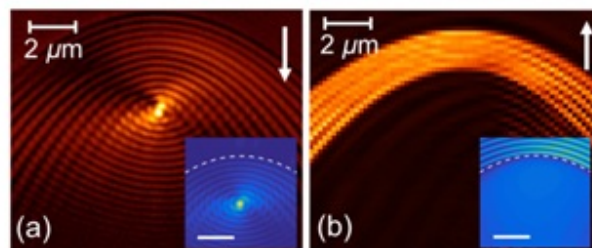


Figure.jpg

Modification of Förster Resonance Energy Transfer using Plasmonic Nanogaps

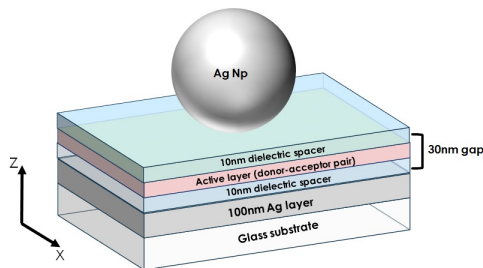
Thursday, 14th September - 15:38 - Photonic & plasmonic nanomaterials - Room 412 - Oral - Abstract ID: 396

Mr. Abdullah Hamza¹, **Mr. Francesco Narda Viscomi**¹, **Dr. Jean-Sebastien G. Bouillard**², **Dr. Ali M. Adawi**³

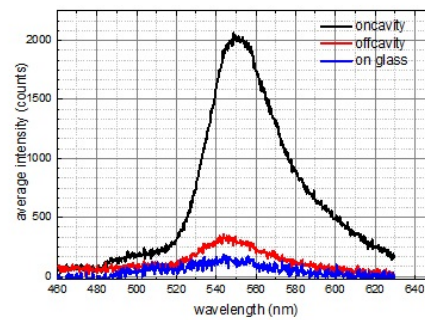
1. School of Mathematics and Physical Sciences -University of Hull, **2.** School of Mathematics and Physical Sciences -University of Hull, G. W. Gray Centre for Advanced Materials-University of Hull, **Department of Physics-King's College London.**, **3.** School of Mathematics and Physical Sciences -University of Hull, G. W. Gray Centre for Advanced Materials-University of Hull.

Förster resonance energy transfer (FRET) is a fundamental phenomenon in photosynthesis, organic photovoltaics and biosensing. FRET is a non-radiative energy transfer process from an excited molecular donor into a nearby molecular acceptor and its efficiency is dependent on the inverse sixth power of the distance between donor and acceptor pair. The rate and range of FRET processes between two quantum emitters can be enhanced by controlling the photonic environment defined by the local density of optical states (LDOS). Successful control over such energy transfers can open the way to range of applications in integrated nano-photonic devices and nano-sensors.

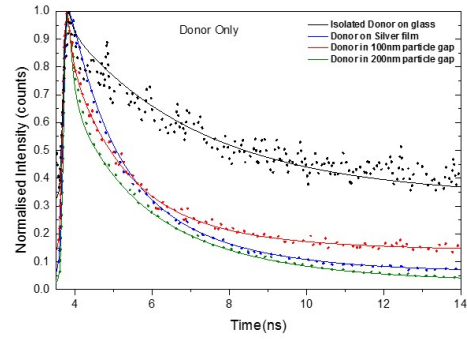
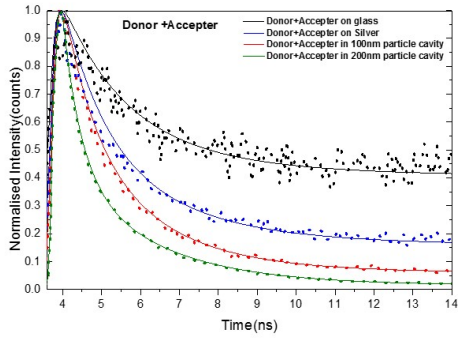
In this work, we present a silver nano-gap, consisting of a silver nanoparticle coupled to an extended silver film, designed to enhance Förster resonance energy transfer. We considered nanoparticles of diameters 100 and 200 nm to form nano-gaps of width 30 nm doped with the laser dye Uranin LC 5520 and the molecular dye Rhodamine 6G as the donor-acceptor pair. Experimentally, up to 14-fold enhancement in acceptor fluorescence emission intensity and 3.6-fold enhancement in the FRET rate were observed in the presence of nano-gaps. To support the experimental observations, the optical properties of the plasmonic nano-gaps were studied using FDTD calculations giving deeper insight in the energy transfer in the presence of plasmonic nanogaps.



Plasmonic nanogap structure.jpg



PL spectra from the energy transfer sample on nanogap black on metal film red and reference is blue.jpg



Normalized time-resolved fluorescence decay profiles of donor in the presence of the acceptor in 100nm cavity 200nm cavity on silver film and on the glass reference .jpg

Normalized time-resolved fluorescence decay profiles of donor in the absence of the acceptor in 100nm cavity 200nm cavity on silver film and on the glass reference .jpg

Characterization of the wavelength-dependent coupling function from nitrogen-vacancy fluorescence into surface plasmon polaritons

Thursday, 14th September - 15:55 - Photonic & plasmonic nanomaterials - Room 412 - Oral - Abstract ID: 388

***Dr. Cesar E. Garcia-Ortiz*¹, *Dr. Victor Coello*², *Dr. Shailesh Kumar*³, *Prof. Sergey I. Bozhevolnyi*³**

1. CONACYT - CICESE Monterrey, 2. CICESE Monterrey, 3. University of Southern Denmark

The nitrogen-vacancy (NV) centers in diamond have gained the attention of an increasing number of research groups due to their property to emit single photons at room temperature, and have become attractive candidates for quantum information processing. The NV centers can be implanted on diamond nanoparticles (NDs), enabling the possibility to couple the emitted light into nanostructured optical systems, e.g. in plasmonic devices. In this work, we have centered our attention in the characterization of the wavelength-dependent coupling of the fluorescence of NV centers in NDs into surface plasmon polaritons (SPPs). The sample consists of NDs ($r = 50$ nm) with multiple NV centers (~ 400) that are spin coated over a 70-nm-thick gold thin film and characterized using leakage-radiation microscopy (LRM) and spectroscopy (LRS), in both the image and Fourier plane [Fig. 1]. The LRM setup allows one to observe the image and intensity distribution of the SPPs that are being excited when pumping the NDs with a 532 nm Nd:YAG laser, while the LRS setup permits to measure the spectra and lifetime of the SPPs coupled from the emitted fluorescence in the Fourier plane. We use the capabilities of leakage-radiation setup to discriminate the coupled, from the uncoupled fluorescence, using filters in the Fourier plane, in order to obtain the wavelength-dependent coupling function. The results showed significant changes in the spectra and a reduction of the lifetime when the coupled fluorescence is compared to the back-scattered fluorescence of the NDs.

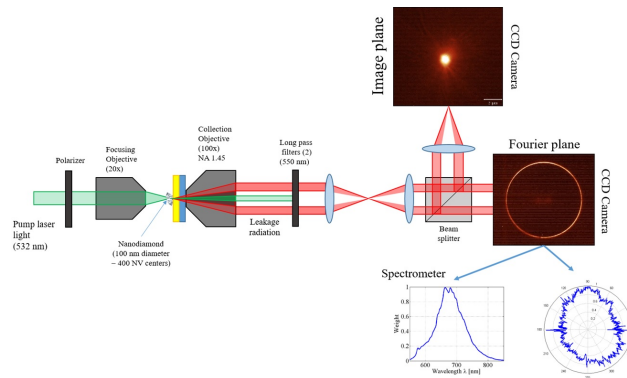


Fig1.jpg

Enhancement and Inhibition of Spontaneous Photon Emission by dielectric photonic antennas

Thursday, 14th September - 16:50 - Optical properties, photonic & plasmonic nanomaterials - Auditorium - Oral
- Abstract ID: 102

Dr. Mathieu Mivelle¹, **Mr. Dorian Bouchet**¹, **Dr. Julien Proust**², **Dr. Bruno Gallas**³, **Dr. Igor Ozerov**⁴,
Prof. Maria Garcia-parajo⁵, **Dr. Yannick De Wilde**¹, **Dr. Nicolas Bonod**², **Dr. Valentina Krachmalnicoff**¹, **Dr. Sebastien Bidault**¹

1. ESPCI Paris, PSL Research University, CNRS, Institut Langevin, 1 rue Jussieu, F-75005, Paris, France, 2. Aix-Marseille Université, CNRS, Centrale Marseille, Institut Fresnel, UMR 7249, 13013 Marseille, France, 3. Sorbonne Universités, UPMC Univ Paris 06, CNRS UMR 7588, Institut des Nanosciences de Paris, 75005 Paris, France, 4. Aix-Marseille Université, CNRS, CINAM, UMR 7325, 13288 Marseille, France, 5. ICFO-Institut de Ciències Fòniques, The Barcelona Institute of Science and Technology, 08860 Castelldefels (Barcelona), Spain

Mie resonators, or high-index dielectric nanoparticles, have recently been proposed as new building blocks to produce metamaterials¹, metasurfaces² or optical antennas³. However, all prior studies have focused on the passive resonant scattering properties of dielectric particles without demonstrating their influence on active materials, a property that is crucial for nanoscale photon management. In this report, we provide the first experimental demonstration that silicon-based nanoantennas can either enhance or inhibit spontaneous emission from fluorescent molecules at the nanoscale (**Figure 1**).

Figure 1: (a) Principal of the experiment: a fluorescent nanosphere is attached at the end of a near-field tip and placed in close proximity to a dielectric photonic antenna. (b, c) Two dimensions of dielectric antennas are considered to be either on resonance or out of resonance at the emission wavelength of the fluorescent nanosphere (d). (e) Enhancement or inhibition of the fluorescent nanosphere spontaneous emission in the vicinity of the dielectric nanoantennas.

Using scanning probe microscopy, we analyse quantitatively the near-field interaction between a fluorescent nanosphere and silicon nanodisks in three dimensions and at the nanoscale. Furthermore, in this study we highlight the ability of dielectric nanoantennas to increase the far-field collection of spontaneously emitted photons, in excellent agreement with numerical simulations. These results are an essential contribution to the new field of Mie resonators, at the crossroads of plasmonics and dielectric microcavities, as they demonstrate the ability of high-index dielectric nanostructures to manipulate solid-state emitters at the nanoscale and at room temperature.

REFERENCES

1. Moitra, P., Yang, Y., Anderson, Z., Kravchenko, I. I., Briggs, D. P. and Valentine, J. "Realization of an all-dielectric zero-index optical metamaterial", *Nat. Photon.* **7**, 791, 2013.
2. Spinelli, P., Verschuuren, M. A. and Polman, A. "Broadband omnidirectional antireflection coating based on subwavelength surface Mie resonators" *Nat. Commun.* **3**, 692, 2012.
3. Fu, Y. H., Kuznetsov, A. I., Miroshnichenko, A. A., Feng Yu, Y. and Luk'yanchuk, B. "Directional visible light scattering by silicon nanoparticles" *Nat. Commun.* **4**, 1527 (2013).

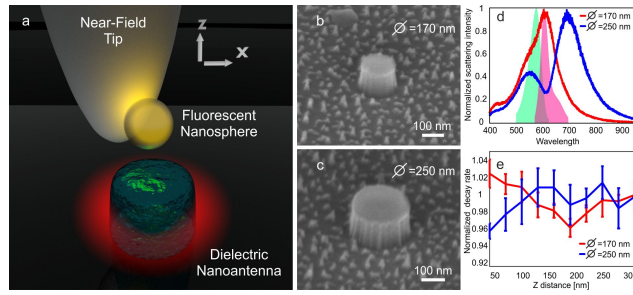


Figure abstract.jpg

Plasmon-exciton coupling evolution by dynamic molecular aggregation

Thursday, 14th September - 17:07 - Optical properties, photonic & plasmonic nanomaterials - Auditorium - Oral
- Abstract ID: 115

*Dr. Francesco Todisco*¹, *Dr. Milena De Giorgi*¹, *Mr. Marco Esposito*¹, *Dr. Luisa De Marco*¹, *Ms. Alessandra Zizzari*¹, *Dr. Monica Bianco*¹, *Dr. Lorenzo Dominici*¹, *Dr. Dario Ballarini*¹, *Dr. Valentina Arima*¹, *Prof. Giuseppe Gigli*¹, *Dr. Daniele Sanvitto*¹

1. CNR Nanotec

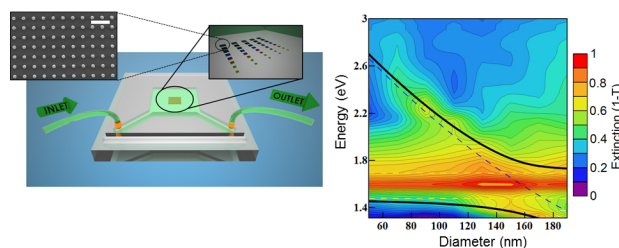
Introduction

The coupling of localized surface plasmons and excitons in semiconductor materials is an extremely powerful strategy to mould the properties of metal nanoparticles and nanoemitters. In fact, when the coupling between the modes dominates over losses, the resulting modes are characterized by a hybrid wavefunction, corresponding to an effective mixture of light and matter components (namely, plasmon-exciton polaritons), thus offering unique possibilities to dress plasmons with excitonic nonlinearities.

Strong coupling between excitons and plasmons has been extensively studied in gold, silver and aluminum nanostructures, either with individual or array of nanoparticles. In this work, by integrating plasmonic nanostructure arrays in a microfluidic device, we show the real time build-up of plasmon-exciton strong coupling, and follow its evolution from the uncoupled modes to the ultra-strong regime.

Results and discussion

By injecting a dilute solution of a near-infrared cyanine dye, we clearly observe the transition from a crossing to an anticrossing behaviour in the plasmon-exciton extinction dispersion, and an increase of the Rabi splitting due to the progressive deposition of injected molecules on the metallic nanostructures surface. In particular, for sufficiently long interaction times, the Rabi splitting increases up to the 35% of the exciton energy (around 600 meV), thus entering the regime of ultrastrong coupling. Our results can open the way towards a full active control of the Rabi splitting in plasmonic systems, spanning from the strong to the ultrastrong regime.



Sample sketch and extinction dispersion.png

Exploring electron induced photon radiation in plasmonic nanostructures by angle and polarization-resolved cathodoluminescence spectroscopy

Thursday, 14th September - 17:24 - Optical properties, photonic & plasmonic nanomaterials - Auditorium - Oral
- Abstract ID: 241

*Dr. Viktor Myroshnychenko*¹, *Prof. Javier García de Abajo*², *Prof. Jens Förstner*¹, *Prof. Naoki Yamamoto*³

1. University of Paderborn, 2. ICFO-The Institute of Photonic Sciences, 3. Tokyo Institute of Technology

Introduction

Localized surface plasmon (SP) resonances of plasmonic nanoparticles have been deeply investigated due to their major role in a wide range of applications such as single-molecule sensing and surface-enhanced Raman scattering. Experimental access to the electromagnetic field distribution associated with SP excitations with high spatial resolution is of fundamental importance. In recent years an electron based cathodoluminescence (CL) spectroscopy has attracted significant attention due to its nanometer spatial resolution and broad spectral range. The CL probes only radiative processes, however, it offers a large set of measurements including spectral, spatial, polarization, and angle dependent properties of the SP modes.

Methods

We use electron-beam lithography to pattern high quality gold nanoprisms and nanoprisms pairs in the bowtie antenna alignment on SiO₂ layers. Angle- and polarization-resolved CL measurements of the optical properties of these nanostructures are performed in a scanning transmission electron microscope equipped with a parabolic mirror and combined with a light detection system (Fig. 1a,b). To interpret the experimental results, numerical simulations are performed using the retarded boundary-element method.

Results and discussion

The optical properties of individual and coupled Au nanoprisms are systematically investigated using the CL with special emphasis on angle and polarization dependences. By exciting nanostructures with an electron beam, we measure spectral features and spatially resolved maps of SPs in the far-field radiation (Fig. 1c,d). By resolving polarization and angular distribution patterns of the far-field emission we access to the symmetry of the modes and interpret them within a group theory description. In particular, the degeneracy of the modes and plasmon hybridization in bow-tie triangles are explored. We demonstrate that combination of the angle and polarization-resolved CL provides a powerful technique with the ability of efficiently detecting and mapping weakly radiative dipole plasmons, higher-order and dark modes. Furthermore, we discuss a link between the CL and the electromagnetic local density of states associated to the SP modes. All our experimental results are supported by numerical simulations showing excellent agreement.

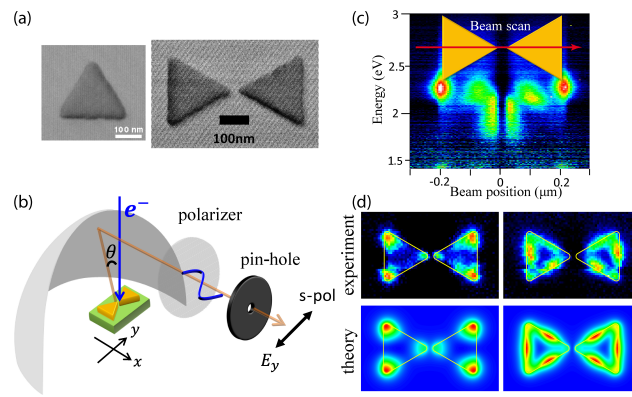


Fig1.experimental setup and photon maps.jpg

Magneto-optics of single-molecule magnets with optical nanoantennas

Thursday, 14th September - 17:41 - Optical properties, photonic & plasmonic nanomaterials - Auditorium - Oral
- Abstract ID: 414

***Dr. Francesco Pineider*¹, *Dr. Addis Mekonnen Adamu*², *Dr. Michele Serri*³, *Dr. Valentina Bonanni*⁴,
*Dr. Giulio Campo*⁵, *Dr. Matteo Mannini*⁶, *Dr. Cesar De Julián Fernández*⁷, *Dr. Claudio Sangregorio*⁸,
*Prof. Massimo Gurioli*⁵, *Prof. Alexandre Dmitriev*⁹, *Prof. Roberta Sessoli*⁶**

1. University of Pisa, 2. Bahir Dar University, 3. Istituto Italiano di Tecnologia, 4. University of Milan, 5. European Laboratory for Non-Linear Spectroscopies, University of Florence, 6. University of Florence, 7. IMEM-CNR, Parma, 8. ICCOM-CNR, Florence, 9. University of Gothenburg

Introduction

Magnetoplasmonics, the interaction of surface plasmons with magnetism, can provide exciting prospects in non-reciprocal nanophotonics, optically-controlled nanomagnetism and highly-efficient chemical sensing.[1,2] To gain these functionalities, one typically combines localized plasmon nanoantennas and ferromagnetic nanostructures.[3,4] Here we investigate the so far unexplored combination of molecular magnets with plasmonic nanostructures to reveal how the magneto-optical response of the former is modified in such hybrids.

Methods

Thin films (2 nm) of the TbPc2 single molecule magnet were prepared by thermal evaporation. Gold nanodisks were prepared by hole-mask colloidal lithography. Low temperature Magnetic Circular Dichroism experiments were carried out on a home-made spectroscopic setup capable of working between 250-2500 nm, 1.4-300 K and ± 11.5 T.

Results

We tuned the geometrical parameters of the nanodisks so that their plasmon resonance would match the main absorption line of TbPc2. We observed a moderate (5x) but clear amplification of the optical and magneto-optical signals.

Discussion

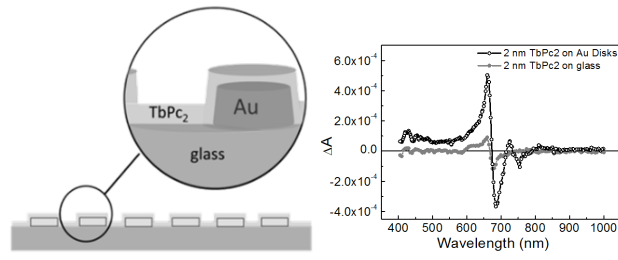
To accurately interpret the magneto-optical response of the molecular-plasmonic hybrid structure, the magnetoplasmonic behavior of the gold nanodisks was modelled and taken into account.[5,6] We found that such contribution is far from being negligible, and it is mandatory to understand the optical and magneto-optical processes taking place in the hybrid nanostructure. This is, to the best of our knowledge, the first report of plasmon-assisted amplification of the magneto-optical signal of a molecular nanomagnet. These results indicate that plasmon-boostered magneto-optics can detect the magnetic properties of single-molecule magnet sub-monolayers, which are currently only accessible through x-ray magnetic circular dichroism at synchrotron radiation facilities.[7,8]

This work has been financed by the EC through grant 737093 — FEMTOTERABYTE — H2020-FETOPEN-2016-2017.

References

- [1] Armelles et al. *Adv. Opt. Mater.* 1 (2013) 10.
- [2] Pellegrini et al. 'Magnetoplasmonics' in *Encyclopedia of Nanotechnology*, Springer 2016.
- [3] Armelles et al. *Nano Lett.* 15 (2015) 2045.
- [4] Lodewijks et al. *Nano Lett.* 14 (2014) 7207.
- [5] Pineider, F. et al. *Nano Lett.* 13 (2013) 4785.
- [6] Sepulveda, B. et al. *Phys. Rev. Lett.* 104 (2010) 147401.
- [7] Mannini, M. et al. *Nature Mater.* 8 (2009) 194.

[8] Mannini, M. et al. Nature Mater. 468 (2010) 417.



Tbpc2 on disks and mcd spectra.png

Active control of transmission and helicity of nanostructured optical beams via magnetoplasmonic vortex lens

Thursday, 14th September - 17:58 - Optical properties, photonic & plasmonic nanomaterials - Auditorium - Oral
- Abstract ID: 177

***Dr. Nicolò Maccaferri*¹, *Dr. Yuri Gorodetski*², *Dr. Pierfrancesco Zilio*¹, *Dr. Francesco De Angelis*¹, *Dr. Denis Garoli*¹**

1. Istituto Italiano di Tecnologia, Department of Nanostructures, 2. Ariel University

Structured optical beams have become a subject of an intense research, due to numerous potential applications in, among many others, super-resolution imaging, optical tweezing, and telecommunications. Special interest is dedicated to the interaction of structured light with metallic nanostructures, resulting in Surface Plasmon Polaritons (SPPs) carrying an orbital angular momentum (OAM). These surface confined electromagnetic distributions are generally defined by a field singularity surrounded by a helical phase front, referred here as plasmonic vortices (PVs). Besides, various practical applications in nanophotonics require fast external control of the emerging beam characteristics. In this regard magnetoplasmonic devices draw a very promising route to active nanophotonics, since an externally applied magnetic field can alter the plasmonic response leading to novel and unexpected effects [1, 2]. The main requirement of these devices is to be fabricated from a material that has both plasmonic and magnetic properties, for instance hybrid noble metal/magnetic materials. Recently we have demonstrated an efficient PV coupling to the free space via adiabatically tapered gold tip at its center [3, 4]. Here we demonstrate an architecture where a PV excited in a gold surface propagates on an adiabatically tapered magnetoplasmonic tip and detaches to the far-field while carrying a well-defined OAM and helicity. We analyze the light transmission and show that, despite generally high losses of flat magnetic surface, our 3D structure exhibits high energy throughput. Moreover we show that the helicity and the OAM of the emitted beam can be tuned by applying an external and relative small (< 0.5 T) magnetic field, providing optimistic opportunities for active magnetically-driven plasmon-based structured optical beams [5].

References

- [1] Armelles, G. et al., *Advanced Optical Materials* **1**, 10-35 (2013).
- [2] Maccaferri, N. et al., *Nature Communications* **6**, 6150 (2015).
- [3] Garoli, D. et al., *Nano Letters* **16**(10), 6636–6643 (2016).
- [4] Garoli, D. et al., *Nanoscale* **9**, 6965-6969 (2017).
- [5] Maccaferri, N. et al., submitted (2017).

Illustration of the helicity locking concept induced by a plasmonic vortex lens (left), and sketch of the magnetic modulation of the helicity locking via a magnetoplasmonic vortex lens (right).

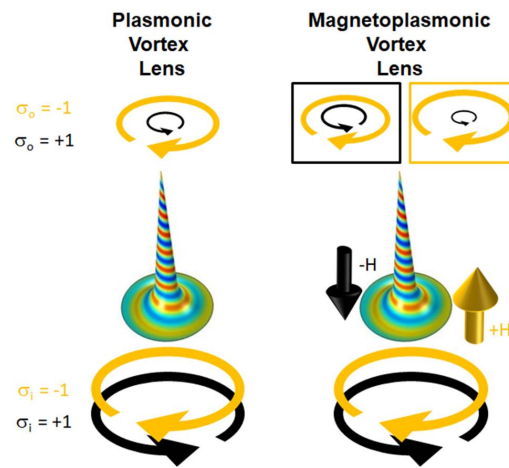


Fig 1 pvl and mpvl concept.jpg

GaSb oxidation for plasmonic enhanced mid-IR molecular spectroscopy

Thursday, 14th September - 18:15 - Optical properties, photonic & plasmonic nanomaterials - Auditorium - Oral
- Abstract ID: 382

Mr. Mario Bomers¹, Ms. Franziska Barho¹, Dr. Aude Mezy², Dr. Maria Jose Milla¹, Dr. Laurent Cerutti¹, Dr. Fernando Gonzalez-Posada Flores¹, Prof. Eric Tournié¹, Prof. Thierry Taliercio¹

1. University of Montpellier / CNRS, 2. Sikemia

Introduction

Plasmonic mid-IR resonators enable surface-enhanced infrared (SEIRA) spectroscopy to improve the detection of minute quantities of molecules. While the field of fabricating plasmonic SEIRA resonators is dominated by metals¹, there is an interest to work with highly-doped semiconductors (HDSC) in the mid-IR range for their tunable optical properties² and their potential to combine plasmonic resonator and detection on one chip. We exploit the oxidation of GaSb (supporting layer) to fabricate pedestals and to blue-shift the mid-IR resonances of our InAs_{0.9}Sb_{0.1} resonators. Additionally, the GaSb oxide layer allows to apply phosphonate-oxide bonding for surface functionalization.

Methods

The resonators used in this study were grown by solid-source molecular beam epitaxy (MBE) and were surface patterned by UV-lithography and acid etching. Self-assembled monolayers (SAM) of phosphonates were deposited by a wet chemical process. The samples were characterized by standard optical techniques including Raman spectroscopy, ellipsometry and FTIR-spectroscopy.

Results and Discussion

We show that 50 nm of GaSb on an InAs_{0.9}Sb_{0.1} supporting layer undergoes a material transition upon exposure to water (Fig. 1). After being exposed for 10h to water, the refractive index of the 50 nm toplayer is reduced by more than 50% and Raman measurements indicate that the material transition involves an evolution of different oxidation states. We demonstrate that this oxidation of GaSb allows to fabricate a pedestal for InAs_{0.9}Sb_{0.1} gratings (Fig. 2). The change of refractive index upon oxidation is a post-fabrication technique to tune plasmonic resonances in the mid-IR range. Finally, we present that phosphonate monolayers are formed by a self-assembling wet-chemical process on native GaSb oxide layers. By depositing a phosphonate monolayer on a InAs_{0.9}Sb_{0.1}/GaSb grating and by comparing the reflection spectra with those of a monolayer on a non-patterned GaSb layer, we can demonstrate enhanced molecular sensing (Fig. 3).

We conclude that the InAsSb:Si / GaSb material system and in particular the oxidation of GaSb can be exploited for surface enhanced molecular spectroscopy.

References

¹ F. Neubrech, C. Huck, K. Weber, A. Pucci, and H. Giessen, Chem. Rev. (2017).

² Y. Zhong, S.D. Malagari, T. Hamilton, and D. Wasserman, J. Nanophotonics 9, 093791 (2015).

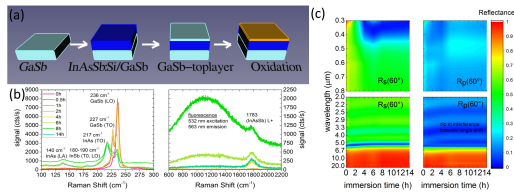


Fig 1 : (a) Illustration of the layer system grown by molecular beam epitaxy. (b) The Raman measurements show the material transition of the GaSb-toplayer after immersion for several hours in water. (c) Changes in reflectance were measured and the refractive index of the oxide could be determined by fitting the data.

01-optical-characterisation-of-material-transition-due-to-gasb-oxidation.jpg

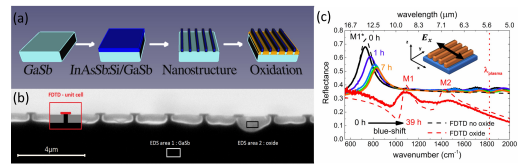


Fig 2 : (a) Illustration of the grating structure used in this study. (b) The scanning electron microscopy image shows the pedestal formation upon immersion for 39h in water. (c) The oxidation of the GaSb supporting layer is blue-shifting the main plasmonic resonance and an additional plasmonic pedestal mode is created.

2-pillar-formation-for-resonance-tuning-by-gasb-oxidation.jpg

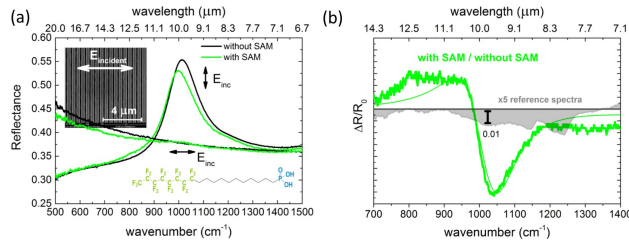


Fig 3 : (a) A self-assembled monolayer (SAM) of phosphonates on the native oxide of the GaSb supporting layer of plasmonic InAsSb resonators is red-shifting the main plasmonic peak. (b) A comparison of the SAM deposited on a flat GaSb layer (on top of a mirror layer) with the SAM deposited on the plasmonic grating reveals surface-enhanced infrared absorption.

3-enhanced-plasmonic-sensing-of-phosphonates-coupled-to-gasb-oxide-surface-update.jpg

Holographic reconstruction via sub-wavelength aperture tips

Thursday, 14th September - 18:32 - Optical properties, photonic & plasmonic nanomaterials - Auditorium - Oral
- Abstract ID: 413

*Dr. Nancy Rahbany*¹, *Dr. Ignacio Izeddin*¹, *Dr. Valentina Krachmalnicoff*¹, *Prof. Rémi Carminati*¹,
*Prof. Gilles Tessier*², *Dr. Yannick De Wilde*¹

1. Institut Langevin, ESPCI Paris - CNRS, 2. Université Paris Descartes, CNRS

Introduction

In this work, we introduce a microscopy method based on full field off-axis holography¹⁻³ which enables performing three-dimensional (3D) reconstruction of scattered light from sub-wavelength aperture tips. While far-field methods, such as back focal plane imaging⁴⁻⁶, can be used to infer the directionality of angular radiation patterns, the advantage of our technique is that a single hologram recorded instantaneously contains information on the amplitude and phase of the scattered light, allowing to reverse numerically the propagation of the electromagnetic field towards the source.

Methods

Our setup is composed of a digital holographic microscope combined with a modified commercial Witec near-field scanning optical microscope (NSOM). Light from the laser is split into sample and reference beams. The sample beam is focused on the nanosized aperture of a metal coated aperture probe that gets in contact with the sample surface. Light emerging through the substrate is directed either to a PMT detector for regular NSOM measurements, or to a CCD camera where it interferes with the reference beam creating a hologram. Using back-propagation, the complex field at any point in space can be reconstructed by computing the scattered field in Fourier space.

Results

We present a comparative study of the reconstructed light from a tip located at various distances from two samples; a glass substrate, and a 40 nm gold film on a glass substrate. Fig.1 shows the field scattered through the tip aperture when placed in contact with a gold film. Directional leaky plasmons are clearly observed. FDTD simulations are performed to measure the angular radiation pattern of a magnetic dipole on a substrate, and show very good agreement with the experimentally obtained results.

Discussion

We have successfully demonstrated 3D reconstruction of scattered light from a NSOM tip through transparent and plasmonic media.

Our experimental and simulation results confirm the lateral magnetic dipole approximation previously studied in the literature for similar aperture probes⁷⁻⁹.

Further work will include applying this technique to investigate the complex field resulting from the propagation through a strongly scattering medium.

Acknowledgments

This work was supported by LABEXWIFI under references ANR-10-LABX-24 and ANR-10-IDEX-0001-02PSL.

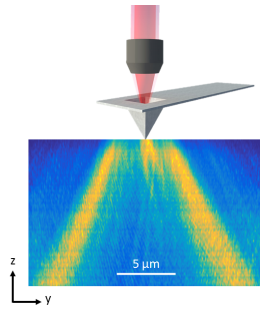


Fig. 1. Reconstructed field propagating in a sample made of a 40 nm gold film on a glass substrate after passing through the nanosized aperture of a NSOM tip.

Fig.1.png

References

1. Suck, S. *et al.* Imaging the three-dimensional scattering pattern of plasmonic nanodisk chains by digital heterodyne holography. *Opt. Lett.* **36**, 849–851 (2011).
2. Absili, E. *et al.* Photothermal heterodyne holography of gold nanoparticles. *Opt. Express* **18**, 780–786 (2010).
3. Martínez-Marrades, A. *et al.* Characterization of plasmonic nanoantennas by Holographic Microscopy and Scanning Near-field Microscopy. *Opt. Commun.* **359**, 455–459 (2016).
4. Lieb, M. A. *et al.* Single-molecule orientations determined by direct emission pattern imaging. *JOSA B* **21**, 1210–1215 (2004).
5. Zhang, D. *et al.* Back focal plane imaging of directional emission from dye molecules coupled to one-dimensional photonic crystals. *Nanotechnology* **25**, 145202 (2014).
6. Hartmann, N. *et al.* Radiation Channels Close to a Plasmonic Nanowire Visualized by Back Focal Plane Imaging. *ACS Nano* **7**, 10257–10262 (2013).
7. Denkova, D. *et al.* Lateral Magnetic Near-Field Imaging of Plasmonic Nanoantennas With Increasing Complexity. *Small* **10**, 1959–1966 (2014).
8. Denkova, D. *et al.* Mapping Magnetic Near-Field Distributions of Plasmonic Nanoantennas. *ACS Nano* **7**, 3168–3176 (2013).
9. Kihm, H. W. *et al.* Optical magnetic field mapping using a subwavelength aperture. *Opt. Express* **21**, 5625–5633 (2013).

References.png

Nanometre scale monitoring of the quantum confined stark effect and emission efficiency droop in multiple GaN/AlN quantum disks in nanowires

Thursday, 14th September - 16:50 - Nonlinear nano-optics - Room 207 - Oral - Abstract ID: 181

Prof. Luiz Fernando Zagonel¹, Dr. Luiz Tizei², Mr. Gabriel Vitiello³, Dr. Gwénoél Jacopin⁴, Dr. Lorenzo Rigutti⁵, Dr. Maria Tchernycheva², Dr. Francois Julien², Dr. Rudeesun Songmuang⁶, Dr. Tomas Ostasevicius⁷, Dr. Francisco De La Peña⁷, Dr. Caterina Ducati⁷, Prof. Paul Midgley⁷, Dr. Mathieu Kociak²

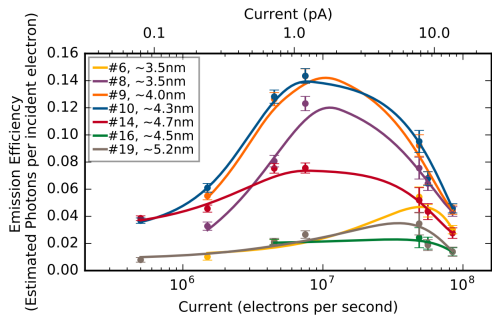
1. University of Campinas – UNICAMP, 2. Univ. Paris-Sud, Université Paris-Saclay, 3. Campinas University, 4. Ecole Polytechnique Federale de Lausanne, 5. Université de Rouen, 6. Institute Neel, 7. University of Cambridge

We report on a detailed study of the intensity dependent optical properties of individual GaN/AlN Quantum Disks (QDisks) embedded into GaN nanowires (NW). The structural and optical properties of the QDisks were probed by high spatial resolution cathodoluminescence (CL) in a scanning transmission electron microscope (STEM).[1] By exciting the QDisks with a nanometric electron beam at currents spanning over 3 orders of magnitude, strong non-linearities (energy shifts) in the light emission are observed. In particular, we find that the amount of energy shift depends on the emission rate and on the QDisk morphology (size, defects and shell thickness).[2] For thick QDisks (>4nm), the QDisk emission energy is observed to blue-shift with the increase of the emission intensity or electron beam current (see Figure). This is interpreted as a consequence of the increase of carriers density excited by the incident electron beam inside the QDisks, which screens the internal electric field and thus reduces the quantum confined Stark effect (QCSE) present in these QDisks. For thinner QDisks (<3 nm), the blue-shift is almost absent in agreement with the negligible QCSE at such sizes. For QDisks of intermediate sizes there exists a current threshold above which the energy shifts, marking the transition from unscreened to partially screened QCSE. From the threshold value we estimate the lifetime in the unscreened regime. These observations suggest that, counterintuitively, electrons of high energy can behave ultimately as single electron-hole pair generators. In addition, when we increase the current from 1 pA to 10 pA the light emission efficiency drops more than one order of magnitude (see Figure). This reduction of the emission efficiency is a manifestation of the ‘efficiency droop’ as observed in nitride-based 2D light emitting diodes, a phenomenon tentatively attributed to the Auger effect.[3]

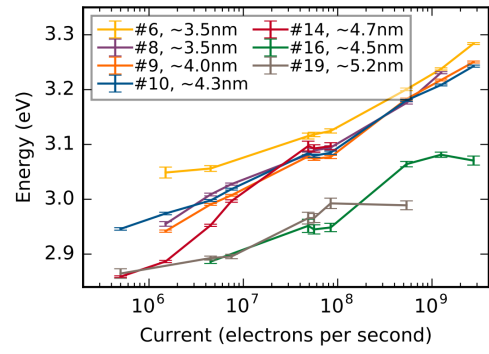
[1] L. F. Zagonel et al. Nanotechnology 23 455205 (2012)

[2] L. F. Zagonel et al. Physical Review B 93 205410 (2016)

[3] Acknowledgements: FAPESP funding 2014/23399-9.



Emission efficiency as function of electron beam current.png



Quantum disk emission energy as function of electron beam current.png

Second harmonic generation in AlGaAs nanodisk dimers

Thursday, 14th September - 17:07 - Nonlinear nano-optics - Room 207 - Oral - Abstract ID: 478

Mr. Valerio Flavio Gili¹, **Mr. Davide Rocco**², **Dr. Lavinia Ghirardini**³, **Dr. Luca Carletti**², **Prof. Andrea Locatelli**², **Dr. Michele Celebrano**³, **Prof. Marco Finazzi**³, **Prof. Costantino De Angelis**², **Dr. Aristide Lemaitre**⁴, **Dr. Ivan Favero**¹, **Prof. Giuseppe Leo**¹

1. Université Paris Diderot, 2. Università di Brescia, 3. Politecnico di Milano, 4. Laboratoire de photonique et nanostructures

All-dielectric nonlinear meta-optics is attracting a great deal of interest thanks to the feasibility of high refractive-index contrast nanostructures available with semiconductor lithography. While $c^{(3)}$ effects have been reported in silicon-on-insulator nanoantennas [1], the AlGaAs-on-insulator platform has recently enabled the demonstration of second harmonic generation (SHG) in $c^{(2)}$ nanoantennas [2]. When one excites them with a plane wave at normal incidence, they exhibit efficient SHG driven by a magnetic-dipole resonance at the pump frequency in the optical telecom range and a polarisation behaviour dominated by a high-order multipole resonance at the second harmonic [3].

Here we focus on SHG from monolithic dimers of $\text{Al}_{0.18}\text{Ga}_{0.82}\text{As}$ -on- AlOx nanoantennas, where AlOx is obtained from selective wet etching of micrometer-thick aluminium-rich AlGaAs epitaxial layer. Such a low refractive index substrate allows to effectively decouple the nanoantenna modes from the underlying GaAs (100) wafer. As a prototype example, we report in the figure the case of a set of coupled nanodisks with height $h = 400$ nm, gap $g = 30$ nm and radii ranging from 175 nm to 225 nm, which we excite with a pump beam linearly polarized along the dimer axis. As in the case of a single nanodisk, the SHG selection rules are mainly set by the properties of bulk AlGaAs $\chi^{(2)}$ tensor: in a good agreement with finite-element calculations, we clearly observe that the main resonance associated to the single pillar splits in two distinct features, owing to near-field coupling between the two pillars. The measured peak conversion efficiency, exceeding 10^{-5} for a 1.6 GW/cm^2 pump intensity, paves the way to the engineering of coupled nanoantennas and nonlinear metasurfaces for molding SHG properties at the nanoscale.

REFERENCES

- [1] M. R. Shcherbakov et al., “Enhanced third-harmonic generation in silicon nanoparticles driven by magnetic response”, *Nano Lett.* 14, 6488 (2014).
- [2] V. F. Gili et al., “Monolithic AlGaAs second-harmonic nanoantennas”, *Opt. Expr.* 24, 15965 (2016).
- [3] L. Ghirardini et al., “Polarization properties of second-harmonic generation in AlGaAs optical nanoantennas”, *Opt. Letters* 42, 559 (2017).

Active near-field probe based on ultrabroadband hot luminescence of Si/Au nanoparticle

Thursday, 14th September - 17:24 - Nonlinear nano-optics - Room 207 - Oral - Abstract ID: 440

***Dr. Anton Samusev*¹, *Dr. Sergey Makarov*¹, *Mr. Ivan Sinev*¹, *Dr. Valentin Milichko*¹, *Mr. Filipp Komissarenko*², *Dr. Dmitry Zuev*¹, *Dr. Elena Ushakova*¹, *Dr. Ivan Mukhin*², *Dr. Yefeng Yu*³, *Dr. Arseniy Kuznetsov*³, *Dr. Pavel Belov*¹, *Dr. Ivan Iorsh*¹, *Dr. Alexander Poddubny*⁴, *Prof. Yuri Kivshar*⁵**

*1. ITMO University, 2. ITMO University; St. Petersburg Academic University, 3. Data Storage Institute, A*STAR (Agency for Science, Technology and Research), 4. ITMO University; Ioffe Institute, 5. ITMO University; Nonlinear Physics Center, Australian National University*

Efficient white-light sources at the nanoscale are of great importance for probing near-field properties of optical nanoantennas and nanophotonics devices operating in a broad spectral range. Tunnelling and scattering near-field scanning optical microscopes (NSOMs) allow to retrieve information on electromagnetic field components in the vicinity of the sample, but the possibility to map the local density of states (LDOS) is crucially important. Here we demonstrate highly-efficient optical NSOM with an active probe operating in unprecedentedly broad UV-VIS-NIR spectral band. The probe is fabricated in two steps. A hybrid nanoparticle with size ranging of 100-200 nm is printed from thin double-layer Si/Au film by means of the laser printing technique. This particle is then transferred to a tip of an atomic force microscopy cantilever by using nanoscale manipulation under an electron beam.

In experiment, the fabricated probe is irradiated by a near-IR femtosecond laser (1053 nm), which results in intense three-photon hot white-light luminescence from the nanoparticle. While the sample is scanned with respect to the tip, the emission spectra are recorded from the substrate side in confocal arrangement.

The measured NSOM signal varies depending on a relative sample-probe position, and the results are in a good agreement with partial LDOS maps simulated numerically as the emission of three incoherent orthogonal electric dipole sources placed in the vicinity of the structure.

The hot luminescence of Si/Au nanoparticle originates from a balance in electron relaxation and recombination times. The latter is strongly increased as compared to purely phonon mechanism by contributing defects and plasmons in silicon. The efficient excitation of plasmons becomes possible due to high nearly metallic-type density of free carriers (of more than 10^{20} 1/cm³) generated by intense femtosecond laser pulses, while gold enables an efficient three-photon absorption and injection of hot electrons.

Thus, we have employed hybrid Si/Au nanoparticles to fabricate an active near-field probe operating in an ultra-broad spectral band. The intense broadband luminescence originates from dense electron-hole plasma generated in silicon by femtosecond radiation. The demonstrated device would be a powerful tool for the study of LDOS of nanoscale systems.

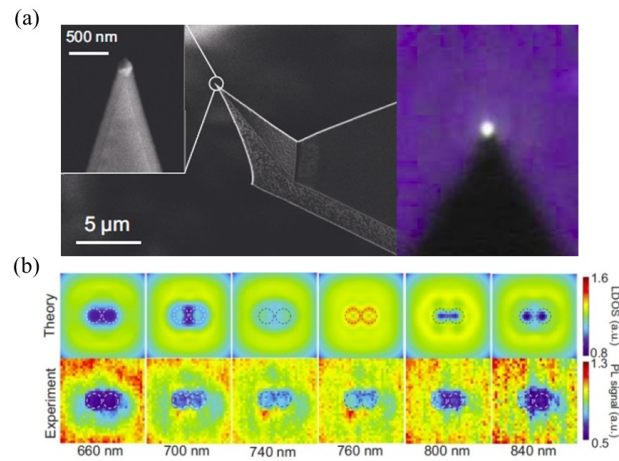


Figure 1. **Active NSOM probe for LDOS measurements.** (a) SEM and optical microscope images of active NSOM probe based on hybrid Si/Au nanoparticle excited by femtosecond laser. (b) Visible-frequency NSOM images of silicon nanodimers measured simultaneously.

Activeprobe.jpg

Generation of continuous terahertz wave by differential-frequency-mixing in a GaAs/AlAs multiple quantum well

Thursday, 14th September - 17:41 - Nonlinear nano-optics - Room 207 - Oral - Abstract ID: 281

***Prof. Osamu Kojima*¹, *Mr. Yuki Tarui*¹, *Prof. Takashi Kita*², *Mrs. Avan Majeed*³, *Dr. Edmund Clark*³,
*Dr. Pavlo Ivanov*⁴, *Prof. Richard Hogg*⁴**

1. Kobe University, 2. Korea University, 3. University of Sheffield, 4. University of Sheffield/University of Glasgow

I. Introduction

As continuous wave (CW) terahertz (THz) sources, the differential-frequency-mixing (DFM) has an advantage for the frequency tunability by changing the energy separation of the two lasers. Considering the inhomogeneous width of the quantum confinement systems, use of the excitons enables wide frequency tuning. The THz sources with the narrow bandwidth and wide frequency tunability will be applied to the high resolution THz spectroscopy. Therefore, in this work, we show the CW-THz wave generation by DFM under the exciton excitation conditions in a GaAs/AlAs multiple quantum well (MQW).

II. Methods

We used an undoped GaAs/AlAs MQW embedded in a p-i-n structure on a (001) n^+ -GaAs substrate. The thickness of GaAs and AlAs layer is 7.5 nm. The measurements of THz wave were carried out at 297 K. As the laser sources, a semiconductor laser and a CW-mode Ti:sapphire laser to change the excitation energy were used. The schematic of the experimental setup is shown in Fig. 1. The two beams were spatially combined on the half mirror in free space with the same polarization, and the combined beam is focused on the sample surface.

III. Results and Discussion

Figure 2 shows the dependence of the signal intensity on the energy of the Ti:sapphire laser. The energy of the semiconductor laser is indicated by an arrow. The dotted lines indicate the exciton energies. While the excitation power of semiconductor laser was kept at 3.40 kW/cm^2 , that of the Ti:sapphire laser was variously changed. When the Ti:sapphire-laser power increases up to 17.0 kW/cm^2 , the peak structure appears in the exciton energy region as indicated by the open circles. In the excitation-power dependence measurement, the signal intensity shows the square dependence on the excitation power. Essentially, the excitons in the zincblende structure semiconductors does not show the second optical nonlinearity because of the inversion symmetry. However, the built-in-field by p-i-n structure breaks the symmetry of the electron and hole envelope functions. This symmetry breaking creates the second optical nonlinear polarization. Therefore, our results demonstrate the possibility of the CW tunable THz source based on the exciton effects.

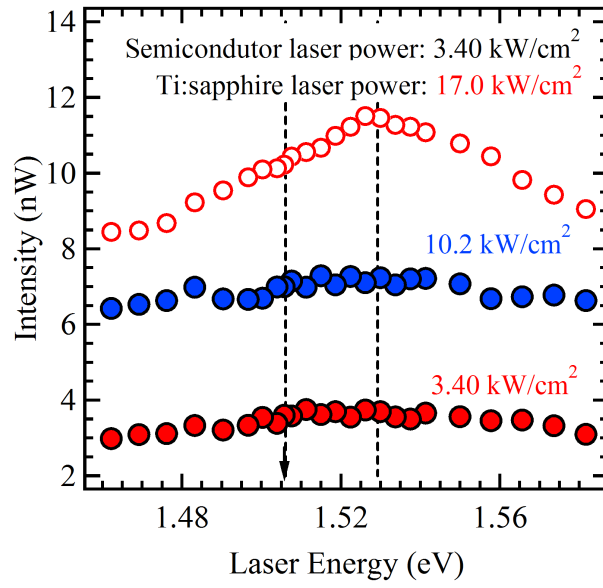


Fig2.png

Mid-infrared nonlinear polaritonics using surface phonon polaritons

Thursday, 14th September - 17:58 - Nonlinear nano-optics - Room 207 - Oral - Abstract ID: 222

*Dr. Christopher Gubbin*¹, *Dr. Simone De Liberato*¹

1. University of Southampton

Introduction

Recently the potential of surface phonon polaritons for light localisation in tailored geometries has been demonstrated. By hybridising photons to coherent oscillations of a polar dielectric crystals ionic lattice, field confinements beyond those theoretically achievable by plasmonic means are possible, with the boon of circumventing Ohmic losses characteristic in metal-based systems. The amalgamation of these features presents a potential platform for mid-infrared nanophotonics. One area where SPhPs present exceptional promise is as a platform for mid-infrared nonlinear optics, where deep-subdiffraction localisation can be exploited to drive fast scattering mediated by the intrinsic anharmonicity of the dielectric. A description of nonlinear optics in these confined systems necessitates theory capable of accounting for real-space variation in the dielectric constant.

Methods

In this work we build from the foundations of a microscopic Hopfield picture, where coupled light-matter modes of the system are linear, polaritonic, superpositions of the bare modes, to develop a quantum theory of perturbative second[1] and third[2] -order optical nonlinearities in polar dielectric systems.

Results

This theory, validated by fits to recent experiments of second harmonic generation in reflection from planar beta-SiC substrates [3] as illustrated in Fig. 1a, provides a methodology to describe nonlinear optical processes in systems with analytically or numerically derived linear solutions. We apply our theory to the describe excitation of SPhPs by difference frequency generation, showing the process to be orders of magnitude more efficient than analogous surface plasmon excitation by four-wave mixing [1]. Furthermore our theory is developed to describe third-order processes, showing that SPhP based parametric oscillators lie within experimental reach [2].

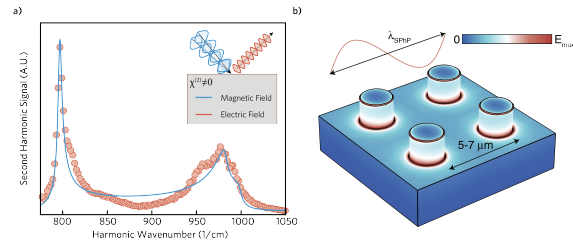
Discussion

The frame for nonlinear polaritonics presented can be expected to find general application as a predictive tool in the emergent field of surface phonon polariton nanophotonics. Our specific results regarding SPhP difference frequency generation and parametric oscillation illustrate the specific potential of polar dielectric systems as a platform for mid-infrared nonlinear optics.

[1] 10.1021/acsphotonics.7b00020

[2] arXiv:1707.06585

[3] 10.1103/PhysRevB.94.134312



Metaimage.png

Second Harmonic generation from an array of gold nanocylinders up to a single nanocylinder.

Thursday, 14th September - 18:15 - Nonlinear nano-optics - Room 207 - Oral - Abstract ID: 64

*Dr. christian jonin*¹, *Prof. Pierre-françois Brevet*¹, *Dr. Emeric Bergmann*¹, *Prof. Pierre-michel Adam*², *Dr. Anne-laure Baudrion*³, *Dr. Sergei Kochtcheev*³

1. universit  de lyon, 2. universit  technologique de troyes, 3. Universit  de technologie de Troyes

1. Nonlinear response of an array of gold nanocylinders

The second harmonic generation process has been performed from hexagonal array of gold nanocylinders. The nonlinear response has been carried out as a function of the input fundamental polarization angle for the on and off-axis transmission geometries and crossed output polarization configurations and for different diameter sizes. The nonlinear response is essentially incoherent in an on-axis transmission geometry while a coherent response appears on off-axis configuration. Indeed for the on-axis configuration the breaking of symmetry shape of the cylinder body leads to a pure electric dipole incoherent response. On the other hand, considering small tilt angle the nonlinear coherent contribution appears from the out-of-plane non linearity. It has also to be noted that as a function of the nanocylinder size the retardation effect play an important role.

2. Nonlinear response of an individual gold nanocylinder.

We have also performed nonlinear studies up to an individual nanocylinder as is displayed on the figure 2. Each gold nanocylinder appears as a circular SHG intensity distribution. This individual mapping indicates clearly that the nonlinear response is due like an array of nanoparticles to the defects at the surface and not to the longitudinal symmetry and the size.

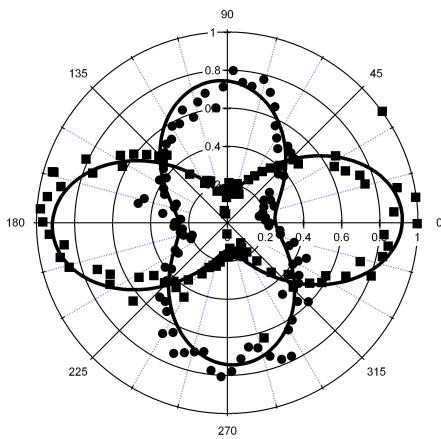


Figure1a.jpg

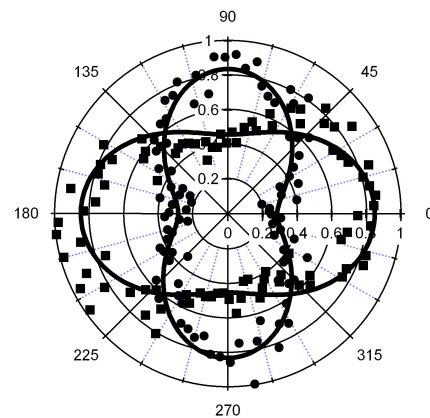


Figure1b.jpg

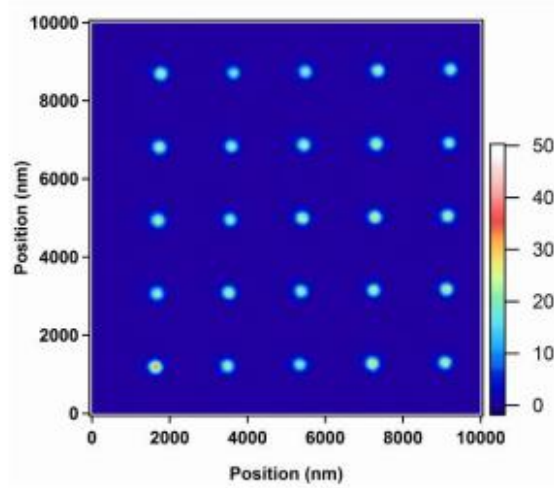


Figure2.jpg

PT-axisymmetric VCSELS

Thursday, 14th September - 18:32 - Nonlinear nano-optics - Room 207 - Oral - Abstract ID: 216

Mr. Waqas W. Ahmed¹, Dr. Muriel Botey², Dr. Ramon Herrero¹, Prof. Kestutis Staliunas³

1. Universitat Politècnica de Catalunya, 2. Univeritat Politècnica de Catalunya, 3. Institució Catalana de Recerca i Estudis Avançats, Catalonia

Optical Parity-Time (PT -) symmetric systems support unusual properties when the symmetric coupling between internal modes is broken [1,2]. The simplest PT -symmetric 1D optical potential may be taken as: $n(x) = n_0 \exp(iqx)$, which at resonance, asymmetrically couples the left-propagating mode, $\exp(-iq/2x)$, to the right-propagating mode $\exp(iq/2x)$, but not vice versa. The question that arises is what happens if such PT -symmetry condition is not met globally. A complex optical potential in the form: $n(x) = n_0 [\cos(iq|x|) - i \sin(iq|x|)]$ imposes a unidirectional coupling towards a selected position, $x=0$. Here, we propose a new class of PT -symmetric potentials with axial symmetry by radial dephased modulations of index and gain/loss: $n(r) = n_0 [\cos(iqr) - i \sin(iqr)]$. This axial potential intrinsically generates an exceptional central point leading to an extraordinary field enhancement and simultaneous confinement [3].

Broad aperture lasers, and VCSELS among them, are relevant laser sources however suffering from a major drawback: a poor beam quality due to the lack of an intrinsic transverse mode selection mechanism. Therefore, as a direct application of the proposed optical potential, we explore the spatio-temporal field dynamics of a 2D complex PT -axisymmetric VCSELS which could have physical realizations present nanophotonic techniques. Indeed, we show that field localization and enhancement is possible at $r=0$, revealing that this 2D axisymmetric system efficiently turns such microlasers into bright and narrow sources.

We expect the proposed PT -axisymmetric configuration to find remarkable applications for the beam quality emission improvement from VCSEL. Besides, the reported effect is universal, and could be extended to different linear or nonlinear physical systems, from optics to Bose condensates, or acoustics among others.

[1] Phys. Rev. Lett. 80, 5243–5246 (1998).

[2] Nat. Mater. 12, 108–113 (2012).

[3] Phys. Rev. A 94, 053819 (2016).

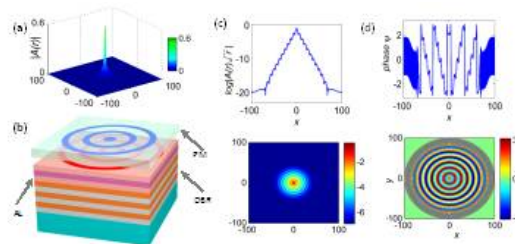


Figure 2 2D PT -axisymmetric VCSEL (a) 3D visualization of the VCSEL output field profile calculated after the steady state ($t \sim 150$ units) for $p = -0.1$ and parameter set $(0.4, 0.4)$ concentrated and enhanced at $r = 0$ (b) Schematic representation of a modified PT -axisymmetric VCSEL; PM-Profiled Mirror, DBR-Distributed Bragg Reflector, AL-active layer. (c) Axial cross-sectional profile and 2D plot of the field in logarithmic scale. (d) Cross-section and 2D distribution of the phase.

Figure.jpg

Biocompatible Random Lasers for Biosensing

Thursday, 14th September - 16:50 - Nanomedicine - Room 412 - Oral - Abstract ID: 150

Ms. Soraya Caixeiro¹, **Dr. Michele Gaio**², **Dr. Van Duong Ta**¹, **Dr. Benedetto Marelli**³, **Prof. Fiorenzo Omenetto**³, **Dr. Francisco Fernandes**⁴, **Dr. Riccardo Sapienza**²

1. King's College London, 2. Imperial College London, 3. Tufts University, 4. Universite Pierre et Marie Curie

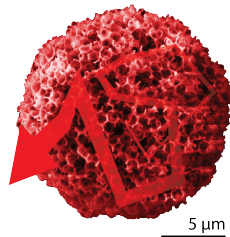
Biocompatible lasers suitable for living tissue integration have begun to captivate the scientific community due to their potential to harness the amplifying power of stimulated emission for bio-sensing and cell tracking [1]. We report a biocompatible self-assembled random laser, made of natural degradable biopolymers such as silk [2].

The biocompatibility, allied with their favorable optical properties and ease of biological functionalisation allows nanostructuring, integration of dyes and lasing. Nanostructuring promotes light confinement while the gain provides light amplification. The lasing action is independent of the overall shape but instead relies on the device's internal porosity; it can therefore easily adapt to biological media with the ability to withstand stretching, wetness and heat.

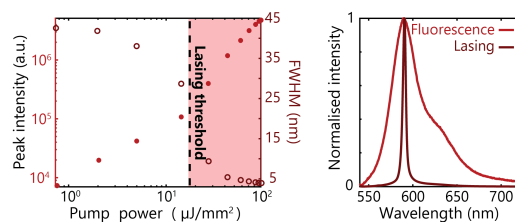
We explore lasing as a mechanism for sensing, demonstrating that bio-random lasing acts as a nonlinear sensor that switches off lasing for high pH values, with a sensitivity ~ 200 times larger than its fluorescent counterpart [3]. The combination of a natural biopolymer and random lasing offers the opportunity for integration of a laser within living tissue, opening a new path at the interface between nanophotonics and medicine.

References:

- [1] Ta, V. D., Caixeiro, S. - Fernandes, F. M., Sapienza, R. *Adv. Opt. Mat.*, 2017, 5, 1601022.
- [2] S. Caixeiro, M. Gaio, B. Marelli, F. G. Omenetto, R. Sapienza, *Adv. Opt. Mat.*, 2016, 4, 7, 998-1003.
- [3] M. Gaio, S. Caixeiro, B. Marelli, F. G. Omenetto, R. Sapienza, *Phys. Rev. Applied* 2017, 7, 034005.



Rl sphere.png



Rl plot.png

Designing Gold Nanoparticles for Photothermal Therapy & Multimodal Therapeutic Strategies

Thursday, 14th September - 17:07 - Nanomedicine - Room 412 - Oral - Abstract ID: 193

Mr. emre doruk önal¹, Prof. Kaan Guven¹

¹. Koc University

Gold nanoparticle (NP) assisted photothermal therapy (PTT) has been actively studied as a minimally invasive approach for treating cancer. With the contemporary fabrication techniques, NPs in a greater spectrum of shapes and sizes become accessible. Thus, laying out some design principles may provide a better start for future implementations.

We compare the optical absorption properties of experimentally realized NP shapes (e.g. rod, tube, disk, ring, and sphere), in the NIR-I and NIR-II biological transparency windows. The optical response of randomly oriented NP ensembles is numerically studied by a boundary element method (MNPBEM) [1]. Unlike many of the existing studies that evaluate the photothermal performance of a NP by its resonant orientation, the present work shows that the random orientation of the NP in host environment has to be taken into account for a realistic assessment and may lead to somewhat counterintuitive results. In particular, we demonstrate that nanodisks can surpass nanorods in terms of photothermal conversion efficiency with almost 3 folds improvement compared to experimentally reported nanorod samples [2, 3]. The improvement is further enhanced in core-shell geometries (nanorings, nanotubes).

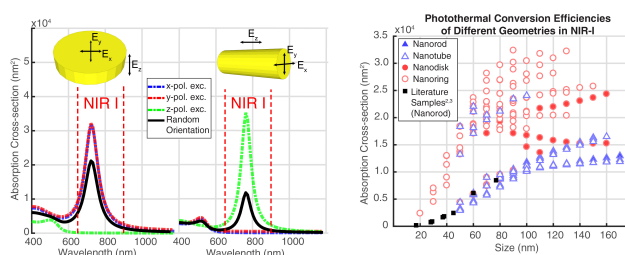
Our study highlights several benchmarks that is relevant to the application environment (i.e. cancer tissue) such as NP size which effects cellular intrusion and retention, and NP dose/mass which is correlated with cytotoxicity. In light of these limitations, we compare the size-dependent tunability of the plasmon resonance in different geometries. We show that mass-sensitive applications favor nanorod design ($\lambda_{\text{res}} \propto m_{\text{NP}}$) instead of nanodisks ($\lambda_{\text{res}} \propto m_{\text{NP}}^2$) at higher wavelengths, i.e. NIR-II.

Conventional PTT as a standalone therapy is currently being challenged by synergistic approaches that require simultaneous utilization of multiple therapeutic schemes (e.g. chemotherapy, immunotherapy and photodynamic therapy) and imaging modalities (NP-assisted optical/thermal imaging). The present work also addresses the optimization of multifunctional NP designs for theranostic applications, e.g. image-guided PTT which utilizes gold NPs both as photothermal transducers and optical contrast agents.

[1] J. R. Cole, et al. J. Phys. Chem. C, 113, 12090 (2009).

[2] M. A. Mackey, et al. J. Phys. Chem. B, 118, 1319 (2014).

[3] L. M. Maestro, et al. RSC Adv., 4, 54122 (2014).



The effects of random orientation photothermal conversion efficiencies of nps.jpg

Nanostructured Color Filter based Wearable Optobiomedical Sensor for Non-invasive Diagnosis

Thursday, 14th September - 17:24 - Nanomedicine - Room 412 - Oral - Abstract ID: 378

Mr. Wenzu Wu¹, Mr. Gregor Scholz¹, Mr. Jan Gülink¹, Ms. C.b. Rojas Hurtado², Dr. Joan Daniel Prades³, Prof. Stefanie Kroker², Prof. Rainer Macdonald², Dr. Hutomo Suryo Wasisto¹, Prof. Andreas Waag¹

1. Institute of Semiconductor Technology (IHT), Technische Universität Braunschweig, 2. Physikalisch-Technische Bundesanstalt (PTB), 3. MIND-IN2UB, Department of Engineering: Electronics, University of Barcelona

Advanced developments in LED technology allow light to become a powerful tool for non-invasive and continuous medical tests. Optical methods avoid people to suffer from discomfort and painfulness during sampling or measurement. However, up to now, most of these sensors in the market have complex operation, bulky dimension, and high cost as well as provide only a few health indicators. Therefore, a small sensor system is designed aiming to capture and measure reliable relevant health data quickly. Differentiating from normal measurement device, e.g., pulse oximetry, which passes two or more wavelengths of light through our body part and detects transmitted or reflected light, our sensor system consists of an LED with wide bandwidth and an image sensor with color filter matrix.

Instead of using color filters made of pigments or dyes, which have low transmission efficiency, imperfect color purity and gradual aging, nanostructured color filters are developed in this work to comprise a color filter matrix. Every image sensor pixel is set under a matrix cell with a certain transmission peak wavelength measuring the intensity to build the spectrum.

Finite-difference time-domain (FDTD) simulations of guided-mode-resonance (GMR) color filter were performed to determine the suitable geometry for each single peak transmission wavelength. In terms of filtering effect, the GMR filter depends on its material, grating period, depth, fill factor, buffer layer, and waveguide layer thickness. Thus, all those parameters were carefully studied to optimize the proposed filters. For GMR, silver has a narrower bandwidth than other metals, because of the poor adhesion between silver and SiO₂, we use ITO instead of Ti or Cr as the adhesion layer, to ensure a higher transmission. A fill factor of 0.9 suppresses subwavelength better and can have high sufficient transmission of about 0.4 to 0.8. From the results, we could determine the metal grating depth of 50 nm, ITO adhesion layer thickness of 5 to 10 nm, buffer layer of 50 nm, waveguide layer of 100 nm, and grating period varies from 380 to 660 nm to cover 600 nm to 988 nm peak transmission wavelength.

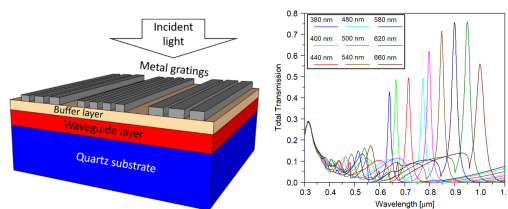


Figure 1 3d structure of guided-mode-resonance gmr color filter left . transmitted spectra of the gmr filter wavelengths at which transmission through each peak versus the grating period from 330 nm to 660 nm right .png

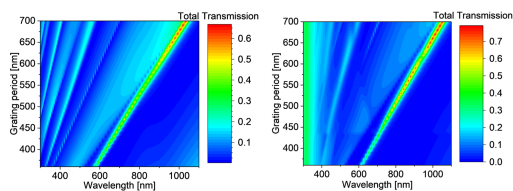


Figure 2 transmitted spectra of aluminum grating with fill factor of 0.9 metal depth of 30 nm buffer layer thickness of 50 nm waveguide layer of 100 nm left and spectra of silver grating .png

Optical scattering and microscopic imaging of cellular exo- and endocytosis

Thursday, 14th September - 17:41 - Nanomedicine - Room 412 - Oral - Abstract ID: 33

*Mr. Dylan Marques*¹, *Dr. Adelaide Miranda*², *Prof. Ana G. Silva*¹, *Dr. Peter Munro*³,
*Dr. Pieter De Beule*²

1. Universidade Nova de Lisboa, 2. INL, 3. University College London

We present a solution to Maxwell’s equations for core-shell nanoparticle scattering near an isotropic substrate covered with an anisotropic thin film, based on an extension of the Bobbert-Vlieger solution for particle scattering near a substrate, delivering an exact solution in the near-field as well as far-field. We successfully apply the developed scattering model to the calculation of light scattering on an optical model representing a lipid vesicle near a lipid bilayer, whereby the lipids are characterized through a biaxial optical model (Figure 1). Hereby, we pave the path for understanding quantitatively how light scatters during a cellular exo- or endocytosis event during microscopic observation taking into account lipid induced anisotropy. Through the application of ellipsometric angles it is effectively demonstrated that realistically small optical anisotropy values significantly alter far-field optical scattering in respect to an equivalent optical model for cellular endocytosis consisting of isotropic components only (Figure 2 & 3). We hereby predict a significant impact of lipid-induced optical anisotropy on the experimental observation of exo- or endocytic microscopic imaging with *e.g.* Differential Interference Contrast (DIC) microscopy. Furthermore, we integrate this extended Bobbert-Vlieger scattering solution into a rigorous model of Differential Interference Contrast (DIC) image formation which allows for characterizing DIC, through simulation, as a tool for imaging of exo- or endocytosis events. We compare theoretical predictions with experimental high numerical aperture DIC imaging of dielectric oxide nanoparticles with organic shell.

Figure 1: optical model for light scattering off a liposome above a lipid bilayer.

Figure 2: Ellipsometry angles Ψ (left) and Δ (right) for wavelength λ (top – angle-of-incidence 70°) and angle-of-incidence θ (bottom – wavelength 488 nm) resolved ellipsometry for liposomes with radii of 50 nm, 150 nm and 250 nm on top of a lipid bilayer ($\delta=R$). We consider light scattering off a structure as depicted in Figure 1 ($n_{\perp,lb} = n_{\parallel,lb} = 1.45$; $n_{\perp,sh} = n_{\parallel,sh} = 1.46$; $n_i = n_s = 1.33$; $d_{1,2} = 5$ nm).

Figure 3: Ellipsometry angles Ψ and Δ for a liposome above a lipid bilayer for varying distance between the liposome and lipid bilayer ($\delta=R$). Model parameters are identical to model considered in Figure 2.

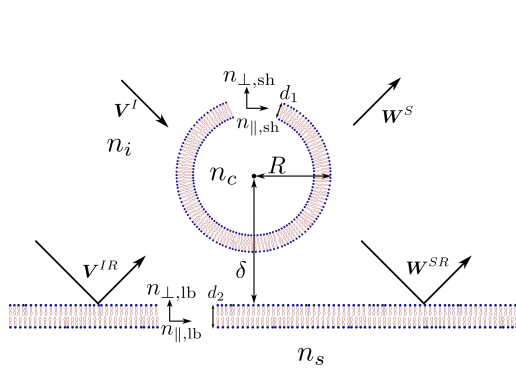


Figure 1.png

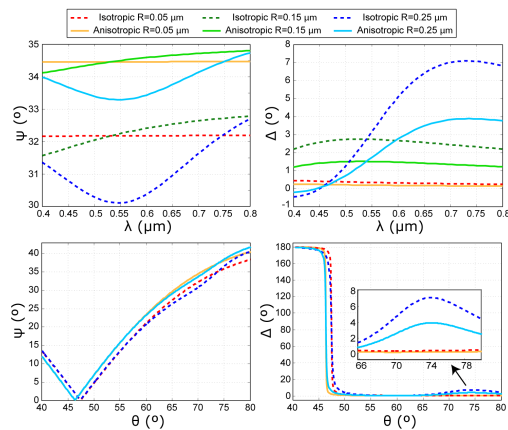


Figure 2.png

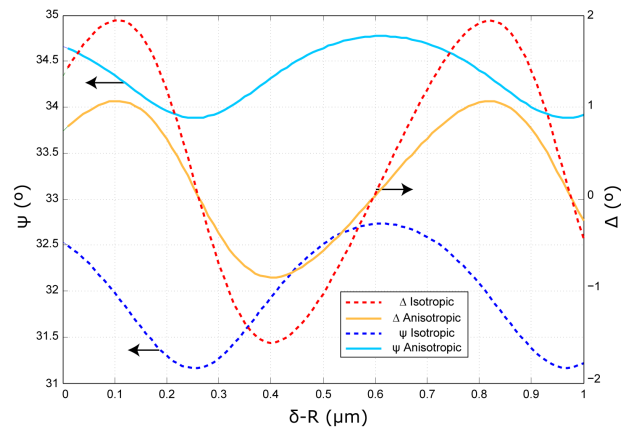


Figure 3.png

Super-resolution imaging of single-molecule DNA interactions with plasmonic nanoparticles

Thursday, 14th September - 17:58 - Nanomedicine - Room 412 - Oral - Abstract ID: 405

***Dr. Adam Taylor*¹, *Dr. Peter Zijlstra*¹**

1. Molecular Biosensing for Medical Diagnostics, Faculty of Applied Physics, Eindhoven University of Technology, P.O. Box 513, 5600 MB, Eindhoven, The Netherlands

Introduction:

Plasmonic nanoparticle-sensors are widely employed to detect analyte binding to receptors on the surface of the particle. The response of a plasmonic sensor strongly depends on the position where an analyte binds due to the spatially heterogeneous near-field. Also, binding kinetics are expected to vary across a nanoparticle surface due to geometry dependent fluid accessibility. It however remains unknown how the location of binding of an analyte correlates with binding kinetics and sensor response.

Method:

Here we employ super-resolution microscopy to establish the location of analyte binding at the single molecule, single-particle level. We use a fluorophore-coupled oligo, which transiently binds to an oligo functionalized gold bipyramid (Fig 1, top) via DNA hybridization. To prevent near-field coupling between the fluorophore and the plasmon resonance we employ a dye (ATTO532, $\lambda_{\text{emission}} = 540 \text{ nm}$) that is spectrally detuned far away from the longitudinal plasmon wavelength ($\lambda_{\text{LSPR}} = 815 \text{ nm}$).

Results:

A resulting time trace showing fluorescence bursts from DNA hybridization events on the surface of a single bipyramid is shown in Figure 1 (middle). Each event is localized, with centroids plotted in Figure 1 as red dots (bottom). The geometry and orientation angle of the underlying nanoparticle is reconstructed by fitting an ellipse to the distribution of localisation coordinates, finding close agreement to dimensions obtained from TEM ($\sim 110 \text{ nm} \times \sim 40 \text{ nm}$ as measured by TEM).

Discussion:

Our approach provides an all-optical method to reconstruct particle geometry. In addition, the localization of each binding event will enable us to establish the connection between binding location, binding kinetics, and sensor response at the single-molecule level. This will further our understanding of nanoparticle-based biosensors and give insight into geometry-dependent interaction kinetics.

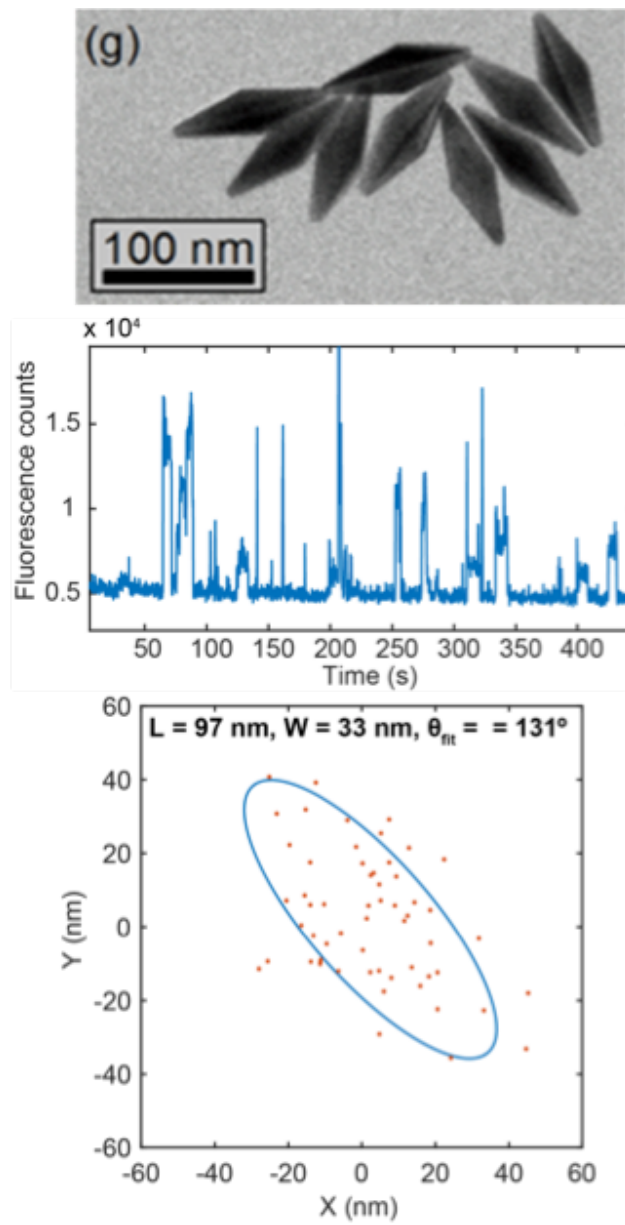


Figure 1.png

Propagation Characteristics of Myelinated and Un-myelinated Nerve Fibres in guiding 200 nm to 2000 nm EM Wave

Thursday, 14th September - 18:15 - Nanomedicine - Room 412 - Oral - Abstract ID: 449

Dr. Enayetur Rahman¹, Dr. Iasonas F. Triantis¹

1. City, University of London

Introduction: Infrared Nerve Stimulation (INS) is becoming popular because of its potential to provide targeted stimulation [1]. Recently it was claimed that myelin sheath can guide light (200nm – 1300nm) [2], however propagation characteristics were not reported for wavelengths $\lambda > 1500\text{nm}$, common in INS [1]. We present them here for λ up to 2000nm for both myelinated and unmyelinated nerve fibres (MNF and UNF).

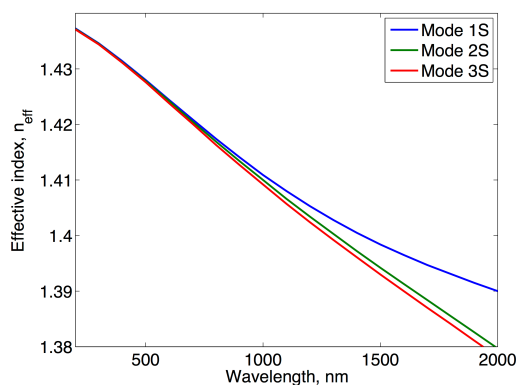
Methods: Maxwell's equations were solved by FDFD (Matlab) on the cross-section of the nerve fibre to obtain its modal characteristics. The effective index (n_{eff}) of the first three modes was evaluated and the single mode operating wavelength range was determined for both MNF and UNF, using a 4 μm diameter axon. The MNF overall diameter was 6.66 μm (StructureNerve). The refractive indices of the fibre cytoplasm, the myelin sheath, and the outside medium were set as 1.34, 1.44 and 1.38 respectively [3].

Results and Discussion: The optical power propagating through UNF is confined by the index of the fibre's cytoplasm (1.38) being higher than its surrounding (1.34). The effective indices of the first three propagating modes were determined and plotted in (PropCharcUnmyelinated) for $200\text{nm} \leq \lambda \leq 2000\text{nm}$. The UNF is single-moded for $\lambda > 1700\text{ nm}$. In the MNF, optical power is confined within the myelin sheath (1.44). The effective indices of the MNF as shown in (PropCharcMyelinated) indicate that it supports more modes than the UNF and the myelin sheath operates in a single-moded condition for wavelengths longer than 1980 nm. This article determines light propagation characteristics of nerve fibres for a range of wavelengths, making it very useful for future INS designs.

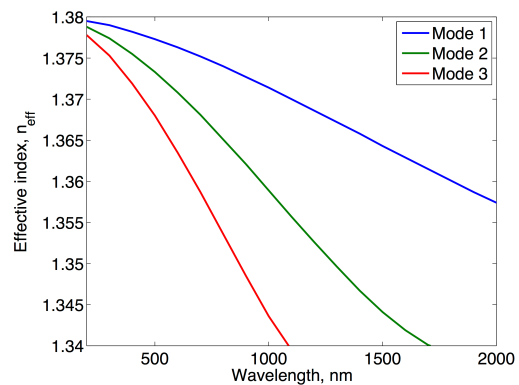
[1] Mou et al. "A Simulation Study of the Combined Thermoelectric Extracellular Stimulation of the Sciatic Nerve of the *Xenopus Laevis*: the Localized Transient Heat Block", IEEE TBME, 59.6 (2012).

[2] Kumar et al. "Possible existence of optical communication channels in the brain" Scientific reports 6 (2016).

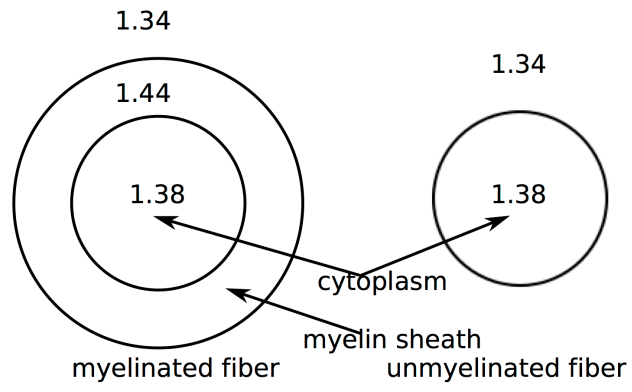
[3] Antonov et al. "Measurement of the radial distribution of the refractive index of the Schwann's sheath and the axon of a myelinated nerve fiber in vivo" J. Applied Spectroscopy 39.1 (1983).



Propcharcmyelinated.png



Propcharcunmyelinated.png



Structurenerve.png

Dielectric and semiconductor nanoantennas

Friday, 15th September - 09:00 - Plenary Speeches - Auditorium - Oral - Abstract ID: 141

Dr. Arseniy Kuznetsov¹

*1. Data Storage Institute, A*STAR (Agency for Science, Technology and Research)*

Over the last decade the research in resonant nanophotonics was mainly focused on metallic nanostructures made out of plasmonic materials such as gold and silver. Plasmonic nanoparticles may provide high field localization and enhancement at their resonances which stimulated a discussion of multiple potential applications of resonant nanophotonics for future technologies. However, at visible and near-IR frequencies these resonances are accompanied by strong Ohmic losses, generating a substantial heat which reduces the stability of plasmonic nanostructures at elevated light intensities and is undesirable for many applications. This significantly limits the areas of practical applications of plasmonics. Recently a new branch of resonant nanophotonics has emerged which has a potential to complement the existing plasmonic approaches and solve the major problem of losses. It is based on optical Mie resonances in high-refractive index dielectric and semiconductor nanoparticles [1]. In contrast to the case of plasmonic nanoparticles, the resonances in high-index dielectric nanoparticles are related to oscillations of bound rather than free charges and thus can be generated without any losses in transparent dielectric or semiconductor materials. In my talk, I will review a recent progress in this rapidly developing field and present several new results from our team revealing the potential of dielectric and semiconductor nanoantennas for various applications. This will include resonant near-field interactions for magnetic and electric near-field concentration, long-range low-loss near-field energy transport and fluorescence enhancement. I will also demonstrate various far-field nanoantenna phenomena related to directional light scattering by single nanoantennas and phased nanoantenna arrays (metasurfaces) whose properties can be precisely controlled by engineering the nanoantenna radiation patterns. In particular I will demonstrate metasurfaces, which can efficiently bend light at extremely high angles (above 80 degrees) and can be used to design visible-range flat lenses with record-high numerical aperture of 0.99. In addition I will discuss different material platforms for dielectric nanoantenna and show how various materials can be used to make active and nonlinear nanoantennas in different spectral ranges.

References:

1) A. I. Kuznetsov et al., "Optically resonant dielectric nanostructures", *Science* 354, aag2472 (2016).

Integrating Nanofluidics with Single Particle Plasmonics

Friday, 15th September - 09:40 - Plenary Speeches - Auditorium - Oral - Abstract ID: 2

Prof. Christoph Langhammer¹

1. Chalmers University of Technology, Department of Physics

The combination of the precise nanoscale mass transport offered by nanofluidics, and the sub-wavelength sensing function provided by a single plasmonic hot spot, creates fascinating opportunities for a range of applications stretching from biosensing and single molecule detection at low concentrations, to single nanoparticle catalysis. In this talk, I will present our efforts towards integrating nanofluidics with single particle plasmonics in these different directions.

Specifically, I will first present our generic platform, which is comprised of nanofluidic channels that are functionalized with single plasmonic nanoantenna sensors and/or catalyst nanoparticles (Figure 1). These structures are locally grown inside the nanofluidic system by means of advanced nanofabrication techniques based on electron beam lithography and reactive ion etching, before sealing with a transparent lid that enables dark-field scattering spectroscopy [1].

For a sensing application in the liquid phase, the dimensions of the nanofluidic system can be tailored such that the entire analyte volume is forced to pass the plasmonic hot spot within the decay length of the near field, thereby significantly enhancing the probability of direct interaction between the sensor surface and the analyte molecules [1].

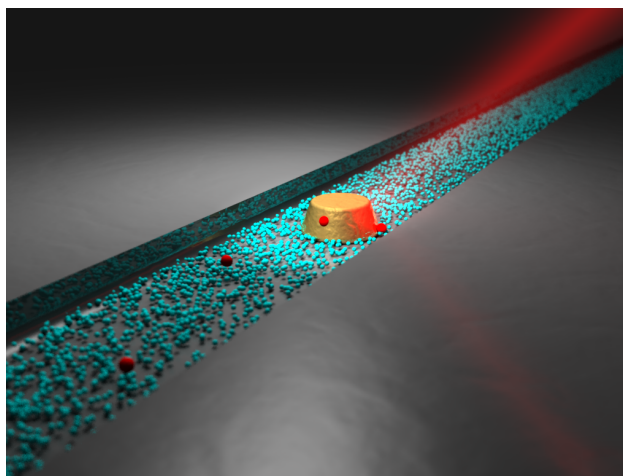
For applications in the gas phase and in heterogeneous catalysis, such a design offers the fascinating prospect of not only addressing individual catalyst nanoparticles by means of plasmonic readout to, for example, derive their hydrogenation [2] or oxidation state [3] *in operando*, but also to use online mass spectrometry connected to the nanofluidic system to analyze reaction products and reaction rates.

In my talk I will illustrate these two applications on specific examples from our recent research, and discuss the potential of nanofluidic devices integrated with single particle plasmonics in a wider perspective by, for example, highlighting the multiplexing potential.

[1] Fritzsche, J., et al. **Nano Letters**, 16 (12), 7857–7864 (2016)

[2] Syrenova, S., et al. **Nature Materials**, 14, 1236–1244 (2015)

[3] Larsson, E.M., et al. **Science** 326, 1091-1094 (2009).



Nanochannel singleau2.png

Exploring the Nanoscale Dynamics of Single Molecules with Optical Microcavities

Friday, 15th September - 10:45 - Plenary Speeches - Auditorium - Oral - Abstract ID: 17

Prof. Frank Vollmer¹

1. Max Planck / University of Exeter

TBA

Metasurfaces with Nonlinear Berry Phases in Space and Time

Friday, 15th September - 11:25 - Plenary Speeches - Auditorium - Oral - Abstract ID: 14

Prof. Thomas Zentgraf¹

1. University of Paderborn

For efficient nonlinear processes, the engineering of the nonlinear optical properties of media becomes important. The most well-known technique for spatially engineering nonlinear properties is the quasi-phase matching scheme for second-order processes like second harmonic generation. However, the widely used technique of periodic polling of natural crystals to obtain quasi-phase matching only provides a binary state for the nonlinear material polarization, which is equivalent to a discrete phase change of π of the nonlinear polarization. A continuous tailoring of the phase of the nonlinear susceptibility would greatly enhance flexibility in the design and reduce parasitic effects.

Here we will discuss a novel nonlinear metamaterial with homogeneous linear optical properties but continuously controllable phase of the local effective nonlinear polarizability. For the demonstration, we use plasmonic metasurfaces with various designs for the meta-atom geometry together with circular polarized light states. The controllable nonlinearity phase results from the phase accumulation due to the polarization change along the polarization path on the Poincare Sphere (the so-called Pancharatnam-Berry phase) and depends therefore only on the spatial geometry of the metasurface. By using a fixed orientation of the meta-atom the nonlinear phase can be spatially arbitrarily tailored over the entire range from 0 to 2π . In contrast to the quasi-phase matching scheme the continuous phase engineering of the effective nonlinear polarizability enables complete control of the propagation of harmonic generation signals, and therefore, it seamlessly combines the generation and manipulation of the harmonic waves for highly compact nonlinear nanophotonic devices. We will demonstrate the concept of phase engineering for the manipulation of second- and third-harmonic generation from metasurfaces and the restriction with respect to symmetry and geometry of meta-atoms. Furthermore, we will discuss a nonlinear Berry phase in the time domain, which arises from the rotational Doppler shift that is observed on spinning objects. Our findings are of fundamental significance in nonlinear optics and for tailored nonlinearities, as they provide a further degree of freedom in the design of nonlinear materials.

Properties of CaF₂ ceramics obtained by Hot Isostatic Pressing

Friday, 15th September - 13:30 - Poster Session - Gallery - Poster - Abstract ID: 416

*Dr. Krzysztof Perkowski*¹, *Dr. Magdalena Gizowska*¹, *Ms. Izabela Kobus*¹, *Dr. Milena Zalewska*¹, *Mr. Gustaw Konopka*¹, *Mrs. Irena Witoławska*¹, *Dr. Marcin Osuchowski*¹

1. Institute of Ceramics and Building Materials

Introduction

Calcium fluoride has a lot of attributes, which caused it is very attractive material for laser application. It characterizes a very good transparency in wide range of electromagnetic radiation, from UV to IR. Additionally, calcium fluoride emits a low photon energy, which prevents an overheating during the laser pumping process.

Methods

Samples were obtained by using two commercial powders of calcium fluoride: C1-Sigma-Aldrich with an average particle size of 20 μm and C2-provided by ABCR with an average particle size of 8 μm. Ytterbium fluoride was added to the powder of calcium fluoride as a source of active ions. Specimens were sintered in temperature range 900 - 1350°C in vacuum. Additionally samples were densificated by hot isostatic pressing under conditions: 2000 bar and 1300°C. The microstructure of specimens was observed using electron microscopy. Qualitative phase analysis was carried out with the use of X-ray diffraction method. Absorbance of CaF₂ sample was measured by spectrophotometer Varian Cary 500. Fluorescence emission was measured by spectrometer SPEX 270M.

Results

XRD analysis confirmed that both powders contains only cubic phase, fig.1. The differences between materials were noticed during thermogravimetric analysis, fig.2. Powder provided by ABCR has contaminations which were analyzed as residual carbon. On basis of SEM CaF₂ sample images it was found that surface was free from macro porosity. On the surface of CaF₂ samples with 2%Yb it can be observed occurrence of porosity, fig.3. Fig. 4. shows cooperative optical process in cluster of Yb³⁺ ions at 504nm. Additionally, we can observe upconversion process $^2H_{11/2} \rightarrow ^4I_{15/2}$ at 516 and 526 nm for Er³⁺ ions, which contaminate of ytterbium fluoride. Luminescence of Yb³⁺ ions are presented at 1030nm.

Discussion

Porosity of calcium fluoride doped Yb ions sample is undesirable for laser materials and further works were focused on elimination of microstructure defects. Basis on fluorescence spectra it can be assumed that ions of ytterbium were incorporated in the crystal lattice of calcium fluoride or ions of calcium were substituted by ytterbium ions.

Acknowledgement

This work was funded by the Polish Ministry of Science and Higher Education.

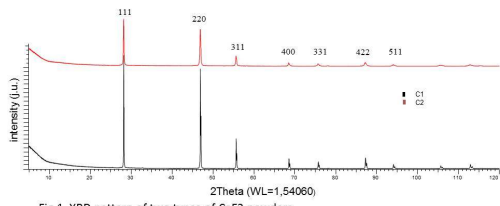


Fig 1. XRD pattern of two types of CaF₂ powders.

Fig 1.jpg

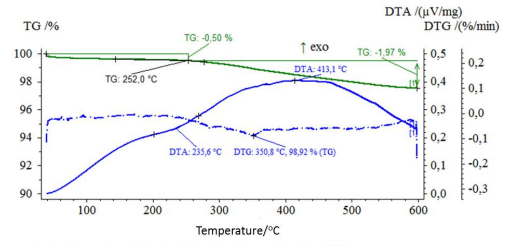


Fig 2. Thermal analysis of calcium fluoride provided by ABCR.

Fig 2.jpg

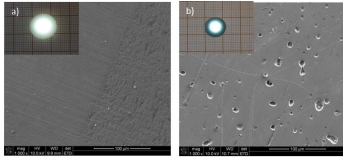


Fig.3 SEM images of the polished surface of calcium fluoride samples and samples illuminated by diode
a)C1-CaF₂ b) C1-CaF₂ with 2%Yb

Fig 3.jpg

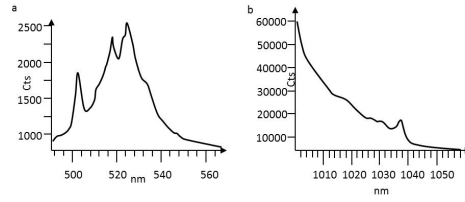


Fig. 4. Fluorescence spectra of calcium fluoride doped 2%Yb a) visible range b) infrared range

Fig 4.jpg

Optical bound state in the continuum in the one-dimensional photonic structures: transition into a resonant state

Friday, 15th September - 13:30 - Poster Session - Gallery - Poster - Abstract ID: 446

*Ms. Zarina Sadrieva*¹, *Mr. Ivan Sinev*¹, *Mr. Kirill Koshelev*¹, *Dr. Anton Samusev*¹, *Dr. Osamu Takayama*², *Dr. Radu Malureanu*³, *Dr. Andrey Bogdanov*¹, *Prof. Andrei Lavrinenko*⁴

1. ITMO University, 2. Department of Photonics Engineering, Technical University of Denmark, 3. Department of Photonics Engineering, Technical University of Denmark, 2800 Kongens Lyngby, Denmark, 4. Technical University of Denmark; ITMO University

Introduction.

Optical bound states in the continuum (BIC) are localized states with energy lying above the light line and having infinite lifetime. Any losses taking place in real systems result in transformation of the bound states into resonant states with finite lifetime.

In this work we analyze transformation of BIC into a resonant state due to surface roughness and leakage into substrate in a grating based on silicon-on-insulator wafer.

Results and discussion.

Since the array is periodic in the x-direction, the eigenstates of the structure are characterized by the frequency f , the wave vector along the bars k_y and by the Bloch quasi-wave vector k_x restricted to the 1st Brillouin zone. For the proposed design, BIC occurs when the k_y component of wave vector is zero.

We consider two cases: (i) 'ideal', because it describes a periodic array in silica medium; (ii) 'practical' with a silicon substrate and surrounding air. For 'ideal' case, the calculated dispersion curves of the three lower TE modes are shown in Fig. 1(d). One can see from Fig. 2(b,e) that the Q-factor of the TE₁ mode tends to infinity at Γ -point of k -space (normal incidence) and field become perfectly confined in grating.

For the 'practical' case, the substrate weakly affects the position of the eigenmode, but results in leaky losses. It might seem that substrate should not destroy the at- Γ BIC since it is protected by in-plane symmetry which is not broken by the substrate. However, it is true only for the subwavelength regime when higher diffraction channels are closed. In our case, evanescent fields of the at- Γ BIC transform in the silicon substrate to propagating waves and BIC becomes a resonant state.

Another inherent feature of experimental samples is surface roughness, which leads to parasitic loss via scattering. Figure 3 shows how two concurrent loss mechanisms – scattering due to surface roughness and leakage into substrate – contribute to the suppression of the resonance lifetime and specify the condition when one of the mechanisms becomes dominant.

To confirm results experimentally, we fabricated a grating from SOI and performed angle-resolved reflectivity measurements.

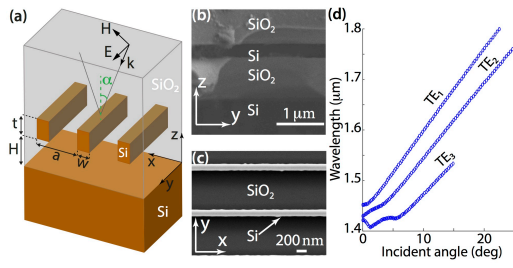


Figure1.jpg

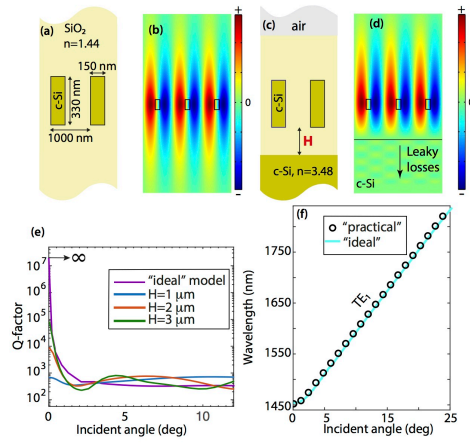


Figure2.jpg

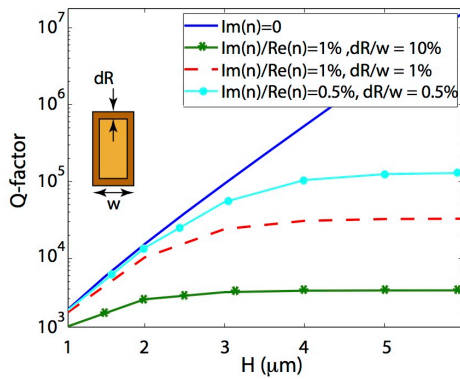


Figure3.jpg

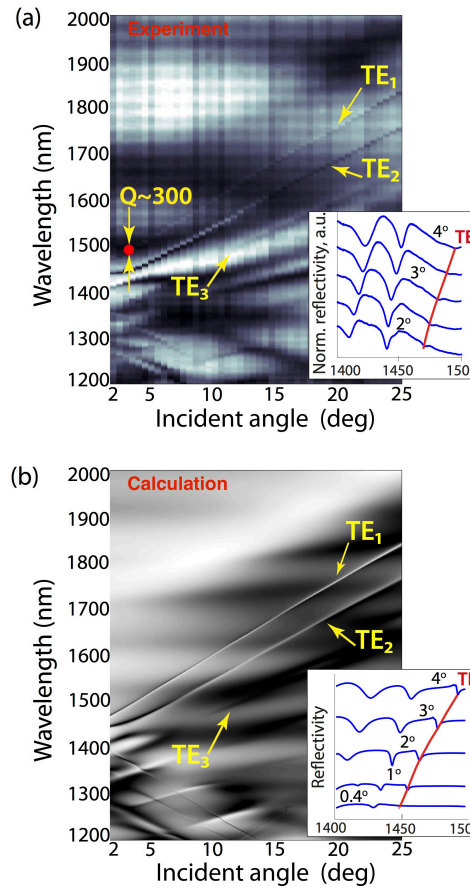


Figure4.jpg

Plasmonic nanohole arrays with thermo-responsive hydrogel for flow-through biosensor

Friday, 15th September - 13:30 - Poster Session - Gallery - Poster - Abstract ID: 452

Mrs. Daria Kotlarek¹, Dr. Jakub Dostalek¹

1. Biosensor Technologies, AIT-Austrian Institute of Technology GmbH

Optofluidics has facilitated rapid and sensitive molecule detection in real time by integrating microfluidics with optical sensing systems [1]. In the typical optofluidic device a sample is flowed over the surface that is functionalized with receptors specific to target analyte. In consequence, the capture of target molecules on the surface is limited by the mass transport that mainly depends on diffusion. In order to overcome mass transport limitations, perforated metallic films have been used in a flow-through format, in which the analyte solution is transported internally through the pores [2-3]. However, existing solutions such as suspended nanohole arrays rely on expensive, low throughput and time-consuming methods including focused ion beam, electron beam lithography and photolithography. These systems offer only a static design and are susceptible to the hydrodynamic deformation due to applied pressure [4].

In order to address these problems, we present a novel system composed of gold nanohole arrays (Au NHAs) with thermo-responsive hydrogel that accommodates array of gold nanodisks for operation in a flow-through format. The Au NHAs were fabricated on permeable substrate by accessible and cost-effective nanoimprint lithography (NIL) combined with template stripping. The nanostructures were subsequently characterized by microscopy and transmission wavelength spectroscopy. In the presented system the transport of the sample is driven by capillary forces and a hydrophilic nature of the porous substrate, improving the efficiency of target delivery to the receptor layer. Furthermore, the thermo-responsive hydrogel empowers the actuation of the optical properties by small changes around *lower critical solution temperature*.

The Au NHAs presented herein offer rapid and sensitive detection of molecules and hold potential to serve as a cost-effective single-step diagnostic device.

1. Fan, Xudong, and Ian M. White. "Optofluidic microsystems for chemical and biological analysis." *Nature photonics* 5.10 (2011): 591-597
2. Eftekhari, Fatemeh, et al. "Nanoholes as nanochannels: flow-through plasmonic sensing." *Analytical chemistry* 81.11 (2009): 4308-4311
3. Yanik, Ahmet Ali, et al. "Integrated nanoplasmonic-nanofluidic biosensors with targeted delivery of analytes." *Applied physics letters* 96.2 (2010): 021101.
4. Tu, Long, et al. "Study of flow rate induced measurement error in flow-through nano-hole plasmonic sensor." *Biomicrofluidics* 9.6 (2015): 064111

Powerful Laser Diode Matrixes for Active Vision Systems

Friday, 15th September - 13:30 - Poster Session - Gallery - Poster - Abstract ID: 65

Mr. Denis Shabrov¹, Dr. Boris Kuntsevich¹

1. Institute of Physics NAS of Belarus

The results of investigations of the matrix of powerful laser diodes (MLD) with quantum well active layer are discussed in this report. Along with creation of MLD with the given parameters and the high operation resource the supply and control electronics units, including the thermostabilizing, ensuring reliable functioning of the semiconductor laser module, were developed.

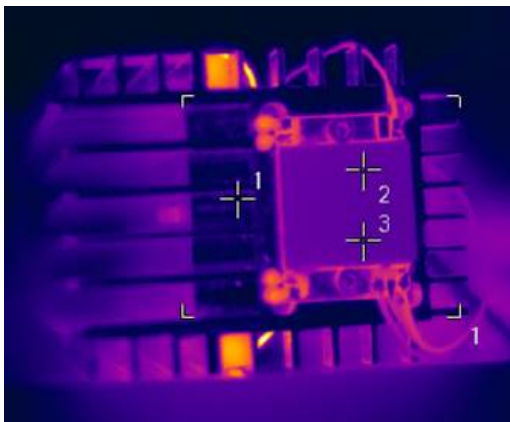
The matrix of laser diodes SLMP-6NP-845N was produced by JSC "Inject" (Russia) based on AlGaAs/GaAs heterostructure. The MLD lasing wavelength is in the vicinity of 846 nm. The spectral width of radiation is 6 nm. The operation temperature is of 30 ± 0.5 °C.

The mirror sides of crystals of laser diodes (cavity mirrors) were created by the method of electron beam evaporation in vacuum. The received reflection coefficients are 25% and 98% for output and high reflective mirrors, respectively.

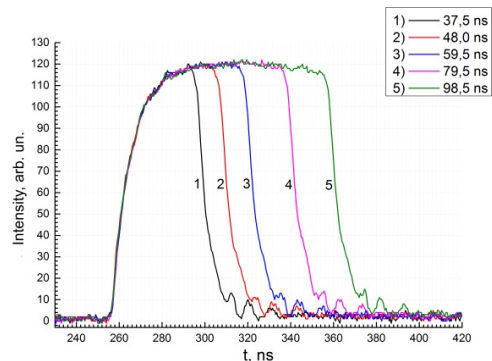
The pulse front of the laser radiation of the MLD reaches 83% of its maximum intensity for the first 12 ns and 100% for 30 ns. At the stage of its switching off, intensity sharply falls approximately through 15 ns. The described behavior is realized for pulses with duration from 35 to 100 ns. Maximal average power of the laser radiation of MLD linearly increases with increase in pulse repetition rate.

Temperature on the matrix surface and heat sink temperature differs on 5°C that demonstrates stable operation of elements of Peltie. However the main contribution to heat-up of the heat sink and air was entered by two resistors connected to both stacks of the matrix sequentially, but this fact doesn't influence on stable operation of the module of laser illumination.

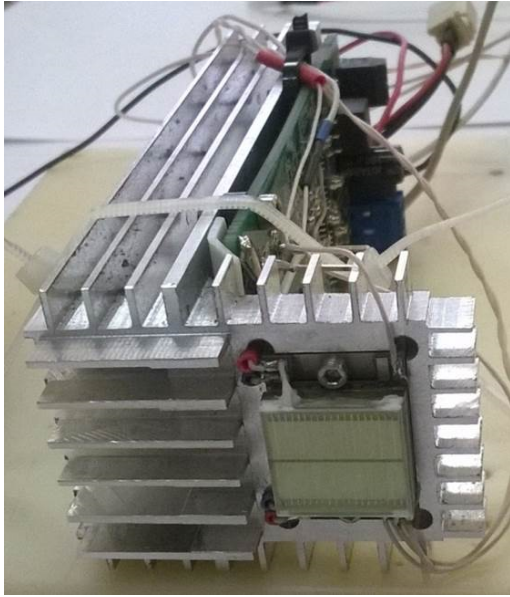
Thus, for effective operation of illumination module based on matrix of powerful laser diodes it is necessary to decrease the temperature gradient near the MLD, which can be done by mounting the resistors and matrix on a general radiator using external culling such as element of Peltie. It was ascertained that an increase in radiation pulse repetition rate from 0.5 to 10 kHz and corresponding change of the power operation mode doesn't influence on the divergence of output radiation of the MLD.



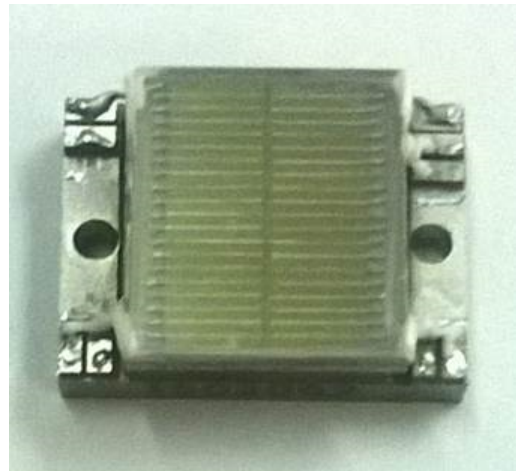
Distribution of temperature on the pulse illumination block.png



Forms of the laser radiation pulse of slmp-6np-845n f 1 khz..png



The pulse illumination block.png



Matrix of laser diodes slmp-6np-845n.png

Numerical investigation of plasmonic metasurfaces for improved MIR absorption

Friday, 15th September - 13:30 - Poster Session - Gallery - Poster - Abstract ID: 80

Dr. Roxana Tomescu¹, Dr. Cristian Kusko¹, Dr. Mihai Kusko²

1. National Institute of R&D in Microtechnologies - IMT-Bucharest, 2. National Institute of R&D for Microtechnologies - IMT-Bucharest

Plasmonic metasurfaces represent a new type of metamaterials which present a large variety of applications. An important use of these structures is focused on absorption increase in the mid infrared domain in a way that one can obtain approximately total absorption on narrow wavelengths intervals. Essentially, the absorption as well as the emissivity of a plasmonic microstructured metasurface can be precisely controlled in a well defined spectral domain by the geometrical parameters of the plasmonic elements of the array [Appl. Phys. Lett. 100, 203508 (2012), Phys. Rev. Lett. 107, 045901 (2011)].

We present a class of plasmonic metasurfaces modeled for achieving an almost total absorption on narrow wavelengths intervals in MIR domain. Our metamaterial is obtain by micro-structuring an array of gold (Au) pillars of 200 nm high on a 200 nm thick silicon (Si) deposited on a thin gold film (200 nm). We performed 3D numerical investigation using finite differential time domain (FDTD) investigating the dependence of the absorption spectrum as a function of the metasurface geometrical and material parameters (Fig.1). We conclude that this type of structure improves the electromagnetic field absorption almost to unitary values for several well defined narrow wavelengths intervals.

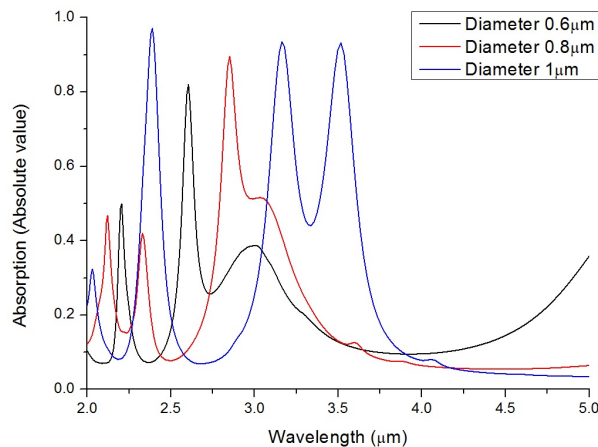


Fig 1 absorption as a function of wavelength for various dimensions of nano-antennas in a metasurface.jpg

Application of luminescent converters for the correction of the spectra of white LEDs

Friday, 15th September - 13:30 - Poster Session - Gallery - Poster - Abstract ID: 444

*Dr. Piotr Pershukevich*¹, *Dr. Pavich Tatsiana*¹, *Dr. Viktoria Lapina*¹

1. The Institute of Physics of NAS Belarus

Introduction.

The growing use of highly efficient blue light-emitting diodes (LEDs) in lighting the premises requires the correction of the primary emission spectra, most prominently, for light-hygienic reasons. Indeed, spectra of the LED sources, particularly, of the ones with a color temperature of 6500 K, are overloaded with a dark-blue component, which affects circadian rhythms and have adverse consequences for the eyes.

Materials: Luminophores (luminescent converters, LC) were used in the work: coumarin 334 (C334), coumarin 343 (C343) and surfactants: Brij 35 (B35), Triton X 100 (T100), Tween 40 (T40) «Sigma-Aldrich».

Methods: Fluorescence spectra (FS), fluorescence excitation spectra (FES), fluorescence quantum yields φ_F were measured on a retrofitted SDL-2 (LOMO, Soviet Union) spectroscopic unit, which consisted of an MDR-12 excitation monochromator and an MDR-23 registration monochromator.

Results:

The peak of the white light LED is in the center of the phosphor excitation (absorption) band, and the spectral dip in the emission spectrum of this LED coincides with the maximum of the fluorescence spectrum of the phosphor (Fig. 1). It can be seen from Fig. 2 that the blue band ~ 450 nm is significantly weakened in the total spectrum obtained after superimposing the polymer film on the LED, owing to the phosphor absorption, and instead of the spectral “dip” of ~ 480 nm, a steep slope of the rising radiation band (460–485 nm).

- Fig 1. Comparison: of FES (1, 2) and FS (3, 4) coumarin 334 (1, 3) and coumarin 343 (2, 4) in the matrix of PC with T40 as a detergent ($I_{\text{mon}} = 505$ nm; $\lambda_{\text{exc}} = 420$ nm); spectra of a LED lamp with a color temperature of 6500 K (5).
- Fig. 2. Normalized spectra of a LED lamp with a color temperature of 6500 K without LC (1) and with LC based on C334 (2) and C343 (3) in PC with T40 as a detergent.

Conclusion: The principal possibility of target correction of the emission spectra of LED lamps by means of luminescent converters based on luminophores in a polymer matrix is demonstrated.

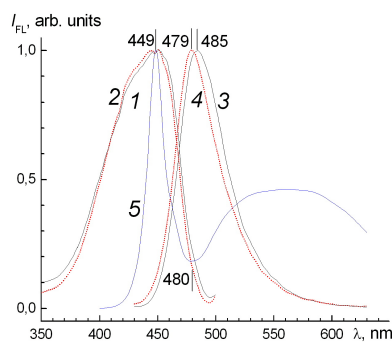


Fig1.jpg

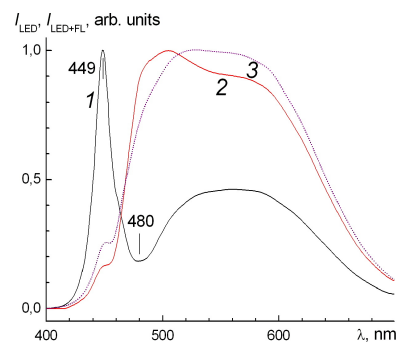


Fig2.jpg

Fabrication and characterization of plasmonic gold Sierpinski nanocarpets

Friday, 15th September - 13:30 - Poster Session - Gallery - Poster - Abstract ID: 119

*Mr. Nikhil Santh Puthiya Purayil*¹, *Dr. Francesco De Nicola*¹, *Mr. Mario Miscuglio*¹, *Dr. Davide Spirito*¹, *Dr. Andrea Tomadin*¹, *Dr. Francesco Tantussi*¹, *Dr. Francesco De Angelis*¹, *Dr. Marco Polini*¹, *Dr. Roman Krahne*¹, *Dr. Vittorio Pellegrini*¹

1. Istituto Italiano di Tecnologia, Genova

Deterministic fractals [1] are self-similar objects generated by geometrical rules having non-integer dimensionality and exhibiting non-discrete Fourier spectra [2]. The multi-scale property of fractals can be exploited to realize broadband spectral response in engineered nanostructures [2,3]. Tunable plasmonic near-field enhancement at multiple frequencies inspires realization of novel structures with potential applications in multi-band antennas [4], bio/chemical sensors [5], solar cells [6], and photodetectors [7]. We present fabrication, optical characterization and finite-difference time-domain simulation of gold plasmonic nanostructures arranged in Sierpinski carpet (SC) fractal [1,4], and propose their application in surface enhanced Raman spectroscopy (SERS) and localized surface plasmon resonance sensing.

Gold SCs were realized starting from a unit cell of side L that is divided into a 3×3 array of sub-cells scaled by $L/3$, with a gold square replacing the central sub-cell. Recursively applying the same rule to each generated sub-cells, fractals of higher orders were obtained. Employing electron beam lithography, evaporation, and lift-off, we fabricated first five orders of gold SCs with element size ranging from $3 \mu\text{m}$ to 40 nm and thicknesses $25\text{-}45 \text{ nm}$ on CaF_2 and Si substrates. In addition, we fabricated periodic arrays of squares with size and period corresponding to the different orders of the SC.

We observed by Fourier transform infrared spectroscopy, a broadband plasmonic response from visible to mid-infrared range, exhibiting a fractal spectrum with multiple resonances. The electric field enhancement was investigated by SERS measurements carried out on SCs coated by Brilliant Cresyl Blue dye. Our results are in good agreement with the electromagnetic simulations.

References:

- 1) B.B. Mandelbrot, *The fractal geometry of nature* (W.H. Freeman, San Francisco, 1983).
- 2) L. Dal Negro & S. Boriskina, *Laser & Photonics Reviews* 6 (2011).
- 3) G. Volpe et al., *Optics Express* 19 (2011).
- 4) T. L. Chen et al., *New J. Phys.* 16, 1-13 (2014).
- 5) E. Aslan et al., *ACS Photonics* 3.11, 20102-20111 (2016).
- 6) L. Zhu et al., *Optics Express* 21.103, A313-A323 (2013).
- 7) J. Fang et al., *Nano Letters* 17, 57-62 (2017).

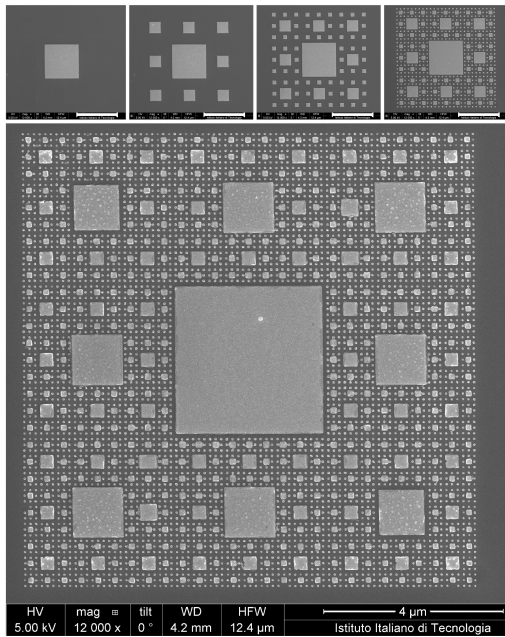


Fig1 sem of fabricated scps.jpg

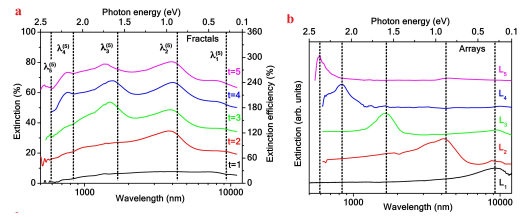


Fig 2 extinction spectra of au scs for 1-5 orders and au periodic arrays.jpg

Evaporated anisotropic nano-structured coatings for polarization control in high-power lasers

Friday, 15th September - 13:30 - Poster Session - Gallery - Poster - Abstract ID: 198

Ms. Lina Grinevičiūtė¹, Mr. Laurynas Petronis¹, Dr. Rytis Buzelis¹, Dr. Tomas Tolenis¹

1. Center for Physical Sciences and Technology

Optical elements for polarization control are one of the main parts in advanced laser systems. The state and intensity of polarized light is typically controlled by optical elements, namely waveplates and polarizers. At high powers, both elements suffer low resistivity to laser radiation. Also, standard waveplates, made from solid or liquid crystals, are fragile and difficult to use in small systems, while Brewster-type polarizers leads to light beam displacement in the optical path. Introducing optical anisotropy to thin film coating structures allows to control the polarized light, therefore, evaporated optical elements do not indicate earlier mentioned drawbacks. In this work serial bi-deposition technique was employed to form nano-structured anisotropic layers evaporating amorphous silica material. Placing the substrate at glancing angle self-shadowing effect is induced, which causes the growth of columnar nano-structure with elliptical shape cross-sections. Anisotropic properties can be improved by rotating the substrate half-turn around surface normal every 5 seconds. Principal illustration and SEM image of anisotropic and dense layers are shown in Fig.1. Combination of porous birefringent and dense isotropic thin films was used to form two spectrally separated Bragg reflection zones for perpendicular polarizations (S-parallel to shadowing direction and P-perpendicular to it). Modeled spectrum of multi-layer design of normal incidence polarizer is shown in Fig.2. Marked transmission district perfectly indicates polarizer properties: high transmission for one polarization, and high reflection for perpendicular polarization. Furthermore, the combination of birefringent nano-structured and isotropic layers allows to form highly transparent ($T \sim 99\%$) waveplates. Both optical elements can be manufactured using only one material by changing only its structural morphology. In this work, silica material was used, which has wide band gap and, therefore, high resistivity to laser radiation in UV region. Optical resistance was tested by measuring laser induced damage threshold of both optical elements at the wavelength of 355 nm in ns regime. Full scale investigation was accomplished to determine optimal optical and structural characteristics of anisotropic nano-structured and isotropic dense silica layers. A novel approach was shown that the combination of both morphologies allows to produce polarizers and waveplates with superior resistivity to laser radiation.

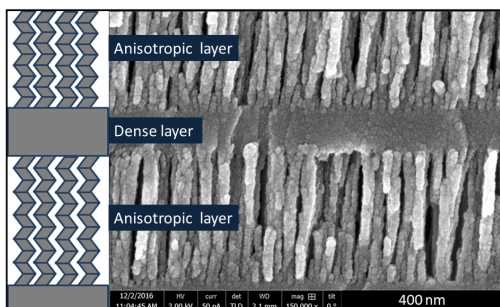


Fig.1 principal illustration and sem image of anisotropic and dense layers.png

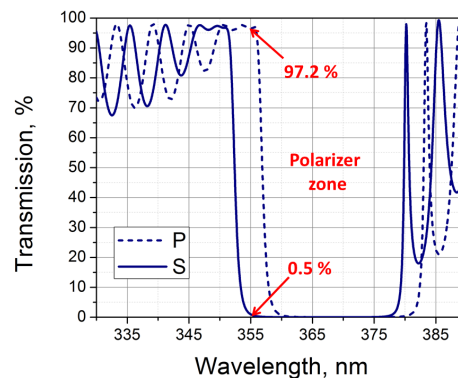


Fig.2 modeled spectrum of multi-layer design of normal incidence polarizer.png

Structural and optical properties of silver-doped gold clusters AgAu_{n-1} (n=1-8): a comparison with pure gold clusters

Friday, 15th September - 13:30 - Poster Session - Gallery - Poster - Abstract ID: 35

Dr. Mohand Akli TAFOUGHALT¹

¹. Faculty of Technology, University A Mira Béjaia

The structural and optical properties of silver-doped gold clusters AgAu_{n-1} (with n=1-8) have been systematically investigated using *ab. initio* method. The structural properties of the ground-states are calculated within the framework of density functional theory using Wu and Cohen generalized gradient approximation functional in the SIESTA code and the optical properties within the framework of TD-DFT using OCTOPUS code.

By substitution of Ag atom, in the optimized lowest energy structures of pure gold clusters, the obtained lowest energy structures resemble the ground-state configurations of the pure gold clusters Au_n in which the Ag atom prefers to occupy higher coordination sites. The calculated binding energies, second-order differences in energies, dissociation energies and HOMO-LUMO energy gaps show pronounced odd-even oscillating behaviors, indicating that clusters with even number of atoms keep a higher relative stability than their neighboring odd-numbered ones. Particularly, the cluster AgAu₅ shows the strongest stability.

The analysis of the calculated absorption spectra shows that in the 1.5-6 eV energy range, the number of transitions in clusters with an odd number of gold atoms is greater than in clusters with an even number. Furthermore, the intensity of transitions is more important in clusters having an even number of Au atoms. The incorporation of Ag atom in the pure gold clusters induces a tightening of the transitions and a shift towards the high energies. This is manifested by the decrease in the intensity of the peaks.

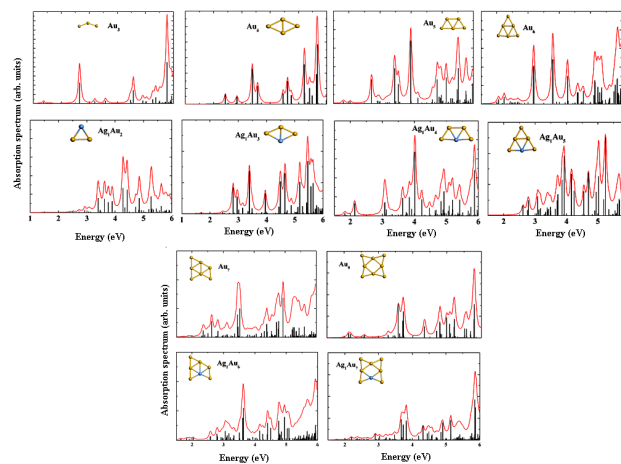


Image.png

Hydrogel-based plasmonic sensor system

Friday, 15th September - 13:30 - Poster Session - Gallery - Poster - Abstract ID: 98

***Mr. Christoph Kroh*¹, *Mr. Roland Wuchrer*², *Dr. Margarita Günther*¹, *Prof. Gerald Gerlach*¹, *Dr. Thomas Härtling*¹**

1. TU Dresden, 2. Fraunhofer Institute for Ceramic Technologies and Systems IKTS

For in-line process monitoring in the fields of water treatment, biotechnology, food and pharmacy industry it is necessary to evaluate several parameters in liquids such as pH, temperature, ethanol-, sugar- or salt concentrations. One approach to tackle the challenge of in-line measurements is the integration of hydrogels on optical sensors. At the Fraunhofer Institute of Ceramic Technologies and Systems a robust optical sensor, based on a plasmonic gold nanostructure, is currently under development. The nanostructure is fabricated by means of nanoimprint-lithography (NIL). The patterning of the sensor substrate makes it possible to excite surface plasmons in the metal layer with light under normal incidence.

It is well known that the spectral transmission properties of the gold nanostructure depends on the refractive index of the surrounding. The concept of using plasmonic sensors with analytically sensitive hydrogels offers an opportunity for an inexpensive and robust system for in-line measurements. Hydrogels change their swelling state with varying values of the parameters listed above. Swelling and deswelling results in a change of the (effective) refractive index. As very thin hydrogel layers (well below 1 μm thickness) can be applied on the gold nanostructure, the diffusion-controlled hydrogel swelling process can fast and, hence, the sensor response time will be short (in the range of seconds).

Initial studies for this concept were carried out with pH-sensitive hydrogels and first results on the pH sensitivity are presented in our contribution which allow us to demonstrate the working principle.

Synthesis of meta-atoms and bottom-up fabrication of three-dimensional plasmonic nanostructures

Friday, 15th September - 13:30 - Poster Session - Gallery - Poster - Abstract ID: 100

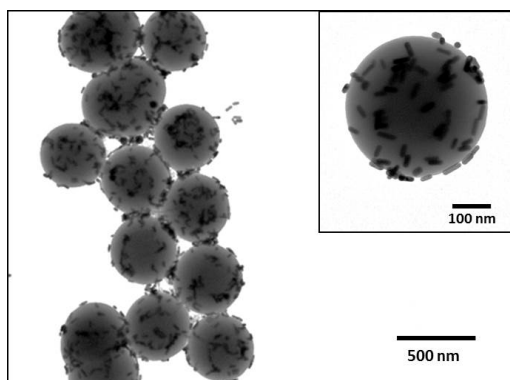
*Ms. Rossella Grillo*¹, *Prof. Thomas Buergi*¹

1. University of Geneva

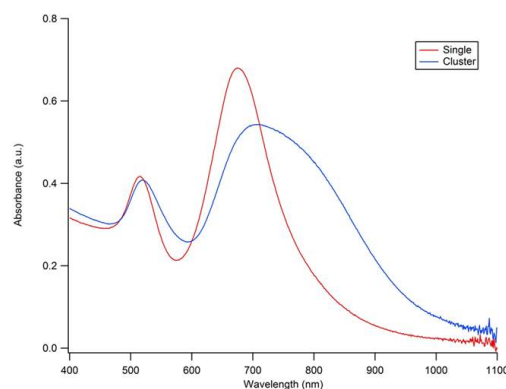
Spherical arrangements of metallic nanoparticles, defined as core-shell nanoclusters, have obtained intense interest in the metamaterials community as they have highly tunable optical properties [1]. It has been proposed that they allow advancements towards materials with double negative properties [2]. Furthermore, they exhibit a strong isotropic magnetic response [3]. The fabrication of these structures is flexible with the possibility to tune the architecture and consequently the optical properties. The key ingredients to achieve such materials are meta-atoms. Other forms such as nanorods provide considerable advantages over the more basic spherical particles due to the introduction of anisotropy, the enhanced extinction coefficients and the wide range of tunability of the longitudinal plasmon resonance. Metal nanoparticles with anisotropic shape have various interesting optical properties, for the reason that the surface plasmon resonance bands split up for orientations along major and minor axes. Moreover, anisotropic metal particles show enhanced nonlinear response [4] when compared to spherically shaped particles, and may thus be used as building blocks in a variety of optical devices. Using bottom-up technique, three-dimensional plasmonic nanostructures were synthesized and characterized. Such structures are sufficiently small to be perceived as an individual object in the far field and exhibit strong and isotropic magnetic response in the visible spectral domain.

References

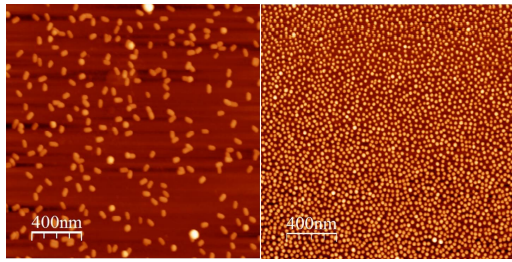
- [1] Shalaev, V.M., Optical negative-index metamaterials. *Nat. Photonics* 1, 41(2006).
 [2] C.R. Simovski, S.A. Tretyakov, Model of isotropic resonant magnetism in the visible range based on core-shell clusters. *Phys. Rev. B* 79(4), 045111 (2009).
 [3] S. Mühlig et al., Self-assembled plasmonic core-shell clusters with an isotropic magnetic dipole response in the visible range. *ACS Nano* 5(8), 6586–6592 (2011).
 [4] K. P. Yuen, M. F. Law, K. W. Yu, P. Sheng, Optical nonlinearity enhancement via geometric anisotropy. *Phys. Rev. E* 56, 1322 (1997).



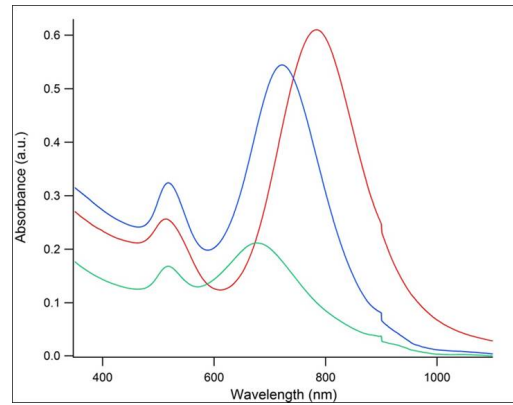
Gold nanorods coated silica spheres.jpg



Measured extinction spectra of the core-shell nanoclusters and of the single gold nanorods.jpg



Afm imaging of gold nanorods and gold nanoparticles deposited on glass.jpg



Extinction spectra of gold nanorods with different aspect ratio.jpg

GaN/AlN Interface Characteristics in Presence of Point Defects

Friday, 15th September - 13:30 - Poster Session - Gallery - Poster - Abstract ID: 213

***Dr. Yahor Lebiadok*¹, *Dr. Tatsyana Bezyazchnaya*², *Dr. Ivan Alexandrov*³, *Dr. Konstantin Zhuravlev*³**

1. SSPA "Optics, Optoelectronics & Laser Technology", 2. Institute of Physical Organic Chemistry, 3. Rzhanov Institute of Semiconductor Physics

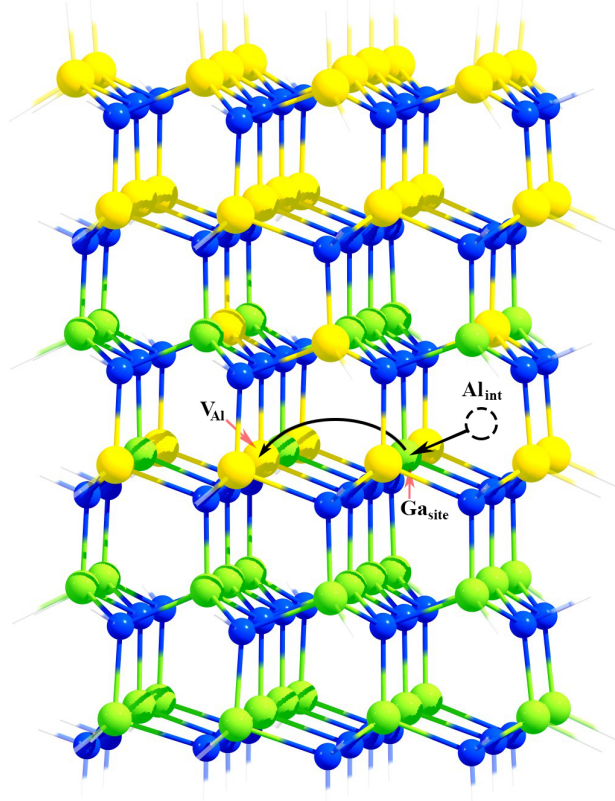
The geometry of point defects in the GaN/AlN interface was calculated in the framework of the cluster approach. The calculations were carried out using two methods: first-principles Hartree-Fock method and the density functional theory with the hybrid functionals B3LYP. This calculation method was realized with the software package GAMESS. The model cluster of GaN/AlN heterointerface with the mixing of gallium and aluminum atoms in the range of 0 – 100 % is under consideration (see Figure).

The comparison of the calculated Ga-Al bond lengths was carried out with the experimental data obtained using EXAFS spectroscopy for GaN/AlN heterostructures. As it follows from the preliminary comparison the bond lengths calculated using the quantum-mechanical first-principles Hartree-Fock method of the self-consistent field are in good agreement with experimental data as opposed to the bond lengths calculated using the density functional theory with the hybrid functionals B3LYP in a combination with Hay-Wadt effective core potentials. As follows from the comparison of calculated and experimental data the most probable locations of nitrogen vacancy in the vicinity of GaN/AlN interface are the location in the GaN/AlN interface and the location in the first Ga layer in respect to the GaN/AlN interface. So, the presence of nitrogen atom vacancy in the heterointerface does not influence on the Al and Ga contacting layers intermixing.

Another types of point defect and structure parameters are discussed in the report.

This work was partially supported by BRFFR, grant F17RM-024

Relaxation path of complex defect
aluminum vacancy + interstitial aluminum atom



1.jpg

Microstructure control of yttria nanopowders obtained by solution combustion synthesis

Friday, 15th September - 13:30 - Poster Session - Gallery - Poster - Abstract ID: 299

*Dr. Magdalena Gizowska*¹, *Ms. Izabela Kobus*¹, *Dr. Krzysztof Perkowski*¹, *Dr. Milena Zalewska*¹, *Mr. Gustaw Konopka*¹, *Mrs. Irena Witosławska*¹, *Dr. Marcin Osuchowski*¹

1. Institute of Ceramics and Building Materials

Introduction

Yttria nanoparticles gained on interest in recent years due to unique properties of doped yttria luminescent particles. The efficiency of luminescence phenomena depends on morphology, particle size, crystallinity of the nanopowder. Solution combustion synthesis (SCS), which is based on the high energy reaction between the metal nitrates and reducing agent, is a promising method for fabrication of nanopowders. Unlike sol-gel or precipitation technique it is less time consuming and requires less technological steps, as the synthesis by-products undergo thermal decomposition.

In the work the relationship between the reaction path with four various reducing agents added in stoichiometric amounts on the morphology of the obtained yttria nanopowder was investigated.

Methods

Thermogravimetric analysis was carried out using thermal analyser TG449 F1 Jupiter (Netzsch Gerätebau GmbH, Germany) in alumina crucibles in argon flow. The powders microstructure was characterized by means of scanning electron microscopy (Nova NanoSEM 200, FEI Company).

Results

Glycine, urea, malonic acid and citric acid were tested as reducing agent for fabrication of $n\text{Y}_2\text{O}_3$. In Fig. 1-4 the results of thermal analysis and micrographs of the obtained powders are presented.

Powders produced with malonic and citric acid have highly porous structure (Fig. 1, 2). After calcination the powder remain in a shape of agglomerates. Reaction of yttrium nitrate with urea (Fig. 3) leads to production of powder in form of platelet. After calcination at temperature of 1100°C nanosized grains are reviled.

Only reaction with glycine (Fig. 4) leads to fabrication of Y_2O_3 without calcination step. Thus obtained powder has highly porous microstructure. After calcination at temperature of 1100°C nanosized grains are visible.

Discussion

All reactions are connected with evolution of big amounts of gases (about 30 mol_{gas}/1 mol_{prod.}) which is supposed to destroy the internal structure of produced oxide to nanopowders. Utilization of substances with carboxyl groups which can create complex compounds with yttrium ion lead to fabrication of porous and spongy ("sponge-like") structures. Using urea, which interaction in the solution with yttria ion is less significant, powders of platelet-like structure are obtained.

Acknowledgement

This work was funded by the Polish Ministry of Science and Higher Education.

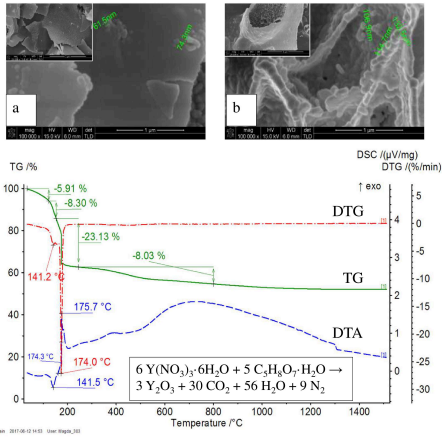


Fig. 1: Thermal analysis of yttrium nitrate and citric acid solution; micrographs of the obtained yttria nanopowder calcined at temperature of: a) 800 °C and b) 1100 °C.

Fig. 1.jpg

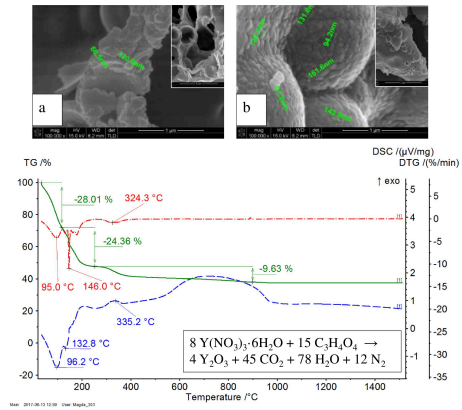


Fig. 2: Thermal analysis of yttrium nitrate and malonic acid solution; micrographs of the obtained yttria nanopowder calcined at temperature of: a) 900 °C and b) 1100 °C.

Fig. 2.jpg

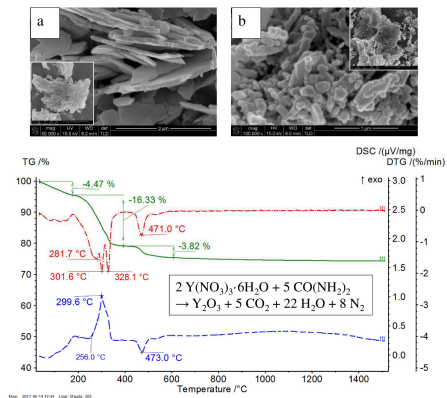


Fig. 3: Thermal analysis of yttrium nitrate and urea solution; micrographs of the obtained yttria nanopowder calcined at temperature of: a) 800 °C and b) 1100 °C.

Fig. 3.jpg

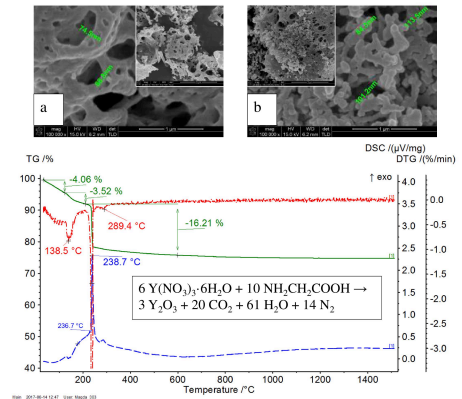


Fig. 4: Thermal analysis of yttrium nitrate and glycine solution; micrographs of the obtained yttria nanopowder calcined at temperature of: a) 800 °C and b) 1100 °C.

Fig. 4.jpg

Micro-Photoluminescence Mapping for evaluation of the Surface Plasmon Enhanced Emissions

Friday, 15th September - 13:30 - Poster Session - Gallery - Poster - Abstract ID: 376

***Mr. Kazutaka Tateishi*¹, *Dr. Pangpang Wang*¹, *Dr. Sou Ryuazki*¹, *Prof. Mitsuru Funato*², *Prof. Yoichi Kawakami*², *Prof. Koichi Okamoto*¹, *Prof. Kaoru Tamada*¹**

1. Kyushu University IMCE, 2. Kyoto University engineering

Photoluminescence (PL) mapping was conducted to elucidate the detailed mechanism of PL enhancement based on energy transfer from excitons to surface plasmon polariton (SPP) observed in silver coated InGaN quantum wells (QWs)[1]. Moreover, recently we reported that the photo-absorption efficiency was also remarkably increased by using Al film [2]. In order to understand the enhancement mechanism, here we measured the microscopic PL mapping.

50-nm-thick of Ag films were deposited onto half part of blue emitting InGaN/GaN QWs with 3-nm-thick InGaN layers which have green emissions. PL spectra mappings were measured by using a fluorescence microscope with a mercury lamp for excitation. The moving stage was electrically controlled by a stepping motor with 1 μm step.

Fig. 1(a) and (b) show the PL peak intensity and the peak wavelength mapping images obtained from metal un-coated part of InGaN QW, respectively. Both of PL peak intensity and peak wavelength values showed some spatial fluctuation in scanned area. The regions with higher PL intensity seem to have longer PL wavelength. This positive correlation between the PL intensities and peak wavelength should be due to the exciton localization effect in emission layer. Fig. 1(c) and (d) show the PL peak intensity and the peak wavelength mapping images obtained from silver coated part of InGaN QW, respectively. In this case the positive correlation was completely disappeared.

PL enhancement by SP on silver film was confirmed to be accompanied with energy transfer from excitons to SPP. If the energy transfer is faster than exciton localization process, the positive correlation can be cancelled. From above, we considered that the positive correlation disappearance suggest the energy transfer from excitons to SPP should be much faster than the exciton localization. Details will be discussed at the conference.

[1] K. Okamoto, I. Niki, A. Shvartser, and Y. Narukawa, *Nat. Mater.* **3**, 601 (2004).

[2] K. Tateishi, M. Funato, Y. Kawakami, K. Okamoto, and K. Tamada, *Appl. Phys. Lett.* **106**, 121112 (2015).

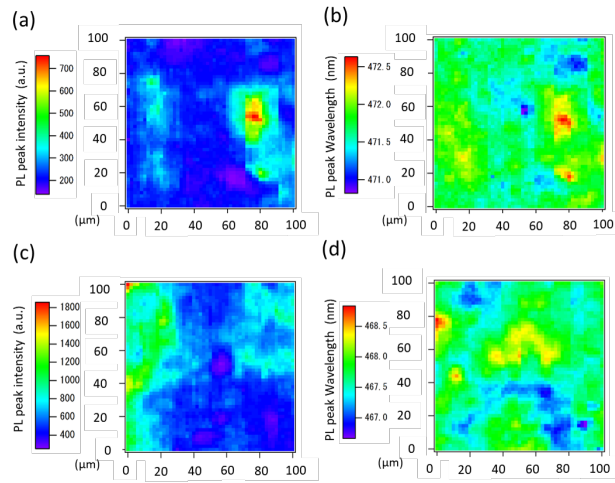


Figure 1 PL peak intensity mapping (a) and peak wavelength mapping (b) of silver uncoated green emitting InGaN QW. PL peak intensity mapping (c) and peak wavelength mapping (d) of silver coated InGaN QW.

Figure.1.png

UV controlled optical properties of polymer porous PET films filled with a liquid crystal

Friday, 15th September - 13:30 - Poster Session - Gallery - Poster - Abstract ID: 459

***Dr. Dina Shmeliova*¹, *Prof. Sergey Pasechnik*¹, *Dr. Alex Dubtsov*¹, *Mr. Sergey Trifonov*¹**

1. Moscow Technological University (MIREA)

In this report we present the results of optical study of polymer polyethelene teraphthalate (PET) porous films filled with a nematic liquid crystal (NLC). Previously such composite system was proposed as perspective material for photonics applications [1,2]. The samples of porous films of thickness $h = 20 \mu\text{m}$, obtained by ion bombarding and further chemical etching, were characterized by normal orientation of pores relatively to the film's plane with a narrow size distribution (the pore diameter's range $d = 0.1 \dots 5 \mu\text{m}$). In present experiments the films were filled with a nematic mixture ZhK 440 (NIOPIK) and irradiated by UV ($\lambda = 365 \text{ nm}$). It induced the time variations $\Delta I_r(t)$ of the red light intensity ($\lambda = 630 \text{ nm}$) passed through the film. It was found, that the value $\Delta I_r(t)$ depended on the irradiation dose $D = I_{UV} * t$ (I_{UV} – the intensinty of UV irradiation). The slow (some hours) backward relaxation of $I_r(t)$ to the initial value was observed after turning off UV irradiation. The observed effects were assigned to the changes of the effective refractive index of NLC imposed by UV induced cis-trans transitions of photo sensitive molecules of LC.

This work was supported by Ministry of Education and Science of Russian Federation, identification number-RFMEFI58316X0058.

1. Chopik A.P., Pasechnik S.V., Semerenko D.A., Shmeliova D.V., Dubtsov A.V., Srivastava A., Chigrinov V.G. Electro-optical effects in porous PET films filled with liquid crystal: new possibilities for fiber optics and THz applications // Optics Letters, Vol. 39, Issue 6, pp. 1453-1456 (2014).

2. Maksimochkin, G.I., Shmeliova, D.V., Pasechnik, S.V., Dubtsov, A.V., Semina, O.A., Kralj, S. Orientational fluctuations and phase transitions in 8CB confined by cylindrical pores of the PET film// Phase Transitions, 89 (7-8), pp. 846-855 (2016).

Contribution of type II quantum dot InAlAs/AlGaAs to enhance solar cell performance

Friday, 15th September - 13:30 - Poster Session - Gallery - Poster - Abstract ID: 276

Dr. Rim Neffati¹

1. Faculty of Sciences of Bizerte 7021 Jarzouna, University of Carthage, Tunisia

The purpose of this research deals with the investigation of optical, electrical and structural properties of III-V semiconductor materials and nanostructures with applications in the development of next generation solar cells. In particular, the focus is on the study of type II quantum dots (QDs) with long carrier lifetimes resulting from the spatial separation of carriers which provides additional advantage in solar cell absorber. AlInAs/AlGaAs QDs is one of the quantum structures that give rise to type-II QDs. Such QDs present a peculiar electronic structure and give the possibility to control and investigate the type-I to type-II crossover. Tailoring of the band alignment, the wave function overlaps and hence the carrier dynamics in these nanostructures is necessary for practical applications. This study presents an band-alignment tailoring of AlInAs/AlGaAs QDs structure for intermediate-band solar cell (IBSCs) application. The intermixing, caused by thermal annealing at the AlInAs/AlGaAs interface, will lead to a favorable electronic band alignment, necessary for high-efficiency solar cell devices. In this study QDs size, material composition and anneal temperature have to be optimised to give the maximum efficiency.

Hexagonal Metamaterial Filter On and Off Embedded Metallic Inclusion for Microwave Applications

Friday, 15th September - 13:30 - Poster Session - Gallery - Poster - Abstract ID: 487

*Dr. toto saktioto*¹, *Mr. Romi Fadli Syahputra*¹, *Mr. Mohammad Fandi Kurnia*¹

1. Department of Physics, Math and Natural Science Faculty, Universitas Riau

The metamaterial has numerous applications for imaging, electromagnetic filters, stealth technology, and biosensor systems. This paper investigates a hexagonal metamaterial structure with a split and a double concentric metallic rings, so-called split ring resonator hexagonal (SRR-H) for frequency filtering applications. SRR-H is designed structurally and operated computationally for microwave frequency. The simulation results showed that SRR-H size will affect the resonant frequency significantly. The resonant frequency goes to red shift when the size of the structure is enlarged. SRR-H structure is able to enhance magnetic permeability. We successfully simulated SRR-H metamaterial to obtain double negative and agreed with Lorentz's model.

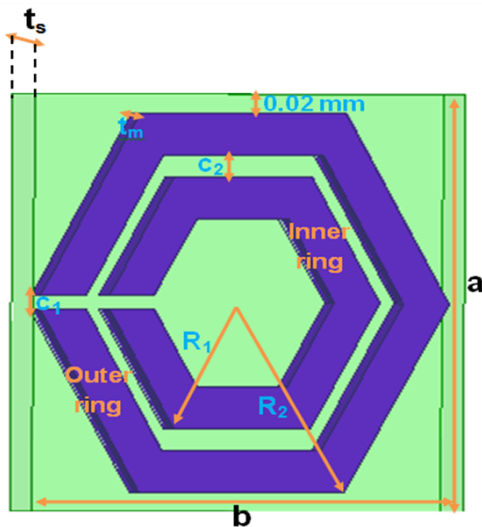


Figure 1 unit cell design.png

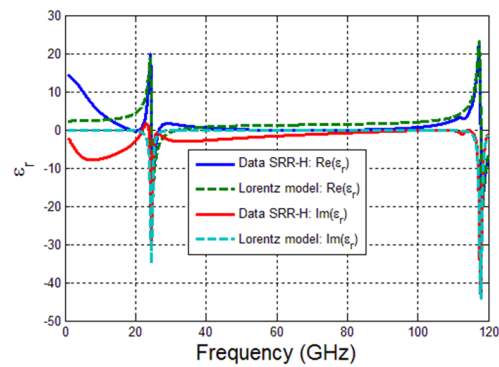


Figure 2 lorentz model for srr-h.png

Superiority of localized surface plasmon resonance technique in characterization of ultra-thin metallic films

Friday, 15th September - 13:30 - Poster Session - Gallery - Poster - Abstract ID: 118

Mr. Sudheer¹, **Ms. P Tiwari**¹, **Ms. S Bhartiya**¹, **Dr. C Mukherjee**¹, **Dr. S. K. Rai**¹, **Dr. A. K. Sinha**¹, **Dr. V. N. Rai**¹, **Dr. A. K. Srivastava**¹

1. HBNI, RRCAT, Indore

The ultra-thin nanostructured metallic films of <10 nm are of great interest because of their potential applications in nano-optics, energy harvesters like thin film solar cell and surface enhanced Raman spectroscopy (SERS) [1-3]. The controlled fabrication of such nanostructures along with accurate and fast characterization is very much important for its useful applications. This article presents, a comparison between UV-visible transmission, x-ray reflectivity (XRR), grazing incidence x-ray diffraction (GIXRD), field-emission scanning electron microscopy (FESEM) and atomic force microscopy (AFM) techniques for the characterization of sputtered-grown Au thin films (1.4 to 8.4 nm thickness) deposited on glass substrate. The optical transmission of 1.4 nm thickness film shows a clear dip at ~530 nm wavelength in the spectra which shift to higher wavelength side and broadened with an increase in the film thickness (Fig.1). These dips are found due to presence of random Au islands in the films (Fig.2) showing excitation of characteristic localized surface plasmon resonance (LSPR). The LSPR minima position and its broadening are intimately dependent on sizes and shapes of the nanoparticles as well as their decoration on the substrate. A linear variation has been found in film thickness and LSPR minima position for lower thickness. The minor modification in the film thickness produces direct feedback with a significant variation in the LSPR profile. The island height variation in different films are determined by AFM. On the other hand, XRR technique shows drastic reduction in the specular reflection with decrease in the film thickness that results in vanished Kossing oscillations in spectra which provides limited information about the thin films (<8.4 nm) (Fig. 3). However, patches of continuous film (~8.4 nm) are supportive in XRR measurement, while devoid of LSPR generation. For lower thickness films (<2.8 nm), GIXRD technique also not able to deliver the significant information (Fig. 4). Finally, we conclude that LSPR spectroscopy can provide much better information about the Au films up to ~1 nm thickness.

1.S. A. Maier et al, Adv. Mater. **19**, 1501 (2001).

2.Y. A. Akimov et al, Opt. Exp. **17**, 10195 (2009).

3.G. Q. Liu et al, Optik **124**, 5124 (2013).

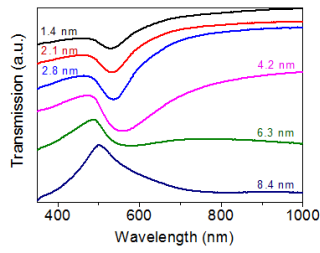


Fig.1 UV-visible transmission spectra of Au thin films.

Fig. 1.png

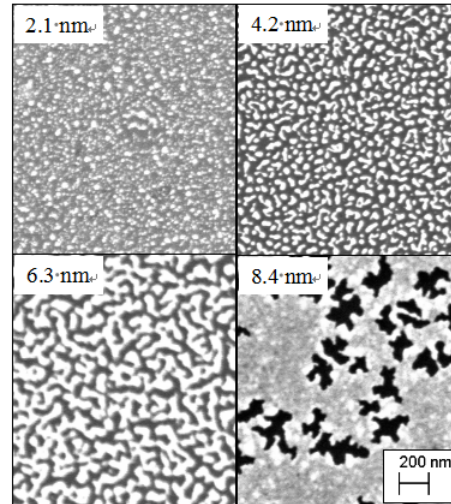


Fig.2 FESEM images of Au thin films

Fig. 2.png

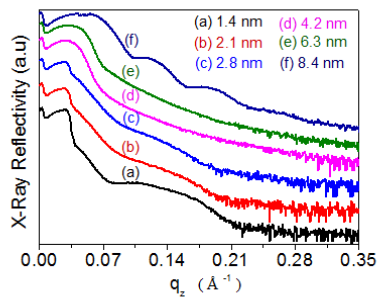


Fig.3 X-ray reflectivity spectra of Au thin films.

Fig. 3.png

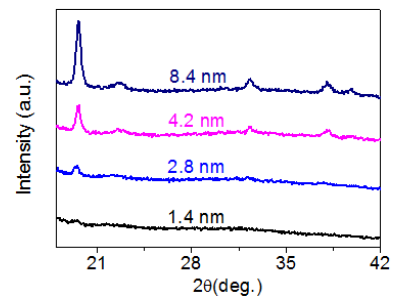


Fig.4 X-ray diffraction spectra of Au thin films

Fig. 4.png

3D Simulations of Spatially Dispersive Metals with a Finite Element Time Domain Method

Friday, 15th September - 13:30 - Poster Session - Gallery - Poster - Abstract ID: 289

*Mr. Nikolai Schmitt*¹, *Dr. Stéphane Lanteri*¹, *Dr. Claire Scheid*¹

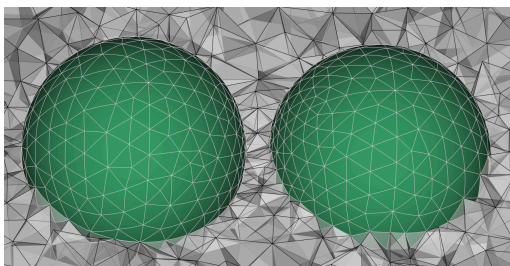
1. INRIA

We present recent advances in the development of a Finite Element Time Domain (Discontinuous Galerkin) solver for computational nanophotonics. Throughout this contribution a particular focus is put on metallic nano structures of sizes between 1 nm and 15 nm. Metal structures at these sizes are well known to show spatial dispersion which can be modeled by a nonlocal dispersion model for the electron gas. Taking such a nonlocal model into account leads to a hydrodynamic fluid equation for the free electrons in the metal. While Maxwell's equations describe the evolution of the electromagnetic fields, the additional fluid equation accounts for the material response and is strongly coupled to Maxwell's equations by means of a source current.

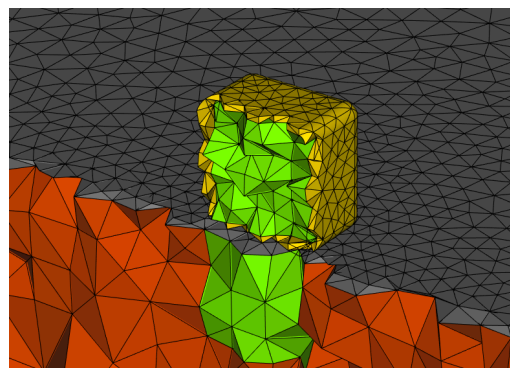
Numerically speaking, the considered 3D finite element time domain method benefits from high-order polynomial solutions on very flexible unstructured tetrahedral meshes. Additionally, working in time domain gives access to broad band frequency solution within a single simulation run due to short pulses. Exploiting distributed memory parallelism eventually allows large computational domains and hence realistic nanophotonic setups.

We assess the performance of our numerical method on multiple nanophotonic scenarios like spherical dimer systems (`simulation_mesh_dimer.png`) and nanocubes (`simulation_mesh_nanocube.png`). We emphasize the importance of highly accurate numerical schemes that guarantee a powerful resolution of surface effects, which is especially indispensable for plasmonic applications since most physics happen in the vicinity of the metal surface.

Moreover, we show the importance of high-order numerical methods including curvilinear tetrahedral meshes in order to properly approximate material interfaces if roundings are of concern.



Simulation mesh dimer.png



Simulation mesh nanocube.png

Solution combustion synthesis as a method of YAG nanopowders obtaining

Friday, 15th September - 13:30 - Poster Session - Gallery - Poster - Abstract ID: 403

*Dr. Milena Zalewska*¹, *Dr. Magdalena Gizowska*¹, *Ms. Izabela Kobus*¹, *Dr. Krzysztof Perkowski*¹, *Mr. Gustaw Konopka*¹, *Mrs. Irena Witosławska*¹, *Dr. Marcin Osuchowski*¹

1. Institute of Ceramics and Building Materials

Introduction

At the present time, YAG is the most widely-used laser material. It is important to synthesize yttrium aluminum garnet ($Y_3Al_5O_{12}$, YAG) ceramics with high transparency. In order to produce laser ceramics with high performance, it is fundamental to synthesize the powders with good dispersity and small particle size, additionally without hard-agglomeration. Solution combustion synthesis (SCS), which is based on the high energy reaction between the metal nitrates and reducing agent, is a promising method for fabrication of YAG nanopowders.

In the work the relationship between the reaction path with three various reducing agents added in stoichiometric amounts on the morphology of the obtained YAG nanopowder was investigated.

Methods

The thermal behavior of reaction mixture (metal oxide precursors and reducing agent) was studied. DSC/TG measurements were realized by using Netzsch STA 449C F1 Jupiter (Netzsch Gerätebau GmbH, Germany). The TG/DSC measurements were carried out from ambient temperature to 1000 °C with a heating rate of 10°C/min under 50 ml/min argon flow.

The microstructure of YAG nanopowders was analyzed by scanning electron microscopy (Nova NanoSEM 200, FEI Company).

Results

Urea, glycine and citric acid were tested as reducing agent for fabrication of YAG. In Fig. 1-3 the results of thermal analysis of the reaction mixture are presented. Fig. 4 show SEM images of the microstructure of YAG nanopowder. The powders obtained in the SCS reactions are highly agglomerated. The solidity, size and structure of the agglomerates depend on the process conditions and the type of fuel used.

Discussion

Solution combustion synthesis (SCS) involves the redox reaction of metal nitrates with reducing agent (urea, glycine, citric acid), where metal oxide precursor is obtained. During the reaction nitrates oxidize reducing agent to form metal oxide and non-toxic gaseous products. Depending on the used reducing agent the course of reaction and ignition temperature are different. These parameters affect the morphology and purity but also dispersibility of the YAG powders.

Acknowledgement

This work was funded by the Polish Ministry of Science and Higher Education.

Synthesis and characterization of new host molecules available as red phosphorescent OLED host material

Friday, 15th September - 13:30 - Poster Session - Gallery - Poster - Abstract ID: 469

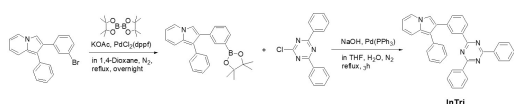
Mr. Dae Ryun Kwon ¹, Prof. Choon Woo Lim ¹

1. Department of Chemistry, College of Life Science and Nano-technology, Hannam University, Daejeon 305-811, Republic of Korea

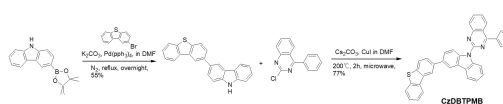
OLED-based displays have good efficiency with self-emission. This is an environmentally friendly display with low power consumption. In theory, phosphorescent organic light-emitting materials is able to harvest internal quantum efficiency (EQE) close to 100% but fluorescent emitter has low EQE to 25%. Phosphorescent OLED materials are demanding more development with better advantages than fluorescence. The host material plays a key role for good energy transfer to the emitter.

Hetero-aromatic system compounds have been widely used as organic electroluminescent materials. Carbazoles and their derivatives are highly interesting because they have fine optical properties, a low redox potential, and high chemical stability. Dibenzothiophene also has high triplet energy of 3.04 eV and good hole-transporting ability. The quinazoline and 1,3,5-triazazine moiety has good electron transport ability due to electron deficiency characteristics. indolizine has good luminescent properties and is likely to be used as an OLED device material. We designed the host material by mixing various hetero-aromatic molecules.

InTri and CzDBTPMB were synthesized as host materials for phosphorescent OLEDs. We used the Spartan 08' program to predict HOMO/LUMO levels and orbital distributions of the host materials. The synthesized host materials were analyzed and confirmed by ¹H NMR, ¹³C NMR, Mass Spectrometer. Also, optical characteristics were examined by UV-Vis spectrophotometer and photoluminescence spectroscopy. The thermal stability of host materials were analyzed by thermo gravimetric analyzer (TGA) and differential scanning calorimeter (DSC).



Scheme1.jpg



Scheme2.jpg

Optical Perturbation of Atoms in weak localization

Friday, 15th September - 13:30 - Poster Session - Gallery - Poster - Abstract ID: 236

Dr. Afifa Yedjour¹

1. Faculté de physique, université des sciences et de la technologie d'Oran USTO-MB

We determine the microscopic transport parameters that are necessary to describe the diffusion process of the atomic gas in optical speckle. Applying the self-consistent theory to calculate the self-energy of the atomic gas in random potential. We will compute the spectral function numerically by an average over disorder realizations in terms of the Greens function. The spectral function behaves as a free space expression $A(\epsilon, k) \propto \delta(\epsilon - \epsilon_k)$ strongly peaked near $k = \sqrt{\epsilon}$. The aim of the present work is to using this theory to discuss the behavior of the energy distribution of the atoms to estimate a correction to the on-shell mobility edge. We have included the real part of the self-energy by incorporating disorder-induced shift of the energy states in the theory. Our results show that the mobility position changes according to the disorder mean value and predict a negative mobility edge.

Simple and Rapid Detection of L-Dopa Based on in Situ Formation of Polylevodopa Nanoparticles

Friday, 15th September - 13:30 - Poster Session - Gallery - Poster - Abstract ID: 133

Mr. Ahmad Moslehi Pour¹, **Dr. Mohammad Reza Hormozi-nezhad**²

1. Sharif University of Technology, 2. Institute for Nanoscience and Nanotechnology, Sharif University of Technology

Introduction

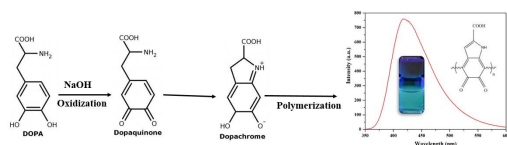
L-DOPA (L-3,4-dihydroxyphenylalanine) is a catecholamine drug that plays important roles in biochemistry and medicinal chemistry which can be converted to dopamine by dopa-decarboxylase to increase dopamine in the brain and also can cross the blood-brain barrier, whereas dopamine itself cannot, which has made it the most effective drug for the treatment of Parkinson's disease. The Abnormal concentrations of L-DOPA in biological fluids (e.g. urine, plasma and serum) can be used for diagnosis of this disease and evaluate the activity of sympathetic nervous system

Methods

First, levodopa solutions were prepared at concentrations ranging from 0.3 to 100.0 μM and the pH for each concentration was adjusted to 7.4 using phosphate buffer. To start the oxidation reaction, NaOH was added to the solution so that the final concentration was 20.0 μM . After 10 minutes, the polymerization reactions were stopped by 20.0 μL of 1.0 M HCl. The reaction stopped between 10 to 20 minutes and we did analysis at 14 min after the start of the reaction. Then, fluorescence spectra of solutions were recorded with excitation wavelength of 340 nm and calibration curves were plotted at an emission wavelength of 419 nm. To evaluate the selectivity of the method, the concentration of L-dopa was 20.0 μM and concentrations of all interfering chemicals were 200.0 μM .

Results and Discussion

In this work, a rapid and sensitive method for levodopa detection was reported which is based on *in situ* formation of polylevodopa nanoparticles. The assay is very simple and low cost and uses only NaOH and HCl as reagents. Under alkaline conditions, levodopa is spontaneously oxidized to its quinone derivative and shows the fluorescence properties. The fluorescence signal of the oxidation product of the levodopa has been explored and used for measurement of levodopa in the presence of dopamine, uric acid, ascorbic acid and other interfering which shows the excellent selectivity of the assay. The limit of detection (LOD) of the method was evaluated to be 29.0 nM with the linear range of 0.3-100.0 μM .



Mechanism.jpg

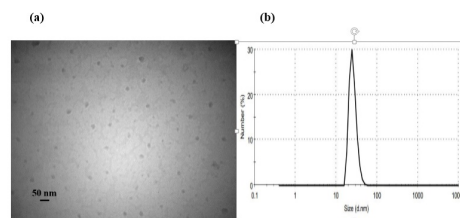
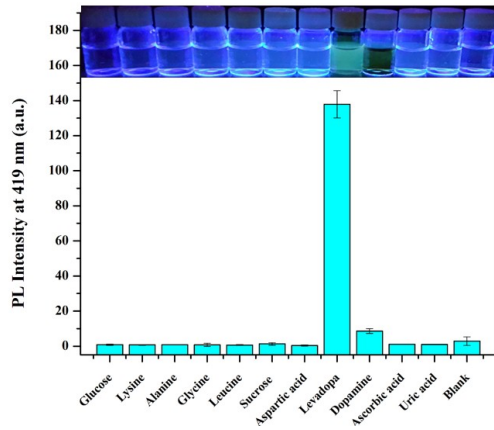
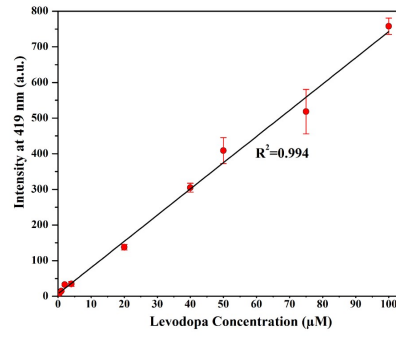


Fig 1. The particle size distribution of polylevodopa nanoparticles over time which were prepared after oxidation of 15.0 μM levodopa solution in the presence of 20 mM NaOH: (a) TEM image (b) DLS

Size.jpg



Selectivity.jpg



Calibration.jpg

Hot-carrier Dynamics in Photoexcited Gold Nanostructures: Analysis of Plasmon Excitation, Interband Transitions and Ballistic Transport

Friday, 15th September - 14:30 - Photonic & plasmonic nanomaterials - Auditorium - Oral - Abstract ID: 197

***Dr. Giulia Tagliabue*¹, *Mr. Adam Jermyn*², *Prof. Ravishankar Sundararaman*³, *Ms. Alex Welch*¹, *Dr. Joseph Du Chene*¹, *Dr. Ragip Pala*¹, *Dr. Artur Davoyan*¹, *Dr. Prineha Narang*⁴, *Prof. Harry Atwater*¹**

1. California Institute of Technology, 2. University of Cambridge, 3. Rensselaer Polytechnic Institute, 4. Harvard University

Plasmon-enhanced photo-excitation and collection of 'hot' charge carriers from metallic nanostructures has the potential to enable new light harvesting mechanisms for optoelectronic devices. While it is now established that plasmon excitation improves device performances, such as responsivity of photo-detectors or incident-photon-to-charge-carrier efficiency of photocatalytic cells, detailed understanding of the role of plasmon in either light absorption or hot-carriers generation, transport and collection (i.e. internal quantum efficiency, IQE) is yet to be achieved. Theoretical ab-initio studies have clarified individual aspects of these processes, establishing the major mechanisms for hot-carriers generation upon plasmon non-radiative decay (inter- and intra-band transitions) as well as the resulting energy distribution, hot-carrier mean free path and momentum. However, the complex convolutions of these aspects is less understood and experimental results are still largely interpreted in terms of the semi-classical Fowler theory.

In this work we combine experimental and theoretical methods to gain a detailed description of hot-carrier transport in nanostructures. We indeed experimentally determine the IQE spectra of several Au-on-GaN photoelectrodes supporting different plasmon resonances and show that plasmon excitation is primarily responsible for absorption enhancement. Furthermore, using a recently developed theoretical framework, we are able to determine the energy distribution of the carriers which reach the Au/GaN interface as well as track the number of scattering events which occurred before extraction. This calculation, whose results agree well to experimental data, predicts ballistic carrier transport and collection for wavelengths greater than 620 nm. Finally, by assessing the relative contribution of intra- and inter-band transitions, we are able to relate the characteristic feature of the IQE spectra to the competing role of these two mechanisms, retrospectively supporting previous experimental results.

Overall the discussed approach coupling experiments with theoretical calculations enables a new level of physical detail in the study of plasmon-enhanced hot-carrier devices.

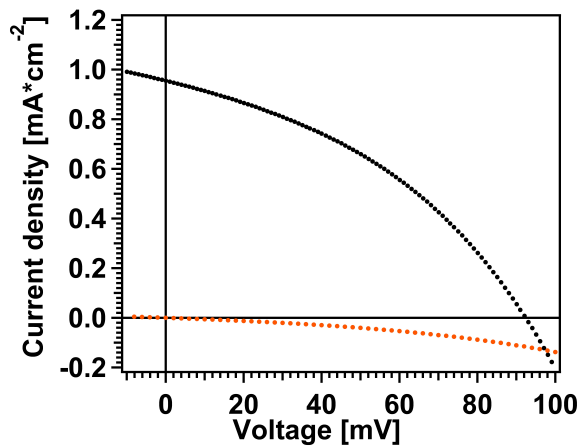
Solid state ITO | Au-NPs | TiO₂ plasmonic based solar cells

Friday, 15th September - 14:47 - Photonic & plasmonic nanomaterials - Auditorium - Oral - Abstract ID: 86

Mr. Adam Ginsburg¹, Dr. Assaf Y. Anderson¹, Prof. Arie Zaban¹

1. Bar-Ilan University

Plasmonic enhanced solar cells are widely studied due to their increased performance arising from the metallic nanoparticles light absorption and scattering. In contrast, there are only few reports on solar cells which are based solely on the plasmonic metallic layer as the absorber. These cells are operating by hot electron injection in a Schottky barrier formed between the metallic nanoparticles and a semiconductor. In this work, we present photovoltaic cells which are based on an ultra-thin tunable Au layer as the only light absorbing material. These cells are in the solid state configuration composed of ITO | Au NP's | TiO₂. High throughput methods are used in order to optimize the performance, which reaches 1 mA cm⁻² of current, and a voltage of 100 mV under one sun illumination. The incident photon to electron conversion efficiency is 5.84 % at 700 nm, the highest reported for a solid-state device so far. These cells are the first step towards a plasmonic based tandem cell.



Iv170207d.jpg

Low-loss Adiabatic Dielectric-Plasmonic Hybrid Waveguide for HAMR Applications

Friday, 15th September - 15:04 - Photonic & plasmonic nanomaterials - Auditorium - Oral - Abstract ID: 258

Mr. Chuan Zhong¹, Mr. Brian Jennings¹, Mr. Patrick Flanigan¹, Mr. Frank Bello¹, Mr. Nicolás Abadía¹, Ms. Gwenael Atcheson¹, Mr. Richard Hobbs¹, Mr. David McCloskey¹, Mr. John Donegan¹

1. Trinity College Dublin

To achieve a feasible heat-assisted magnetic recording (HAMR) system, a near-field transducer (NFT) is necessary to focus the optical field to a lateral region measuring tens of nanometres in size. Coupling light effectively into the NFT is a key challenge in the design of a HAMR system. In this work, we theoretically and experimentally investigate the properties of coupling between a slab Si₃N₄ waveguide and a long tapered Au plasmonic waveguide through an evanescent coupling mechanism. The most important insight is how to construct an adiabatic taper with a length on the order of 10 μm (two orders of magnitude longer than typical devices) that can efficiently extract the incident light from the waveguide core to the NFT while overcoming the ohmic losses incurred by increasing the optical path length. Our study shows that in the fully optimized system, a maximum coupling efficiency between the photonic mode and the plasmonic mode of ~77% is achieved with a 6 μm long taper. The system can be characterized in terms of the coupling length (the distance between constructive interference points) and the field intensity enhancement at the tip, which is estimated to be 16× for an NFT with a 50 × 50 nm² tip. All these factors, particularly the system's ability to remove light from the dielectric waveguide to prevent optical interference in other parts of the system, make this a viable candidate for HAMR implementation.

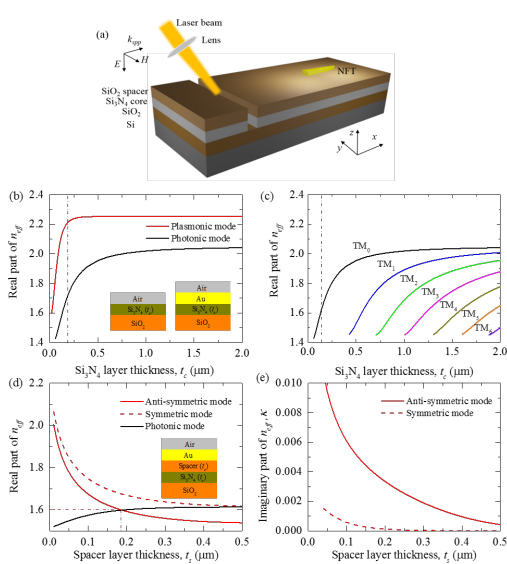


Figure 1 diagram of the system and momentum matching.png

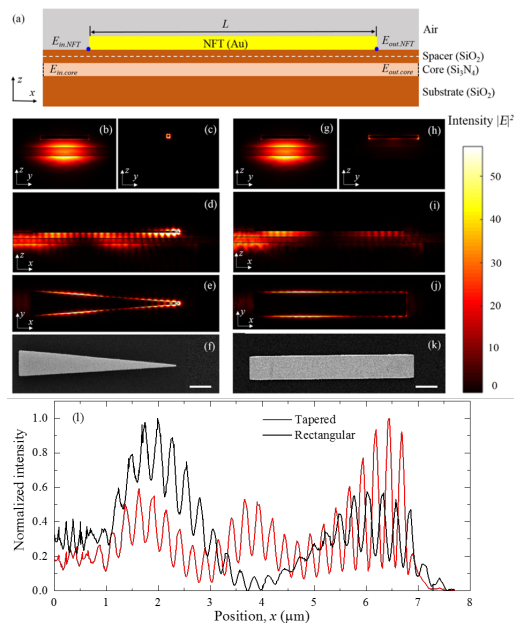


Figure 2 3-d comsol simulations.png

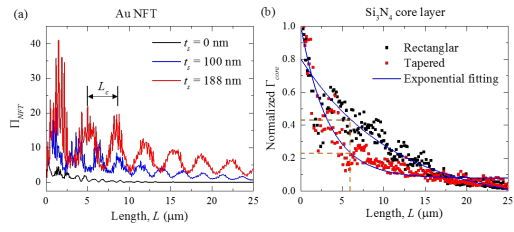


Figure 3 field enhancement and coupling efficiency.png

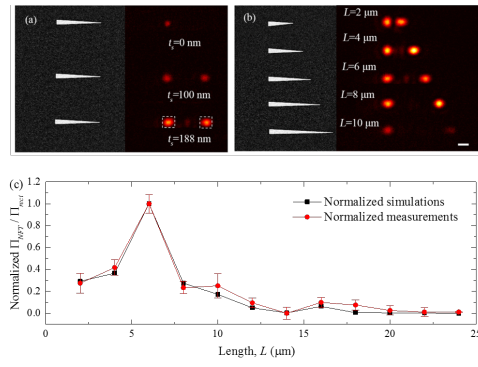


Figure 4 far-field measurement results.png

Microspectroscopy of plasmonic crystal cavity by cathodoluminescence STEM

Friday, 15th September - 15:21 - Photonic & plasmonic nanomaterials - Auditorium - Oral - Abstract ID: 232

*Dr. Hikaru Saito*¹, *Prof. Naoki Yamamoto*²

1. *Kyushu University*, 2. *Tokyo Institute of Technology*

The use of surface plasmon-polaritons (SPPs) is one of the most promising ways to achieve nano-cavities with ultra-small mode volumes, leading to enhanced spontaneous emission and nanolasers. We have performed a detailed characterization of a plasmonic crystal (PIC) cavity, and visualize standing plasmonic waves localized inside the cavity by using angle-resolved cathodoluminescence (CL) technique combined with scanning transmission electron microscopy (STEM) [1]. The investigated PIC cavity was composed of silver pillar arrays with a square lattice. An angle-resolved spectroscopy (ARS) pattern indicates a plasmonic bandgap at the Γ point in the crystalline area (Fig. 1a), where SPPs are forbidden to propagate in the PICs. In the ARS pattern taken from the cavity area sandwiched by two PICs, an energy level is observed in the energy range of the crystalline bandgap (Fig. 1b). To identify the character of the new mode appearing in the bandgap, we have performed photon map imaging around the cavity area (Fig. 1c and 1d), indicating the new mode is confined in the cavity.

In detailed analyses about dependence of the cavity mode on the cavity width (W), the modal symmetry and the quality factor showed periodic changes as a function of W , and these behaviors were related to the characteristics of the band-edge modes. As a result, the formation mechanism of the cavity mode has been elucidated, which provides a clear design guide for the PIC cavity to control the coupling between SPPs and photons in plasmonic devices.

This work was supported by the Japanese Ministry of Education, Culture, Science, and Technology (MEXT) Nanotechnology Platform 12025014.

[1] H. Saito and N. Yamamoto, *Nano Lett.* 15, 5764–5769 (2015).

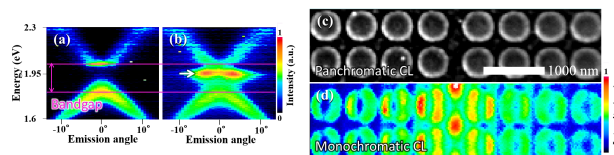


Figure 1. CL-STEM analyses for the PIC cavity. The PIC has the pillar height h (100 nm) and period P (600 nm), and the cavity width W is 100 nm. (a and b) ARS patterns taken from (a) the crystalline area and (b) the cavity area. (c) Panchromatic photon map. (d) Monochromatic photon map viewed at the energy corresponding to the cavity mode.

Figure1.png

UV light driven synthesis of plasmonic nanoparticles on ceria support: optimisation and potential applications in photocatalysis

Friday, 15th September - 15:38 - Photonic & plasmonic nanomaterials - Auditorium - Oral - Abstract ID: 81

***Mrs. Eva Raudonyte-Svirbutaviciene*¹, *Dr. Arturas Katelnikovas*²**

1. Faculty of Chemistry and Geosciences, Vilnius University, Naugarduko 24, LT-03225 Vilnius, Lithuania; SRI Nature Research Centre, Institute of Geology and Geography, Akademijos 2, LT-08412 Vilnius, Lithuania, **2.** Faculty of Chemistry and Geosciences, Vilnius University, Naugarduko 24, LT-03225 Vilnius, Lithuania

Light still remains an exotic tool for the control of particle shape, size and composition, even though light-mediated synthesis provides advantages of a uniform distribution of the reducing agent and tunable wavelength with regard to the conventional chemical approaches. On the other hand, utilization of solar energy for catalytic chemical transformations has been considered as an environmentally friendly alternative to traditional thermally driven heterogeneous catalysis for decades [1,2]. The aim of this work was to prepare and characterize Ag-CeO₂ system, a potential photocatalyst with the visible light activity, via photochemical inorganic synthesis. Synthesis of Ag-CeO₂ was carried out in deaerated aqueous CeO₂ dispersions containing dissolved AgNO₃. Metallic silver was photocatalytically generated on the surface of ceria as a result of UV irradiation with 0 W mercury discharge lamp NIQ40/18-45000024. Irradiation of deaerated CeO₂ suspensions in the presence of AgNO₃ resulted in the rise of a strong band with the maximum at 391 – 422 nm in the absorption spectra of the solutions. Faster formation of Ag nanoparticles with the lower amount of silver being required was observed when ethanol was introduced to the reaction solution before the irradiation. Alcohols with α -hydrogens are known to easily form α -hydroxyalkylradicals upon α -H atom abstraction. Hence, reductive reactions can be strongly enhanced in deaerated ethanol containing solutions with respect to the pure aqueous media.

Not only is the proposed synthesis pathway a clean route to the formation of the nanoparticles with no potential damage to the environment being expected, it also provides the possibility to create small uncoated nanostructures with a “clean” surface. From the viewpoint of applications, any residue of amines, polymers or organic solvents, which are usually required in a photochemical synthesis mixture, should affect the performance of the nanoparticles significantly. Thus, the proposed photochemical approach with no additives, but uncoated ceria nanoparticles being required, should enable us to produce particles with remarkably improved photocatalytic properties.

1. A. Fujishima and K. Honda. Nature, 1972. **238**(5358): 37-38

2. M.J.Kale, T. Avanesian, P. Christopher. ACS Catalysis, 2014. **4**(1): 116-128.

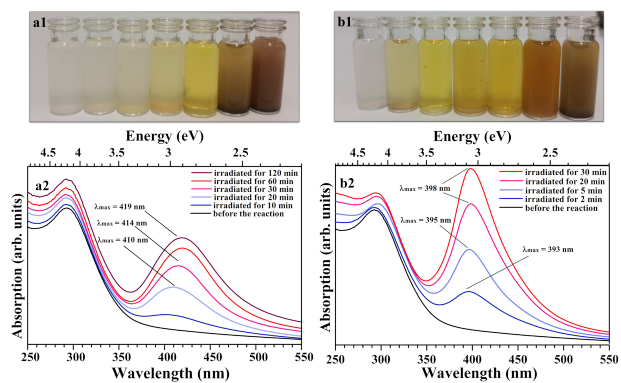


Figure 1. Irradiation time-dependent final color of the colloidal solutions and absorption spectra of the Ag-CeO₂- dispersions: a – 3.5 mmol/L AgNO₃, b – 0.035 mmol/L AgNO₃, 20% vol EtOH solution. Irradiation time as follows: 0; 10; 20; 30; 60; 90; 120 min for a1 and 0; 2; 5; 30; 60; 90; 120 min for b1

Figure 1. irradiation time depending final color and absorption spectra of the colloidal ag-ceo2 solutions.png

Analytical Investigation of In-plane Focusing Surface Plasmon Modes by a Dielectric Lens

Friday, 15th September - 15:55 - Photonic & plasmonic nanomaterials - Auditorium - Oral - Abstract ID: 428

Ms. Fahimeh Armin¹, Prof. Mir Mojtaba Mirsalehi¹

1. Ferdowsi University of Mashhad

A dielectric lens placed on a metal-dielectric interface (Fig. 1) can be used for in-plane focusing surface plasmon (SP) modes. The propagation behind the lens is usually studied using scalar diffraction theory which is not accurate in nanometer regime and cannot explain the propagation and energy flow of SP modes. Here, we have used vectorial derivation of Huygens-Fresnel principle [1] to analytically calculate the diffracted fields behind the lens to study the energy flow of SP modes in a focusing system.

In a plasmonic structure, a dielectric lens cannot be considered as a thin lens. In the first step, we have derived the phase delay of a SP mode considering the lens thickness. This phase delay in conjunction with the vectorial form of Huygens-Fresnel principle is then used to calculate the diffraction pattern of a SP mode. The resulted electric field is

$$\mathbf{E}(\mathbf{r}) = (1/2\pi) \int \mathbf{E}(k_y) \exp(i\sqrt{K^2 - k_y^2}z + ik_y y + ik_x x) dk_y,$$

where k_x and k_y are the components of wavevector in the x and y directions, respectively. The wave propagates along the z direction and K indicates the tangential element of the wavevector. The above equation can be considered as the Fourier transform of the product of the phase function of SP and its complex amplitude. This relation can be expressed in the form of a convolution integral and its solution provides the diffracted fields behind the lens. The resulted fields have the form of higher order SP modes [2] which means that passing through a dielectric lens has excited higher order modes. Using the Poynting vector, one can calculate the energy flow behind the lens. The results are shown in Fig. 2 for different points on a metal-dielectric interface. Using the vectorial Huygens-Fresnel principle and accurate SP phase delay, we have shown that higher order SP modes are excited behind a lens in an in-plane focusing system. This is equivalent to more energy loss from the surface since the higher SP modes are less bounded to the surface than the fundamental mode.

References

- [1] A. Archambault, *et al.* Phys. Rev. B 79, 2009.
 [2] M. Kordi, *et al.* Phys. Rev. A 95, 2017.

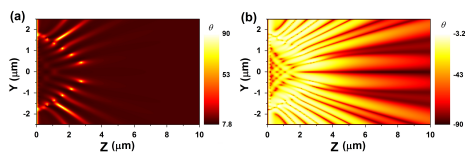


Fig. 2. The energy flow of SP mode behind the dielectric lens in (a) metal and (b) dielectric. θ is the angle of Poynting vector with respect to the surface. The results are calculated for silver-air interface at the wavelength of 780 nm. The lens is made of PMMA and has a curvature of 5 μm . It can be seen that at some points θ has even increased to 90° from the surface which explains the energy loss.

Fig2.png

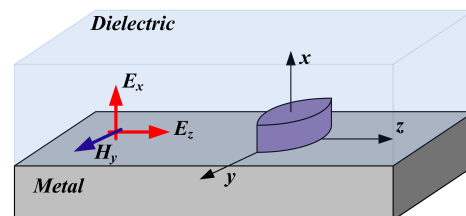


Fig. 1. Schematic diagram of the dielectric lens on a metal-dielectric interface as the fundamental SP mode propagates in front of the lens.

Fig1.png

Subnanometric control of the coherent coupling between a single molecule and a plasmonic nanocavity

Friday, 15th September - 14:30 - Strong light-matter interactions at the nanoscale - Room 207 - Oral - Abstract ID: 313

Dr. Yao Zhang¹, Dr. Qiu-shi Meng², Dr. Yang Zhang², Mr. Yang Luo², Mr. Yun-jie Yu², Mr. Li Zhang², Dr. Ruben Esteban¹, Prof. Zhen-chao Dong², Prof. Javier Aizpurua¹

1. Center for Material Physics (CSIC - UPV/EHU and DIPIC), 2. University of Science and Technology of China

The interaction between excitons and plasmons provides useful information about the coupling strength and the coherence of the hybrid system. A single molecule can be regarded as an ideal two-level system, and a plasmonic nanocavity in a tip-substrate configuration can sustain ultra-localized electric fields that serve as atomic-scale optical probes to study plasmon-exciton interactions. We have previously applied a plasmonic nanocavity formed by the tip-substrate configuration to enhance the Raman signal of a single molecule and retrieve the information of the dipole-dipole coupling regime at sub-molecular level. However, the intrinsic properties of the coherent coupling between a single molecule and the plasmon have not been studied yet, especially at sub-nanometer level. In this work, we use a scanning tunneling microscope (STM) tip/substrate nanocavity to generate a localized plasmonic field, and a zinc phthalocyanine (ZnPc) molecule as a quantum emitter to study the coherent coupling between the plasmon and a single molecule at the sub-nanometer scale (as depicted in the schematics of Fig. 1, left). If there is no molecule under the STM tip, an emission spectrum of the nanocavity plasmon is observed (blue spectrum in Fig. 1, right). However, if the STM tip is placed in the proximity of the single molecule, a dramatic change in the fluorescence spectra is observed, evolving from a pure plasmonic peak to a Fano lineshape (red spectrum in Fig. 1, right), indicating a coherent coupling between the molecular excitation and the plasmonic resonance. The coupling strength can be tuned in a controlled manner by varying the lateral distance between the STM tip and the molecule, due to the spatial confinement of the local electric field. Furthermore, the detuning between the nanocavity plasmon resonance and the molecular transition can be carefully modified, with the strongest coupling strength obtained when both excitations are resonant. All these results can help to provide a better understanding of the exciton-plasmon coupling mechanism at the sub-nanometer level with implications in molecular sensing, optical modulators, and quantum information devices.

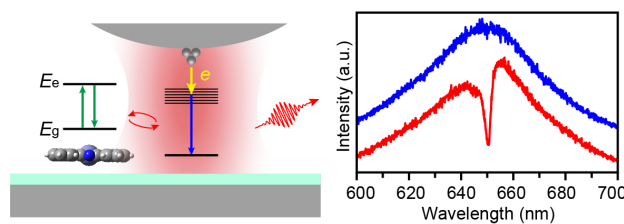


Figure-01.jpg

All optical band engineering of Dirac materials

Friday, 15th September - 14:47 - Strong light-matter interactions at the nanoscale - Room 207 - Oral - Abstract ID: 124

Mr. Kevin DINI¹, Dr. Ivan Iorsh², Prof. Oleg Kibis³, Prof. Ivan Shelykh¹

1. University of Iceland, 2. ITMO University, 3. Novosibirsk State technical university

We demonstrate theoretically that the interaction between electrons in Dirac materials and a strong off-resonant electromagnetic field (dressing field) substantially renormalizes different parameters of the band structure of Dirac materials (such as monolayer graphene, bilayer graphene, Transition Metal Dichalcogenides). Moreover, we show that different effects strongly depend on the polarization of the field. Namely, an example of the found features is the opening of a gap in graphene with the circularly polarized light whereas with a linear polarization we observe a modification of the Fermi velocity [1]. Another example is the closure of the gap and the modification of the spin splitting in both valence and conduction bands in TMDC materials using linearly polarized light [2]. As a consequence the dressing field can serve as an effective tool to control spin and valley properties of Dirac materials and be potentially exploited in optoelectronic applications.

[1]: K. Kristinsson, O. V. Kibis, S. Morina, I. A. Shelykh, Sci Rep. 6 20082 (2016)

[2]: O. V. Kibis, K. Dini, I. V. Iorsh, I. A. Shelykh, Phys. Rev. B 95, 125401 (2017)

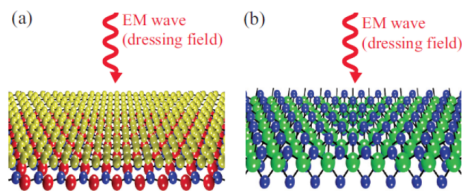


FIG. 1. Sketch of the considered gapped Dirac materials subject to an electromagnetic wave (dressing field): (a) Graphene grown on the substrate of hexagonal boron nitride; (b) transition-metal dichalcogenide monolayer MoS_2 .

Sketch.png

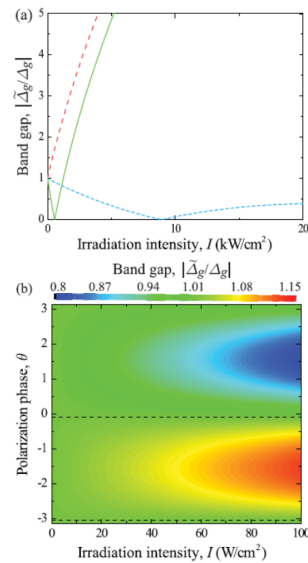


FIG. 3. Dependence of the band gap in irradiated gapped graphene ($\Delta_g = 2$ meV, $\gamma/\beta = 10^6$ m/s) on the irradiation intensity, I , and the polarization, θ , for the photon energy $\hbar\omega = 10$ meV. In part (a) the dotted line corresponds to the linearly polarized dressing field, whereas the dashed and solid lines correspond to the different circular polarizations ($\tau\xi = -1$ and $\tau\xi = 1$, respectively). In part (b) the dashed lines correspond to the polarizations, θ , which do not change the band gap.

Polarization dependence.png

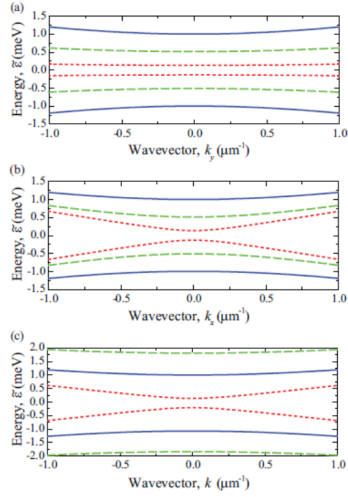


FIG. 2. The energy spectrum of dressed electron, $\tilde{E}(k)$, near the band edge of gapped graphene ($\Delta_g = 2$ meV, $\gamma/\hbar = 10^6$ m/s) irradiated by a dressing field with the photon energy $\hbar\omega = 10$ meV and the different intensities, I . In parts (a) and (b) the dressing field is linearly polarized along the x axis; the irradiation intensities are $I = 0$ (solid lines), $I = 7.5$ kW/cm 2 (dashed lines), and $I = 15$ kW/cm 2 (dotted lines). In part (c) the dressing field is circularly polarized; the solid line describes the energy spectrum of “bare” electron ($I = 0$), whereas the dotted and dashed lines correspond to the different circular polarizations ($\tau\xi = -1$ and $\tau\xi = 1$, respectively) with the same irradiation intensity $I = 300$ W/cm 2 .

Dispersion.png

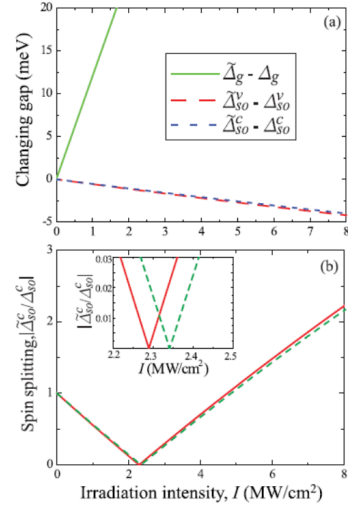


FIG. 4. Dependence of the band gap, $\tilde{\Delta}_g$, and the spin splitting of conduction and valence bands, $\Delta_{g0}^{C,V}$, on the irradiation intensity for MoS $_2$ monolayer ($\Delta_g = 1.58$ eV, $\Delta_{g0}^C = 3$ meV, $\Delta_{g0}^V = 147$ meV, $\gamma/\hbar = 7.7 \times 10^5$ m/s) irradiated by a circularly polarized field with the photon energy $\hbar\omega = 10$ meV: (a) The field-induced changing of the band gap and the spin splitting of the circularly polarized field with $\tau\xi = -1$; (b) The renormalized spin-splitting of conduction band for different field polarizations (the solid and dashed lines correspond to $\tau\xi = -1$ and $\tau\xi = 1$, respectively).

Spin splitting.png

Guided mode resonance enhanced upconversion fluorescence of rare earth nanoparticles in aqueous solution using a low refractive index resonant waveguide grating

Friday, 15th September - 15:04 - Strong light-matter interactions at the nanoscale - Room 207 - Oral - Abstract ID: 215

Prof. C. C. Hsu¹, Mr. V. D. Vu¹, Mr. H. W. Chiu¹, Ms. R. Nababan¹, Prof. Q. M. Le², Prof. S. W. Kuo³, Prof. L. K. Chau⁴, Prof. C. C. Ting⁵, Prof. H. C. Kan¹

1. Department of Physics, National Chung Cheng University, 2. Institute of Materials Science, VAST of Vietnam, 3. Department of Materials and Optoelectronic Science, National Sun Yat Sen University, 4. Department of Chemistry and Biochemistry, National Chung Cheng University, 5. Graduate Institute of Opto-Mechatronics, National Chung Cheng University

We demonstrated that upconversion fluorescence (UCF) produced from rare earth upconversion nanoparticles (UCNPs) in aqueous solution could be greatly enhanced using a low refractive index resonant waveguide grating (low-n RWG). The low-n RWG comprised of a low refractive index porous silica ($n=1.22$) sinusoidal grating layer in the bottom and a thin high refractive index TiO_2 waveguide layer on the top (see Fig. 1 (a)). The surface of the TiO_2 layer was biotinylated and then covered with aqueous solution (PBS). After drop-coating of streptavidin-conjugated UCNPs on the biotinylated TiO_2 surface, streptavidin-coated UCNPs were immobilized on biotinylated surface. Strong local field was built near the interface between TiO_2 and PBS aqueous solution, when the low-n RWG was illuminated with a near IR laser with an incident angle matching with the guided mode resonance (GMR) angle of the low-n RWG. Figure 1(b) depicts the UCF spectra of the low-n RWG sample obtained with different excitation angles. As displayed, UCF intensities from all emission peaks were dramatically increased when the low-n RWG was illuminated under GMR condition, i.e., $q = 1.5^\circ$. As the excitation angle was shifted to $q = 2.0^\circ$, UCF intensities collapsed and became barely higher than those from a non-RWG area. We also compared UCF spectra of biotinylated (labelled) and non-biotinylated (non-labelled) low-n RWG samples under resonant excitation. As shown in Fig. 1(c), the UCF emissions of the labelled sample were much stronger than those of non-labelled one, indicating higher numbers of UCNPs immobilized on the TiO_2 surface of the labelled low-n RWG, and thus validating the biotinylated functionalization process workable for our low-n RWG structured surface. The result confirms that the low-n RWG is powerful for enhancing UCF of UCNPs which paves a good foundation of using the low-n RWG in UCF biosensing and bioimaging applications.

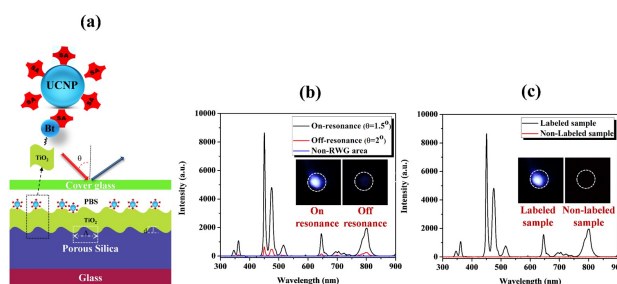


Figure 1: (a) Schematic of the 1D low-n RWG via streptavidin-biotin interaction. (b) UCF spectra of the low-n RWG obtained on-resonance and off-resonance conditions and that from a non-RWG area. (c) UCF spectra of the labelled and non-labelled low-n RWGs obtained under the excitation resonance condition.

Picture1 1 .jpg

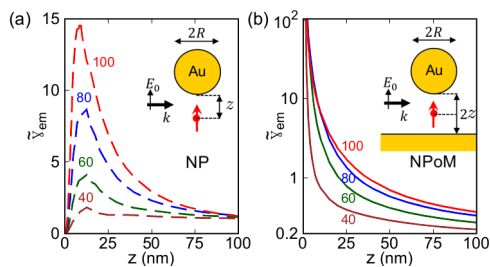
Suppression of fluorescence quenching in plasmonic nanocavities

Friday, 15th September - 15:21 - Strong light-matter interactions at the nanoscale - Room 207 - Oral - Abstract ID: 231

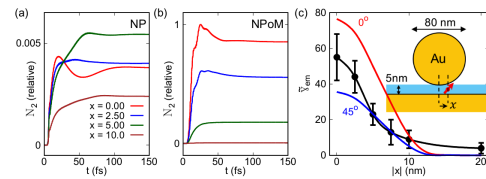
Mr. Nuttawut Kongsuwan¹, **Dr. Angela Demetriadou**¹, **Mr. Rohit Chikkaraddy**², **Dr. Felix Benz**², **Dr. Vladimir A Turek**², **Dr. Ulrich F Keyser**², **Prof. Jeremy J Baumberg**², **Prof. Ortwin Hess**¹

1. Imperial College London, 2. University of Cambridge

An emitter in the vicinity of an isolated metal nanoparticle is quenched by its decay through non-radiative channels, leading to a zone of inactivity for emitters placed within <10nm of the nanoparticle. Here we demonstrate that in tightly-coupled plasmonic resonators forming nanocavities quenching is suppressed due to plasmon mixing. Unlike isolated nanoparticles, plasmonic nanocavities show mode hybridization which massively enhances emitter excitation and decay via radiative channels. This creates ideal conditions for realizing and observing single-molecule strong-coupling with plasmons, evident in dynamic Rabi-oscillations and experimentally confirmed by laterally dependent emitter placement through DNA-origami.



1-suppression of quenching in plasmonic nanocavities.png



2-strong-coupling dynamics in plasmonic nanocavities.png

Knife-Edge Method At Nanoscale: Why It Fails And How To Correct It?

Friday, 15th September - 15:38 - Strong light-matter interactions at the nanoscale - Room 207 - Oral - Abstract ID: 426

*Dr. Sergej Orlov*¹

1. Center for Physical Sciences and Technology, Industrial Laboratory for Photonic Technologies

The knife-edge method is an established technique for profiling light beams. As the beams become tighter focused, sizes of their focal spots can be even smaller than the wavelength. Though the cases, when the knife-edge method can reconstruct projections of tightly focused beams, were reported they rather represent an exception than the rule. The knife-edge method at the nanoscale is proven to be exceptionally sensitive to the material choice, geometry of the knife-edges, polarization of the beams and even the choice of the substrates of the knife-pads.

As a rule, two types of distortions are observed for linearly polarized Gaussian beam, see Fig 1 (a): 1) displacement $d_{s,p}$ of the projection from the knife-edge and b) changes in the beamwidths $w_{s,p}$ of the projections. Both distortions are polarisation sensitive. The main cause for the failure of the knife-edge method at the nanoscale is due to the plasmonic interaction of the light with the knife and its edge. A rather large number of interaction scenarios leads to the failure of the knife-edge method at the nanoscale.

Here, we systematically study different knife-edge pad geometries, materials, substrates and collection geometries. Relative shifts $d_{s,p}$ are introduced for higher order HG and LG modes, see Fig. 1 (b) and we can report on the consistency with the cases of a linearly polarized Gaussian beam. We use our previous developments and introduce a set of corrections into the standard knife-edge evaluation method. It seems that an adapted knife-edge reconstruction technique can be successfully developed. Very first attempts to “save” the knife-edge method at the nanoscale are reported here. The algorithm can even account for various aberrations (like koma, astigmatism etc.) introduced by the focussing system.

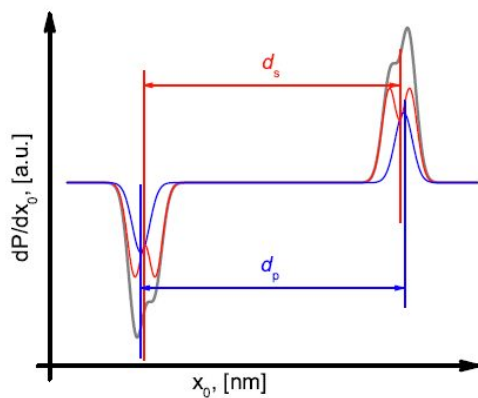


Fig1c.jpg

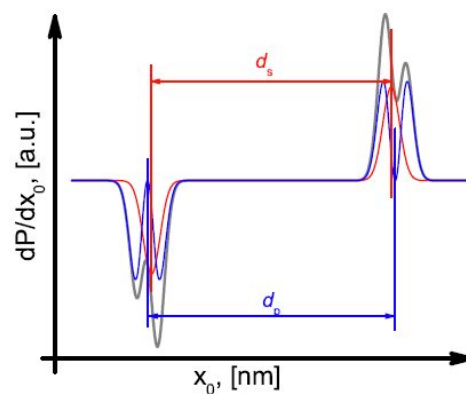


Fig1b.jpg

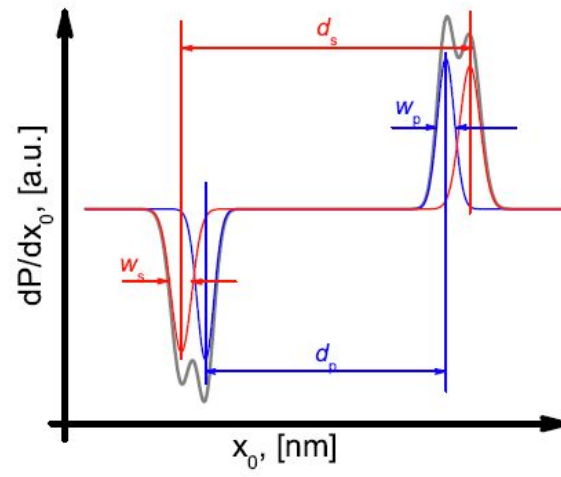


Fig1a.jpg

Hybrid Plasmons in Graphene Nano-slits

Friday, 15th September - 15:55 - Strong light-matter interactions at the nanoscale - Room 207 - Oral - Abstract ID: 490

Mr. Paulo André Gonçalves¹, **Prof. Sanshui Xiao**¹, **Prof. Nuno Peres**², **Prof. N. Asger Mortensen**³

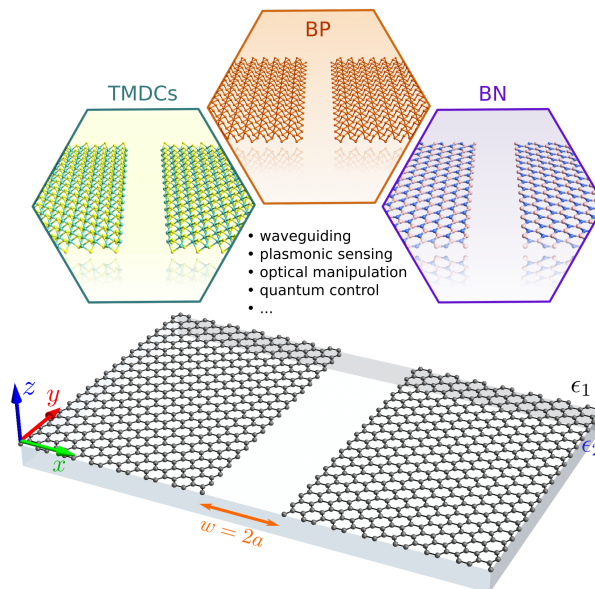
1. Technical University of Denmark, 2. University of Minho, 3. University of Southern Denmark

Introduction: Plasmon coupling and hybridization in complex nanostructures constitutes a fertile playground for controlling light at the nanoscale. Here, we present a semi-analytical model to describe the emergence of hybrid plasmon modes guided along 2D nano-slits. In particular, we find two coupled plasmonic resonances arising from symmetric and antisymmetric hybridizations of the edge plasmons of the constituent half-sheets.

Methods: We develop a semi-analytical model based on the Green's functions and an orthogonal polynomials expansion in order to fully determine the plasmon spectrum and corresponding field distribution of the plasmon modes. We then benchmark our results against full-wave numerical simulations having obtained a very good agreement.

Results: We find a 2D slit antibonding and a bonding mode, lying above and below the energy of the bare edge plasmon. We further compare the plasmons of the nano-slit with those of a nanoribbon (the slit's complementary structure), and compare them with 3D MIM/IMI waveguides.

Discussion: Our treatment is notably generic, being able to account for slits of arbitrary width, and remains valid irrespective of the 2D conductive material (e.g., doped graphene, 2D transition metal dichalcogenides, or black phosphorus).



2d nano-slits.png

Large angle directional beaming control by metal aperture-corrugation structures

Friday, 15th September - 14:30 - Optical properties of nanostructures - Room 412 - Oral - Abstract ID: 287

Dr. Guoguo Kang¹

1. Beijing Institute of Technology

The beaming effect of subwavelength holes and slits has attracted more and more attention since it was first observed. A subwavelength metal aperture with symmetric periodic surface corrugations has an effect of on-axis directional beaming and the effect is attributed to the excitation of surface plasmon polariton (SPP) and its diffraction by the corrugations. Correspondingly, breaking the symmetry of the structure will lead to the off-axis directional beaming effect. But it is difficult to achieve larger angle directional beaming because the radiation field of a subwavelength aperture is not consistent with spherical distribution and the energy is confined to a limited divergence angle. However, the previous reports on the angle control are confined in $\pm 30^\circ$ and seldom approach the limited angle of about $\pm 60^\circ$.

To control the beaming angle, a mathematic model of a metal slit-grating structure is built and calculated with Finite-Difference Time-Domain method. A design methodology is proposed in terms of two aspects: the phase modulation of the light radiated from the surrounding gratings and the reverse process of the SPP wave coupling. The corrugation spacing can be modulated to generate the constructive interference of a specific beaming angle or destructive interference of the angle needed to be weakened. With the designed asymmetric structures, the beaming angle varied in $\pm 60^\circ$ can be achieved, as is shown in the attached figure.

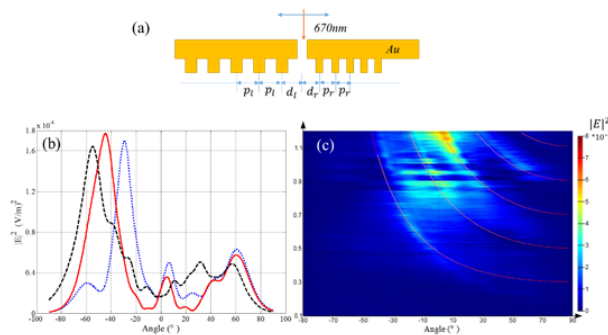


Figure. 1.png

Light controlled conductivity of graphene on photorefractive lithium niobate

Friday, 15th September - 14:47 - Optical properties of nanostructures - Room 412 - Oral - Abstract ID: 435

***Mr. Jon Gorecki*¹, *Dr. Nikitas Papasimakis*¹, *Dr. Sakellaris Mailis*¹, *Dr. Vasilis Apostolopoulos*²**

1. Optoelectronics Research Centre, University of Southampton, 2. University of Southampton

We demonstrate non-volatile control by light of electrical conductivity of graphene deposited on iron doped Lithium Niobate (LN).

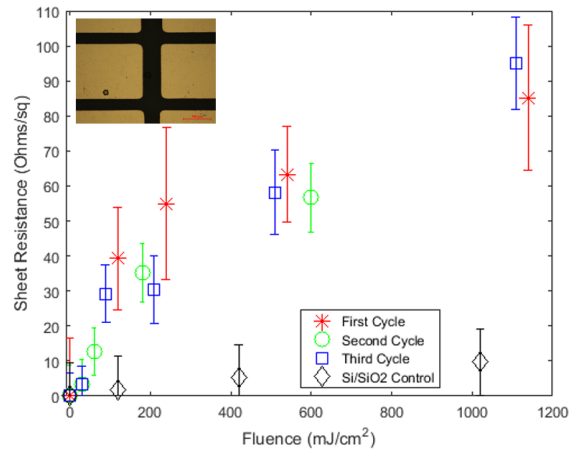
Doped LN under non-uniform illumination exhibits photorefractive behaviour with electrons diffusing from areas of higher light intensity towards darker areas becoming trapped resulting in a non-uniform charge distribution in LN [1]. This distribution can be “erased” by a thermal cycle which redistributes charge carriers.

Here we employ photorefractive effects in LN to control the carrier concentration of graphene. Owing to its atomic thickness, the electronic and optical properties of graphene are controlled by injecting small numbers of charge carriers [2]. Single-layer CVD graphene was deposited on iron doped LN substrates. A graphene on SiO₂/Si control sample was used owing to the absence of photorefractive effect. To measure sheet resistance an array of metallic (Cr/Au 5nm/100nm) electrodes were defined via a shadow-mask (see inset to Fig. 1) at spacings ranging from 50 μm-750μm. The electrodes also act as an illumination mask creating light and dark regions which lead to non-uniform charge distribution in the LN, and therefore to changes in the graphene carrier concentration. In Fig. 1, we show the variation in the sheet resistance of graphene on LN after white light illumination. After final illumination the device is heated to ‘erase’ the charge distribution, this cycle is performed three times. Graphene on LN experiences substantial increase of resistivity. Variation in the graphene/SiO₂/Si control sample was within experimental error. We note during electrical measurements the samples were not illuminated.

In conclusion, we have shown that the electrical properties of graphene can be controlled through light illumination mediated by the presence of a photorefractive LN substrate. Our results provide a route towards local control of charge carrier concentration in graphene and consequently of its electronic and electromagnetic properties. Implications for reconfigurable plasmonics and metamaterials will be discussed at the conference.

[1] K. Buse and E. Kratzig, “Three-valence charge-transport model for explanation of the photorefractive effect”, *Appl. Phys B* 61, 27-32 (1995).

[2] K. S. Novoselov, A. K. Geim, S. V. Morozov, et al. “Electric field effect in atomically thin carbon films,” *Science*. 306, 666-669 (2004).



Graphene on photorefractive substrate.png

Enhancement of light transmission through random copper thin-films near the percolation threshold

Friday, 15th September - 15:04 - Optical properties of nanostructures - Room 412 - Oral - Abstract ID: 271

***Dr. Luis Guillermo Mendoza Luna*¹, *Prof. José Luis Hernández Pozos*¹, *Ms. Eva Mayra Rojas Ruiz*¹**

1. Departamento de Física, Universidad Autónoma Metropolitana Iztapalapa

In this work, we report the absorption and transmission properties of thin copper films deposited on glass slightly below the percolation limit produced by laser ablation; said films are analyzed as a function of the material deposited (measured by the number of pulses). Copper films produced through this method are deposited in a random fashion.

It has been found experimentally that upon approaching the percolation threshold the light experiences an enhancement in transmission, and it is hypothesized that this is due to the surface plasmon polariton of copper; this finding is at odds with the observed transmission of light in related $\text{TiO}_2/\text{Cu}/\text{TiO}_2$ multilayer systems, in which such enhancement does not happen, even though the same amount of copper has been deposited compared to the copper-only samples.

To better understand the observed phenomena, a host of numerical calculations with the open-source DDSCAT software have been carried out to simulate the optical behavior of the copper films: transmission simulations across a set of random islands show an enhancement in transmission consistent with the experiments (similarities and differences between experiment and numerical calculations are discussed); this enhancement is independent of the size of the unit cell; also, when the occupation rate of the islands is varied the qualitative behavior of the transmission is unchanged; simulations with different metals are also analyzed.

Finally, the potential of these films as sensors is explored.

Cathodoluminescence characteristics of light emission properties of axial ZnO/Zn_{1-x}Mg_xO multiple quantum wells on vertical ZnO microrods

Friday, 15th September - 15:21 - Optical properties of nanostructures - Room 412 - Oral - Abstract ID: 178

*Ms. Agnieszka Pieniążek*¹, *Dr. Henryk Teisseyre*², *Mr. Dawid Jarosz*², *Dr. Bartłomiej S. Witkowski*², *Mrs. Anna Reszka*², *Mr. Krzysztof Kopalko*², *Prof. Adrian Kozanecki*², *Prof. Marek Godlewski*², *Prof. Bogdan J. Kowalski*²

1. Institute of Physics, Polish Academy of Sciences, Warsaw, Poland, 2. Institute of Physics PAS

We have fabricated axial ZnO/ZnMgO multiple quantum well (MQW) heterostructures consisting of five ZnO wells with different thicknesses separated by thin ZnMgO barriers on the top of ZnO microrods and investigated the optical properties of such structures by spatially and spectrally resolved cathodoluminescence (CL) spectroscopy and imaging.

ZnO microrods have been prepared by the microwave-assisted hydrothermal method and then overgrown by plasma-assisted molecular beam epitaxy technique which has been employed for control of well widths and compositions of the axial MQW heterostructures.

To study local optical properties, CL spectrum line scans have been recorded for a number of the axial MQW heterostructures. Example of results is seen in Fig. 1(a). The orientation of the line scan is illustrated in Fig. 1(b). The CL line scan shows the spatial distribution of the emission bands with respect to the microrod position. It is visible that the ZnO QWs with different thicknesses and the ZnMgO layers are located on the top end of the microrod. The spectra measured at the bottom of the microrod, where no QW and barrier are present, show only the ZnO emission band at 3.35 eV related to recombination of the donor bound exciton. Relative intensity of the emission bands depends on position in the microrod.

The CL-intensity image of individual MQW heterostructure (Fig. 1(c)) composed of two images taken for the two spectral features (QW and barrier emission) confirms that the ZnMgO barrier is only grown on the top end of the microrods and that nearly no lateral growth of the material along the microrod axis takes place under our growth conditions. Emission at 3.36 eV is localized between the ZnMgO layers and most likely is related to recombination in QW.

In conclusion, the presence of the axial heterostructure grown on the top of ZnO microrods is confirmed by low-temperature CL. Luminescence lines are observed at the spectral positions expected for the QW and barrier emissions from the top part of the microrods.

Terahertz Generation via Excitation of Surface States Formed from Spatially Separated Electrons and Holes in Nanocomposites

Friday, 15th September - 15:38 - Optical properties of nanostructures - Room 412 - Oral - Abstract ID: 191

***Dr. Oleg Khasanov*¹, *Dr. Olga Fedotova*², *Mr. Grigory Rusetsky*², *Dr. Vladimir Gayvoronsky*³, *Prof. Sergey Pokutnyi*⁴, *Dr. Eugenijus Gaizauskas*⁵, *Dr. Virgilijus Vaicaitis*⁵**

1. Scientific-Practical Material Research Centre, NAS of Belarus, 2. Scientific-Practical Material Research Centre, NAS of Belarus, 3. Physics Institute NAS Ukraine, 4. Chuiko Institute of Surface Chemistry, 5. Vilnius University Laser Research Centre

Terahertz (THz) generation in nanocomposites consisted of metal-oxide semiconductor nanocrystals incorporated into a dielectric matrix is studied. We consider the THz emission from excitons formed by spatially separated electron and hole in above nanostructures when the quantum dot (QD) dielectric permittivity is substantially higher than the dielectric matrix one and the QD sizes are large enough. According to our calculations starting from the critical QD radius the electron-hole binding energy asymptotically approach the binding energy of corresponding 2D exciton. Another reason of the large binding energy of the excitonic states is the dielectric enhancement effect originated from the field produced by the nanoparticles in matrix. We study frequency down-conversion processes in nanocomposites with the large permanent dipole moment (PDM). Dielectric matrix is supposed to be non-centrosymmetric and transparent in THz spectral range. We consider THz generation by a femtosecond laser pulse being in resonance with the QDs and out of resonance with dielectric matrix. As a result, the nonlinear polarization response of the medium consists of resonant and non-resonant components. One- and two-photon resonances are under study. The local field effects are also accounted for. The resonant mechanism of down-frequency conversion is shown to be more effective than non-resonant one. As a first step, solitonic regimes of the input pulse propagation and harmonic formation in its field have been studied. The local field and the PDM impact is revealed to modify sufficiently the pump pulse envelope in comparison with hyperbolic secant form. When such influence is weak, the dependence of the THz field on the pump pulse is quadratic. In this case the maximal THz field is observed for pump pulse area $\theta=3\pi$ but its generation efficiency does not exceed 10^{-3} . With increasing the PDM magnitude the underlying two-photon processes modify the pump pulse form to a great extent and lead to stronger dependence providing more efficient frequency conversion. According to our numerical results, for nanocomposites with optimal parameters the THz generation can reach 2% in magnitude under phase capture conditions.

Microstructured photonic polymer membranes for modulation of the reflectivity in the mid infrared

Friday, 15th September - 15:55 - Optical properties of nanostructures - Room 412 - Oral - Abstract ID: 465

Mr. Salim Assaf¹, Ms. Maud Viallon¹, Dr. Alexander Korovin¹, Prof. Yan Pennec², Dr. Anthony Treyzebre¹, Dr. Vincent Thomy¹, Dr. Vincent Senez¹, Dr. Daniel Dupont³, Mr. Michel Caillibotte⁴, Prof. Bahram Djafari-rouhani²

1. Institut d'Electronique, de Micro-électronique et de Nanotechnologie, UMR CNRS 8520, Cité Scientifique, 59652 Villeneuve d'Ascq Cedex, 2. Institut d'Electronique, de Micro-électronique et de Nanotechnologie, UMR CNRS 8520, Université de Lille, Cité Scientifique, 59652 Villeneuve d'Ascq Cedex, 3. HEI, 13 Rue de Toul, 59800 Lille, 4. Société DAMART, Lille

Recently, photonic crystals (PC) have attracted much attention in several fields of applications like in photovoltaic or optomechanic, and various implementations have been tested using either silicon or polysilicon. Our goal is to develop a polymer based photonic membrane to control heat losses through radiative exchange in the mid infrared (MIR) range for applications such as wearable textiles, building insulation or food packaging.

We first studied numerically and experimentally silicon based PC, constituted of either ridges or holes, with dimensions of the lattice parameter about tens microns. These structures have been simulated with numerical models (finite differences and finite elements methods) and characterized in the 5-15 μm range. Various geometries have been studied to understand the effects of the geometry on the reflective spectrum of the silicon membrane. An experimental comparison of the spectra has been done with a good agreement.

We then investigate the case of a microstructured polymer membrane of benzocyclobutene (BCB) in the MIR. Numerical simulations have been undergone in order to study the influence of the geometry on the reflectivity. These membranes show narrow Fano's type bands presenting high reflectivity together with Fabry-Perot oscillations. The efficiency of the various designs is compared by integrating the reflected energy on 5-15 μm spectrum divided by the energy produces by a black body in the same spectrum. The following figure represents the evolution of the efficiency as a function of the diameters of the air holes in the membrane and for different periods of the photonic lattice. One can clearly see that the variation of the diameter induces a modulation of the efficiency.

This work permits to quantify the efficiency of the polymer membranes and paves the way for the design of a smart responsive membrane which modifies its reflectance in response to external stimuli like temperature or the embedded medium.

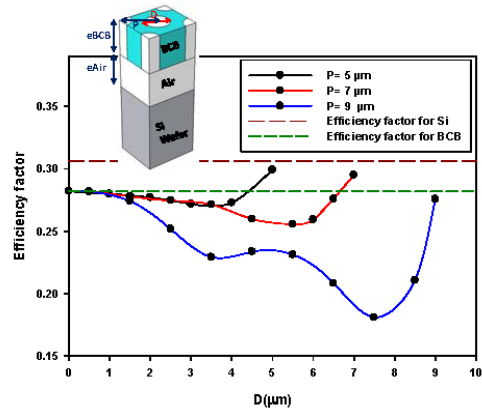


Figure: Evolution of the efficiency rate as a function of the radius of the air holes drilled inside a polymer BCB membrane for different periods.

Fig1.png

Gain Media In Plasmonic Nanostructures: From Superradiance To Lasing

Friday, 15th September - 16:40 - Photonic & plasmonic nanomaterials - Auditorium - Oral - Abstract ID: 110

Dr. Renaud Vallée¹, Dr. Pierre Fauché², Dr. Atsushi Yamada³, Prof. Daniel Neuhauser⁴, Prof. Brahim Lounis²

1. University of Bordeaux, Centre de Recherche Paul Pascal, 2. University of Bordeaux, 3. Kent State University, 4. University of California, Los Angeles

Hybridisation of quantum emitters and plasmonic nano-structures has attracted much attention over the last years, due to their interest in the design of plasmon-based nano-lasers [1,2] or to achieve long-range qubit entanglement [3,4]. Recent theoretical studies [5,6] suggest a plasmonic super-radiant mechanism to increase the rate of emitters, similar to Dicke super-radiance [7].

1. In this work, we provide experimental evidence of plasmonic super-radiance of organic emitters close to a metal nanosphere at room temperature. A silica shell acts as a spacer between the grafted emitters and the Au core. A single particle study performed on 1400 nanohybrids with controlled core sizes, spacers and numbers of grafted emitters shows that the emission rate dramatically increases with the numbers of emitters and as the emitters get closer to the core. This observation of plasmonic superradiance at room temperature opens questions about the robustness of these collective states against decoherence mechanisms which are of major interest for potential applications.
2. We propose a new type of nanodevice, capable of both path-selectivity and anisotropic lasing that is based on loss-compensation and amplification by a localized plasmon polariton. The nano-device is a Y-shaped plasmonic nanostructure embedded in an anisotropic host medium with gain. The anisotropy leads to the path selectivity, an effect which is more pronounced once gain is included. Such a device is potentially realizable via bottom-up techniques. The path-selectivity may be coupled with activation of a rotation of the anisotropic host medium for inducing a light-guiding switching functionality.

References

[1] J.G. Bohnet et al. *Nature***484**, 78–81(2012). [2] M.A. Noginov et al., *Nature***460**,1110–2 (2009). [3] R. Kolesov et al., *Nature Physics***5**,470–474 (2009).[4] A. Gonzalez-Tudela et al., *Phys. Rev. Lett.***106**, 020501 (2011).[5] V.N. Pustovit et al., *Phys. Rev. Lett.***102**, 077401 (2009).[6] D. Martín-Cano et al., *Nano Letters***10**, 3129–3134(2010).[7] R.H. Dicke. *Phys. Rev.***93**, 99-110 (1954).

NanoPlasmonic Sensing spectroscopy as a novel route for monitoring CH₃NH₃PbI₃ perovskite formation in mesoporous TiO₂ films

Friday, 15th September - 16:57 - Photonic & plasmonic nanomaterials - Auditorium - Oral - Abstract ID: 286

*Dr. Fahd Rajab*¹, *Prof. Farid Harraz*¹

1. Najran University

Here, we demonstrate a facile formation-controllable sequential deposition of CH₃NH₃PbI₃ perovskite within a mesoporous TiO₂ film by using a novel route of NanoPlasmonic Sensing (NPS). In-splorion Sensors, with plasmonic Au nanodisks (diameter: 100 nm; height: 20 nm) with 10 nm dense layer of compact TiO₂ were initially spin coated with a mesoporous TiO₂ films (~350 nm -650 nm thickness and particle size <20 nm). The mesoporous TiO₂ films were infiltrated with PbI₂ solution by spin coating. For the in situ monitoring of perovskite formation, different concentrations of CH₃NH₃I at different operating temperatures were introduced into the above Au sensors/compact TiO₂/mesoporous TiO₂/PbI₂. The dynamics of CH₃NH₃PbI₃ perovskite formation at the lower interface of the mesoporous TiO₂ films can be monitored with this approach via the time-resolved spectral shifts of the Localized Surface Plasmon Resonance (LSPR) peak induced by the embedded plasmonic Au sensors. X-ray diffraction (XRD), scanning electron microscopy (SEM) and photoluminescence (PL) measurements were further used to confirm the perovskite formation. This study suggests the viability of the current, developed experimental NPS approach for precise control of the standard two-step sequential solution deposition of CH₃NH₃PbI₃ perovskite, and thus to further improve the performance of photovoltaic and light-emitting based devices. In a broader context, it would offer a unique opportunity to detect minute local changes of several materials of interest at the localized interfaces either in solid or mesoporous systems.

Nanomechanical membrane resonator as a novel platform for the detection and analysis of FEBID plasmonic nanostructures

Friday, 15th September - 17:14 - Photonic & plasmonic nanomaterials - Auditorium - Oral - Abstract ID: 369

Ms. Miao-Hsuan Chien¹, Dr. Mostafa Shawrav¹, Dr. Heinz Wanzenboeck², Prof. Silvan Schmid¹

1. Micro and Nanosensors group, Institute of Sensor and Actuator Systems, TU Wien, 2. Bionanobeam group, Institute of Solid State Electronics, TU WIEN

Localized surface plasmon resonance (LSPR) in nanostructures has been extensively studied during the last decades due to its remarkable optical properties. The understanding and analysis of LSPR in various nanostructures is important for the optimizations of devices. Focused electron beam induced deposition (FEBID) is a mask-free, resist-free direct write additive nanofabrication method where noble metal plasmonic nanostructures can be deposited in-situ in a single process step with minimum limitation on geometry and with high purity. In this work, as a proof of principle, nano-ellipsoids were deposited on a 50 nm-thick rectangular silicon-rich silicon nitride membrane using 3 kV acceleration voltage and 1 nA beam current. A LEO 1530 VP SEM with home-built gas injection system was used to inject precursors inside the system. By exploiting the thermoplasmonic effect of nanostructures, we use a nanomechanical membrane resonator as a novel optical detection scheme for the experimental analysis of LSPR, as shown in figure 1. The FEBID nano-ellipsoids on membrane resonator are scanned with a 633 nm pumping laser with linear polarization to investigate the effects of aspect ratio and orientation on LSPR. During scanning, the excitation of LSPR in the nano-ellipsoids results in a heat influx into the membrane. The heating-induced detuning of the membrane resonance frequency was monitored with a laser Doppler vibrometer incorporated with a phase-locked loop. The results in figure 2 demonstrate the corresponding relative frequency detuning in the membrane resonator caused by the specific absorption cross-section of nano-ellipsoids with different aspect ratio and orientation. Due to the red-shift of LSPR with increasing aspect ratio of nano-ellipsoids, the enhanced absorption at 633 nm in high aspect ratio nano-ellipsoids results in larger relative frequency shift. The effect of nano-ellipsoid orientation relative to polarization is also observable. With the current setup, we are able to detect a dissipated power of 300 fW, which result in extremely high signal-to-noise ratio in plasmonic nanostructure with LSPR around VIS-NIR regime even with small pumping powers of only 300 μ W. With this new plasmonic characterization technique, in combination with FEBID, LSPR with various nanostructures can easily be investigated with almost no limitation in geometry.

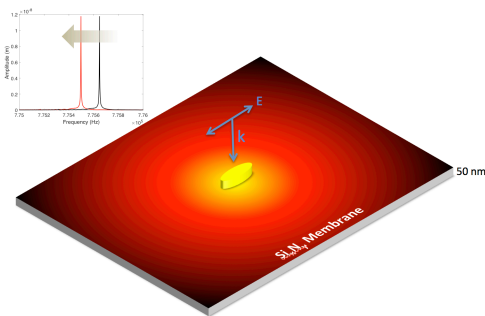


Fig1.png

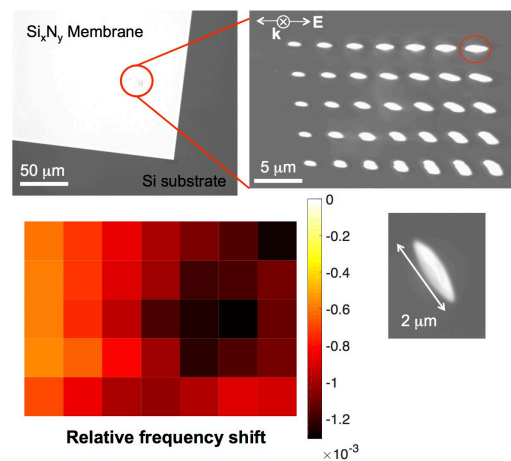


Fig2.jpg

Transmission of optical signals in coupled cavity resonators based on quasi-one-dimensional periodic nanobeam based structures

Friday, 15th September - 17:31 - Photonic & plasmonic nanomaterials - Auditorium - Oral - Abstract ID: 457

Dr. Alexander Korovin¹, Prof. Yan Pennec¹, Prof. Bahram Djafari-rouhani¹

1. Institut d'Electronique, de Micro-électronique et de Nanotechnologie, UMR CNRS 8520, Université de Lille, Cité Scientifique, 59652 Villeneuve d'Ascq Cedex

Recently, phononic and photonic properties have been combined into one platform that provided a new tool for controlling light and sound simultaneously. Such artificial materials are called phoXonic or optomechanical crystals. Recently, a structure consisting of a corrugated nanobeam containing an array of holes in the middle and an array of rectangular plugs from the side was proposed. Detailed development of photonic modes and its interaction is necessary for the implementation of chip photon/phonon networks.

We study here the coupling between two silicon nanobeams with a quasi-periodic system of holes with single defects forming cavity resonances in the photonic bandgap. Using 3D-FDTD simulations, two configurations of “side-by-side” or “top-on-top” nanobeams were studied (**Fig.1**) by changing periodic arrays supporting mirror or scattering properties of the photonic structure for the transfer of the incoming TE-polarized wave from the first nanobeam input (red-port) to the output of the second (blue-port). **Fig.2(a,b)** present transmission spectra at the exit (port-blue) corresponding to a sharp transmission inside the photonic bandgap of the perfect structure that comes from a complex process including the excitation, the coupling and the transfer of the incoming wave based on the two modes localized inside the cavities (green arrows). As it follows from **Fig.2(a,b)** excitation/coupling/transfer process of the optical signal is more efficient in the “top-on-top” configuration and the output signal quickly falls down by increasing the air gap from 0.5 μm to 1.5 μm . The vertical air gap decreasing from 500nm to 300nm in the “top-on-top” configuration (**Fig.2c**) leads to clearly observable mode splitting on symmetric and antisymmetric states. In addition, the efficiency of the transferred splitted signal can be improved by increasing of number of perfect cells forming the Bragg mirror along unwanted directions of propagation (**Fig.2d**).

We show that the coupling condition between two nanobeams plays a crucial role in the process of excitation and transfer of an incident optical signal. The results of the coupling allow to the tunability of both frequency and quality factors that can be used in the design of chip based cavity optical or optomechanical devices for further applications in sensing, metrology, and quantum information science.

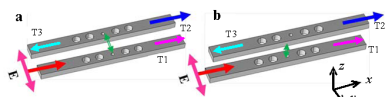


Fig. 1: Coupling of photonic cavity modes in 'side by side' (a) and 'top on top' (b) configurations of quasi 1D-periodic system of holes with single defect (central hole with different diameter).

Fig1.png

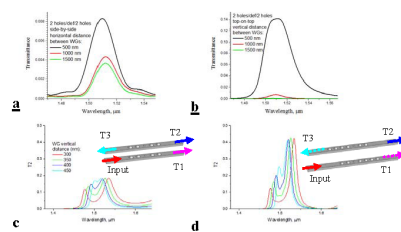


Fig. 2: (a, b) Guided mode transmittance spectra in the second nanobeam (blue port) for various nanobeam distances in the case of the two configurations “side-by-side” (a) and “top-on-top” (b). (c,d) Observation of the splitting of the transferred mode in the case of “top-on-top” configuration for low distances between the nanobeams. (d) coincides with (c) with different conditions of the Bragg mirror to avoid propagation to the ports T1 and T3 (the number of perfect cells is increased in these directions).

Fig2.png

Accurate detection of resonance by monitoring wavepacket width

Friday, 15th September - 16:40 - Enhanced spectroscopy and sensing - Room 207 - Oral - Abstract ID: 344

Dr. Rémi Pollès¹, Dr. Martine Mihailovic¹, Prof. Emmanuel Centeno¹, Dr. Antoine Moreau¹

1. Université Clermont Auvergne

Surface Plasmon Resonances (SPR) are detected through the dip they provoke in the reflection coefficient of a light beam send in a prism coupler. The reflected beam has two components (i) the part that is reflected by the prism-metal interface and (ii) the part coming from the surface plasmon itself, leaking back trough the prism. One would thus expect a distortion of the reflected beam, characterized at resonance by a lateral shift and a change in the beam width.

Studying this phenomenon, we came to the surprising conclusion that while the beam should indeed be larger off resonance, it is theoretically narrower exactly at resonance. At resonance, the beam reflected by the bottom of the prism out of phase with the leakage coming from the surface plasmon. When the incident beam is narrow, the two components do not overlap, which actually results in a lateral shift of the beam and in a larger reflected beam. But when the incident beam is large, the two components overlap and interfere destructively. This counter intuitive phenomenon can be difficult to detect when the beam is very large, but we have shown that in the right conditions the reflected beam can be 10% narrower at resonance, a feature easy to measure.

It is particularly interesting to notice that, even slightly off resonance, the beam is larger, so that the change in the beam width occurs on a very narrow angular range. Monitoring the change is the width of the reflected beam can thus allow to measure more precisely the position of the resonance, than monitoring the reflection coefficient - thus improving the resolution of the SPR device. This is all the more interesting as SPR apparatus are reaching their theoretical limits in terms of resolution. Using this technique could allow to overcome these problem.

We finally underline that this phenomenon occurs not only in the case of SPR. Our conclusions can be extended to wave packets in general, even temporal ones, and are not limited to plasmonics.

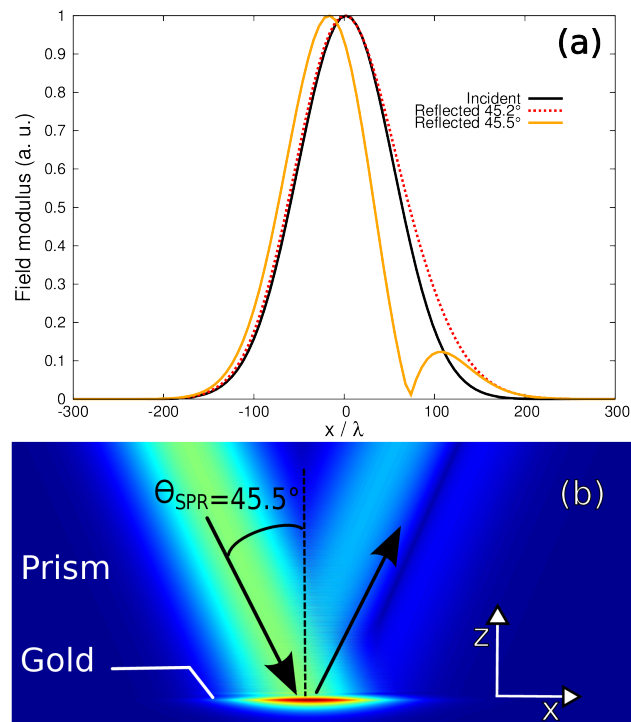


Figure.png

Non-plasmonic nanoparticle heaters with temperature control

Friday, 15th September - 16:57 - Enhanced spectroscopy and sensing - Room 207 - Oral - Abstract ID: 383

Mr. George Zograf¹, Dr. Mihail Petrov², Dr. Dmitriy Zuev¹, Dr. Valentin Milichko¹, Dr. Sergey Makarov¹, Prof. Pavel Belov¹

1. Department of Nanophotonics and Metamaterials, ITMO University, 2. ITMO University

There is a wide range of modern applications where use of the nanoscale heaters are of great importance, such as photochemistry, photocatalysis, photothermal therapy and biosensing. The plasmonic nanoparticles are considered as the most efficient heat sources, and the heating is achieved through the excitation of the localized surface plasmon resonance in metal nanospheres, nanorods, nanoshells and others. However, in order to preserve nanoparticles from temperature overheating and even melting the precise temperature control is needed. This is a challenging problem to solve with plasmonic nanoparticles, and it often requires additional thermal sensors. To overcome this limitation, and to expand the applicability of nanoscale heaters, we propose novel non-plasmonic heating approach. It uses non-metallic crystalline nanoparticles, for example silicon, which in contrast to metals silicon has active optical phonon modes Raman, which are suitable for nanoscale thermometry, due to the thermal shift of the Raman frequency. There are several advantages of using silicon structures, as it has a melting point above 1500 K, and nanosized silicon particles possess resonant Mie optical modes (see measured scattering spectrum of 260 nm silicon spherical particle shown in Fig. 1).

In this work, we experimentally and theoretically demonstrate that in some cases silicon nanoparticles may be more effective than the heating plasmonic nanoparticles and can be heated up to 900 K under moderate laser power [Zograf, G. P., et. al. *Nano Letters*, 17(5), 2945–2952 (2017)]. This is provided by the resonant excitation of Mie modes in silicon nanoparticles, which results in strong resonant temperature increase under 632 nm CW laser excitation. In spite of the low level of optical losses, the concentration of Mie modes inside nanoparticles and large mode volume comparing to plasmonic modes results in effective light-to-heat conversion. Moreover, we have experimentally demonstrated the possibility of precise optical temperature detection simultaneously with optical heating of silicon nanoparticles, which also allows for nanoscale spatial temperature mapping with Raman spectroscopy. The efficiency of other non-plasmonic materials for potential optical heating purposes is discussed in the work as well.

Our results pave the way for a new non-plasmonic approach to nanoscale heating with temperature feedback.

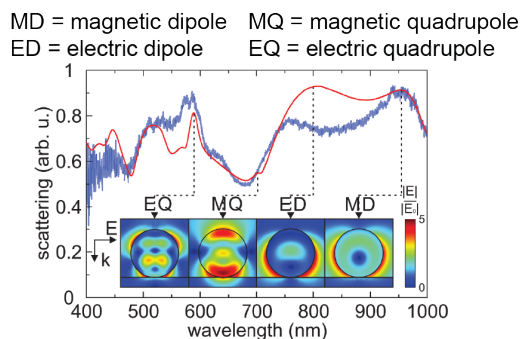


Fig1.png

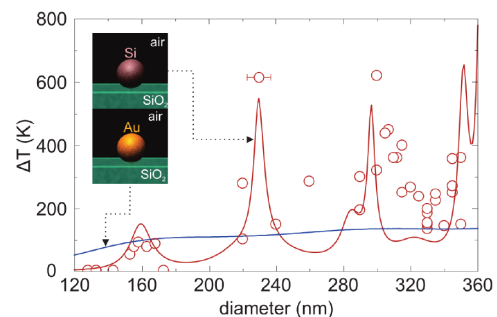


Fig2.png

Dielectric nanoantennas for surface-enhanced fluorescence spectroscopy and efficient harmonic generation

Friday, 15th September - 17:14 - Enhanced spectroscopy and sensing - Room 207 - Oral - Abstract ID: 224

Dr. Gustavo Grinblat¹, **Dr. Yi Li**¹, **Mr. Toshihiko Shibanuma**¹, **Mr. Javier Cambiasso**¹, **Dr. Michael Nielsen**¹, **Dr. Emiliano Cortes**¹, **Dr. Pablo Albella**¹, **Dr. Aliaksandra Rakovich**¹, **Dr. Rupert F Oulton**¹,
Prof. Stefan Maier¹

1. Imperial College London

Dielectric nanoantennas have recently emerged as promising alternative candidates to plasmonic systems in the visible range.^{1,2} When excited above their bandgap energies, high-refractive-index dielectric nanostructures can highly concentrate electric and magnetic fields within subwavelength volumes while presenting ultra-low absorption compared to metals.³ In particular, by locally enhancing the incident light intensity, dielectric nanoantennas are expected not only to produce negligible heating, but also boost nonlinear phenomena and surface-enhanced spectroscopies, since their efficiencies increase with the excitation density.

In this presentation, GaP and Ge nanoantennas will be introduced as promising nanosystems for surface-enhanced fluorescence and second and third harmonic generation on the nanoscale at visible wavelengths.³⁻⁵ Fluorescence enhancement factors of over 3000 and harmonic conversion efficiencies of 10⁻³% will be demonstrated for suitably engineered dielectric nanostructures. Finally, hybrid dielectric/metallic Si/Au nanoantennas will also be analyzed.⁶

¹Albella, P.; Poyli, M. A.; Schmidt, M. K.; Maier, S. A.; Moreno, F.; Sáenz, J. J.; Aizpurua, J. *J. Phys. Chem. C* **2013**, *117*, 13573-13584.

²Shorokhov, A. S.; Melik-Gaykazyan, E. V.; Smirnova, D. A.; Hopkins, B.; Chong, K. E.; Choi, D. Y.; Shcherbakov, M. R.; Miroshnichenko, A. E.; Neshev, D. N.; Fedyanin, A. A.; Kivshar, Y. S. *Nano Lett.* **2016**, *16*, 4857-4861.

³Grinblat, G.; Li, Y.; Nielsen, M., Oulton R. F.; Maier S. A. *Nano Lett.* **2016**, *16*, 4635-4640.

⁴Grinblat, G.; Li, Y.; Nielsen, M., Oulton R. F.; Maier S. A. *ACS Nano* **2017**, *11*, 953-960.

⁵ Cambiasso, J.; Grinblat, G.; Li, Yi.; Rakovich, A.; Cortés, E.; Maier, S. A. *Nano Lett.* **2017**, *17*, 1219-1225.

⁶ Shibanuma, T.; Grinblat, G.; Albella, P.; Maier S. A. *Nano Lett.* **2017**, DOI: 10.1021/acs.nanolett.7b00462.

Plasmon Voltammetry to Sense pH-dependent Surface Oxidation of Gold

Friday, 15th September - 17:31 - Enhanced spectroscopy and sensing - Room 207 - Oral - Abstract ID: 317

***Mr. Bernhard Steinhauser*¹, *Dr. Cynthia Vidal*¹, *Mrs. Ruxandra-Aida Barb*¹, *Prof. Johannes Heitz*¹,
*Dr. Calin Hrelescu*¹, *Prof. Thomas Klar*¹**

1. Johannes Kepler University Linz - Institute of Applied Physics

Extraordinary chemical stability and unique optical properties render gold as excellent material for all kinds of plasmonic sensing applications. These attributes allowed the development of localized plasmon voltammetry (LPV), where the optical response of a plasmonic nanostructure is monitored while applying an electrochemical potential sweep. This technique is capable to optically detect the electrochemical charging of plasmonic nanostructures as well as the adsorption of ionic species. However, for large electrochemical potentials, the region of stability of elemental gold is exceeded and gold oxides are formed on the surface. As plasmonic sensing is based on the dielectric properties of the interface region, it is of great necessity to investigate the plasmonic response during surface oxide formation.

Therefore, we report LPV measurements on a plasmonic gold nanowire array with electrolytes of different pH values. The plasmonic gold nanowire arrays are produced by oblique evaporation of gold on a nanostructured poly-ethylene terephthalate foil. The plasmonic nanowires exhibit transverse localized plasmon resonance modes at a resonance wavelength of ca. 800nm and are used as nanometer-sized working electrodes in an electrochemical three electrode cell.

To correlate the optical response with redox processes we concurrently measure the electrical current through the electrochemical cell. By changing the pH values of the electrolyte solutions, we tune the oxidation and reduction potentials of the gold redox system. We observe an excellent agreement for the oxidation and reduction potentials determined optically with the LPV method or with the current measured by cyclic voltammetry for all tested pH values.

Furthermore, we apply electrochemical potentials that exceed the applicable potential region for electrical current measurements in aqueous solutions, i.e. potentials where currents from the formation of elemental hydrogen and oxygen gas cover currents originating from other sources. Our results show that the evolution of gaseous species has little to no influence on optical signals detected by the LPV method. Moreover, they reveal an additional redox reaction happening on the plasmonic electrode.

[1] Dondapati et.al. *Nano Lett.*,2012,12(3),1247

[2] Dahlin et.al. *Nanoscale*,2012,4,2339

[3] Brown et.al. *ACS Photonics*,2015,2(4),459

[4] Byers et.al. *Nano Lett*,2016,16(4),2314

Broadening effects of absorption and emission bands in InP/ZnS quantum dots

Friday, 15th September - 16:40 - Optical properties of nanostructures - Room 412 - Oral - Abstract ID: 367

Mr. Sergey Savchenko¹, **Dr. Alexander Vokhmintsev**¹, **Prof. Ilya Weinstein**¹

1. Ural Federal University, NANOTECH Centre

Colloidal core/shell quantum dots (QD) based on non-toxic indium phosphide surrounded by more widegap zinc sulphide are being extensively investigated [1]. At the same time, the effect of temperature on the optical properties of InP/ZnS nanocrystals remains insufficiently studied both from the standpoint of experimental analysis and consistent theoretical justifications [2]. This work aims to investigate temperature behavior of optical absorption (OA) and photoluminescence (PL) spectra of InP/ZnS QD in the range of 6.5-296 K.

Two colloidal samples of 2.1 nm (QD-1) and 2.3 nm (QD-2) average sizes capped with modified polyacrylic acid (Research Institute of Applied Acoustics, Dubna) were studied. Control, change and monitoring of temperature were carried out by means of a CCS-100/204N model Janis closed cycle refrigerator system and Model 335 controller. OA spectra were measured using the module integrated in Shimadzu UV-2450 spectrophotometer. To detect PL response under UV LED excitation the module was coupled with Andor Technology Shamrock SR-303i-B spectrograph and Newton^{EM}DU-970P-BV-602 CCD-camera.

The OA spectra at 296 K feature the first exciton absorption bands of InP with the energies of 2.60 (QD-1) and 2.38 (QD-2) eV determined by the second-order derivative technique. Blueshift of the bands upon cooling is analyzed by virtue of the formalism assuming efficient exciton-phonon interaction. FWHM of the first exciton absorption band are found to be temperature-independent (Fig.1). Numerical simulation shows that FWHM of resulting band for the dots ensemble does not vary with temperature changes of Gaussian spectral components (shift, broadening, area) for the individual nanocrystals allowing for its distributions in size, shape etc. The calculated model parameters are analyzed based on comparison with independent data for bulk crystals and QDs. It is observed that PL spectra represents asymmetrical bands at 2.32 (QD-1) and 2.14 (QD-2) eV. Intensity of the exciton PL bands increases by a factor of 7 when cooled. Simultaneously the spectra reveal hidden components which intensity rises more than 15 times (Fig.2). Mechanisms of the observed luminescence and band broadening effects in the InP/ZnS quantum dots are discussed.

[1] S.S.Savchenko, A.S.Vokhmintsev, I.A.Weinstein, J.Phys.:Conf.Series, 741, 012151 (2016).

[2] S.S.Savchenko, A.S.Vokhmintsev, I.A.Weinstein, Opt.Mater.Express, 7, 354 (2017).

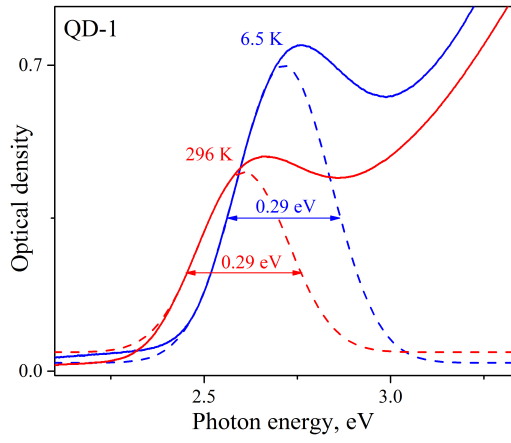


Figure 1. inhomogeneous broadening of the qd-1 first exciton absorption band. solid lines experimental results dash lines gaussian approximations.jpg

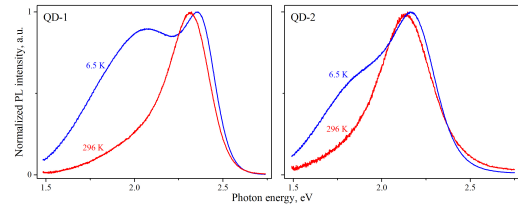


Figure 2. normalized pl spectra of the qds under study.jpg

Multi-color luminescent ZnO nanoparticles produced by pulsed laser ablation in water

Friday, 15th September - 16:57 - Optical properties of nanostructures - Room 412 - Oral - Abstract ID: 184

***Prof. Marco Cannas*¹, *Dr. Pietro Camarda*¹, *Dr. Lavinia Vaccaro*¹, *Dr. Fabrizio Messina*¹, *Dr. Gianpiero Buscarino*¹, *Prof. Simonpietro Agnello*¹, *Prof. Franco Gelardi*¹**

1. Department of Physics and Chemistry, University of Palermo

One of the most intriguing challenges of nanophotonics is the development of materials with controlled physical/chemical properties favorable for highly efficient and color tunable lighting. To this purpose, ZnO is a material of choice: the direct bandgap ($E_g=3.4$ eV) and the large exciton-binding energy (60 meV) allow the observation of an UV emission even at room temperature; in addition, defects in the ZnO network introduce deep-levels in the forbidden band thus originating different colors emission. One of the most versatile methods to synthesize ZnO nanoparticles with specific defects is the pulsed laser ablation in liquid (PLAL); the ablation conditions that determine the end product are indeed dependent both on laser and liquid parameters. In this work, we used two pulsed laser sources, ns Nd:YAG (1064 nm) and fs Ti:Sapphire (800 nm), to irradiate a Zn target immersed in water, by which ZnO wurtzite nanocrystals result from the Zn oxidation [1]. Photoluminescence was investigated by time-resolved spectra acquired under a tunable laser excitation. We observed three PL bands that are excited by band-to-band transition: the first, peaked at 3.3 eV and decaying in a sub-ns timescale, is due to the excitonic recombination; the second, centered at 2.3 eV and decaying in μ s-ms, is associated with oxygen vacancies [2]; the third, centered at 2.8 eV and decaying in ns, is peculiar to ZnO produced by fs PLAL, its origin being unclear yet. These results are promising in view to the realization of multi-color ZnO nanosystems thus increasing their application in lighting technologies

References

- [1] P. Camarda, L. Vaccaro, F. Messina, and M. Cannas, *Appl. Phys. Lett.*, 107 (2015) 013103.
- [2] P. Camarda, F. Messina, L. Vaccaro, S. Agnello, G. Buscarino, R. Schneider, R. Popescu, D. Gerthsen, R. Lorenzi, F. M. Gelardi, and M. Cannas, *Phys. Chem. Chem. Phys.*, 18 (2016) 16237.

Silicon Oxycarbide Waveguides for Photonics Applications

Friday, 15th September - 17:14 - Optical properties of nanostructures - Room 412 - Oral - Abstract ID: 448

***Dr. Faisal Ahmed Memon*¹, *Dr. Francesco Morichetti*², *Prof. Andrea Melloni*²**

1. Politecnico di Milano Italy, Mehran University of Engineering & Technology Jamshoro Pakistan, 2. Politecnico di Milano Italy

The photonics technology has seen a dramatic growth over the past decades. Several material platforms have been explored to cater day-to-day needs of the integrated optics industry. However, the well-established platforms such as SiO₂, SiN, Si, and InP are limited in their refractive index tunability. Silicon oxycarbide (SiOC), on the other hand, has a potential of wide refractive index tunability extending from silica to silicon carbide.

In the present work, comprehensive study of silicon oxycarbide (SiOC) films prepared with reactive rf magnetron sputtering and the use of SiOC as a core material for optical waveguides have been demonstrated for the very first time. Thanks to the refractive index tunability (1.45 to 3.0) and lower extinction coefficient offered by SiOC in the near-infrared spectrum, development of a range of passive optical devices is possible on a single material platform.

We have fabricated channel waveguides with SiOC core using UV photolithography and reactive ion etching techniques. SiOC cores with two high index values, $n = 1.578$ and 1.82 at 1550 nm, have been buried in SiO₂ giving a high index contrast optical waveguides (8% and 18%) respectively.

The SiOC waveguides have been characterized at telecom wavelength 1550 nm and propagation losses of 0.4 dB/mm and 0.8 dB/mm are estimated for two high contrast SiOC waveguides, respectively. Using the dispersion information from ellipsometry, the group dispersion of the optical waveguides has been estimated that agrees with experimental results.

In conclusion, we have been successful in demonstrating SiOC films characteristics and fabricating photonic waveguides with two high refractive indices. Our study solves the problem of refractive index tunable optical material providing acceptable losses in the telecom wavelength range and opens a door for the use of SiOC as a potential candidate in integrated optics.

Demultiplexing surface waves with silicon nanoantennas

Friday, 15th September - 17:31 - Optical properties of nanostructures - Room 412 - Oral - Abstract ID: 423

***Mr. Ivan Sinev*¹, *Dr. Andrey Bogdanov*¹, *Mr. Filipp Komissarenko*², *Ms. Kristina Frizyuk*¹, *Dr. Mihail Petrov*¹, *Dr. Ivan Mukhin*², *Dr. Sergey Makarov*³, *Dr. Anton Samusev*¹, *Prof. Andrei Lavrinenko*⁴, *Dr. Ivan Iorsh*¹**

1. ITMO University, 2. ITMO University; St. Petersburg Academic University, 3. Department of Nanophotonics and Metamaterials, ITMO University, 4. Technical University of Denmark; ITMO University

One of the crucial building blocks for optical devices operating in 2D is a spectral demultiplexer, which allow simultaneous operation at multiple wavelengths, thus dramatically accelerating the performance of the integrated photonic circuit. Usually, excitation of surface waves as well as their demultiplexing is performed using 1D and 2D structures like gratings, structured nanoslits, or arrays of nanoholes. However, severely limited amount of space available on a modern integrated optical circuit calls for using more compact structures for surface waves excitation and routing.

In this work, we reveal that a very basic dielectric nanoantenna (silicon nanosphere) provides unmatched performance serving as a highly efficient source and spectral demultiplexer for surface plasmon polaritons (SPPs). The unique opportunities for manipulation of directivity pattern of SPP are delivered by mutual interference of inherently strong electric and magnetic dipole resonances of the dielectric nanoparticle. Using analytical approach based on Green function and measurements with leakage radiation microscopy integrated with Fourier plane imaging optics, we predict and demonstrate experimentally the rapid switching between directional forward and backward excitation of SPP by silicon nanosphere on gold substrate within extremely narrow (<50 nm) spectral band. Importantly, inherently strong magnetic dipole response of the silicon particle provides extremely efficient excitation of a SPP wave, whereas mutual interference of the electric and magnetic dipole resonances of the nanoantenna provides high front-to-back ratio contrast and directivity values for the excited surface waves.

The theoretical framework that we formulate to describe the physics behind the observed phenomena can be easily extended to more complex interfaces supporting other types of surface waves. Furthermore, the combination of tunability of the nanoantenna radiation pattern that we demonstrate here and dispersion engineering of states supported by a 2D interface would be an important step forward to efficient routing of surface waves.

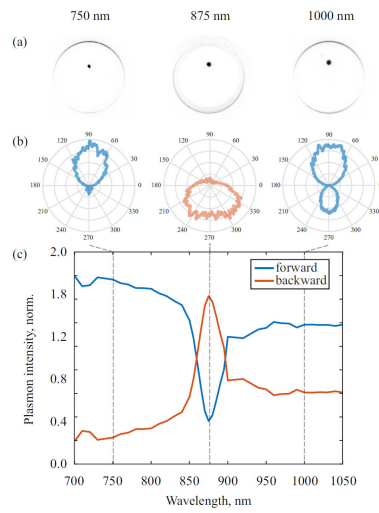


Fig. 1: (a) (False color) Fourier plane images of SPP excited by a 275 nm silicon nanosphere on 40 nm gold layer at 750, 875 and 1000 nm wavelengths. (b) SPP directivity patterns reconstructed from the measured Fourier images. (c) Spectral dependence of forward and backward SPP intensity demonstrating fast switching between SPP excitation directions. The wavelengths corresponding to data presented in (a,b) are marked with dashed lines.

Spp from si sphere - experiment.jpg

Multiple Spherical Reactor

Friday, 15th September - 19:00 - Video Presentation - Online - Video - Abstract ID: 204

Prof. Humberto Ramirez Hernandez¹, **Prof. Francisco Espinosa**², **Prof. Salvador Fernandez Tavizon**³,
Prof. Alfonso Mercado³, **Prof. Armando Zaragoza**²

1. CIMAV, 2. CIMAV (Center for Advanced Materials Research), 3. CIQA (Center for Research in Applied Chemistry)

Introduction

It is a pilot system for the synthesis of carbon nanostructures that can be scalable to fit the production needs of such nanostructures.

Methods

One of the improvements in its usefulness is that studies were also carried out on the use of graphite powder in MSR tubes, the efficiency of the synthesis and especially the synthesis time, and practically avoid the control system of the bars of Graphite to maintain constant the distance of the plasma arc in the MRS which will consist of a multiple Spherical reactor (MSR) graphite electrode bar; It can work with many graphite electrodes simultaneously; But the distance on all electrodes must be kept constant. It will be placed on the secondary coil or by multiple operators; In the case of a larger coil voltage (250 or 500 Kv or more) will be in the toroidal coil, we are working on the design of a real-time control system to optimize the distance between the graphite electrodes based on the Electric field and magnetic all the electrodes at the same optimum distance for that operation is steady and steady state.

As for the structural dimensional characterization of nanostructured materials, the carbon is realized by means of Raman spectroscopy, XRD and Transmission Electron Microscopy (TEM). Scanning Electron Microscopy (SEM) and EELS

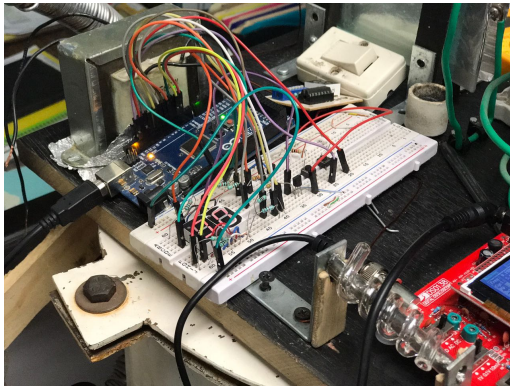
ANALYSIS OF RESULTS

The following table 1 shows the statistics of the synthesis that was carried out for three weeks. And it shows the statistical variables, mean, standard deviation and their respective means of each week and that of the total of the synthesis.

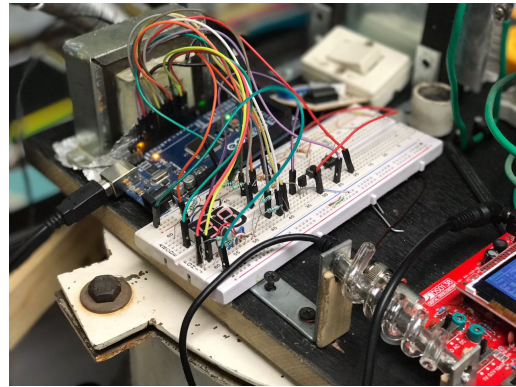
Table 1: Synthesis results

1 ^a week	2 ^a Week	3 ^a Week
58.7 gr.	64.5 gr.	59.9 gr.
60.4 gr.	71.3 gr.	68.8 gr.
59.3 gr.	60.7 gr.	72.4 gr.
60.1 gr.	68.6 gr.	72.1 gr.
64.4 gr.	73.4 gr.	70.9 gr.
$\Sigma=302.9$ gr.	$\Sigma=338.5$ gr.	$\Sigma=344.1$ gr.
= 60.58 gr. \bar{x}		
=67.70 gr \bar{x}		
= 68.82 gr \bar{x}		
$\sigma=2.001$ gr.	$\sigma=4.593$ gr.	$\sigma=4.363$ gr.

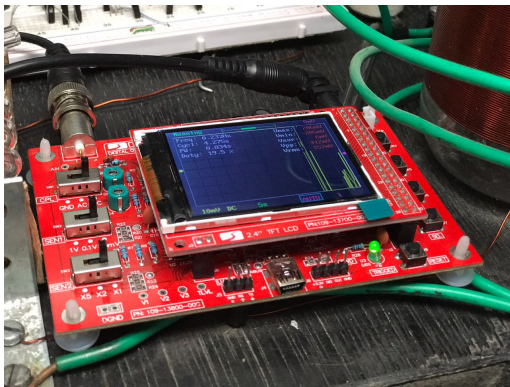
Of separation by magnetic fields and solubilization procedures in different organic solvents hexane and benzene PVP (polyvinyl pyridone) and PVA (polyvinyl alcohol)



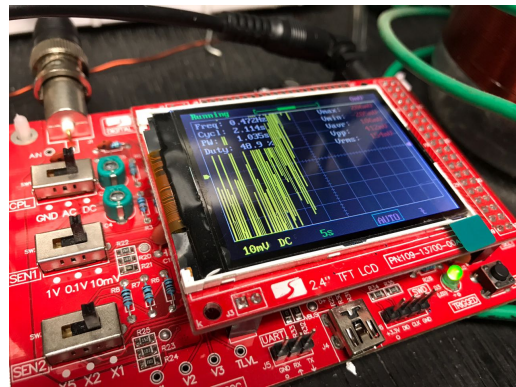
06db6e9a-07ec-469e-986a-81631d39cd81.jpg



6ca08e55-b40e-476d-9ae1-5e3fddcaddfb.jpg



216034d5-c020-4ab7-9421-5bde3009d8b4.jpg



E43da61e-4a15-403f-b798-9e3c3c7405e2.jpg

Authors Index

., S.	203	Barho, F.	56, 149
Abadía, N.	214	Baudrion, A.	162
Adam, P.	162	Baumberg, J.	224
Adhikari, S.	37	Belacel, C.	9
Agnello, S.	247	Bellessa, J.	74, 118, 136
Aguilar, J.	14	Bello, F.	214
Ahmed, W.	164	Belov, P.	63, 156, 242
Aizpurua, J.	58, 220	Beneš, L.	19
Akimov, A.	63	Benoit, J.	118
Al Hafidh, M.	50	Benson, O.	97
Albella, P.	243	Benz, F.	224
Alekseeva, S.	60	Bergmann, E.	162
Alexandrov, I.	194	Bernard, R.	135
Alfadhli, S.	84	Berthel, M.	74, 136
Alfaro Mozaz, F.	58	Bertru, N.	135
Alivisatos, A.	10	Bezshlyakh, D.	21
Alonso González, P.	58	Bezyazychnaya, T.	194
Alshalfouh, A.	31	Bhartiya, S.	203
Alwakil, a.	75	Bianco, M.	142
Aly, M.	87	Bidault, S.	140
Amra, C.	75	Bisio, F.	53
An, J.	83	Blaize, S.	25
Anderson, A.	213	Blanquer, G.	54
Anokhin, M.	20	Boer Duchemin, E.	121
Antipov, Y.	105	Bogdanov, A.	76, 180, 249
Apostolopoulos, V.	229	Bomers, M.	56, 149
Arima, V.	142	Bonanni, V.	145
Armin, F.	219	Bonod, N.	140
Armstrong, R.	46, 47	Borkunov, R.	105
Askes, S.	133	Botey, M.	91, 164
Assaf, S.	234	Bouchet, D.	140
Atcheson, G.	214	Bozhevolnyi, S.	90, 139
Atwater, H.	1, 212	Brand, U.	21
Atxabal, A.	58	Brevet, P.	162
Auad, Y.	17	Brickus, D.	16
Autore, M.	58	Brito Da Silva, T.	108
Aviv, H.	32	Bryukhanov, V.	105
Bakan, E.	107	Buergi, T.	192
Ballarini, D.	142	Buscarino, G.	247
Barb, R.	244	Buzelis, R.	129, 189
		Byungjun, K.	132

Caillibotte, M.	234	De Liberato, S.	160
Caixeiro, S.	165	De Marco, L.	142
Caldarola, M.	48	De Melo, A.	108
Calderon, J.	106	De Nicola, F.	187
Caldwell, J.	45	De Rosa, M.	42
Camarda, P.	247	De Wilde, Y.	54, 140, 151
Cambiasso, J.	243	Demetriadou, A.	224
Campo, G.	145	Demin, M.	105
Canepa, M.	53	Derbal, M.	23
Cannas, M.	247	Di Fabrizio, E.	53
Cao, S.	121	Dias, E.	90
Carletti, L.	155	Ding, B.	27
Carminati, R.	151	Ding, Z.	27, 66
Carvalho, E.	17	Dini, K.	221
Casanova, F.	58	Djafari Rouhani, B.	234, 239
Cazier, N.	62	Dmitriev, A.	145
Celebrano, M.	155	Dobrovolsky, A.	34
Centeno, E.	33, 240	Dobrykh, D.	63
Cerutti, L.	56, 149	Dolado, I.	58
Chau, L.	223	Dominici, L.	142
Chen, J.	30	Donegan, J.	214
Chien, M.	124, 238	Dong, Z.	220
Chikkaraddy, R.	224	Dostalek, J.	28, 101, 182
Chiu, H.	223	Drezet, A.	74, 121, 136
Choi, J.	94	Du Chene, J.	212
Choi, K.	94	Duan, X.	7
Chu, J.	36	Dubertret, B.	9
Clark, E.	158	Dubtsov, A.	200
Coello, V.	25, 139	Ducati, C.	153
Contreras, B.	14	Dujardin, G.	121
Coolen, L.	9	Dupont, D.	234
Cooper, J.	50	Durand, O.	135
Cornet, C.	135	Dussan, A.	106
Corre, A.	135		
Cortes, E.	243	Elewah, I.	87
Cox, J.	40	Engheta, N.	77
Crai, A.	123	Escorcía Carranza, I.	99
Cumming, D.	99	Esparza, J.	9
		Espinosa, F.	251
Da Silva Moreira, C.	108	Esposito, M.	142
Das, G.	53	Esteban, R.	58, 220
Davoyan, A.	212		
De Angelis, C.	155	Fauché, P.	236
De Angelis, F.	53, 71, 147, 187	Favero, I.	42, 155
De Beule, P.	168	Fedotova, O.	233
De Giorgi, M.	142	Fernanda Da Silva Santiago, M.	108
De Julián Fernández, C.	145	Fernandes, F.	165
De La Peña, F.	153	Fernandez Tavizon, S.	251

Finazzi, M.	155	Gorecki, J.	229
Flanigan, P.	214	Gorodetski, Y.	147
Fossati, S.	101	Grange, R.	38
Frizyuk, K.	249	Grant, J.	99
Fu, A.	66	Greffet, J.	118, 121
Fu, Y.	119	Grillo, R.	192
Fujii, M.	132	Grillot, F.	41
Fujiwara, Y.	132	Grinblat, G.	243
Funato, M.	198	Grinevičiūtė, L.	129, 189
Förstner, J.	68, 143	Gubbin, C.	160
		Guedes, R.	17
G. Bouillard, J.	137	Guo, W.	102
G. Silva, A.	168	Gurioli, M.	145
Gaio, M.	165	Guyen, K.	166
Gaizauskas, E.	233	Guzmán Gutiérrez, E.	14
Galieni, V.	102	Gülinc, J.	167
Gallas, B.	140	Günther, M.	191
Garcia De Abajo, J.	40, 114		
Garcia Etxarri, A.	35	Hageneder, S.	101
Garcia Meca, C.	126	Hamza, A.	137
Garcia Ortiz, C.	139	Han, J.	72
Garcia Parajo, M.	140	Harraz, F.	237
Garcia Vidal, F.	80	Hayashi, S.	132
Garcés, R.	14	Hayran, Z.	91
García De Abajo, J.	143	Heitz, J.	244
Garnett, E.	133	Hellberg, L.	60
Garoli, D.	147	Hendricks, N.	38
Gayvoronsky, V.	233	Hernández Pozos, J.	231
Gelardi, F.	247	Herrero, R.	91, 164
Genet, C.	74, 136	Hess, O.	123, 224
Genevet, P.	81	Hildebrandt, A.	68
Gerlach, G.	191	Hillenbrand, R.	58
Gharib, K.	68	Hinczewski, M.	71
Ghimire, G.	37, 112	Hobbs, R.	214
Ghirardini, L.	155	Hogg, R.	158
Gibson, N.	10	Honey, S.	29, 103
Gigli, G.	142	Hormozi Nezhad, M.	110, 210
Gili, V.	155	Horáček, M.	46
Ginsburg, A.	213	Hrelescu, C.	244
Gisbert Quilis, N.	28	Hsu, C.	223
Gizowska, M.	178, 196, 206	Huang, K.	27
Glidle, A.	50	Huant, S.	74, 121, 136
Glorieux, Q.	54	Hueso, L.	58
Godlewski, M.	232	Hugonin, J.	121
Goh, G.	102	Humphreys, M.	99
Gonzalez Hernandez, R.	106	Hurtado, C.	167
Gonzalez Posada Flores, F.	56, 149	Hwang, C.	94
Gonçalves, P.	90, 227	Härtling, T.	191

Iorsh, I.	76, 156, 221, 249	Kivshar, Y.	38, 156
Isa, L.	38	Klar, T.	244
Ishaq, A.	103	Knoll, W.	28, 101
Isoniemi, T.	71	Knotek, P.	19
Ivanov, P.	158	Kobus, I.	178, 196, 206
Izeddin, I.	151	Kochtcheev, S.	162
Jacopin, G.	153	Kociak, M.	153
Janiček, P.	19	Kojima, O.	158
Jarosz, D.	232	Komissarenko, F.	156, 249
Jennings, B.	214	Kongsuwan, N.	224
Jermyn, A.	212	Konopka, G.	178, 196, 206
Jiang, J.	37	Konstantinova, E.	105
Jiang, Q.	74, 136	Kontoleta, E.	133
Jo, S.	37	Kopalko, K.	232
Jonas, U.	28, 101	Korovin, A.	234, 239
Jonin, c.	162	Koscher, B.	10
Joo, J.	37	Koseoglu, D.	107
Joos, M.	54	Koshelev, K.	180
Julien, F.	153	Kotlarek, D.	182
Kabanau, D.	86	Kowalski, B.	232
Kabanava, V.	24	Kozanecki, A.	232
Kalds, M.	87	Krachmalnicoff, V.	54, 140, 151
Kamin, S.	7	Krahne, R.	187
Kan, H.	36, 223	Kroh, C.	191
Kang, G.	228	Kroker, S.	167
Kang, H.	94	Kuhn, T.	123
Kapitanova, P.	63	Kumar, D.	96
Kapon, O.	61	Kumar, S.	139
Karpinska, K.	102	Kuntsevich, B.	183
Karsli, K.	107	Kuo, S.	223
Katelnikovas, A.	217	Kurnia, M.	202
Kawakami, Y.	198	Kurt, H.	91
Kazanov, D.	117	Kusko, C.	185
Kelly, A.	50	Kusko, M.	185
Kenney, M.	72, 99	Kusmartsev, F.	84
Keyser, U.	224	Kutálek, P.	19
Khasanov, O.	233	Kuznetsov, A.	119, 156, 174
Kibis, O.	221	Kuzyk, A.	113
Kim, C.	96	Kwon, D.	208
Kim, G.	94	Langfahl, J.	21
Kim, H.	37, 94	Langhammer, C.	60, 175
Kim, J.	37, 112	Lanteri, S.	33, 205
Kim, T.	72	Lapina, V.	12, 186
Kim, Y.	94	Larochelle, S.	41
Kita, T.	158	Lavrinenko, A.	76, 180, 249
Kitaev, V.	30	Le Moal, E.	121
		Le, Q.	223

Lebbou, K.	23	Martínez, A.	5, 8, 82
Lebiadok, Y.	86, 104, 194	Maître, A.	9
Lechago, S.	126	Mažulė, L.	129
Lee, C.	112	Mccloskey, D.	214
Lee, J.	96, 112	Mekonnen Adamu, A.	145
Lee, W.	94	Melloni, A.	248
Lee, Y.	37	Melnikova, E.	24
Lemaitre, A.	42, 118, 155	Melninkaitis, A.	129
Leo, G.	42, 155	Memon, F.	248
Leone, S.	10	Mendoza Luna, L.	231
Leuthold, J.	2	Meng, Q.	220
Levi, S.	43	Mercado, A.	251
Li, L.	102	Mercadé Morales, L.	8
Li, P.	58	Merdasa, A.	34
Li, S.	72	Mesa, F.	106
Li, Y.	77, 243	Messina, F.	247
Liang, X.	119	Mezy, A.	149
Liberal, I.	77	Midgley, P.	153
Lim, C.	83, 208	Mihailovic, M.	240
Lin, J.	36	Mikami, A.	130
Lin, T.	36	Milichko, V.	156, 242
Linden, S.	68	Milla, M.	56, 149
Liu, N.	7	Miranda, A.	168
Liu, S.	60	Mirsalehi, M.	219
Lober, L.	17	Miscuglio, M.	187
Locatelli, A.	155	Mivelle, M.	140
Loo, V.	54	Morais, N.	42
Losada, J.	5	Moreau, A.	33, 240
Loung, D.	37	Morichetti, F.	248
Lounis, B.	236	Mortensen, N.	90, 227
Luo, Y.	220	Moslehi Pour, A.	110, 210
Léger, Y.	135	Mourran, A.	28
		Mukherjee, C.	203
M. Adawi, A.	137	Mukhin, I.	76, 156, 249
Maaza, M.	103	Munro, P.	168
Maccaferri, N.	71, 147	Myroshnychenko, V.	143
Macdonald, R.	167	Möller, M.	28
Maier, S.	243		
Mailis, S.	229	Nababan, R.	223
Majeed, A.	158	Narang, P.	212
Makarov, S.	70, 156, 242, 249	Naseem, S.	103
Maldonado, A.	14	Nasilowski, M.	9
Malureanu, R.	76, 180	Naydenova, I.	18
Mannini, M.	145	Neffati, R.	201
Marelli, B.	165	Nesterenko, D.	132
Marini, A.	114	Neuhauser, D.	236
Marques, D.	168	Ni, S.	38
Marti, J.	126	Nielsen, M.	243

Nikitin, A.	58	Pokutnyi, S.	233
Niv, A.	43	Polini, M.	187
Novotny, L.	4	Pollès, R.	240
Nugroho, F.	60	Porvatkina, O.	93
		Poshakinskiy, A.	117
Okamoto, K.	198	Prades, J.	167
Omenetto, F.	165	Pradhan, B.	48
Orfanelli, M.	17	Prins, F.	67
Orlov, S.	16, 225	Proietti Zaccaria, R.	53
Orrit, M.	48	Proust, J.	140
Ostasevicius, T.	153	Pusch, A.	123
Osuchowski, M.	178, 196, 206	Puthiya Purayil, N.	187
Otsuji, T.	115		
Oulton, R.	243	Quidant, R.	65
Ouyang, C.	72	Rahbany, N.	151
Oyarzun, P.	14	Rahman, E.	172
Ozerov, I.	140	Rai, S.	203
		Rai, V.	203
Paarmann, A.	45	Raj Dhawan, A.	9
Pala, R.	212	Rajab, F.	237
Palatnik, A.	32	Rakovich, A.	243
Palhares, L.	17	Ramirez Hernandez, H.	251
Paniagua Dominguez, R.	119	Raudonyte Svirbutaviciene, E.	217
Papasimakis, N.	229	Rauschenbeutel, A.	79
Park, C.	96	Ravaro, M.	42
Park, K.	112	Razdolski, I.	45
Pasechnik, S.	200	Reboud, J.	50
Passler, N.	45	Reiter, D.	123
Pellegrini, V.	187	Rekik, B.	23
Pennec, Y.	234, 239	Renaut, C.	38
Peres, N.	90, 227	Resch Genger, U.	97
Perkowski, K.	178, 196, 206	Reszka, A.	232
Permyakov, D.	76	Rigo, I.	17
Perotto, S.	71	Rigutti, L.	153
Pershukevich, P.	12, 186	Ritter, N.	30
Peter, M.	68	Rocco, D.	155
Petri, C.	28, 101	Rohel, T.	135
Petronis, L.	189	Rojas Ruiz, E.	231
Petrov, M.	38, 242, 249	Roland, I.	42
Peña Román, R.	17	Roy, S.	37
Pham, A.	74, 136	Rusetsky, G.	233
Pi, J.	94	Ryuazki, S.	198
Piatkowski, L.	6		
Pieniżek, A.	232	Sadhegi, P.	62
Pineider, F.	145	Sadrieva, Z.	180
Pitelet, A.	33	Saito, H.	216
Poddubny, A.	156	Saktioto, t.	202
Pogoda, B.	21	Salas Montiel, R.	25

Samusev, A.	76, 156, 180, 249	Steiger Thirsfeld, A.	62
Samusev, I.	105	Steinhauser, B.	244
Sandoghdar, V.	78	Strangi, G.	71
Sangregorio, C.	145	Strikhanov, M.	20, 93
Santa Cruz, R.	108	Sun, H.	72
Santana, L.	17	Sundararaman, R.	212
Sanvitto, D.	142	Susarrery Arce, A.	60
Sapienza, R.	165	Svedendahl, M.	65
Sarraute, J.	41	Syahputra, R.	202
Sauvan, C.	118	Symonds, C.	118
Savchenko, S.	245		
Savelev, R.	70	Ta, V.	165
Saveliev, S.	84	Tafoughalt, M.	190
Scheblykin, I.	34	Tagliabue, G.	212
Scheid, C.	33, 205	Takayama, O.	76, 180
Schell, A.	65	Takele, W.	6
Schires, K.	41	Taliercio, T.	56, 149
Schlickriede, C.	68	Tamada, K.	198
Schmid, S.	62, 124, 238	Tantussi, F.	187
Schmitt, N.	33, 205	Tarasenko, S.	117
Scholz, G.	167	Tarui, Y.	158
Schwob, C.	9	Tateishi, K.	198
Sekkat, Z.	132	Tatsiana, P.	12, 186
Senellart, P.	9, 118	Taylor, A.	170
Senez, V.	234	Tchernycheva, M.	153
Seo, C.	112	Teisseyre, H.	232
Serri, M.	145	Tellez Limon, R.	25
Sessoli, R.	145	Tessier, G.	151
Sezer, Y.	107	Thomy, V.	234
Shabrov, D.	183	Timpu, F.	38
Shadrivov, I.	63, 70	Ting, C.	223
Shah, Y.	99	Tischler, Y.	32, 61
Shalayeva, A.	104	Tishchenko, A.	20, 93
Shawrav, M.	62, 238	Tiwari, P.	203
Shelykh, I.	221	Tizei, L.	153
Sheppard, A.	102	Todisco, F.	142
Shibanuma, T.	243	Tolenis, T.	129, 189
Shmeliova, D.	200	Tolstik, A.	24
Shubina, T.	117	Toma, A.	53
Sinev, I.	76, 156, 180, 249	Tomadin, A.	187
Sinha, A.	203	Tomescu, R.	185
Songmuang, R.	153	Tournié, E.	56, 149
Soshenko, V.	63	Tremblay, R.	135
Spirito, D.	187	Treyzebre, A.	234
Srivastava, A.	203	Triantis, I.	172
Staliunas, K.	91, 164	Trifonov, S.	200
Stanescu, S.	102	Tsarkov, M.	105
		Turek, V.	224

Unger, E.	34	Wu, W.	167
Ushakova, E.	156	Wuchrer, R.	191
Vaccaro, L.	247	Xiao, S.	90, 227
Vaicaitis, V.	233	Yamada, A.	236
Vallée, R.	236	Yamamoto, N.	143, 216
Van Dongen, M.	28	Yang, J.	94
Van Hulst, N.	3	Yartsev, A.	34
Vasilevskiy, M.	90	Yedjour, A.	209
Velez, S.	58	Yermakov, O.	76
Viallon, M.	234	Yu, Y.	119, 156, 220
Vidal, C.	244	Zaban, A.	213
Vieira, R.	17	Zagonel, L.	17, 153
Vilain, S.	102	Zalewska, M.	178, 196, 206
Viscomi, F.	137	Zalogina, A.	70
Vitiello, G.	153	Zaluzny, M.	109
Vokhmintsev, A.	245	Zaragoza, A.	251
Vollmer, F.	176	Zawadzka, M.	18
Vorobyov, V.	63	Zentgraf, T.	68, 177
Vu, V.	223	Zerrad, M.	75
Vázquez Lozano, J.	82	Zhang, L.	220
Waag, A.	21, 167	Zhang, S.	72
Wabnitz, S.	42	Zhang, W.	48, 72
Waluk, J.	6	Zhang, X.	72
Wang, D.	72	Zhang, Y.	220
Wang, P.	198	Zhao, X.	52
Wanzenboeck, H.	238	Zhong, C.	214
Wasisto, H.	21, 167	Zhuravlev, K.	194
Wei, C.	102	Zijlstra, P.	46, 47, 170
Weinstein, I.	245	Zilio, P.	147
Welch, A.	212	Zizzari, A.	142
Winta, C.	45	Zograf, G.	242
Witkowski, B.	232	Zuev, D.	70, 156, 242
Witosławska, I.	178, 196, 206	Özelci, E.	97
Wolf, H.	38	önal, e.	166
Wolf, M.	45	Černošková, E.	19
Wright, S.	102		
Wu, D.	72		

PremC Upcoming Conferences

PremC
Conferences, Events & Workshops

ICONAN 2017

International Conference on **NANOMEDICINE**
And **NANOBIOTECHNOLOGY**

Sept 25-27, 2017
in **Barcelona**



PremC
Conferences, Events & Workshops

ANNIC 2017



**APPLIED NANOTECHNOLOGY
AND NANOSCIENCE
INTERNATIONAL CONFERENCE**

OCT 18-20, 2017
ROME

PremC
Conferences, Events & Workshops



PEMED 2018

Personalized and Precision Medicine
International Conference

April 11-13, 2018 | Paris

PremC
Conferences, Events & Workshops



ICREN 2018

INTERNATIONAL CONFERENCE ON **RENEWABLE ENERGY**

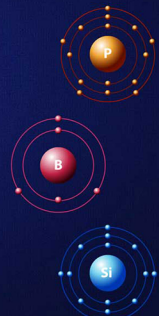
APRIL 25-27, 2018 | BARCELONA

PremC
Conferences, Events & Workshops

PBSi 2018

International Conference On
Phosphorus, Boron and Silicon

Dec 10-12, 2018 | Barcelona



Prem 
Conferences, Events & Workshops